UNRAVELLING THE ROLE OF GLYCOSYLATION IN *CLOSTRIDIUM DIFFICILE* INFECTION

A thesis submitted for the degree of Ph. D.

By

Izabela Marszalowska, B. Sc. (Hons)

Under the supervision of

Prof. Christine E. Loscher

Based on research carried out at

School of Biotechnology

Dublin City University

Ireland

September 2015

DECLARATION

I hereby certify that this material, which I now submit for assessment on the programme of study leading to the award of Doctor of Philosophy is entirely my own work, that I have exercised reasonable care to ensure that the work is original, and does not to the best of my knowledge breach any law of copyright, and has not been taken from the work of others save and to the extent that such work has been cited and acknowledged within the text of my work.

Signed: _____ (Candidate) ID No.: 57749040 Date: _____

TABLE OF CONTENTS

ACKNOWLEDGMENTS

First and foremost I would like to express my special appreciation and thanks to Professor Christine Loscher. Christine, thank you for giving me the opportunity to join the Immunomodulation Laboratory. Thank you for encouraging my research and for allowing me to grow as a research scientist. Your enthusiasm for science and your career is truly inspiring.

The successful completion of this project would have not been possible without the members of Immunomodulation Laboratory. I have been lucky to work with a wonderful group of people. I would like to acknowledge all the help that I have received during completion of my PhD - I literally couldn't do it without you guys. On a more personal note, I know that I made lifelong friends that had such a big impact on my life. Laura, thank you for all the advices and encouragement, but also for being wonderful friend, and always going beyond expected. Maja, it was always great to have these Crolish & Crolski chats that nobody else could understand and appreciate! Catherine, thank you for being such a lovely and kind person, and I will never forget your first day in the lab! Still makes me laugh! Fiona, thank you for all the help in recent weeks and being so kind to me all that time. Kathy, not long left now, we will have plenty of meerkatea breaks for MeerKathy to keep you going! Lab twins Niamh & Kim, you are such a lovely addition to the lab, I have no doubts you will do great in your PhDs! There is also a special thanks to the previous members of the lab, Mary, Ciara, Mark and Joey. Mark, the founding member of the Team SLP! I admire your never-ending enthusiasm for science and thank you for the advice, support, and kind words in the final stages of my project. Mary, thank you for being such a patient supervisor during my first project in the lab. *Loscher Lab - Go raibh míle maith agaibh.*

I would also like to thank my wonderful friend Joanna Stanicka. I am so lucky to have you in my life, you are such an inspiring person, not only as a scientist but also as a friend. You remind me every day that *impossible is nothing.* Now that I have more time, I am looking forward to our late night chats, and dancing all night *like the ceiling can't hold us*.

There also special thank you to my lifelong friends Ewa, Natalia, Iwona, Ola and Kuba. Thank you for always finding time for me when I am back home, even when you are busy family lives and work. And it is a great feeling to know that no matter what is going to happen next, no matter where our future takes us, we will always have a place to meet in Janikowo.

Completing my PhD was long but fascinating journey and I could not do it without my family. There are special thanks to Banaś and Westfal family and Drzewiecki and Walczak family for enthusiastic support in all those years.

I would also like to thank my sister Ewa and her husband Jarek. Thank you for inviting me all these years ago to visit you in Ireland, and showing me this wonderful place. Thank you for your constant support and advise when I decided to move to Dublin and start college. And I can't wait to visit you soon and play with Robert and Bruno. *Love you guys*.

Last but not least, I would like to thank my mum Bożena and my dad Adam. The words cannot describe how grateful I am for all these years of support, long and late night Skype calls, patiently waiting for me at the airport, spoiling me rotten with all my favourite dinners and snacks. And thank you for always reminding me what is really important in life. *Dziękuję*.

ABBREVIATIONS

AAL	*Aleuria aurantia* lectin
ANOVA	Analysis of Variance
APC	Antigen Presenting Cell
BCA	Bicinchoninic acid assay
BHI	Brain Heart Infusion Broth
bp	Base pairs
BSA	Bovine Serum Albumin
BW	Body Weight
C57BL/6J	Strain of mice used this project
CCL	Chemokine ligand
CD	Cluster of differentiation
cDNA	complementary Deoxyribonucleic Acid
ConA	Concanavalin A lectin
Cq	Threshold cycle (in RT qPCR)
DAPI	4',6-diamidino-2-phenylindole
DBA	*Dolicos biflorus* lectin
DDAI	Daily Disease Activity Index
DEPC	Diethylpyrocarbonate
DMEM	Dulbecco's Modified Eagle's Medium
dNTP	Deoxyribonucleotide Triphosphates
DPBS	Dulbecco's Phosphate-buffered Saline
DSS	Dextran Sulphate Sodium
DTT	Dithiothreitol
ECL	*Erythrina cristagalli* lectin
EDTA	Ethylenediaminetetraacetic acid
ELLA	Enzyme-linked Lectin Assay
EU	Endotoxin Units
FAB	Fastidious Anaerobic Broth
FDA	Food and Drug Administration
FITC	Fluorescein isothiocyanate
FMT	Faecal Microbiota Transplant

FPLC	Fast Protein Liquid Chromatography
GalNAc	N-Acetylgalactosamine
GI	GI (tract)
GlcNAc	N-Acetylglucosamine
GNL	*Galanthus nivalis* lectin
GSL I/II	*Griffonia simplicifolia I/II* lectin
HMW	High Molecular Weight subunit of Surface Layer Protein
HRP	Horseradish Peroxidase
H&E	Haematoxylin and Eosin Staining
IBD	Inflammatory Bowel Disease
IFNγ	Interferon gamma
IL	Interleukin
IP	Intraperitoneal injection
kDa	kilodalton (unified atomic mass unit)
LAL	Limulus Amebocyte Lysate assay
LCA	*Lens culinaris* lectin
LMW	Low Molecular Weight subunit of Surface Layer Protein
LPS	Lipopolysaccharide
Mal I/II	*Maackia amurensis I/II* lectin
MCP1	Monocyte Chemoattractant Protein 1
MIP1/2 α	Macrophage Inflammatory Protein 1 or 2 alpha
MIQE	Minimum information for publication of quantitative real-time PCR experiments
mRNA	Messenger Ribonucleic Acid
MUC	Mucin
NF-κB	Nuclear Factor kappa-light-chain-enhancer of activated B cells
NOD	Nucleotide-binding Oligomerisation Domain
NPL	*Narcissus pseudonarcissus* lectin
OCT	Optimum Cutting Temperature (medium)
OD	Optical density
PaLoc	Pathogenicity locus
PAGE	Polyacrylamide Gel Electrophoresis
PAS	Periodic Acid-Schiff staining
PBS	Phosphate-buffered Saline
PNA	Peanut lectin

PPR	Pathogen Recognition Receptor
RANTES	Regulated on Activation, Normal T cell Expressed and Secreted
RegIIIγ	Regenerating islet-derived protein 3 gamma
RLR	RIG-I-like receptor
RNA	Ribonucleic Acid
RPMI	Roswell Park Memorial Institute medium
RT	Ribotype
RT qPCR	Reverse Transcriptase quantitative Polymerase Chain Reaction
SBA	Soybean lectin
SBT	Soybean Trypsin
SDS	Sodium Dodecyl Sulphite
S-layer	Surface Layer
SLP	Surface Layer Protein
SNA	*Sambucus nigra* lectin
STAT	Signal transducer and activator of transcription
sWGA	Succinylated Wheat Germ lectin
TBST	Tris-buffered saline with Tween
TAE	Tris base, Acetic Acid and EDTA buffer
TEMED	N, N, N', N'-tetramethylethylenediamine
TGFβ	Transforming Growth Factor beta
Th1/17	Helper T cells (type 1 and type 17)
TLR	Toll-like receptor
TMB	3,3',5,5'-Tetramethylbenzidine
TNFα	Tumour Necrosis Factor alpha
Tregs	Regulatory T cells
UC	Ulcerative Colitis
UEA-1	*Ulex europaeus I* lectin
UV	Ultraviolet
VRE	Vancomycin-resistant *Enterococcus*
WGA	Wheat Germ lectin

LIST OF TABLES

LIST OF FIGURES

PUBLICATIONS

Surface Layer Proteins isolated from *Clostridium difficile* induce clearance responses in macrophages.
L. E. Collins, M. Lynch, I. Marszalowska, M. Kristek, K. Rochfort, M. J. O'Connell, H. Windle, D. Kelleher, C. E. Loscher
Microbes and Infection (2014; 1-10)

Profiling Humoral Immune Response to *Clostridium difficile*-Specific Antigens by Protein Microarray Analysis.
O. Negm, M. Hamed, E. Dilnot, C. Shone, I. Marszalowska, M. Lynch, C. E. Loscher, L. Edwards, P. Tighe, M. Wilcox, T. Monaghan
Clinical and Vaccine Immunology (2015: CVI.00190-15)

Surface Layer Proteins from virulent *Clostridium difficile* ribotypes exhibit signatures of positive selection with consequences for innate immune response.
M. Lynch, T. A. Walsh, I. Marszalowska, A. E. Webb, M. MacAogáin, T. R. Rogers, H. Windle, D. Kelleher, M. J. O'Connell, C. E. Loscher
Submitted to PLOS Pathogens

Examining glycosylation patterns of Surface Layer Proteins from infectious ribotypes of *Clostridium difficile*.
I. Marszalowska, M. Lynch, R. Larrgy, A. Ravida, M. MacAogáin, T. Rogers, H. Windle, B. O'Connor, S. M. O'Neill, C. E. Loscher
To be submitted to Microbes and Infection

***Clostridium difficile* ribotype 001 infection induces early clearance mechanism via IL-22, while ribotype 027 delays this clearance mechanisms via IL-22.**
I. Marszalowska, M. Lynch, M. Kristek, J. DeCourcey, P. Casey, M. MacAogáin, T. Rogers, C. E. Loscher
Manuscript in preparation

***Clostridium difficile* ribotype 027 induces more severe infection *in vivo* compared to ribotype 001.**
M. Lynch, M. Kristek, J. DeCourcey, I. Marszalowska, K. Kennedy, P. Casey, M. MacAogáin, T. Rogers, C. E. Loscher
Manuscript in preparation

PRESENTATIONS

Unravelling the dynamics of mucosal immune response during *Clostridium difficile* infection
I. Marszalowska, M. Lynch, A. Ravida, C. E. Loscher
4th European Congress of Immunology
Vienna, Austria, September 2015
Poster Presentation and Travel Award

Changes in glycosylation patterns in the gut contribute to infection with *Clostridium difficile.*
I. Marszalowska, M. Lynch, A. Ravida, C. E. Loscher
Keystone Symposia Meeting: "Gut Microbiota Modulation of Host Physiology: The Search for Mechanism"
Keystone, Colorado, USA, March 2015
Poster Presentation

Changes in glycosylation patterns in the gut contribute to infection with *Clostridium difficile.*
I. Marszalowska, M. Lynch, A. Ravida, R. Larrgy, B. O'Connor, C. E. Loscher
DCU School of Biotechnology Annual Research Day
Dublin, January 2015
Oral Presentation

Factors contributing to *Clostridium difficile* infection.
I. Marszalowska, M. Lynch, A. Ravida, C. E. Loscher
Irish Society for Immunology Annual Meeting
Dublin, September 2014
Poster Presentation

Can we use sugar to treat infection?
I. Marszalowska and C. E. Loscher
Tell It Straight Competition organised by DCU Graduate Studies Office
Dublin, March 2014
Oral Presentation

Can we use sugar to treat infection?
I. Marszalowska, M. Lynch, M. MacAogáin, R. Larrgy, H. Windle, T. Rogers, B. O'Connor, C. E. Loscher
DCU School of Biotechnology Annual Research Day
Dublin, January 2014
Oral Presentation Winner

Unravelling the role of glycosylation in C*lostridium difficile* infection.
I. Marszalowska, M. Lynch, M. MacAogáin, R. Larrgy, H. Windle, T. Rogers, B. O'Connor, C. E. Loscher
6th Annual GlycoScience Meeting
Westport, Ireland, November 2013
Poster Presentation

Do bacteria use sugar to stick to your gut?
I. Marszalowska, M. Lynch, C. E. Loscher
Why my research matters? Organised by Irish Research Council
Annual Research Day, Irish Research Council,
Dublin, September 2013
Poster Presentation

Unravelling the role of glycosylation in C*lostridium difficile* infection.
I. Marszalowska, M. Lynch, M. MacAogáin, R. Larrgy, H. Windle, T. Rogers, B. O'Connor, C. E. Loscher
Irish Society for Immunology Annual Meeting,
Dublin, September 2013
Poster Presentation

ABSTRACT

Unravelling the Role of Glycosylation in *Clostridium difficile* Infection

Izabela Marszalowska, B. Sc. (Hons)

Alterations to the normal composition of our gut microbiota can result in disturbance of gut homeostasis. Opportunistic pathogens such as *Clostridium difficile* can profit from this environment, leading to colonisation of the gut.

Clostridium difficile infection (CDI) is the most common healthcare associated disease in Ireland and with the incidence of occurrence on the rise. CDI represents a major health and economic burden to society. The primary pathogenesis of *C. difficile* has been attributed to its toxins; however the mechanisms that promote the initial colonisation and adherence of the pathogen still remain unclear. Glycosylation is an important factor affecting host-pathogen interactions in the gastrointestinal (GI) tract. We have, however discovered that the Surface Layer Proteins (SLPs) of *C. difficile* are not glycosylated and therefore do not contribute to host-pathogen interactions in this context. Subsequently, we examined the glycosylation profile on the surface of the colonic epithelium. To mimic the immunocompromised state of CDI patients, we used an *in vivo* model of antibiotic treatment to induce a susceptibility state in mice. Antibiotic treatment, and presumably the disturbance in microbiota composition, induced a protective state. This was evidenced by the glycan profile on the surface of the epithelium which was rich in fucose, a sugar known to promote the recovery of commensals, and depleted of sialic acid, an essential sugar used by *C. difficile* as an energy source. This protective state was further confirmed by the increased expression of anti-inflammatory cytokines IL-10 and TGFβ, and the increase in mucin and tight junction protein expression. We also observed decreased IL-22 expression, an essential cytokine for maintaining the integrity of the epithelium. For these reasons we propose that susceptibility to CDI is a result of compromised expression of IL-22 and the immunosuppressive environment induced by IL-10 and TGFβ that may delay the initial immune response to the pathogen. These findings are further supported by our observations of *C. difficile* infection *in vivo* where the increased sialic acid correlated with increased pathogen load and decreased IL-22 expression correlated with the excessive damage to the epithelial barrier.

In this project we have identified novel mechanisms with an important role in CDI. These mechanisms may provide attractive targets for therapeutic intervention. Specifically, modulation of the fucose and sialic acid balance in the gut of immunocompromised patients may aid in commensal recovery and prevent *C. difficile* from thriving. Furthermore, enhancing IL-22 signaling may reinforce the integrity of the mucosal barrier in susceptibility state and infection.

CHAPTER 1 INTRODUCTION

1. 1 CO-EVOLUTION OF HOST IMMUNE SYSTEM AND MICROBES

The human immune system and microbes co-evolved in parallel in a mutualistic relationship (Ley *et al.* 2008). The mammalian gastrointestinal (GI) tract provides a unique niche for microbes. The human colon is by far the largest microbial community in the human body, harbouring more than 100 trillion microbial cells (Guarner 2015). These microbes became human symbionts by complementing the host's digestive and anabolic pathways that the mammalian genome lack (Zaneveld *et al.* 2008). However, harmful pathogens were also present at very early stages of human evolution. *Helicobacter pylori*, a common gastric pathogen was shown to be associated with *Homo sapiens* host since before humans started the migration from Africa (Linz *et al.* 2007). This indicates that the human immune system had to evolve at a very early stage to provide protection against invading pathogens (Ohnmacht *et al.* 2011).

1. 1. 1 Definition of Commensal Microbiota

Microbes that reside in the human body can be referred to in the literature as microflora, microbiota or the more recently coined term microbiome. By definition, microbiota is understood as the ecological community of commensal, symbiotic, and pathogenic microorganisms that share our body space (Lederberg 2001). Recently coined "microbiome" is defined as the microbiota and its collective genomes (Bäckhed *et al.* 2005).

1. 1. 2 GI Tract as an Example of Dynamic Host-Microbial Interactions

1. 1. 2. 1 General Structure

The GI tract is the largest surface of the body that is exposed to the outer world (Pelaseyed *et al.* 2014). It is organised into the oral cavity, stomach, small and large intestine (colon). The intestines are divided in the duodenum, jejunum, ileum, caecum and colon (Pott & Hornef 2012). Distinct structural and functional differences are found along the intestines. This include variations in luminal water, ion and nutrient concentration, pH, microbiota composition and density, thickness and composition of mucus and spectrum of antimicrobial peptides (Robbe *et al.* 2003; McGuckin *et al.* 2011). Variations in the mucus thickness and composition have implications in host-microbiota and host-pathogen interactions, and this topic is further explored in this thesis.

The primary function of the GI tract is to digest food and provide the body with nutrients, but also, it is a residence site for many bacteria, both commensal and pathogenic. As the GI tract is constantly exposed to bacterial antigens, it has developed several mechanisms that protect it from bacterial invasion and overstimulation by commensals.

The first line of defence is composed of a chemical barrier, which results in the destruction of potentially harmful species by chemical lysis. These barriers are composed of highly concentrated hydrochloric acid in the stomach that can hydrolyse chemical bonds, digestive proteases that are capable of cleaving all types of peptide bonds and bile salts that are able to dissolve cell membranes (Pelaseyed *et al.* 2014).

1. 1. 2. 2 Intestinal Epithelial Cells as a Barrier

In the GI tract, a single layer of intestinal epithelial cells provides a physical barrier between the lumen colonised by bacteria and the subepithelial tissue that harbours various cells of immune system. The intestinal epithelial layer also actively participates in communication between both environments and the coordination between all these components is essential to maintain intestinal homeostasis.

The epithelial cells that cover the GI tract are structurally and functionally polarised. An apical surface faces the intestinal lumen and a basolateral surface faces the underlying basement membrane and the lamina propria (Abreu 2010). This polarised structure is established through distribution of membrane proteins to the either apical or basolateral surface, and it is also supported by the presence of tight junction proteins. Additionally, the apical surface is covered by mucus. This organisation of the intestinal epithelial barrier is generally thought to be impermeable to commensal bacteria (Peterson & Artis 2014).

The individual cells of the intestinal epithelial layer fulfil different tasks depending on their location along the GI tract. Enterocytes are the most abundant cells in the small intestine and they are interspersed by goblet cells, which produce heavily glycosylated mucins (Johansson & Hansson 2013). The Paneth cells and enterocytes actively sense microbiota and secrete antimicrobial peptides in response, including defensins, angiogenin 4, secretory phospholipase A2, lipopolysaccharide-binding protein, collectins, histatins, REGIIIα and REGIIIγ (Lindén *et al.* 2008; McGuckin *et al.* 2011). Fresh mucus is secreted by goblet cells and mixed with antimicrobial peptides secreted from the Paneth cells and enterocytes. This generates an

antimicrobial gradient in the mucus that facilitates the separation of microbiota from the epithelial cell surfaces (Pelaseyed *et al.* 2014).

The mucosal surface area is significantly increased by the formation of villi and crypts. Villi are small intestinal protrusions and are indispensable for nutrient absorption. Crypts are gland-like invaginations known to generate a protected stem cell niche (Kim *et al.* 2014).

Adjacent epithelial cells are held together through interactions between tight junction proteins (Ivanov 2012). Tight junction proteins in the intestinal epithelium prevent the free movement of luminal bacteria, toxins and antigens to the subepithelial layer (Suzuki 2012). Instead, tight junction proteins allow for selective permeability in the intercellular space between the adjacent cells (Ulluwishewa *et al.* 2011).

All the components of this system co-operate in harmony to maintain the integrity of this barrier. When one of the components is compromised, it has a detrimental effect on the homeostasis of the GI environment. The structure of the colonic epithelial layer is outlined on Figure 1. 1.

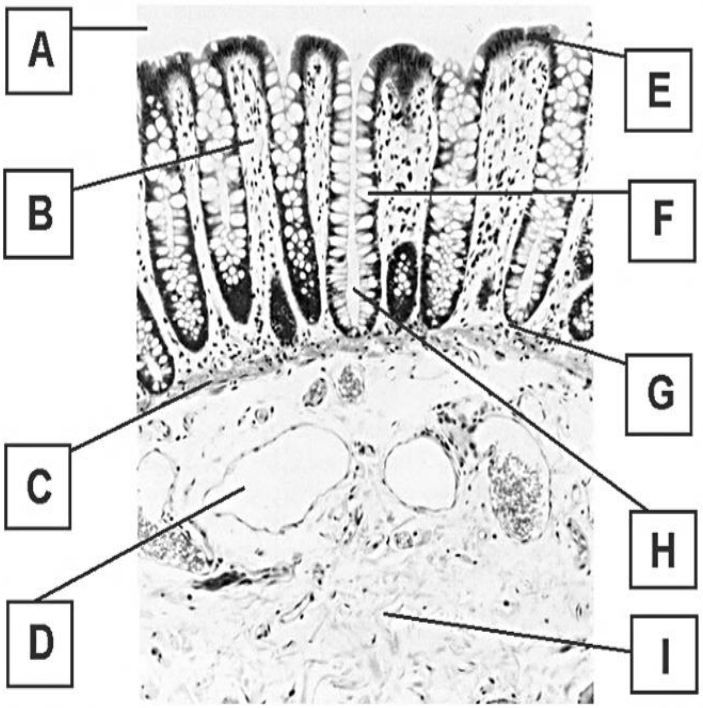

Figure 1. 1 The structure of the human colon (large intestine). Cross section of the human colonic epithelium reveals basic structures of the epithelium. Colonic epithelium lacks villi (present in the small intestine), the invaginations of the surface epithelium form intestinal crypts, which contain goblet cells and their secretions. **A**. Intestinal lumen; **B**. Lamina propria; **C**. Muscularis mucosae; **D**. Blood vessel; **E**. Surface epithelium; **F**. Goblet cell; **G.** Stem cell; **H.** Crypt of Lieberkühn; **I.** Tunica submucosa. Image sourced form: http://www.bmb.leeds.ac.uk/teaching/icu3/mdcases/ws3/.

1. 1. 2. 3 Intestinal Epithelial Cells and Their Role in Inducing the Immune System

Intestinal epithelial cells were thought to play a passive role in the separation of bacterial lumen and subepithelial layers saturated with immune cells. However, intestinal epithelial cells express pattern-recognition receptors (PPRs) to detect microbial ligands, indicating that these cells actively participate in the surveillance of the mucosal immune system (Kabat *et al.* 2014). The PPRs expressed in intestinal

epithelial cells include NOD-like receptors (NLRs), RIG-I like receptors (RLRs) and Toll-like receptors (TLRs). Nucleotide-binding oligomerisation domain 1 (NOD1) and (NOD2) receptors are intracellular receptors that recognise bacterial peptidoglycans, while retinoic acid-inducible gene (RIG) receptors recognise viral RNA, and the subsequent downstream signalling of these receptors involves engaging cell death and autophagy pathways (Saxena & Yeretssian 2014).

Of particular interest to this thesis are Toll-like receptors (TLRs), which play an important role in recognising pathogens and commensals but also viruses via pathogen-associated molecular patterns (PAMPs) and eliciting a subsequent immune response (Imler & Hoffmann 2001). There are 10 members of the TLR family in humans and 13 in mice (O'Neill *et al.* 2013). TLR2/TLR1 and TLR2/TLR6 heterodimers recognise lipopeptides of the bacterial cell wall (Round *et al.* 2011). TLR4 is known for recognising lipopolysaccharide, a component of the outer membrane of Gram negative bacteria (Takeuchi *et al.* 1999). TLR5 recognises flagellin, a protein component of flagella (Vijay-Kumar *et al.* 2008). TLR9 recognises the hypomethylated CpG DNA, which is specific to bacteria (Hemmi *et al.* 2000). TLR11 identifies uropathogenic bacteria (Zhang *et al.* 2004). Viruses are also detected via TLRs, as TLR3 participates in recognition of RNA from double- and single-stranded viruses (Alexopoulou *et al.* 2001). The intestinal epithelium of the GI tract has been shown to express all of the above TLRs, which highlights the abundance of the antigen load that the epithelium encounters (Abreu 2010).

TLR binding to its specific ligand initiates a cascade of proinflammatory cytokines and chemokines, and subsequent recruitment of effector immune cells to the site of infection (Min & Rhee 2015). Specifically, the activation of most of TLRs results in the induction of cell signalling through Myeloid differentiation primary response 88

protein (MyD88), a universal adapter protein. This in turn activates a signalling cascade within the cell that leads to activation of Nuclear Factor kappa B transcription factor (NF-κB). Consequently, NF-κB induces transcription of proinflammatory mediators such as cytokines and chemokines, which orchestrate the subsequent immune cell recruitment and immune response (Kawai & Akira 2010).

A healthy GI tract is colonised with commensal microbiota, therefore it is essential for the TLRs of the intestinal epithelial barrier to adapt to this antigen-rich environment, to prevent eliciting an immune response to commensal antigens. This is achieved by the spatial arrangement of the TLRs. For instance, TLR2, TLR4 and TLR5 have been shown to be expressed on the basolateral surface of the epithelium, while TLR3 and TLR9 are restricted to the intracellular space (Abreu 2010). Therefore TLRs become activated by their ligands only when the epithelial barrier has been breached.

Activation of TLRs by commensals under steady state conditions is also crucial for maintaining the integrity of the barrier. It has been shown that recognition of commensal antigens by TLRs is essential for the stimulation of factors that protect the epithelium. This is evident from studies of MyD88 deficiency in mice. Inability of commensals to activate protective pathways through MyD88 in these mice results in increased mortality rate due to intestinal epithelium injury (Rakoff-Nahoum *et al.* 2004). Furthermore, the TLR signalling has been shown to be important in maintaining a healthy epithelial barrier by inducing epithelial cell proliferation, IgA production, maintenance of tight junction proteins and secretion of antimicrobial peptides (Abreu 2010). Therefore, the TLRs in intestinal epithelial barrier have at least two distinct functions, protection from pathogens and maintenance of tissue homeostasis.

1. 1. 2. 4 Breach of Intestinal Epithelial Barrier Results in Recruitment of Innate Immune Response

Despite the highly organised protection system within the intestinal epithelial barrier, the immune system is essential when the physical and chemical barriers have been breached. To facilitate these functions, the immune system of the GI tract is composed of a wide network of interactions between innate and adaptive immune cells, and the cytokines and chemokines facilitate the cell communication (Kayama *et al.* 2013).

Breach of the intestinal epithelial barrier results in immediate activation of an immune response. As previously mentioned, intestinal epithelial cells are able to sense bacterial antigens via their TLRs. Activation of TLRs results in the secretion of proinflammatory cytokines and chemokines which orchestrate the subsequent immune response and cell recruitment. Specifically, innate immune cells, such as dendritic cells and macrophages are recruited from the lamina propria to clear the invading pathogens (Garrett *et al.* 2010). These cells act as innate effector cells by actively phagocytosing bacteria (Cerovic *et al.* 2014). Additionally, dendritic cells also sample the environment of the intestinal lumen by extending their dendritic processes (Hooper & Macpherson 2010). Intestinal macrophages contribute to tolerance at the epithelial barrier by secreting anti-inflammatory IL-10 cytokine (Cerovic *et al.* 2014).

Chemokine release is essential for the recruitment of neutrophils to the site of the infection (Fournier & Parkos 2012). Neutrophils have chemokine receptors on their surface that detect molecules such as IL-8 (CXCL8), Macrophage inflammatory protein 2 (MIP-2) or complement molecule C5a (Maloy & Powrie 2011; Ohtsuka *et al.* 2001). Neutrophils present in the blood detect the gradient of chemokines and

traverse the vascular endothelium to reach the intestinal lamina propria within minutes (Fournier & Parkos 2012). Their main role of the neutrophils at the site of the infection is to phagocytose the bacteria, however the neutrophils can orchestrate further immune responses by secreting chemokines for further recruitment of immune cells, anti-inflammatory IL-10 to contain the inflammation, and IL-22, which is essential for restoring the epithelial barrier (Zindl *et al.* 2013).

The sequential innate response to a breached epithelial barrier is quite complex but it is contained in order to control the recovery of gut homeostasis. When this balance is somehow compromised, it can lead to conditions such as Inflammatory Bowel Disease (IBD). While the etiology of IBD is clearly multifactorial, intestinal injury observed in IBD is largely attributed to the massive recruitment of neutrophils of an unknown origin (Maloy & Powrie 2011). However, the depletion of neutrophils in chemically-induced colitis resulted in exacerbated collapse of the epithelial structure (Kühl *et al.* 2007). This suggests that a balanced innate response is essential for the clearance of the pathogen, but also for maintaining homeostasis in the gut.

1. 1. 2. 5 Induction of Adaptive Immune Response

The activation of the innate immune cells has further implications for initiating the adaptive immune response. Activated macrophages and dendritic cells act as antigen-presenting cells (APC) to T cells (Garrett *et al.* 2010). T cells are classified into two groups; $CD4^+$ and $CD8^+$. $CD4^+$ T cells play a significant role in the GI tract, residing mostly in mesenteric lymph nodes and Peyer's patches (Hooper & Macpherson 2010). When APCs present PAMPS from pathogenic antigen via their PPRs to naïve T cells they develop into effector T cells (Helper T cell, Th cell). Certain pathogenic antigens have associated Th subsets; Th1 (intracellular bacteria and viruses), Th2

(helminths) and Th17 (bacteria and fungi) while naïve T cells presented with commensal antigen develop into Regulatory T cell (Tregs) (Nutsch & Hsieh 2012). The maturation of T cells is also influenced by the nature of the cytokines released by APCs. For example, secretion of IL-12 cytokine and IFNγ by APCs induces the maturation of Th1 cells, while IL-6, IL-23 and TGFβ have been shown to drive Th17 development (Maloy & Kullberg 2008). Transforming growth factor β (TGFβ) is an important mediator of Tregs maturation (Ouyang *et al.* 2011; Peterson & Artis 2014). Each subset of T cells plays a particular role in the immune response in the GI tract; however the balance between Th cells and Treg cells is also essential for the maintenance of gut homeostasis.

Th17 cells in the GI tract play an important role in both infection and homeostasis (Maloy & Kullberg 2008). They exert these actions via the secretion of IL-17 and IL-22 (Ivanov *et al.* 2009). IL-17 has an essential role in enhancing tight junction protein formation and secretion of antimicrobial peptides, which is of particular importance when the epithelial layer is compromised (Liang *et al.* 2006). Additionally, IL-17 can regulate the expression of another cytokine, IL-22 (Sonnenberg *et al.* 2010). IL-22 is a member of the IL-10 family of cytokines and plays a critical role in inflammation, immune surveillance and recovery of the epithelial barrier (Sonnenberg *et al.* 2011). This is evident by the wide spectrum of pathways affected by IL-22 signalling. It induces proliferation and anti-apoptotic pathways in the epithelium, which are important during disruption of the epithelial barrier (Mühl 2013). IL-22 strengthens the recovering epithelium by inducing the expression of antimicrobial peptides (Zheng *et al.* 2008) and mucus (Sonnenberg *et al.* 2010; Zenewicz *et al.* 2007; Radaeva *et al.* 2004), and it also shapes the sugar profile available for the recovering commensals (Pham *et al.* 2014). IL-22-deficient

mice suffered from increased epithelial damage, increased systemic burden of bacteria and higher mortality (Sonnenberg *et al.* 2010).

Treg cells have a mostly immunosuppressive function through the release of IL-10 cytokines. The main role of IL-10 is to repress the expression of proinflammatory cytokines during recovery to prevent tissue damage (Mühl 2013). Mice deficient in IL-10 and TGFβ develop a spontaneous colitis in response to commensal bacteria (Kühn *et al.* 1993; Shull *et al.* 1992), which highlights the importance of the TGFβ-Tregs-IL-10 axis in regulating commensal microorganisms and maintaining gut homeostasis (Ohkusa *et al.* 2009). However, the overexpression of IL-10, together with TGFβ, is thought to lead to chronic persistent infections with pathogens such as *Mycobacterium tuberculosis* (Ouyang *et al.* 2011).

1. 1. 2. 6 Mucus Composition

The GI mucus system is important for minimising the exposure of antigens to the immune system, but is also crucial for the protection from self-digestion (Johansson *et al.* 2011). The mucus layer is secreted by goblet cells and typically contains several major components such as mucins and their associated glycans, antimicrobial peptides and secretory peptides (Juge 2012). Mucins are the main scaffolding component of the mucus layer (Moran *et al.* 2011). They are heavily glycosylated proteins that are capable of assembling into a viscous gel-like layer on the surface of the epithelium. The glycosylation chains attached to mucins are highly hydrophilic and absorb a large volume of water, hence the gel-like appearance. The high water content (>98%) provides an additional physical barrier as the mucus acts as a diffusion barrier protecting the epithelial layer (Pelaseyed *et al.* 2014). Moreover,

due to the carbohydrates that are attached to mucins, the intestinal proteases cannot reach the peptide bonds, rendering the mucus layer and epithelial layer resistant to self-digestion (Pelaseyed *et al.* 2014).

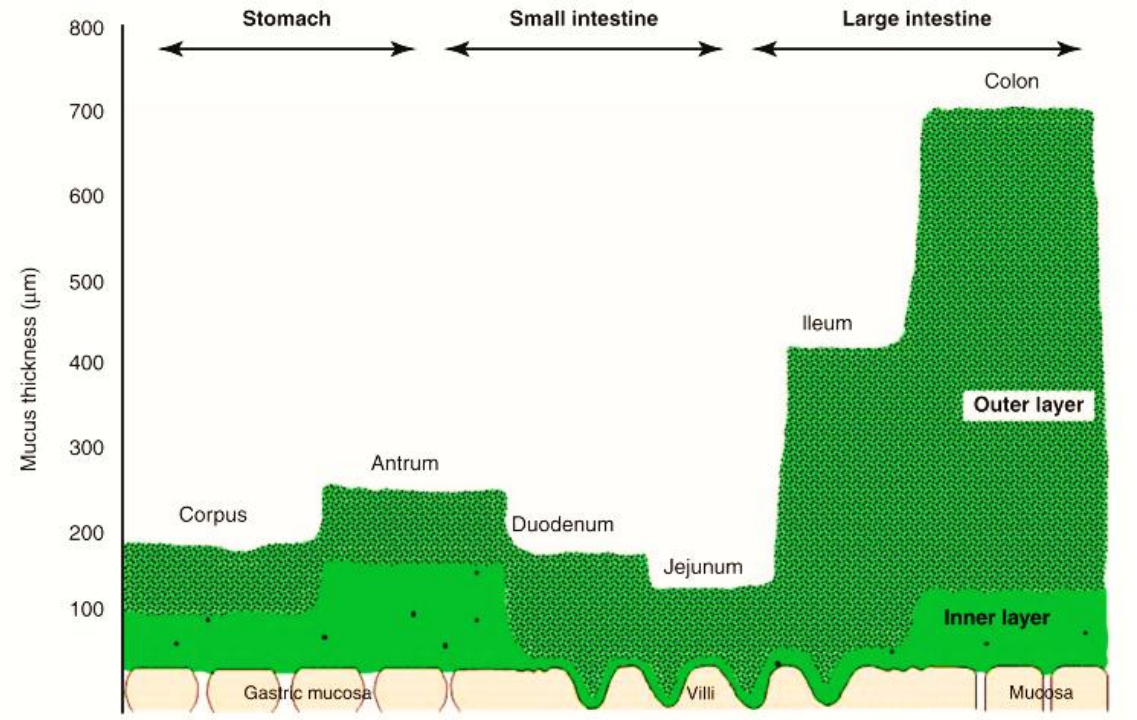

Figure 1. 2 Organisation of the mucus layers within the human GI tract. The mucus layer varies in thickness along the GI tract, but also its organisation in to layers. Sourced from Juge 2012.

The mucus layer has varying thickness along the GI tract (Figure 1. 2). It extends from 200 µm outwards from the epithelium in the stomach to up to 700 µm outwards from the epithelium in the colon (Hooper & Macpherson 2010; Juge 2012). The structure within the mucus layer allows for the spatial limitation of bacteria, both commensals and pathogens, and prevents microbes from interacting with the epithelium. In the stomach, there are two layers of mucus and the rate of mucus

production is relatively higher than other parts of the GI tract, which allows for the protection of the stomach lining from the action of acid and self-digestion. The small intestine has only one layer of mucus that is non-attached and is easily removed to facilitate the peristaltic movement of the food. The colonic mucus consists of two layers. The outer layer of colonic mucus harbours microbiota and facilitates the commensal metabolism by providing nutrients from glycosylated mucins. The inner mucus layer is firmly attached to the epithelial layer and it is considered sterile, due to the high level of antimicrobial peptides (Hooper & Macpherson 2010).

The properties of the mucus layer are largely influenced by the mucin proteins that are secreted in any given part of the GI tract. Up to 20 different mucin genes have been identified to date (Kim & Ho 2010). These genes are expressed in a tissue- and cell-specific manner and are classified into two types, secretory and membrane-associated. The mucins known to be expressed in GI tract are summarised in Table 1. 1. MUC2 is the most prevalent mucin secreted in the colon (Peterson & Artis 2014; Johansson & Hansson 2013; Bergstrom *et al.* 2010). Other mucin genes that have been shown to be expressed and secreted in colon of mice, such as MUC1 (Petersson *et al.* 2011), MUC3 (Mack *et al.* 2003), MUC4 (Hoebler *et al.* 2006), MUC5AC (Shaoul *et al.* 2004), MUC6 (Walsh *et al.* 2013), MUC13 (Sheng *et al.* 2013), MUC15 (J. Huang *et al.* 2009) and MUC20 (Moehle *et al.* 2006).

Table 1. 1 Expression of mucins throughout the GI tract. Adapted from Moran *et al.* 2011 and McGuckin *et al.* 2011.

Mucin	Distribution	Type
MUC1	Oral cavity, stomach, gallbladder, pancreas, duodenum, small intestine, colon	Cell surface-associated
MUC2	Small intestine, colon	Secreted gel-forming
MUC3	Small intestine, colon, gall bladder, duodenum	Cell surface-associated
MUC4	Oral cavity, stomach, small intestine, colon	Cell surface-associated
MUC5AC	Stomach, small intestine, colon	Secreted gel-forming
MUC5B	Salivary glands, gallbladder, stomach	Secreted gel-forming
MUC6	Stomach, gallbladder, pancreas, duodenum, colon	Secreted gel-forming
MUC7	Salivary glands	Secreted non-gel-forming
MUC12	Stomach, pancreas, small intestine, colon	Cell surface-associated
MUC13	Stomach, small intestine, colon	Cell surface-associated
MUC15	Small intestine, colon, foetal liver	Cell surface-associated
MUC16	Oral cavity, peritoneal mesothelium, stomach, small intestine, colon	Cell surface-associated
MUC17	Stomach, duodenum, small intestine, colon	Cell surface-associated
MUC19	Sublingual gland, submandibular gland	Secreted gel-forming
MUC20	Colon	Cell surface-associated

1. 1. 2. 7 Glycosylation of the GI tract

In addition to its protective role, the mucus layer that lines the GI tract is rich in glycans. The diversity of the glycan moieties serves an ideal habitat for commensals and pathogens, by providing both binding sites and energy to sustain the growth

(Hooper & Gordon 2001). In colonic mucus, the glycans are attached to the backbone of the mucin proteins.

In glycoproteins, the oligosaccharide chains are attached to either to the oxygen in the side chain of serine or threonine (termed O-linked glycosylation), or the amide nitrogen in the side chain of asparagine (termed the N-linked glycosylation), see Figure 1. 3. Mucins have large numbers of O-linked oligosaccharides, and the glycan chains account for about 80% of the total mucin mass. Furthermore, the attached glycans are highly hydrophilic, which determines the rheological and biological properties of the mucins and mucus (Juge 2012). N-linked glycosylation is relatively uncommon in GI tract mucins. O-linked glycans contain from 1 to 20 residues connected in a linear or branched manner. The glycan chain structure is not genetically determined, rather it is a product of the genes coding for the glycosylating enzymes (Freitas *et al.* 2002). O-linked glycosylation biosynthesis takes place exclusively in the Golgi complex, whereas N-linked glycosylation begins in the endoplasmic reticulum and continues in the Golgi complex (Freitas & Chantal 2000).

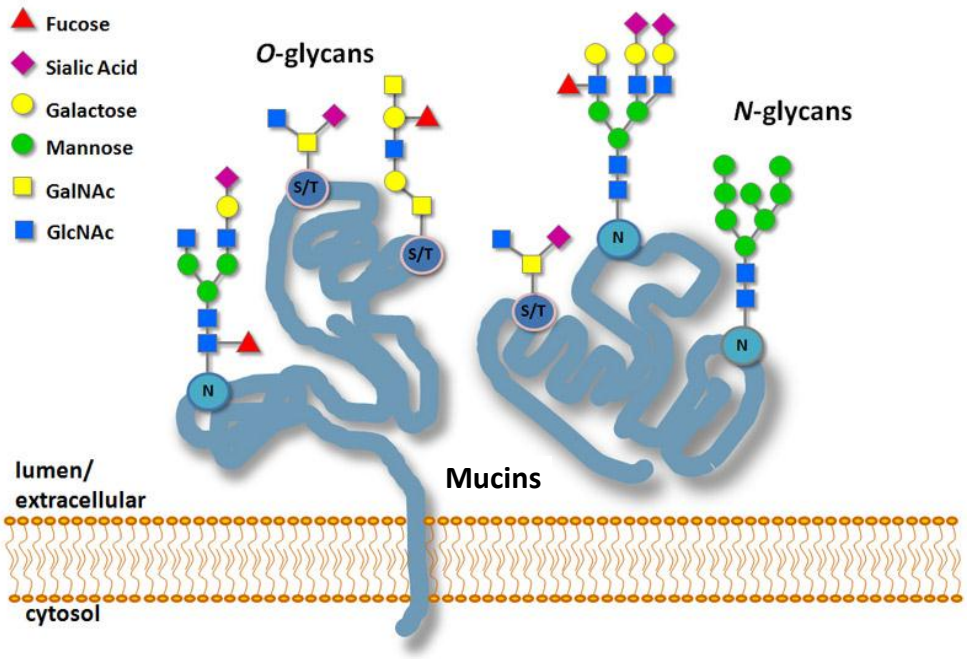

Figure 1. 3 Representation of O- and N-linked glycosylation found in GI tract. O-linked glycans are added to hydroxyl groups of mucin protein via serine (S) or threonine (T) amino acids, while N-linked glycans are attached to amide nitrogen of asparagine (N). The glycan chains can be linear or branched and are composed of one of four core structures and terminated with outlined glycans. Sourced from www.neb.com.

The O-linked glycosylation is initiated by the addition of N-Acetylgalactosamine to the hydroxyl group of a serine or threonine of the mucin protein backbone. Following this, one of eight core structures of glycan chain is added. Core 1, core 2, core 3 and core 4 structures are most prevalent in the GI tract (Figure 1. 4). Next, the chains are elongated by the addition of new glycan units and capped with terminal glycans such as fucose, galactose, N-Acetylgalactosamine or sialic acid (also known as N-Acetylneuraminic acid) (Juge 2012; Varki 2009). While core structures of glycan chains are constant, the terminal glycan sequences are determined by the environment and the commensal microbiota.

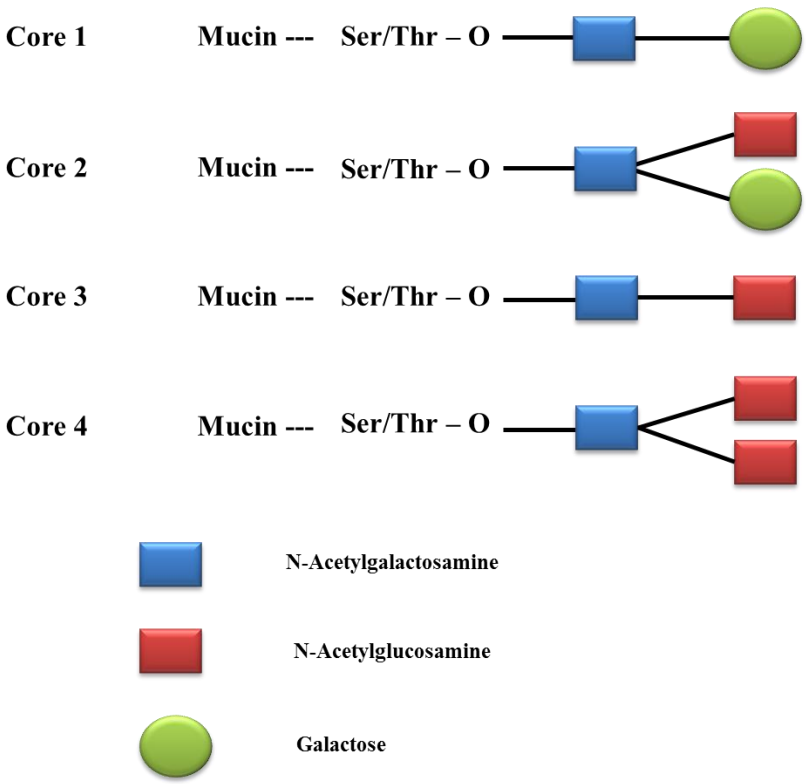

Figure 1. 4 Diagrammatic representation of the core O-glycosylation structures present on mucins in the GI tract. The core glycans are then elongated by the addition of further glycan units, such as N-Acetylgalactosamine, N-Acetylglucosamine, Galactose, fucose or sialic acid, in branched or linear manner. Adapted from Moran *et al.* 2011and Juge 2012.

The terminal glycans along the GI tract are region specific, and there is a reverse gradient of fucose and sialic acid along the GI tract. Fucose is most prevalent in the stomach, with low levels of sialic acid, while sialic acid is highly abundant in the colon where there are low levels of fucose. However, under disease conditions, this ratio becomes reversed, with high fucose and low sialic acid presented in the colon (Robbe *et al.* 2003).

Aberrant mucin glycosylation leading to shorter carbohydrate chains, or altered composition is frequently associated with many pathological conditions. Altered O-linked glycosylation of mucins has been associated with increased incidence of

Escherichia coli diseases as the altered glycosylation aids the pathogen adherence (Rhodes 2007). Also, patients with Ulcerative Colitis (UC) had altered glycosylation of MUC2 and this glycosylation profile was correlated with the severity of the intestinal inflammation (Larsson *et al.* 2011). Furthermore, altered glycosylation in UC increased risk of developing colon cancer (Saeland *et al.* 2012; Kawashima 2012; Campbell *et al.* 2001). This highlights the importance of correct mucin glycosylation in the maintenance of gut homeostasis.

There is a large body of evidence to suggest that commensal bacterial influence the glycosylation of the mucins (Freitas *et al.* 2002; Sommer *et al.* 2014; Xu *et al.* 2013). Disturbance of the microbiota, due to antibiotic use, and its subsequent effect on glycosylation and composition of the mucus remains unexplored despite its important role in homeostasis (Wlodarska *et al.* 2011; Hill *et al.* 2010).

1. 1. 2. 8 Microbiology of the GI tract

Human microbiota is essential for the postnatal maturation of mucosal and systemic immunity (Zeissig & Blumberg 2014). The inability to culture the majority of the GI microbiota compounded by the limited technology has inhibited research in this area. However, recent culture-independent approaches have advanced our understanding of the human microbiome (Tremaroli & Bäckhed 2012). These methods combine the molecular sequencing of nucleic acids with powerful bioinformatic tools capable of sorting the outcomes into taxonomic identification (Dave *et al.* 2012). A small subunit ribosomal RNA gene, 16S rRNA, has become the standard reference gene in prokaryote phylogenetic research, including the human microbiome project (Turnbaugh *et al.* 2007).

Use of these methods has led to discovery that only 9 out of 55 phyla of the Bacteria domain are detected in the human GI tract (Guarner 2015). The bacterial phyla that are present in the mammalian gut microbiota include Firmicutes, Bacteroidetes, Actinobacteria, Proteobacteria, Verrucomicrobia, Cyanobacteria, Fusobacteria, Spirochaetes and TM7 (Brown *et al.* 2013). Out of this, 90% of all taxa belong to just two phyla, Bacteroidetes and Firmicutes (Kim & Ho 2010).

Bacterial composition varies along the intestinal tract, as each species of bacteria colonises a specific niche (Brown *et al.* 2013). This is also largely influenced by the nutrient availability and pH along the tract. The number of bacteria increases in distal colon direction. The stomach harbours very few microbes, whereas more than one kilogram of microbes reside in the human colon (Figure 1. 5) (Pelaseyed *et al.* 2014). Moreover, even within the large intestine, bacterial composition varies from cecum to rectum (Guarner 2015).

Microbiota plays a number of crucial roles for the host, including assistance in digestion of certain nutrients (Sommer & Bäckhed 2013), protection from invading pathogens by colonisation resistance (Buffie & Pamer 2013), shaping the mucosal immune response (Thaiss *et al.* 2014) and mucus composition (Jakobsson *et al.* 2015).

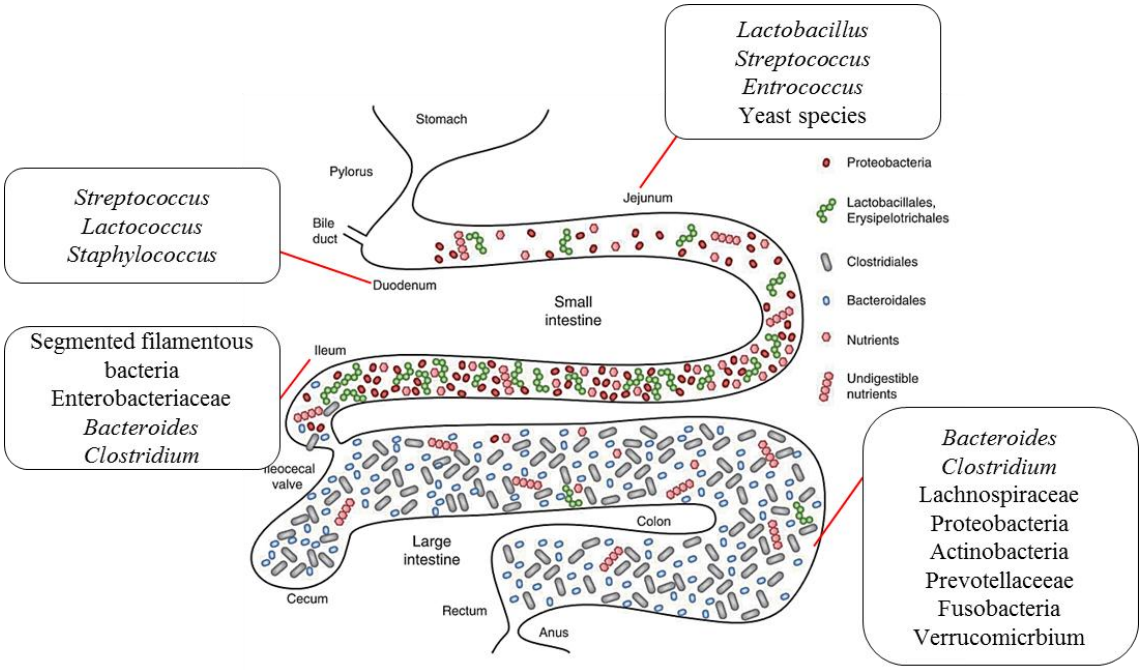

Figure 1. 5 The composition of the main bacterial phyla present in the GI tract. Most of the bacterial species found in the mammalian intestine are from the phyla Bacteroidetes or Firmicutes. Archaeal and eukaryotic microorganisms also can colonize the intestine in low abundance. Adapted from (Kamada *et al.* 2013; Brown *et al.* 2013)**.**

1. 1. 2. 9 Colonisation Resistance

Beneficial commensal bacteria can prevent pathogens from colonising the gut by directly competing with them in a process known as colonisation resistance (Sassone-Corsi & Raffatellu 2015). Commensal bacteria can contribute to colonisation resistance in both direct and indirect manners such as adhesion exclusion, competition for carbon and micronutrient sources, secretion of antimicrobials such as bacteriocins and microcins and direct delivery of toxins upon contact with competitor (Sassone-Corsi & Raffatellu 2015). In indirect colonisation

resistance, the microbiota restricts the invading pathogens by enhancing the innate and adaptive immune response of the host, as well as the mucosal barrier composition (Buffie & Pamer 2013).

The use of antibiotics is known to compromise the composition of the microbiome. Ubeda and Pamer reported that a single dose of clindamycin has the ability to diminish 90% of microbial taxa usually found in the human microbiome (Ubeda & Pamer 2013). This in turn has a several implications for the host-microbiota relationship. These include lack of competition for nutrients and space and secondary metabolites available in the GI tract, namely bile salts and short-chain fatty acids (SCFA). Sugars are important nutrients for bacteria, and the availability of sugars may influence the colonisation of various species. There is region-specific presentation of glycans along the gastrointestinal tract, which influence the species that colonise particular part of the gastrointestinal tract, especially in infancy (Robbe et al. 2003). Additionally, commensals and the pathogens compete for the nutrients, and in healthy gut, commensals outcompete pathogens for nutrients in process known as colonisation resistance (Britton & Young 2014). Fucose, one of the glycans used as a nutrient, is important for the commensals, as commensals have readily available enzymes to digest the fucose. Pathogens are disadvantaged in the presence of fucose, as they either have to switch their metabolism to express appropriate enzymes, this include *Salmonella*, or do not possess enzyme that digest fucose, this include *C. difficile* (Ng et al. 2013). Additionally, glycans such as sialic acids have been shown to facilitate the infection with opportunistic pathogen such as *C. difficile* (Ng et al. 2013).

Commensals play a role in converting primary bile salts into secondary bile salts, essential for lipid metabolism (Wlodarska *et al.* 2015). SCFA are a product of fiber

digestion by commensals and these SCFA are essential to ameliorate inflammatory conditions in the gut (Kelly et al. 2015). Therefore, the disturbance of commensals may additionally affect the host metabolism, but additionally this lack of balance may be used by opportunistic pathogens such *C. difficile.*

While the role of the microbiota in the health of the GI tract has always been appreciated, it is only recently that greater efforts have been made to utilise the microbiota to restore homeostasis. This includes the use of prebiotics that are non-digestible food ingredients that selectively promote the microbiota (Tremaroli & Bäckhed 2012). Other approaches involve the administration of probiotics, live microorganisms that confer a health benefit for the host (Kanai *et al.* 2015). Finally, the administration of faecal matter from a healthy donor to compromised patients has proven to be an effective method of restoring the colonisation resistance in compromised individuals (Rao *et al.* 2014; Pamer 2014).

1. 1. 2. 10 Opportunistic Pathogens Employ Range of Mechanisms to Evade Host's Protective Mechanisms

Despite the variety of host defence mechanisms, the enteric pathogens have evolved methods to overcome these protective barriers. In some cases, pathogens take advantage of innate host responses to enter the body (Hornef *et al.* 2002). Furthermore, some of them act as opportunistic pathogens, as they co-exist with the commensal microbiota in the gut and only invade the gut when the host defence mechanisms are compromised (Linden *et al.* 2008; Pham *et al.* 2014; Kabat *et al.* 2014). *H. pylori* attaches itself to mucins secreted in the stomach (Van De Bovenkamp *et al.* 2003), while *Campylobacter jejuni* load increases when the mucosal barrier is compromised (McAuley *et al.* 2007). *Vibrio cholera* has been

shown to produce a toxin that disrupts the epithelial integrity in the gut through the destruction of the tight junction proteins, aiding its colonisation post disruption of the barrier (Guichard *et al.* 2013).

Pathogens can also actively evade immune recognition. *Salmonella* has been shown to modulate its surface features so it cannot be recognised by the innate immune system receptors such as TLRs (Guo *et al.* 1997). *Listeria monocytogenes* is able to survive within phagocytosing cells such as macrophage and even lyse these cells to escape back into the cytosol (Dramsi & Cossart 2002). Additionally, all of the aforementioned can also modulate their own metabolisms to resist antibiotic treatment. This mechanism includes bacterial surface pumps that remove unprocessed antibiotics, hydrolysis of the antibiotic or actively changing the target site of the antibiotic (Blair *et al.* 2014).

This project is focused on another enteric pathogen, *Clostridium difficile*. We aim to elucidate the critical mechanisms that this bacterium utilises to evade the host immune system and clearance and to establish successful colonisation in the gut.

1. 2 *CLOSTRIDIUM DIFFICILE* AS AN EXAMPLE OF ENTERIC PATHOGEN

1. 2. 1 Impact

C. difficile is a well-recognised causative agent of *Clostridium difficile* infection (CDI), the leading hospital-acquired infection in Ireland, United Kingdom and the United States (Barbut *et al.* 2007; Cheknis *et al.* 2009). *C. difficile* bacterium is resistant to commonly used broad-spectrum antibiotics like clindamycin, erythromycin, and fluoroquinolones (H. Huang *et al.* 2009; Redgrave *et al.* 2014).

Increased age (>65) is a well-accepted risk factor for the development of CDI. The majority of these patients are hospitalised and severely immunocompromised (Rodriguez *et al.* 2014; Shields *et al.* 2015). Recently, there has been increased prevalence of CDI in younger populations with no prior contact with hospital or antibiotic therapy, which is known as community-acquired infection (Lessa 2013).

The clinical outcome for patients with CDI are diverse, ranging from asymptomatic colonisation to mild diarrhoea, to more severe cases of pseudomembranous colitis and toxic megacolon and even death (Karadsheh & Sule 2013). Another feature of CDI is the high relapse rate (up to 60% of patients) due to reinfection or reactivation of infection (Kim *et al.* 2014). Infection routinely requires isolation of affected patients, additional antibiotic therapy, and a prolonged hospital stay, which has implications for both patient turnover and health economics (Ghantoji *et al.* 2010; Hill 2014; Teena Chopra *et al.* 2015).

1. 2. 2 *Clostridium difficile* Bacterium

C. difficile is a Gram-positive, obligate spore-forming anaerobe rod-shaped bacterium (Stanley *et al.* 2013). It was initially described as a part of the microbiota of healthy neonates and named *Bacillus difficilis* due to difficulty in isolation and culture of the bacterium in the laboratory (Hall & O'Toole 1935). *C. difficile* was identified as a pathogen relatively recently. The first confirmed case of CDI was reported in 1977, when the introduction of clindamycin as the primary antibiotic of choice led to a rapid increase in the number of pseudomembranous colitis cases (Larson *et al.* 1978). In 1978, *C. difficile* was recognised as a causative agent of CDI by fulfilling the criteria of Koch postulates (George *et al.* 1978). Bartlett *et al.*

confirmed that the main pathogenicity of *C. difficile* was attributed to toxin production (Bartlett *et al.* 1978).

1. 2. 3 Infection Route

The infection route of *C. difficile* is complex and largely dependent on the immunocompromised state of the host (Figure 1. 6). *C. difficile* spores are ingested via the oral route, survive the acidic environment of the stomach and germinate into vegetative forms when they reach the anaerobic conditions of the colon (Paredes-Sabja *et al.* 2014). *C. difficile* can only colonise the gut if the normal intestinal microbiota is disturbed or absent as happens following antibiotic therapy (Britton & Young 2012). As a result, the antibiotic-resistant *C. difficile* is not eliminated by the prescribed antibiotic treatment, and due to lack of competition, it proliferates to reach high densities in the intestinal lumen (Buffie & Pamer 2013). The lack of colonisation resistance from commensals has various implications, including the obvious lack of competition for energy sources, but also disturbed bile salt metabolism contributes to spore germination (Figure 1. 7) (Sorg 2014). Upon proliferation, *C. difficile* penetrates through the intestinal mucus and adheres to the epithelium. This process is recognised as colonisation and is known to be a critical step of infection (Denève *et al.* 2009). Successful adherence allows *C. difficile* to thrive and produce toxins, which induce epithelial damage and acute inflammation (Genth *et al.* 2008).

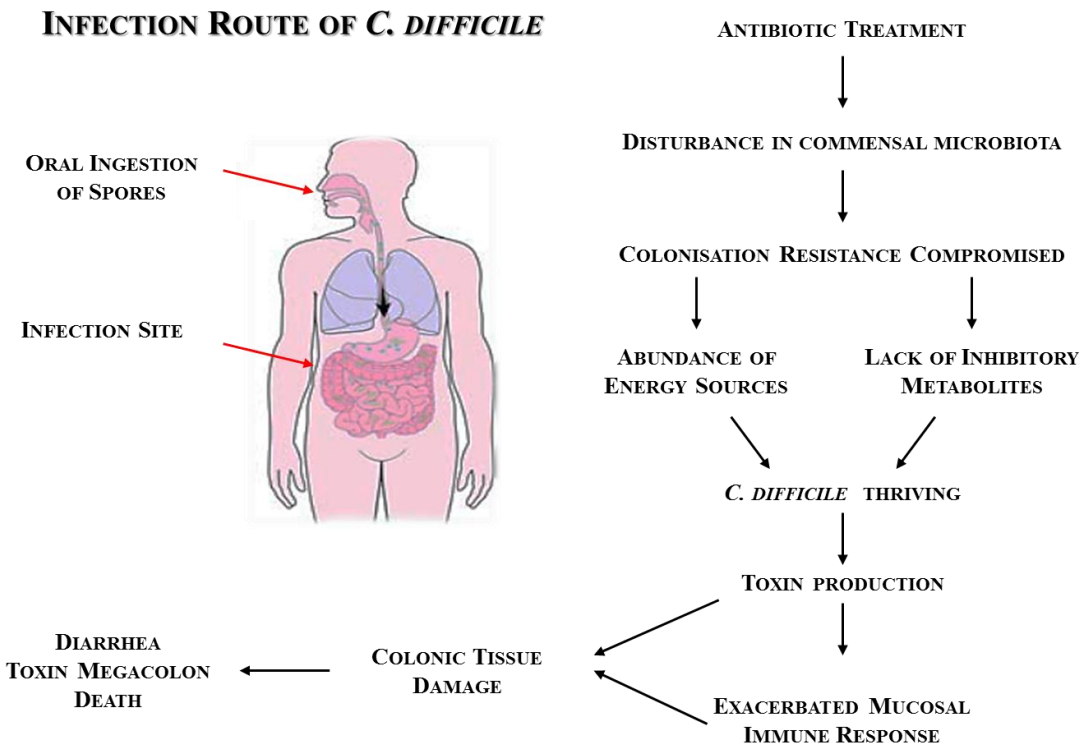

Figure 1. 6 Current understanding of *C. difficile* infection route. *C. difficile* takes advantage of the immunocompromised state of the host and lack of colonisation resistance from commensal microbiota. The pathogen proliferates then due to the abundance of nutrients and lack of inhibiting metabolites. This allows for toxin productions, that damages the epithelial layer. The influx of immune cells to the site of infection exacerbates the inflammation rather than clearing the pathogens. The resultant systemic organ failure can lead to death. Adapted from literature described in Section 1. 2. 3.

1. 2. 4 Virulence Factors Contributing to CDI Pathogenicity

1. 2. 4. 1 Toxins

Biochemical and molecular studies have shown that the main clinical symptoms and signs of CDI, such as diarrhoea and inflammation of the colonic mucosa are largely explained by the actions of the TcdA and TcdB toxins produced by *C. difficile* (Rolfe & Finegold 1979). *C. difficile* produces three toxins, toxin A and toxin B, and binary toxin CDT (Rupnik 2005). All three toxins disrupt host actin filamentation via

different enzymatic activities. Toxin A and B achieve this by glucosylating and inactivating the Rho-GTPases, regulatory proteins of actin (Kuehne *et al.* 2010). Binary toxin CDT binds to intestinal cells and sabotages host actin polymerisation (Schwan *et al.* 2009). Overall, the toxins lead to depolymerisation of the actin filaments with loss of internal architecture of the cells, microtubule disorganisation and disruption of the tight-junctions that hold cells together. This results in accelerated breakdown of the epithelial membrane. Destruction of villus and brush border membranes is followed by mucosal loss, fluid accumulation and a pronounced inflammatory response, which results in increased bacterial adherence (Schwan *et al.* 2014).

The majority of the hypervirulent *C. difficile* strains co-produce both the TcdA and TcdB (toxinotype A^+B^+), whereas only a minority of *C. difficile* produces TcdB only (toxinotype A^-B^+) (Genth *et al.* 2008). As mentioned previously, toxins are described as the main virulence factors associated with CDI. In fact, delivery of the TcdA and TcdB toxins alone reproduced clinical symptoms of CDI in hamsters (Mullany & Roberts 2010). However, vaccines against toxins did not confer protection against CDI (Mullany & Roberts 2010). Furthermore, toxins are not produced until the late log and stationary phase of infection, when the population of *C. difficile* is well-established (Hundsberger *et al.* 1997). This evidence suggests that other features of *C. difficile* may contribute towards its virulence.

1. 2. 4. 2 Surface Layer Proteins

The Surface layer (S-layer) of *C. difficile* is formed by the self-assembly of monomeric proteins into a regularly spaced, two-dimensional array (Fagan & Fairweather 2014). The S-layer of *C. difficile* is assembled from one protein, Surface

Layer Protein (SLP). SLPs are the most abundant proteins on the surface of *C. difficile* and are encoded by the s*lpA* gene (Fagan *et al.* 2009). *SlpA* is translated into a single precursor protein, which is cleaved by Cwp84 protease into two subunits, High Molecular Weight (HMW) and Low Molecular Weight (LMW) (Bradshaw *et al.* 2014). The two subunits of SLP assemble on the surface of the bacterium into the paracrystalline lattice known as the S-layer (Fagan *et al.* 2009). The SLP gene cluster encodes a variety of other proteins such as Cwp66, Cwp84, which aid the processing of the precursor SLP protein. It is separated from the Pathogenicity Locus (PaLoc) region, which includes genes encoding toxins (Denève *et al.* 2009).

The S-layer provides cell shape, cell adhesion and a protective coat (Schäffer *et al.* 2001). S-layer proteins have been described in other bacteria as virulence factors such as *Aermonas salmonicida* and *Campylobacter fetus* (Thompson 2002; Noonan 1997). SLPs of *C. difficile* have been shown to be essential for the adhesion to the epithelium (Calabi *et al.* 2002; Merrigan *et al.* 2013; Spigaglia *et al.* 2013). Furthermore, SLPs from *C. difficile* have been demonstrated to be potent immune stimulators of immune cells (Ausiello *et al.* 2006). In our previous studies we have demonstrated that SLPs are recognised by the immune system specifically via TLR4 (Ryan *et al.* 2011) and they activated clearance mechanisms in macrophages, specifically, the phagocytosis by macrophages (Collins *et al.* 2014). Also, the immune response to SLPs is dependent on the ribotypes of the *C. difficile* (Bianco *et al.* 2011; Vohra & Poxton 2012). This suggests that SLPs may contribute to disease severity, however, this correlation has not yet been reported in the literature. Therefore, the exact role of SLPs in CDI is yet to be determined.

1. 2. 4. 3 Other Surface Features and Their Implication for Adhesion

Adherence is a pivotal step during the colonisation process. Several surface-associated proteins of *C. difficile* have been investigated for their possible role in adhesion and virulence. Flagella of *C. difficile* have been extensively researched for their role in adhesion and colonisation (Tasteyre *et al.* 2001). In general, the primary function of the flagella is to enable the motility of the bacterium. It also facilitates in the adherence to host cells, force-driven motility to nutrients and acts as an immunomodulator by triggering a proinflammatory reaction via TLR5 (Stevenson *et al.* 2015). Enteric pathogens such as *C. jejuni*, *V. cholera* and *H. pylori* employ flagella to facilitate their motility through the host GI tract. Contribution of flagella to the pathogenesis of *C. difficile* is complex, and it is not yet fully understood. While flagella genes are upregulated extremely early during *in vivo* infection with *C. difficile* (Janoir *et al.* 2013), it has been shown that flagella may not be essential for survival and colonisation (Janoir *et al.* 2013; Baban *et al.* 2013). However, it is thought the flagella may modulate the expression of TcdA and TcdB (Aubry *et al.* 2012) and sporulation (Pettit *et al.* 2014) and for this reason its role in *C. difficile* pathogenicity cannot be overlooked.

Several cell wall proteins of *C. difficile*, including Cwp84 and Cwp66, have also been investigated for their role in adherence (Fagan *et al.* 2011). Cwp84 is cysteine protease that is essential for processing of the immature SLPs and assembling them into the S-layer (Bradshaw *et al.* 2014). Cwp84 is also known to play a role in degrading the extracellular matrix of the host tissue, possibly aiding the docking of the bacterium on the epithelial surface (Janoir *et al.* 2007). Antibodies raised against Cwp66 were able to partially inhibit the adherence of *C. difficile* to cultured cells (Waligora *et al.* 2001). The gene cluster encoding for Cwp66 and Cwp84 was shown

to be under high evolutionary pressure, suggesting its role in evolution of the pathogen and immune evasion (Dingle *et al.* 2013). Pechine *et al.* determined that in patients sera, antibodies against Cwp66 and Cwp84 could be found until up to two weeks after the initial CDI diagnosis, suggesting their strong antigenic properties (Péchiné, Janoir, *et al.* 2005; Péchiné, Gleizes, *et al.* 2005).

GroEL is a classical heat-shock protein, secreted by *C. difficile* upon heat challenge but also under other stresses including high osmolarity, low pH, nutrient starvation or the presence of subinhibitory concentrations of antibiotics (Mizrahi *et al.* 2014; Jain *et al.* 2011; Hennequin, Collignon, *et al.* 2001). The involvement of GroEL in *C. difficile* adhesion is controversial as it is a membrane-associated rather than a cell wall protein. However, Hennequin *et al.* demonstrated that antisera against GroEL was able to partially inhibit the *C. difficile* attachment to cells in culture (Hennequin, Porcheray, *et al.* 2001). Also, Pechine *et al.* showed that immunisation against GroEL may decrease the rate of *C. difficile* colonisation in the colon (Péchiné *et al.* 2013). Fibronectin-binding protein (Fbp) is an adhesin that recognises the extracellular matrix fibronectin on the surface of the host tissues (Hennequin *et al.* 2003). Hennequin *et al.* demonstrated that antibodies raised against this protein inhibited the adhesion of *C. difficile* to immobilised fibronectin (Hennequin *et al.* 2003). Deletion of Fbp in *C. difficile* affected its adhesion to cultured intestinal epithelial cells, via unknown mechanisms (Barketi-Klai *et al.* 2011). The addition of fibronectin to the cell culture increased the adherence rate of *C. difficile* (Schwan *et al.* 2014). Moreover, the same authors were able to determine that infection with *C. difficile* induced changes in secretion of fibronectin, to form clusters on the surface of the epithelial layer, presumably to aid the adhesion (Schwan *et al.* 2014). Deneve *et al.* demonstrated that exposure of *C. difficile* to various antibiotics upregulated the

expression of genes suspected to be involved in the adherence such as Cwp66, Cwp84 and Fbp (Denève *et al.* 2008).

1. 2. 4. 4 Spores

Like other clostridia, *C. difficile* produces spores that are metabolically inert (Stanley *et al.* 2013). *C. difficile* spores are able to withstand harsh environmental conditions such as desiccation, chemicals and extreme temperatures (Rupnik *et al.* 2009). *C. difficile* is a strict anaerobe and therefore dormant spores play a key role in transmission of the pathogen (Paredes-Sabja *et al.* 2014). Spores frequently contaminate the environment around patients with CDI, with the potential to persist for months and even years (Burns & Minton 2011). Furthermore, *C. difficile* spores were recently shown to survive the temperatures and disinfectant treatments of typical hospital laundering cycles and to cross-contaminate bed linens during a wash cycle (Hellickson & Owens 2007). *C. difficile* strains have various sporulation capabilities, which adds this feature as another virulence factor (Burns & Minton 2011). Enhanced germination of spores was connected with increased colonisation of the gut during infection with epidemic RT 027, which sporulates more readily than non-epidemic ribotypes (Akerlund *et al.* 2008). Furthermore, Carlson *et al.* recently determined that the germination of spores of various strains correlates with disease severity (Carlson *et al.* 2015). Germination of spores into vegetative cells in the GI tract occurs under the influence of primary bile salts and it is tied to commensal bacteria metabolism. Specifically, the action of commensal bacterial completes conversion of host-derived primary bile salts to secondary bile salts, which are essential for the lipid metabolism, see Figure 1. 7 (Sorg 2014). Spores of *C. difficile* germinate in presence of primary bile salts, however under normal conditions,

secondary bile salts inhibit the vegetative cells of *C. difficile* (Theriot & Young 2014). When intestinal microbiota is disturbed, for example due to antibiotic treatment, the bile salts metabolism is compromised. In that instance, there is accumulation of primary bile salts, which result in excessive germination of *C. difficile* spores. Simultaneously, due to lack of inhibitory effect of secondary bile salts, the vegetative cells are actively proliferating in order to establish infection (Taur & Pamer 2014; Seekatz & Young 2014).

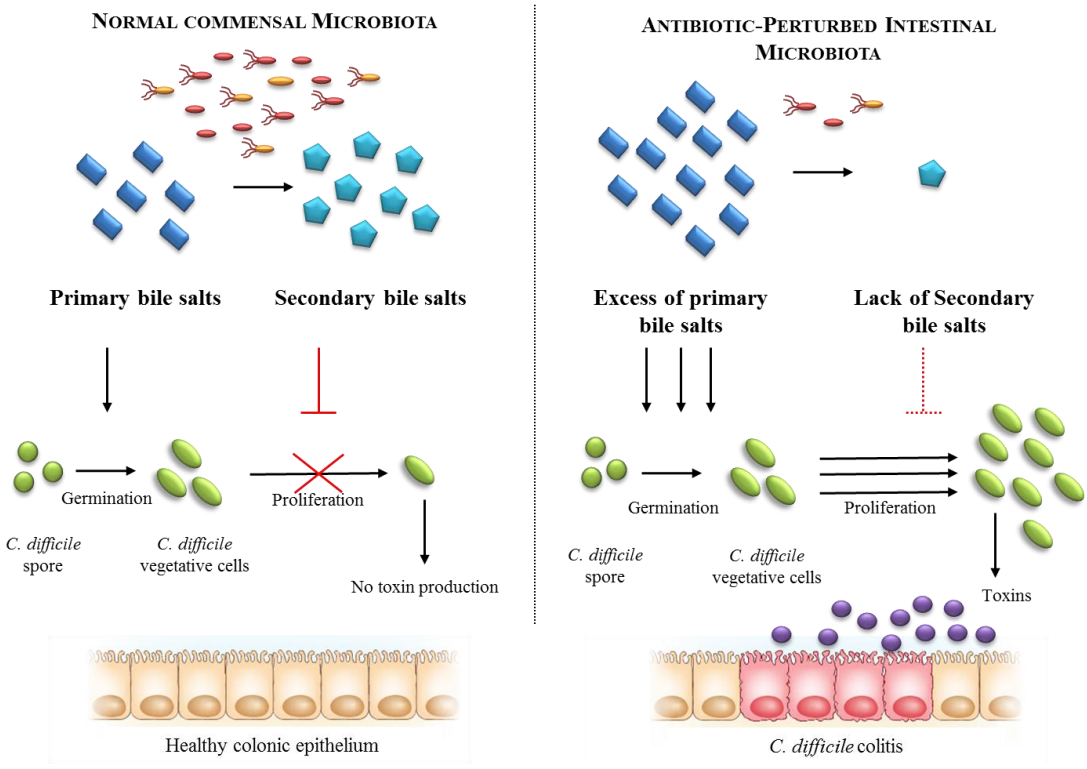

Figure 1. 7 The role of commensal microbiota in bile salt metabolism. Commensal microbiota metabolises primary bile salts into secondary bile salts. While the primary bile salts facilitate *C. difficile* spore germination, secondary bile salts actively inhibit the vegetative cells of *C. difficile*. When microbiota is disturbed, there is an excess of primary bile salts (facilitating the germination of spores) and lack of secondary bile salts to abolish the vegetative cells. This results in *C. difficile* colonisation and toxin production that damages the epithelial barrier. Adapted from Taur & Pamer (2014) and Seekatz & Young (2014).

1. 2. 5 Mucosal Immune Response to *C. difficile*

The mucosal immune response to *C. difficile* is quite complex, given that the host is already immunocompromised (Figure 1. 8). The early stages of infection are characterised by acute intestinal inflammation mediated by the innate immune response. This defence is mediated by antimicrobial peptides such as defensins, which dampen the toxins effect on the epithelium (Solomon 2013). Furthermore, the epithelial layer recognises the pathogen via TLRs, specifically, SLPs are recognised via TLR4 (Ryan *et al.* 2011) and TLR5 detects flagella (Jarchum *et al.* 2012). Proinflammatory signalling results in recruitment of innate immune cells, such as neutrophils via secretion chemokines such as of IL-8 and MIP-2 (Hasegawa *et al.* 2011). Despite the involvement of these innate immune mechanisms, *C. difficile* toxins act rapidly to disrupt the epithelial layer. This results in the loss of tight junction proteins and collapse of the intestinal epithelial barrier (Solomon 2013). Once this barrier is breached, toxins come in contact with submucosal macrophages and dendritic cells. This triggers an aggravated cascade of proinflammatory cytokines such as IL-1β, IL-6, IL-8 and TNFα via NF-κB signalling (Madan & Petri Jr 2012). Furthermore, toxin A has been shown to block the secretion of mucins from goblets cells (Branka *et al.* 1997), resulting in a thinner mucus layer, which allows *C. difficile* and its toxins even closer to the intestinal epithelial barrier (Engevik *et al.* 2014).

The recruitment of neutrophils to the site of infection is a central part of *C. difficile* infection (Madan & Petri Jr 2012). While neutrophils are essential for the innate immune response and clearance of the pathogens via phagocytosis (Fournier & Parkos 2012), when the epithelial barrier is compromised, the influx of these cells results in exacerbated acute inflammation and further damage to the epithelium (Sun

& Hirota 2015). In our previous study we have shown that mice infected with *C. difficile* had increased the neutrophil infiltration into the colonic tissue, and this correlated with collapsed epithelial structure and acute inflammation (Lynch 2014, unpublished). The extensive acute inflammatory response appears to be a major factor contributing to injury in CDI, subsequently leading to organ failure and even death (Kelly & Kyne 2011).

Among the cascade of secreted cytokines are those essential for inducing an adaptive immune response. In our previous research we have demonstrated that the type of adaptive response to *C. difficile* is largely influenced by the ribotype of *C. difficile* (Lynch 2014, unpublished). We determined that the persistence of infection with *C. difficile* RT 027 and lack of clearance mechanisms in mice were due to elevated levels of anti-inflammatory IL-10 which provides the environment for Treg development suggesting an immune evasion mechanism employed by the pathogen. Conversely, infection with *C. difficile* RT 001 resulted in activation of IL-17 cytokine and promoting a Th17 environment. Th17 cells secrete IL-22 which is known to play role in epithelial layer recovery (Sadighi Akha *et al.* 2015). However, the exact role of Th17 cells and IL-22 in the clearance of *C. difficile* and restoration of the epithelial barrier remains unclear and warrants further investigation.

Induction of adaptive immune response results in maturation of B cells and production of antibodies that aid the clearance of the pathogen. Antibodies detected in CDI patients' sera include IgG, IgA and IgM, specific for toxins, SLPs, flagella and cell wall proteins. This indicates the complexity of the adaptive response against *C. difficile* (Drudy *et al.* 2004; Kelly & Kyne 2011).

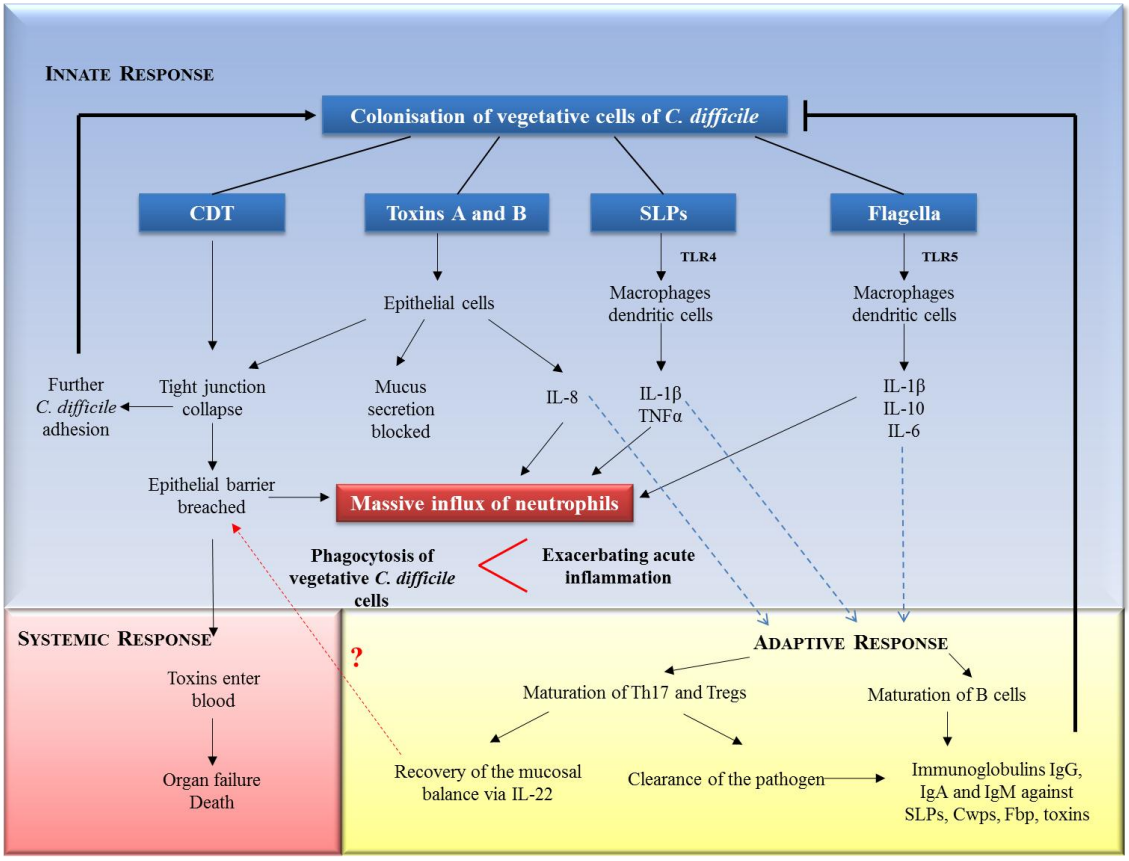

Figure 1. 8 The interactions between *C. difficile* and the immune system. Vegetative cells of *C. difficile* induce a cascade of reactions upon recognition via innate immune response. While the pathogen produces the toxins that damage the tight junction proteins and the epithelium, the innate immune response recruits the neutrophils to the site of infection, while trying to mount the specific adaptive immune reaction. Neutrophils become detrimental to the epithelial damage, as the massive influx exacerbates the acute inflammation rather than phagocyting the pathogen. Infection resolution relies on how prompt the adaptive immune response, ie. the production of antibodies specific for the bacterial antigens. Furthermore, the exact role of IL-22 in recovery of the epithelial cells during infection is yet to be determined. Adapted from Sun & Hirota 2015 and the literature described in section 1. 2. 5.

1. 2. 6 Ribotyping

C. difficile has been identified as a pathogen relatively recently. The epidemiology of CDI has been very dynamic, with the emergence of new virulent strains and an

increase in the incidence of community-acquired CDI. Since the disease outcome is directly related to the strain of the *C. difficile* involved, there was a need for standardising the typing schemes and referencing, as several approaches to categorising *C. difficile* were in development (Manzo *et al.* 2014). This was to aid in tracking new outbreaks, the epidemiology of the pathogen and also to facilitate communication between research communities.

Initial work focused on typing phenotypic features like toxin production (Wüst *et al.* 1982) or isolation of plasmids (Clabots *et al.* 1988), and these approaches were based on clinical isolates which were cultured into pure colonies (Tortora *et al.* 2010). This method allowed for the identification of "type strains" and is a classic method of classifying bacteria. Genotyping gradually replaced the phenotypic procedures mentioned previously. Advances in molecular methods allowed for the classification of organisms based on having the same sequences in their housekeeping genes. Methods like pulse-field electrophoresis, restriction endonuclease analysis, and toxinotyping have since been used and have provided a greater insight into the classification of *C. difficile* (Mullany & Roberts 2010).

PCR-ribotyping exploits the differences in the spacer regions between 16S and 23S of the ribosomal RNA. Both the number of operons and length of the spacer regions are different between the strains and these criteria are used for discrimination between the strains (Weisburg *et al.* 1991). In this case, the pattern generated by the DNA is visualised by gel electrophoresis and is referred to as ribotype (Brazier 2001). PCR-ribotyping was first used to classify *C. difficile* in 1993 (Gurler 1993) and it is now the most widely accepted method with more than 100 distinguishable groups of *C. difficile* isolates identified to date (Martinson *et al.* 2015; Behroozian *et al.* 2013). In this project, *C. difficile* strains are referred to as ribotypes.

1. 2. 7 Current Therapies

Treatment of CDI is far from straightforward, due to the fact that broad-spectrum antibiotics exacerbate the disease (Dawson *et al.* 2009). During the past few years, more severe and more resistant strains of *C. difficile* have emerged, which are able to overcome the standard treatment approach (H. Huang *et al.* 2009). Traditional therapies such as metronidazole and vancomycin (Vardakas *et al.* 2012) or corticosteroids (Wojciechowski *et al.* 2014) are still able to dampen the CDI symptoms. However, overuse of antibiotics such as fluoroquinolones has led to the emergence of resistance among the most prevalent strains of *C. difficile* (Redgrave *et al.* 2014). Thus, this has prompted the search for alternative treatment approaches. The Food and Drug Administration (FDA) has fast-tracked novel combination antibiotic treatments such as ramoplanin and actagardine (Mathur *et al.* 2013). Another new narrow-spectrum antibiotic with antimicrobial activity specific against *C. difficile*, but not the commensal microbiota, thuricin CD was recently reported (Rea *et al.* 2010). Furthermore, Ling *et al.* have reported the development of the antibiotic teixobactin, which was shown to be exceptionally active against *C. difficile* without any sign of antibiotic resistance emerging in the pathogen (Ling *et al.* 2015).

While antibiotics promptly ameliorate the disease symptoms, most common and hypervirulent *C. difficile* strains demonstrate very high rates of antibiotic resistance (H. Huang *et al.* 2009) and therefore there is a need to develop alternative treatment therapies. Previously there were several attempts to develop vaccines, including vaccines against whole, or fragments, of toxin A and B (Foglia *et al.* 2012; Karczewski *et al.* 2014; Senoh *et al.* 2015), SLPs (O'Brien *et al.* 2005), fibronectin-binding protein (Brun *et al.* 2008) and GroEL heat shock protein (Péchiné *et al.* 2013). Tam Dang *et al.* reported the development of protease inhibitors that targeted

the assembly of the S-layer in *C. difficile* (Tam Dang *et al.* 2012). Another study proposed a treatment that utilises membrane perforation with the use of nisin and lysozyme (Chai *et al.* 2015). However the efficiency of these treatments is still under question.

To date the most effective approach implemented in treating *C. difficile* has been Faecal Microbiota Transplant (FMT), with over 90% of patients with reoccurring CDI being successfully cured (Khoruts & Weingarden 2014). It consists of the transfer of a homogenised faecal suspension from a healthy donor to the GI tract of a diseased recipient (Di Bella *et al.* 2015). While it was known that this therapy is successful, its mechanism of action was poorly understood for many years (Aas *et al.* 2003; Koenigsknecht & Young 2013). Recently it was reported that the delivery of healthy microbiome via FMT allows for the metabolism of the primary bile salts into secondary bile salts (Seekatz *et al.* 2014; Weingarden *et al.* 2014). In an immunocompromised state, the lack of commensal metabolism results in accumulation of primary bile salts and lack of secondary acids. This in turn has a great impact on *C. difficile* germination, as the primary bile salts facilitate the germination of spores, while lack of secondary bile salts allows for the proliferation of vegetative cells. Also, lack of commensal metabolism limits the digestion of fiber into short-chain fatty acids (SCFA), which are known for their inhibitory properties on vegetative cells of *C. difficile* (Britton & Young 2012). FMT restores the microbiota balance but also the commensal metabolism essential for the colonisation resistance.

1. 3 REASONING BEHIND THE STUDY AND AIMS

The GI tract is a very tightly regulated system with all its components finely tuned to keep pathogens at bay. *C. difficile* is an opportunistic pathogen that exploits the situation when the host is immunocompromised. Recent research has shed more light on the factors contributing to infection, such as the role of microbiota. However, not many studies have explored the role of differences in SLP structure between different ribotypes as a potential virulence factor. The differences in SLPs could play a significant role in the adherence, recognition by the immune system and clearance mechanisms mounted in response to various ribotypes.

Our hypothesis states that the SLPs of different ribotypes differentially interact with host mucosal epithelial barrier, and hence mount different responses. Post-translational modifications, such as glycosylation, could contribute to SLPs being differentially recognised by the immune system. Furthermore, the susceptibility state may modify host's responses to the pathogen and its initial recognition and induction of clearance pathway; however this area is largely unexplored in the pathogenicity of *C. difficile*. Finally, the glycans available on the surface of the epithelium are used by the pathogen for growth and we wanted to examine whether the glycans available in susceptibility state and during the infection with *C. difficile* promotes the pathogen growth.

To address the above research questions, the aims of this thesis were:

- ✓ To optimise the methods to grow a range of *C. difficile* and purify the SLPs from these ribotypes and compare the *ex vivo* response of colonic tissue to SLPs

- ✓ To examine glycosylation patterns of SLPs from these ribotypes, as glycosylation was proposed to potentially contribute to adherence and colonisation

- ✓ To examine factors that could contribute to the susceptibility state *in vivo* in a murine model, namely glycosylation profile of the colonic epithelium, immune response and mucosal integrity state

- ✓ To examine the glycosylation profile of the colon during *C. difficile* infection *in vivo* and clearance mechanism of the pathogen

CHAPTER 2 MATERIALS AND METHODS

2.1 MATERIALS

Table 2. 1 Microbial Cell Culture

Anoxomat Anaerobic Jar	Mart Microbiology
Brucella Agar with 5% Horse Blood	BD
Anaerobic Gas Generating Kit	Thermo Fisher Scientific
Anaerobe Indicator Test	Sigma-Aldrich
Dulbecco's Modified Eagle's Medium	Sigma-Aldrich
Glycerol	Sigma-Aldrich
Cryovials	Lennox
Mr. Frosty Freezing Container	Thermo Fisher Scientific
Fastidious Anaerobic Broth	Oxoid
Brain Heart Infusion Broth	Oxoid
Hemin	Sigma-Aldrich
Vitamin K	Sigma-Aldrich
Sodium Thioglycolate	Sigma-Aldrich
10 µl Inoculation Loops	Cruinn
Presept Tablets	VWR

Table 2. 2 S-layer Isolation and SLPs Purification	
50 ml Unskirted Centrifuge Tubes	Sarstedt
2 ml Screw Cap Centrifuge Tubes	Sarstedt
Trizma Base	Sigma-Aldrich
NaCl	Sigma-Aldrich
Urea	Sigma-Aldrich
cOmplete™ Protease Inhibitor Cocktail	Roche
Slide-A-Lyzer™ Dialysis Cassettes 10 K Molecular Weight Cut Off	Pierce
$ÄKTA_{FPLC}$	GE Healthcare
MonoQ HR 10/10 Chromatography Column	GE Healthcare
10 ml Injection Loop	GE Healthcare

Table 2. 3 SDS PAGE	
30% Bis-acrylamide	Sigma-Aldrich
Sodium Dodecyl Sulfate (SDS)	Sigma-Aldrich
Ammonium Persulfate (APS)	Sigma-Aldrich
N, N, N', N'-tetramethylethylenediamine (TEMED)	Sigma-Aldrich
PageRuler™ Plus Prestained Protein Ladder	Fermentas
Methanol	Lennox
Acetic Acid	Sigma-Aldrich
Glycine	Sigma-Aldrich
Brilliant Blue	Sigma-Aldrich

Table 2. 4 SLP Characterisation	
Pierce™ BCA Protein Assay Kit	Thermo Fisher Scientific
Amicon® Ultra-4 Centrifugal Filter 10 K Molecular Weight Cut Off Devices	Merck Millipore
ToxinSensor™ Chromogenic LAL Endotoxin Assay Kit	GeneScript
VERSA Amax Microplate Reader	Molecular Devices, CA, USA

Table 2. 5 SLP Glycosylation	
The Pierce™ Gycoprotein Staining Kit	Thermo Fisher Scientific
Asialofetuin	Sigma-Aldrich
Fetuin (Bovine)	Sigma-Aldrich
Glucose Oxidase	Sigma-Aldrich
Invertase (from *Saccharomyces cervisiae*)	Sigma-Aldrich
Thyroglobulin (Porcine)	Sigma-Aldrich
Transferrin	Sigma-Aldrich
PBS	Biosciences
Nunc 96-well Plate	Sarstedt
Carbo-Free™ Blocking Solution	Vector Laboratories
Biotinylated Lectins*	Vector Laboratories
$CaCl_2$	Sigma-Aldrich
$MgCl_2$	Sigma-Aldrich
$MnCl_2$	Sigma-Aldrich
Trizma Base	Sigma-Aldrich
Tween® 20	Sigma-Aldrich
Streptavidin-conjugated Horseradish Peroxidase	Sigma-Aldrich
3,3',5,5'-Tetramethylbenzidine (TMB)	BD
10% H_2SO_4	Sigma-Aldrich
iBlot System	Biosciences
iBlot Nitrocellulose Blots	Biosciences
Bovine Serum Albumin	Sigma-Aldrich
Luminata Chemiluminescence Substrate	Merck Millipore
G-Box Fluorescence Gel Analysis System	Syngene

*Complete list of biotinylated lectins and their corresponding specificities are summarised in Table 2. 15.

Table 2. 6 Animal Model	
C57BL/6J Female Mice (aged 9-15 weeks)	Charles River
Metronidazole	Sigma-Aldrich
Gentamicin	Sigma-Aldrich
Colistin	Sigma-Aldrich
Kanamycin	Sigma-Aldrich

Vancomycin	Sigma-Aldrich
Clindamycin	Sigma-Aldrich
1 ml Syringe	BD
27 G Needle	BD
PBS	Biosciences
Penicillin-Streptomycin (10,000 U/mL)	Gibco
RPMI	Invitrogen
LPS from *E. coli*	Enzo Lifesciences
6- and 24-well Tissue Culture Plates	Nunc

Table 2. 7 RNA Isolation and cDNA Synthesis Reagents

NucleoSpin® RNA II Total Isolation Kit	Macherey-Nagel
DEPC-treated dH_2O	Invitrogen
High Capacity cDNA Reverse Transcription Kit	Applied Biosystems
Molecular Grade Ethanol	Sigma-Aldrich
β-Mercaptanol	Sigma-Aldrich
RNaseZap®	Sigma-Aldrich
MJ Research PTC-200 Thermal Cycler	GMI

Table 2. 8 RNA and DNA Integrity by Gel Electrophoresis

Agarose	Thermo Fisher Scientific
TAE	Sigma-Aldrich
RNA Sample Loading Buffer, without ethidium bromide	Sigma-Aldrich
Gene Ruler 100 bp Plus DNA ladder	Thermo Fisher Scientific
SYBR® Safe DNA Gel Stain	Invitrogen
6X DNA Loading Dye	Fermentas

Table 2. 9 RT qPCR Reagents	
FastStart Essential DNA Green Master	Roche
FastStart Essential dH_2O	Roche
Lightcycler® 96-well Plates	Roche
Optical Adhesive Film	Roche
LightCycler® 96	Roche
PrimeTime qPCR Primers	IDT

Table 2. 10 PrimeTime qPCR Primers (mixture of forward and reverse). All primers sourced from IDT. Complete sequences, corresponding protein products and exon locations are summarised in Table A2 (Appendix C).

Mucins	*Muc1, Muc2, Muc3, Muc4, Muc5ac, Muc6 Muc13, Muc15 and Muc20*
Inflammatory Cytokines	*Il1β, Il2, Il6, Il10, Il17a, Il22b, Ifng, Tnfa, Tgfb and Stat3*
IL-12 Family cytokines	*Il12a and Il23*
Chemokines	*Ccl2, Ccl3, Cxcl2 and Ccl5*
Toll-like Receptors	*Tlr2, Tlr4, Tlr5 and Tlr9*
Tight junction proteins	*Cdh1 and Ocln*
Glycosylation Enzymes	*Nans and Fut2*
Reference Genes	*B2m, Gusb, Ppia, Rps18 and Tbp*

Table 2. 11 Tissue Processing and Sectioning	
Optimum Cutting Temperature (OCT) Medium	VWR
Leica TP1020 Tissue Processor	Leica
Tissue Processing/Embedding Cassettes	Sigma-Aldrich
Formaline	Sigma-Aldrich
Ethanol	Lennox
Xylene	Sigma-Aldrich
Paraffin	Sigma-Aldrich

Cryostat	Leica
SuperFrost® Plus Adhesion Slides	VWR
Microtome	Leica

Table 2. 12 Haematoxylin and Eosin Staining

Harris Heamatoxylin	Sigma-Aldrich
Eosin	Sigma-Aldrich
Xylene	Sigma-Aldrich
Ethanol	Lennox
Sodium Biocarbonate	Sigma-Aldrich
HCl	Sigma-Aldrich
Histoclear	Thermo Fisher Scientific
DPX Mounting Medium	Sigma-Aldrich

Table 2. 13 Lectin Histochemistry

FITC-conjugated lectins*	Vector Laboratories
Vectashield Hardset Mounting Medium with DAPI	Vector Laboratories
Bovine Serum Albumin (BSA)	Sigma-Aldrich
$CaCl_2$	Sigma-Aldrich
$MgCl_2$	Sigma-Aldrich
Trizma Base	Sigma-Aldrich
Methyl α-D-mannopyranoside	Sigma-Aldrich
L-Fucose	Sigma-Aldrich
L-Fucose	Sigma-Aldrich
N-Acetyl-D-galactosamine	Sigma-Aldrich
N-Acetyl-D-glucosamine	Sigma-Aldrich
N-Acetyl-D-glucosamine	Sigma-Aldrich
N-Acetylneuraminic acid	Sigma-Aldrich

* Complete list of fluorescently-labelled lectins and their corresponding specificities are summarised in Table 2. 22.

2.2 METHODS

2. 2. 1 Microbial Cell Culture

All microbial cell culture was carried out using aseptic techniques in BIOMat^2 class II Microbiological Safety Cabinet in Institute of Molecular Medicine (Trinity College, Dublin), based in St. James's Hospital. All *C. difficile* ribotypes used in this project were a kind gift from Professor Thomas Rogers from Department of Clinical Microbiology, School of Medicine, Trinity College, Dublin. These ribotypes were sourced from patients with *C. difficile* infection.

2. 2. 2 Overview of SLP Isolation from *C. difficile.*

The steps involved in the isolation and purification of SLPs from *C. difficile* are summarised in Figure 2. 1. Each step in described in details in Sections 2. 2. 3 – 2. 2. 7.

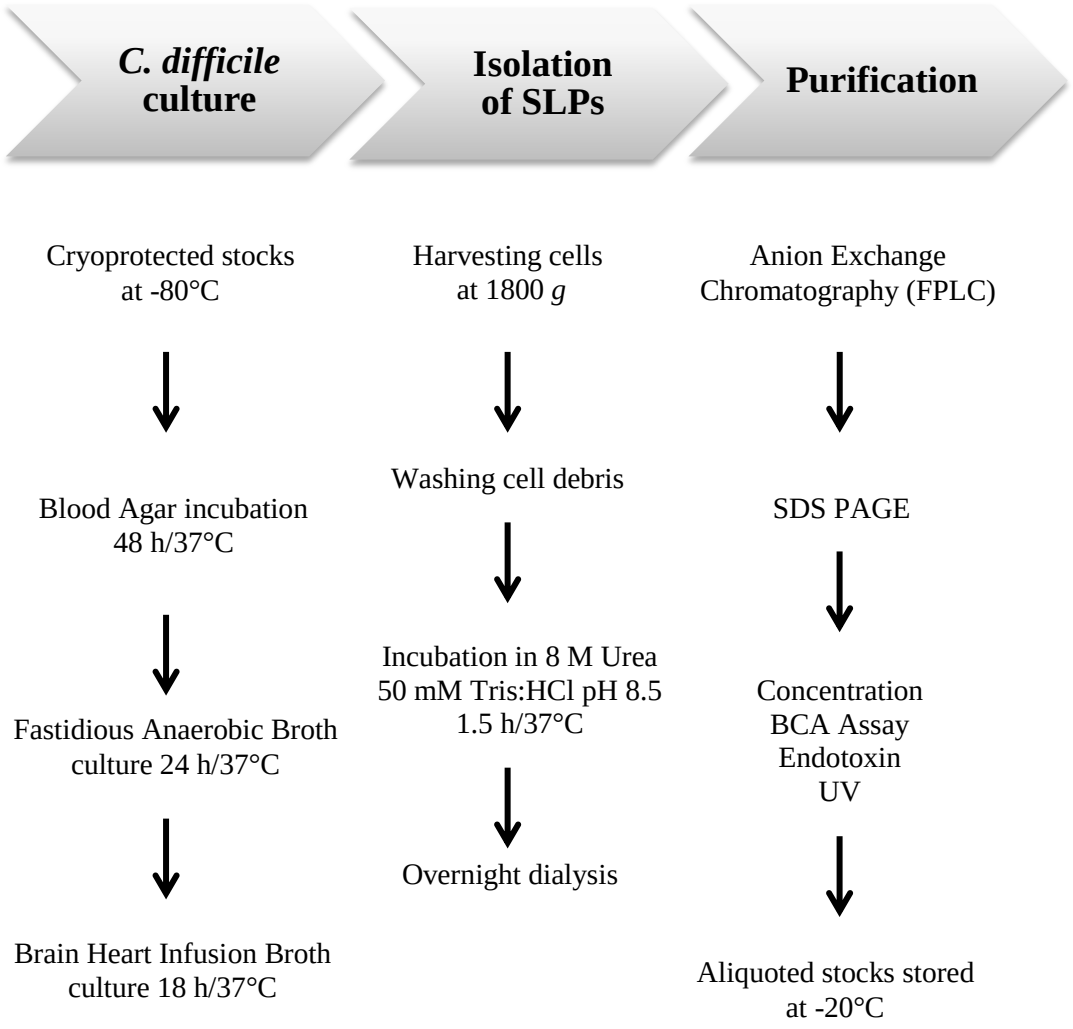

Figure 2. 1 Overview of SLP isolation. The method is briefly described in section 2. 2. 2, and in detail in Sections 2. 2. 3 – 2. 2. 7.

2. 2. 3 Bacterial Culture on Solid Medium

An inoculum of a given ribotype was streaked of surface Brucella Agar with 5% Horse Blood with a sterile inoculating loop using standard streaking method (Figure 2. 2). Plates were incubated upside down at 37°C for 48 h in anaerobic jar. An anaerobic Gas Generating Kit was used to generate anaerobic conditions in the jar. Furthermore, an Anaerobe Indicator Test was also inserted in the jar to monitor whether anaerobic conditions occurred in the sealed container. A colour change from pink to white indicated anaerobic conditions.

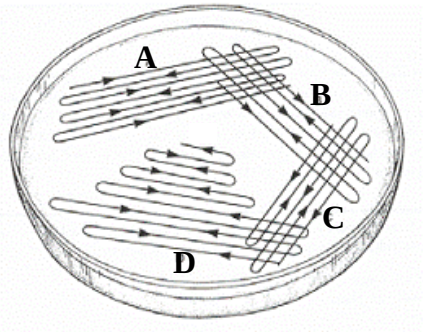

Figure 2. 2 Principle of plate streaking. Fresh loop was used between A, B, C and D.

2. 2. 4 Preparation of Microbial Spore Stocks

To prepare fresh stock for each new isolate, a single colony was streaked onto the surface of blood agar as described in section 2. 2. 3.

Two approaches for preserving stocks were developed. Initially, a solution of PBS with 15% glycerol was used for whole cell stock solution. In this case, colonies were incubated for 48 h and all colonies from one plate were swabbed from the surface of the agar and transferred into 2 ml of PBS/glycerol in a cryovial. Cell stocks were then immediately frozen at -80°C. A second approach involved preserving spores of

C. difficile. In this case agar plates were incubated for seven days under anaerobic conditions to generate spores. The cultures were harvested with disposable loops into 1 ml of PBS in screw cap tubes. Tubes were then spun down at 5600 *g* and the supernatant was removed. The cell pellet was washed in 1 ml PBS, and heat-shocked at 56°C for 10 min to kill surviving vegetative cells. The spores were centrifuged and re-suspended in 1 ml DMEM with 15% glycerol. Cryovials were labelled, dated, and frozen overnight at -80°C using a Mr. Frosty freezing container. The next day cryovials were transferred to a box and returned to -80°C. The latter approach was preferred to prevent the culture forming mutations.

2. 2. 5 Reviving of Microbial Spore Stocks

The bacterial spore stock cryovial was kept on ice. Using a sterile loop, the surface of the stock was scraped and streaked onto the surface of blood agar plate. The stock cryovial was returned to -80°C, while the plates were incubated upside down at 37°C for 48 h in an anaerobic jar, as described in Section 2. 2. 3. One passage was sufficient to produce enough colonies to inoculate liquid broth culture.

2. 2. 6 Liquid Broth Culture of *C. difficile* for Isolation of SLPs

Fastidious Anaerobic Broth (FAB) and Brain Heart Infusion (BHI) broth were prepared according to manufacturer's guidelines and autoclaved at 121°C and 15 lb/in^2 for 15 min. BHI broth was supplemented with 0.05% Sodium thioglycolate to ensure reducing conditions, and with vitamin K and hemin to support *C. difficile* growth (accordingly, 0.1 ml of 1% alcohol solution per litre of broth and 0.5 ml of 1% solution per litre of broth).

FAB broth was inoculated with a single *C. difficile* colony from blood agar plates. Broth tubes were placed in a 5 L anaerobic jar and incubated anaerobically for 24 h. After 24 h incubation, there was visible growth of suspended *C. difficile* colonies. In the meantime, Brain Heart Infusion Broth was aliquoted into 50 ml tubes (approximately 48 ml) and incubated in an anaerobic jar for 1-24 h to remove oxygen. Using sterile transfer pipettes, approximately 1 ml of FAB inoculum was transferred into tubes with BHI broth. BHI broth was incubated for approximately 16 h, under anaerobic conditions, until the turbid growth was observed.

2. 2. 7 Isolation of SLPs

2. 2. 7. 1 Removal of S-layer

Bacterial cells were harvested by centrifugation at 3200 *g* for 20 min at 4°C. Supernatant was discarded into a container filled with Presept solution to inactivate any remaining bacterial cells or spores. Each pellet was washed twice in ice-cold 50 mM Tris/HCl pH 7.4 by centrifuging at 3200 *g* for 20 min at 4°C. The pellets were then resuspended in 8 M urea/50 mM Tris/HCl pH 8.5, supplemented with protease inhibitor (5 tablets per 100 ml of 8 M urea/50 mM Tris/HCl pH 8.5) and incubated for 90 min at 37°C. Cells were then centrifuged at 12 500 *g* for 30 min at 4°C. Supernatant containing crude S-layer was carefully removed into fresh 50 ml tubes for storage at -20°C or dialysed immediately.

2. 2. 7. 2 Dialysis of Crude S-layer Preparation.

The crude protein extract underwent dialysis to remove urea from the solution. Dialysis cassettes (35 ml) with 10 K Molecular Weight Cut Off were rehydrated in

dialysis buffer (20 mM Tris/HCl pH 8.5) for 2 min. Dialysis buffer was compatible with running buffer for FPLC (described in Section 2. 2. 7. 3).

The crude protein extract was added to the dialysis cassette and the excess air was removed in the cassette by pressing the membrane gently on both sides. The cassette was placed in 5 L of dialysis buffer (300 X volume of the crude SLP extract) and floated vertically. Buffer was placed on a stirring plate and moved to a 4°C room. The crude protein extract was dialysed for 2 h and the buffer was changed three times. The third change of buffer was left overnight at 4°C. The crude extract was dialysed in a total of 20 L of dialysis buffer. The next day the sample was retrieved and filtered through 0.2 µm filters to remove any solid impurities. The crude protein extract was aliquoted into 10 ml tubes and stored in -20°C before proceeding to purification.

2. 2. 7. 3 Purification of SLPs using Fast Protein Liquid Chromatography (FPLC)

The crude S-layer was purified using ÄKTA$_{FPLC}$, which is a high-performance liquid chromatography for fast and easy purification of proteins. The assembled system allowed for ion exchange type of chromatography and was equipped with a MonoQ HR 10/10 chromatography column and a 10 ml injection loop (allows for introduction of large sample volumes into a pressurised fluid system). After assembling the instrument, the system was primed with running buffer (Buffer A; 20 mM Tris/HCl pH 8.5) and elution buffer (Buffer B; 0.3 M NaCl/20 mM Tris/HCl pH 8.5). The system was controlled by UNICORN™ Software (3.21v) which provided full control of purification process (Table 2. 14).

Crude S-layer fractions, comprised of isolated SLPs and other cell wall/cell surface-associated proteins in 100% running buffer, were pumped into the column with the injection loop. Proteins bound to the column resin by a charge interaction. The flow rate of the mobile phase was kept constant, however the proportion of Buffer B to Buffer A was gradually increased from 0% to 100% (known as gradient). Proteins dissociated from the column upon increasing the gradient of elution buffer. The slope of the salt gradient was adjusted by changing the amount of total volume flowing through the column (measured in number of column volumes) and final salt concentration.

The effluent containing the dissociated proteins passed through the flow cell. This allowed for detection of the NaCl concentration by conductivity (mS/cm) and protein concentration by absorption of UV light at 280 nm (mAU). As each protein was eluted and detected, it appeared as a peak on the chromatogram. The height and area of the peak was directly proportional to the concentration of the detected protein. The effluent fractions were set to 2 ml and were collected on a rotating rack (fractions numbered A1-A15, B1-B15, C1-C15 etc.) and approximately 45 fractions were collected in total per run. This allowed for satisfactory resolution between the eluted protein fractions.

Depending on the slope of the NaCl gradient, several elution profiles were observed. The main peak observed on the chromatogram generated by the software corresponded to the eluted SLP fraction (eluted at approximately 40 min).

To confirm the protein identity, 100 µl aliquots were kept frozen for SDS PAGE analysis. Before shutting down, the system was washed with Buffer B (0.3 M

NaCl/20 mM Tris/HCl pH 8.5) to remove any remaining proteins and Buffer A (20 mM Tris/HCl pH 8.5) to calibrate the system. The system was stored in 20% ethanol.

Table 2. 14 UNICORN™ Software (3.21v) Settings Applied to Purify SLPs using ÄKTA$_{FPLC}$. CV: Column Volume; B: Eluting buffer (Buffer B).

Parameter	Setting
UV Averaging Time	5.10
Flow Rate	4.00 ml/min
Starting Concentration Buffer B	0.00% B
Equilibrate with	1 CV
Flowthrough Fraction Size	0.00 ml
Start Flowthrough at	Next Tube
Empty loop with	10 ml
Wash Column with	5 CV
Start Fractionation at	60% B
Eluate Fraction Size	2.0 ml
Start Eluate Fraction at	First Tube
Peak Fraction Size	0.00 ml
Start Peak Fraction at	Next Tube
Peak Start Slope	100.00 mAU/min
Peak End Slope	75.00 mAU/min
Minimum Peak Width	0.31 min
End Fraction at	100% B
Target Concentration B 1	60% B
Length of Gradient 1	20 CV
Target Concentration B 2	100% B
Length of Gradient 2	4 CV
Target Concentration B 3	100% B
Length of Gradient 3	2 CV
Concentration of Eluent B	100% B
Clean with	5 CV
Reequilibrate with	2 CV

2. 2. 7. 4 SDS Polyacrylamide Gel Electrophoresis

To confirm the identity of the detected protein peaks, proteins were separated by SDS denaturing polyacrylamide gel electrophoresis. Acrylamide gels (10% (w/v)) were cast between two glass plates and affixed to the electrophoresis unit using spring clamps. Samples were diluted with 5X Loading Buffer supplemented with 1 M Dithiothreitol (DTT) and heated to 96°C for 5 min to denature any protein structures (See Appendix A). To run the samples on the gels, electrode running buffer was added to the upper and lower reservoirs. Prepared samples (10 µl) were loaded into wells and run at 30 mA per gel for approximately 45 min. Protein ladder containing pre-stained protein molecular weight markers was added to the first lane in each gel.

2. 2. 7. 5 Identification of SLPs by Coomassie Staining

When protein samples were separated completely, gels were removed from the casts, washed extensively with deionised water, and submerged in 10 ml of Coomassie Blue stain to identify any proteins present. The gels were then stained for 1 h with gentle agitation. After the incubation, the Coomassie stain was removed and the gels were washed briefly with dH_2O. Destain solution was added and gels were left for 10 min. Destain solution was then removed and the destaining was repeated four times. The gels were then left rocking in destain solution overnight at 4°C. The next day gels were examined for the presence of protein bands. Lanes with two bands (weights corresponding to both SLP subunits, High Molecular Weight at ~55 kDa and Low Molecular Weight at ~35 kDa) were selected. Corresponding crude protein fractions in 2 ml tubes were identified and defrosted.

2. 2. 7. 6 Concentration of Purified SLPs

Samples were concentrated using centrifugal filters with 10 K Molecular Weight Cut Off to retain both subunits of SLP (HMW ~55 kDa and LMW ~35kDa). The filters were centrifuged at 4000 g for 15 min at 4°C. Concentrated protein samples were recovered from filter device. Furthermore, samples were subjected to UV radiation for 15 minutes to ensure sterility, aliquoted and stored at -20°C.

2. 2. 7. 7 Measuring Protein Concentration with BCA assay

Purified SLP concentration was measured using BCA Protein Assay Kit according to manufacturer's guidelines. The assay uses the well-documented reduction of Cu^{+2} to Cu^{+1} by protein in a base, along with the colourimetric detection of Cu^{+1} using bicinchoninic acid (BCA). A purple colour is observed in the presence of protein, with darker colour signifying a higher concentration.

Briefly, a standard curve was prepared from Bovine Serum Albumin (highest standard 2000 pg/ml, followed by 1500, 1000, 750, 500, 250, 125, 25 and 0 pg/ml) in 20 mM Tris:HCl pH 8.5 and plated in triplicate on a 96-well plate. Samples (diluted and neat) were also plated in triplicate. BCA solution was added to all wells and the plate was incubated at 37°C for 30 min. The plate was cooled to room temperature and the absorbance was read at 562 nm on a microplate reader. Standard curve and the protein concentrations were calculated using GraphPad Prism 5.01.

2. 2. 7. 8 Endotoxin Test and UV Radiation

Samples of concentrated SLP were tested for the presence of endotoxin. LAL assay kit was used as a quantitative *in vitro* end-point endotoxin test. It utilises a modified Limulus Amebocyte Lysate, which is an aqueous extract of blood cells

(amoebocytes) from the horseshoe crab, *Limulus polyphemus.* A synthetic colour producing substrate is used to detect endotoxin chromogenically. Reagents were prepared according to manufacturer's instructions, and the test procedure was followed as per guidelines. Briefly, a measurable concentration ranges of 0.005 to 1 Endotoxin Units/ml (EU/ml) were prepared. Standards and samples (100 µl) were placed in specific endotoxin-free vials in duplicate. A blank of LAL reagent water was also prepared. LAL (100 µl) was added to each vial and the samples were incubated at 37°C for 10 min. Chromogenic substrate solution (500 µl) was then added, the samples were gently mixed and incubated for 6 min. Stop solution (500 µl) and colour stabiliser were added and samples were gently swirled to avoid generation of bubbles. Absorbance was read at 545 nm on a microplate reader.

2. 2. 8 Confirmation of *slpA* Sequences

The strains used in this study included R13537 (ribotype 001) and R12885 (ribotype 014). The sequence of the *slpA* gene of these strains has been previously determined (accession numbers DQ060626 and DQ060638 respectively). To determine the *slpA* gene sequences of our clinical strains belonging to ribotypes 027 and 078, whole-genome sequencing was performed. DNA was extracted from *C. difficile* using the Roche High-pure PCR template preparation kit (Roche, West Sussex, UK). Nextera XT library preparation reagents (Illumina, Eindhoven, The Netherlands) were used to generate multiplexed sequencing libraries of *C. difficile* genomic DNA, and resultant libraries were sequenced on an Illumina MiSeq®. Short-read data obtained has been deposited in the European Nucleotide Archive (ENA); project accession number PRJEB6566. Genome assemblies were performed using the Velvet short-

read assembler and *slpA* gene sequences were retrieved for each isolate using BLAST (Altschul *et al.* 1990).

2. 2. 9 Periodic Acid–Schiff Glycoprotein Staining

The periodic acid-Schiff (PAS) method was used to detect glycosylated proteins that have sialic acid and other oxidisable carbohydrate groups. In this method, a gel or membrane containing separated proteins is treated with a periodate solution (Oxidising reagent), which oxidizes cis-diol sugar groups in glycoproteins. The resulting aldehyde groups are detected through the formation of Schiff-base bonds with a reagent that produces magenta bands. Crude and purified SLPs samples were separated by electrophoresis on a 12.5% (w/v) SDS denaturing polyacrylamide gel a as described before (Section 2. 2. 7. 4). Protein ladder containing molecular weight markers was added to the first lane in each gel. Soybean Trypsin Inhibitor was used as a negative control and Horseradish Peroxidase was used as positive control (included in the kit). A total of 10 µg of protein per sample was prepared, and loaded into wells and run at 30 mA per gel for approximately 45 min. When proteins were separated, gels were removed from casts and stained with Coomassie Brilliant Blue stain to confirm the protein identity. Schiff staining was performed according to the manufacturer guidelines. After completing the procedure, the glycols were stained, yielding magenta bands with a colourless background, while proteins with no glycosylation remained dark blue.

2. 2. 10 Enzyme-Linked Lectin Assay (ELLA)

An Enzyme-Linked Lectin Assay was used to probe the surface of the SLPs for the presence of various sugar moieties using a range of lectins (Figure 2. 3). SLPs were

diluted to a concentration of 5 µg/ml in PBS and 50 µl was added to 96-well plates. PBS was used as a negative control while a range of glycoproteins with known glycosylation patterns were used as positive controls. The plate was incubated overnight at 4°C. The plate was then aspirated and blocked for non-specific binding for 2 h at room temperature with Carbo-Free™ Blocking Solution. Plates were washed four times with TBST supplemented with 1 mM Ca^{2+}/Mg^{2+}/Mn^{2+}. Biotinylated lectins (Table 2. 15) were diluted in TBST to a concentration of 5 µg/ml and 50 µl was added to corresponding wells and incubated for 1 h at room temperature. TBST was used as negative control for lectin specificity. Wells were aspirated and washed four times with TBST. Horseradish Peroxidase conjugated to streptavidin was diluted and 50 µl was added per well (1:10 000 dilution in TBST) and incubated for 1 h at room temperature. Wells were washed again four times in TBST and 90 µl of TMB was added, left for approximately 10 min and stopped with 10% H_2SO_4. Absorbance was read at 450 nm using a microplate reader. The assay was run along with positive controls which are outlined in the Table 2. 16.

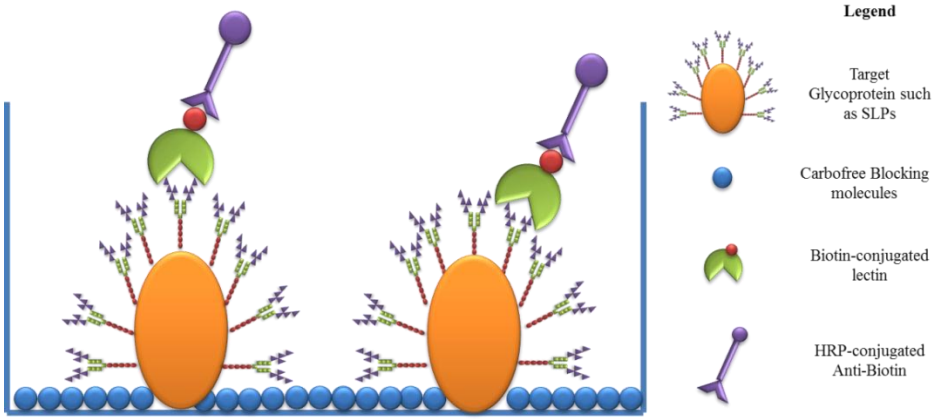

Figure 2. 3 Schematic diagram of ELLA. SLPs were coated onto the surface of the 96-well plate and were probed with biotinylated lectins. This interaction was quantified by addition of HRP-conjugated Anti-Biotin antibody and addition of substrate solution that change colour proportionally to the amount of lectin bound. Adapted from Thompson *et al.* (2011).

Table 2. 15 List of Biotinylated Lectins used in ELLA and Lectin Blotting. All lectins were sourced from Vector Laboratories and stored in -80°C. Recommended manufacturer concentrations were used. Table information was adapted from information provided on www.vectorlabs.com.

Lectin	Abbreviation	Source	Glycan Specificity
Aleuria aurantia	AAL	*Aleuria aurantia* mushrooms	Fucose-(α-1,6)-N-Acetylglucosamine
Concanavalin A	ConA	*Canavalia ensiformis* (Jack Bean) seeds	Core Mannose
Dolichos biflorus	DBA	*Dolicos biflorus* (Horse Gram) seeds	α-N-Acetylgalactosamine
Erythrina cristagalli	ECL	*Erythrina cristagalli* (Coral Tree) seeds	Galactosyl-(β-1,4)-N-Acetylglucosamine
Galanthus nivalis	GNL	*Galanthus nivalis* (Snowdrop) bulbs	(α-1,3)-Mannose
Griffonia simplicifolia I	GSL I	*Griffonia simplicifolia* seeds	α-N-Acetylgalactosamine and α-Galactose
Griffonia simplicifolia II	GSL II	*Griffonia simplicifolia* seeds	α/β-N-Acetylglucosamine
Jacalin	Jacalin	*Artocarpus integrifolia* (Jackfruit) seeds	Galactosyl-(β-1,3)-N-Acetylgalactosamine
Lens culinaris	LCA	*Lens culinaris* (lentil) seeds	α-Mannose
Maackia amurensis II	MAL II	*Maackia amurensis* seeds	Galactosyl-(α-2,6)/(α-2,3)-Sialic Acid-(β-1,4)-N-Acetylgalactosamine
Narcissus pseudonarcissus	NPL	*Narcissus pseudonarcissus* (Daffodil) bulbs	Terminal and High Mannose
Peanut	PNA	*Arachis hypogaea* peanuts	Galactosyl-(β-1,3)-N-Acetylgalactosamine
Soybean	SBA	*Glycine max* (soybean) seeds	Terminal α/β-N-Acetylgalactosamine
Sambucus nigra	SNA	*Sambucus nigra* (Elderberry) bark	Galactosyl-(α-2,6)/(α-2,3)-Sialic Acid

Table 2. 16 Most abundant glycans found on glycoproteins used as positive controls used in ELLA. Adapted from Thompson et al. 2011, Larrgy 2011 and Kalisz et al. 1997.

Asialofetuin	Terminal Galactose and N-Acetylgalactosamine
Fetuin (Bovine)	Terminal and High Sialic Acid
Glucose Oxidase	N-Acetylglucosamine
Invertase (from *Saccharomyces cervisiae*)	High Mannose
Thyroglobulin (Porcine)	Sialic Acid
Transferrin	Terminal Sialic Acid, Fucose and Galactose

2. 2. 11 Lectin Blotting

Crude S-layer fractions and purified SLPs (10 µg of total protein) of *C. difficile* RT 001, 002, 027 and 078, along with pre-stained molecular markers, were separated by SDS PAGE on 10% (w/v) acrylamide gels under denaturing conditions. Gels were washed in water to remove salts and were transferred onto a nitrocellulose membrane using the iBlot system, and stained with Ponceau S to confirm the transfer of proteins. Non-specific lectin binding sites were blocked for 1 h at room temperature using Carbo-Free™ Blocking Solution. Afterwards, membranes were washed four times in wash buffer (TBS with 0.01% Tween20® supplemented with 1 mM $Ca^{2+}/Mg^{2+}/Mn^{2+}$). Samples were then incubated for 1 h at room temperature with 1:2000 dilution of biotinylated lectin made up in lectin buffer (TBS with 0.01% Tween20® supplemented with 1% Bovine Serum Albumin and 1 mM $Ca^{2+}/Mg^{2+}/Mn^{2+}$), followed by a wash step. Membranes were then incubated with 1:250 dilution of streptavidin-conjugated horseradish peroxidase in lectin buffer for 1 h at room temperature, followed by another wash step. Chemiluminescent substrate was then added to the membranes to detect HRP-lectin complexes. The intensity of the signals was detected by the G-Box fluorescence gel analysis system and exposed for a range of times (from 30 s to 120 s).

2. 2. 12 Animal Models

2. 2. 12. 1 Housing

Female C57BL/6J mice aged 9 to 15 weeks were used in this study. Mice were purchased from Charles River (UK) and were certified to be specific-pathogen free. Animals were housed in licenced facility in Bioresource Unit in Dublin City University and had *ad libitum* access to water and animal chow. Facility was monitored daily for temperature and humidity.

2. 2. 12. 2 Project Approval and Ethics Statement

All procedures were carried out in accordance with the Health Products Regulatory Authority and performed under project licence number AE19115_P001, project titled *"Interaction between Surface Layer Proteins from Clostridium difficile and the gut epithelium"*. All animal protocols received ethical approval from Dublin City University Research Ethics Committee.

2. 2. 12. 3 *In vivo* susceptibility model

Animals were assessed for the overall health on day 0 of the study to exclude any individuals that possibly experienced barbering (See Section 2. 2. 12. 4). Animals were divided into two groups, control and treatment. The control group received filtered water from day 0 to day 7, and this group was injected intraperitonially with body-temperature PBS on day 5. The treatment group received a cocktail of antibiotics in drinking water from day 0 to day 3 (and filtered water from day 4 to day 7), which was followed by an intraperitoneal injection of clindamycin on day 5. The antibiotics, their mode of action and relevant dosage are outlined in Table 2.17.

Table 2. 17 Antibiotics used to induce susceptibility state in mice. Dosage and route of delivery was adapted from Chen *et al.* (2008). Information about primary specificity of the antibiotics and associated mode of action were sourced from Walsh (2003).

Antibiotic	Antibiotic Conc.	Daily Dosage	Delivery	Specificity	Mode of action
Metronida-zole	0.215 mg/ml	21.5 mg/kg	Oral in water	Anaerobic bacteria	Nucleic acid synthesis inhibitor (disrupting DNA structure)
Gentamicin	0.035 mg/ml	3.5 mg/kg	Oral in water	Gram-ve bacteria	Protein synthesis inhibitor (blocking 30S subunit)
Colistin	850 U/ml	4.2 mg/kg	Oral in water	Gram-ve bacilli	Bactericidal action by solubilising the membrane
Kanamycin	0.4 mg/ml	40 mg/kg	Oral in water	Gram-ve bacteria	Protein synthesis inhibitor (blocking 30S subunit)
Vancomycin	0.045 mg/ml	4.5 mg/kg	Oral in water	Gram+ve bacteria	Cell wall synthesis inhibitor (blocking peptidoglycan assembly)
Clindamycin	n/a	10 mg/ml	IP injection	Anaerobic bacteria	Protein synthesis inhibitor (blocking 50S subunit)

Animals were assessed daily for appearance, behaviour, water intake, weight and stool consistency. All scores were noted in Monitoring Score Sheet (Table 2. 18) and there was an individual sheet for each animal used in the study. The total score was used to determine Daily Disease Activity Index to assess animal welfare and any possible disease progress.

As mentioned, water intake was monitored for welfare purpose. However, it was also correlated with the body weight of each animal (dosage per kg body weight) to

ensure that sufficient amount of the antibiotics was ingested to eradicate the microbiota. The general approach to susceptibility model is outlined in Figure 2. 5.

Table 2. 18 Daily Disease Activity Index was determined based on the factors outlined below. Actions taken based on the total score for any given day: 0-2 normal; 4-6 monitor carefully, but notify Project Manager; 6-8 seek opinion from named animal care and welfare officer; consider termination; >9 terminate. Animal with >20% body weight loss should be euthanised regardless of the Total Score for any given day. The criteria were based on Wolfensohn & Lloyd (2012) and University of Colorado Denver/Anschutz Medical Campus (www.ucdenver.edu).

Score	0	1	2	3
Appearance	Normal	General lack of grooming, barbering	Coat staring, ocular or nasal discharges	Piloerection, hunched up
Behaviour	Normal	Minor changes	Abnormal: reduced mobility, inactive	Unsolicited vocalisation, self-mutilation, restless or immobile
Water intake	Normal	Limited <15% body weight	Below 10% body weight	No intake
Weight	Normal	<5% weight loss	5-15% weight loss	>15% weight loss*
Stool Consistency	Normal	Soft but still formed	Very soft, no shape	Diarrhoea (defined as mucus/faecal material adherent to anal fur)

Animals were sacrificed humanely by cervical dislocation on day 7 and colons were removed. The colon was opened longitudinally and faecal matter was removed. The colon length and colon weight were recorded as an indication of colitis. The distal part of the colon was used for the subsequent experiments. Colonic tissue was preserved as follows, for RNA isolation, 0.5 cm of colon was stored in RNAlater at -80°C, for lectin blotting 0.5 cm was snap-frozen in liquid nitrogen and stored at -80°C, for *ex vivo* analysis 1 cm pieces of colon were washed in PBS and PBS with 10 000 U/ml penicillin and 10 000 µg/ml streptomycin and incubated as per Section

2. 2. 12. 6. Finally, for tissue embedding, 1.5 cm of colon was rolled using Swiss Roll technique (Moolenbeek & Ruitenberg 1981) and inserted into plastic cassettes and stored in formaline.

2. 2. 12. 4 Barbering

In early stage of handling mice, we have noticed that female C57BL/6J mice were prone to barbering. Barbering is a behaviour-associated hair loss and includes trimming, nibbling, and plucking of fur and whiskers (Figure 2. 4 B). It may include barbering of cage mates (hetero-barbering) or oneself (self-barbering) and it is commonly observed in mice (Nicholson *et al.* 2009). It is particularly common in certain strains, such as C57BL/6J, suggesting a strong genetic component (Kalueff *et al.* 2006). The signs of barbering were used as an indicator of appearance and were accounted for in daily disease index.

A **B**

Figure 2. 4 Female C57BL/6J were used in this project. Animals were sourced from Charles River (UK) and were used between ages of 9 to 15 weeks. Animals were monitored daily for the appearance (**A**). Any case of barbering (**B**) was monitored carefully and animals experiencing hair loss were removed from this study. Sourced from www.criver.com (**A**) and from Kalueff *et al.* (2006) (**B**).

2. 2. 12. 5 *In Vivo Clostridium difficile* Infection Model

C57BL/6J mice were subjected to antibiotic treatment as described in section 2. 2. 12. 3. On day seven, animals were divided into two groups. First group was challenged with oral gavage of 10^3 of *C. difficile* spores, RT 001. The control group was allowed to restore microbiota and was not challenged with any infectious agent. Animals were weighed daily and monitored for overt disease, including diarrhoea. Moribund animals with >15% loss in body weight were humanely killed. At day three and day seven post-infection, animals were sacrificed and cecum content was harvested to assess the CFU counts. Also, colon tissue was rolled using Swiss roll technique, preserved in OCT medium and snap-frozen in liquid nitrogen and subsequently stored at -80°C for further analysis. The general approach to infection model is outlined in Figure 2. 5.

The *in vivo* infection model was carried out in collaboration with Pat Casey and Professor Colin Hill in the Alimentary Pharmabiotic Centre, University College Cork. Isolation of colonic samples was carried out by Dr Maja Kristek, Dr Mark Lynch and Dr Joseph deCourcey.

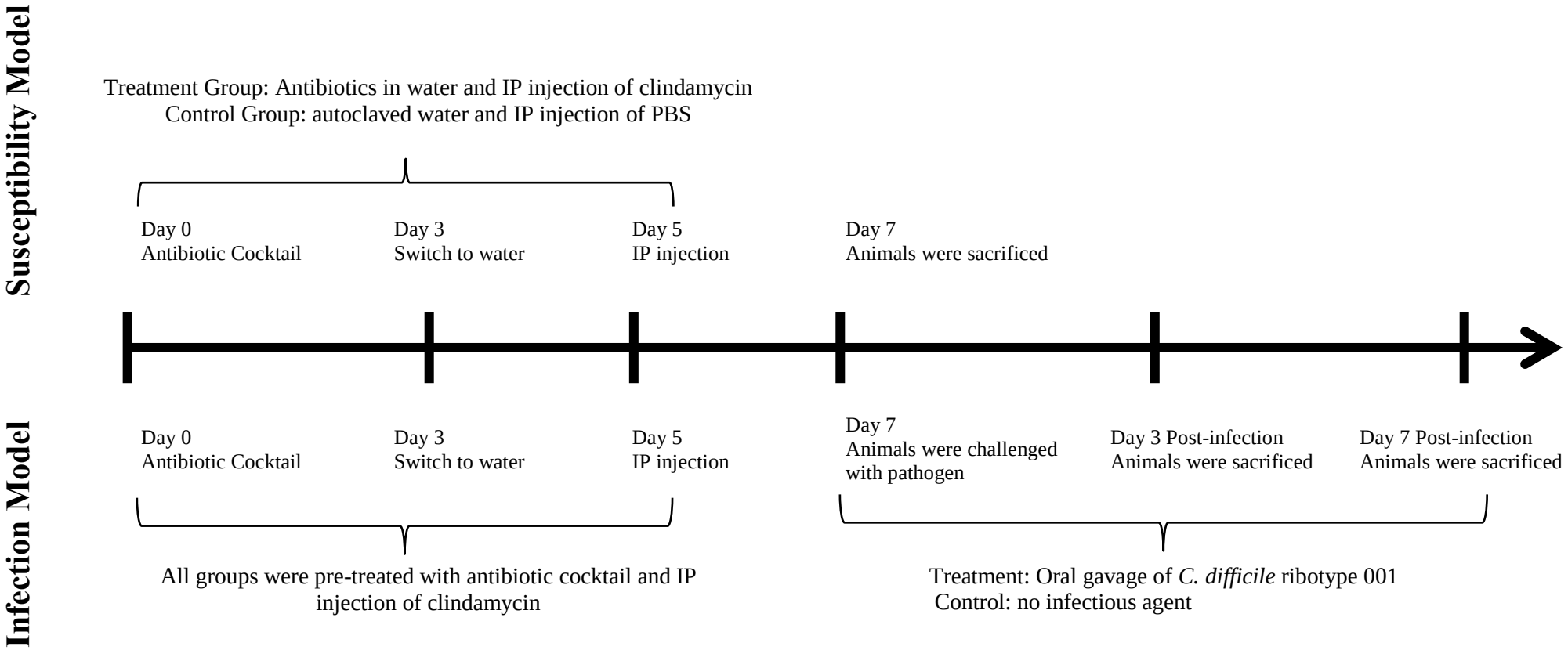

Figure 2. 5 Outline of *in vivo* approach of two animal models investigated during this project. The first study, the susceptibility model, investigated the effect of disturbance in commensal microbiota on susceptibility to infection. Second study, the infection model, involved infecting susceptible animals with *C. difficile* RT 001. This model focused on host's mucosal response to infection and mechanisms involved in clearing the pathogen and the recovery of the epithelial structure.

2. 2. 12. 6 *Ex vivo* Colon Culture

Mice were sacrificed by cervical dislocation and the abdominal cavity was opened aseptically. The GI tract was removed and the cecum and colon were identified. The colon was cut out and faeces were removed. The colon was then opened longitudinally and the distal colon was cut into 1 cm pieces (colon explants). These colon explants were washed in sterile PBS for 1 min, followed by a wash in PBS with 10 000 U/ml penicillin and 10 000 µg/ml streptomycin. Explants were then transferred into individual wells in a 24-well plate and cultured in 1 ml of RPMI supplemented with 100 U/ml penicillin and 100 µg/ml streptomycin. Explants were stimulated with 100 ng/ml of LPS, 20 µg/ml of SLP 001 or 20 µg/ml of SLP 027, respectively, and left for 6 h incubation at 37°C/ 5% CO_2.

After incubation, explants were stored stored in 300 µl of RNAlater at -80°C overnight and processed as per section 2. 2. 15.

2. 2. 13 Mammalian Cell Culture

All cell culturing techniques were carried out using aseptic technique in a class II laminar airflow unit (Holten 2010 - ThermoElectron Corporation, USA). Cell cultures were maintained in a 37°C incubator with 5% CO_2 and 95% humidified air (Model 381 – ThermoElectron Corporation, USA). Cell cultures were and visualised with an inverted microscope (Olympus CKX31, Olympus Corporation, Toyko, Japan).

2. 2. 14 Basic Principles of Reverse Transcription quantitative Polymerase Chain Reaction (RT qPCR)

Reverse Transcription quantitative Polymerase Chain Reaction (RT qPCR) is a molecular method based on the principles of PCR where a region of DNA is amplified using primers to surround a specific targeted portion of DNA and amplify it exponentially using a heat stable DNA polymerase. In RT qPCR the amount of DNA amplified is real time and allows for absolute (total copies) or relative quantification (normalisation to a gene of choice) of target DNA.

RT qPCR has become the most precise and accurate method for analysing gene expression. RT qPCR has the advantage of measuring the starting copy number and detecting small differences in expression levels between samples because amplification and quantification occur simultaneously.

The intercalating dyes are nonsequence-specific fluorescent dyes that exhibit a large increase in fluorescence emission when they intercalate into double-stranded DNA. Intercalating dye of choice for these experiments was SYBR® Green. During the RT qPCR, the primers amplify the target sequence and multiple molecules of the dye are inserted between the bases of the double-stranded product, causing fluorescence. The background fluorescence from SYBR® Green when in solution as a free dye and stimulated by light of appropriate wavelength is very low. In contrast, when double-stranded DNA product is formed and SYBR® Green becomes incorporated into the minor grove of DNA helix, there is a proportional increase in fluorescence roughly 2000x the initial fluorescent signal.

The main advantage of using intercalating dye is that they are not specific to a particular sequence, therefore are inexpensive and versatile to a range of molecular targets.

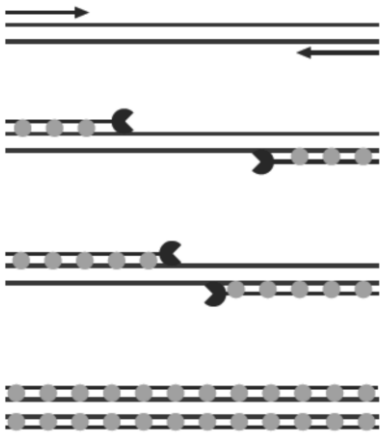

Figure 2. 6 The Principle of Fluorescence Produced by Intercalating Dye. During the annealing step, the primers hybridise in sequence-dependent manner to the complementary DNA strand. During the extension step, the intercalating dye (grey circles) incorporates to newly formed double-stranded product. Fluorescence increases proportionally to the length of the amplicon. The process is repeated in each cycle with increasing total fluorescence.

2. 2. 15 RNA Isolation

All work involving nucleic acids was carried out in an RNase-free environment. This was ensured by the use of dedicated bench space, dedicated pipettes and sterile RNase-free consumables (pipette tips with filters, 1.5 ml and 0.2 ml microcentrifuge tubes). All surfaces and pipettes were wiped with RNase Zap solution.

RNA was isolated from frozen tissue samples using NuceloSpin® RNA II Total Isolation Kit. Frozen tissue samples weighing 30 mg were homogenised in 350 µl of lysis buffer using a rotor-stator homogeniser. Next, 3.5 µl of β-mercaptanol was added and mixed thoroughly. The viscosity of the lysate was reduced by filtration through NuceloSpin® filters (violet ring) and centrifuged for 1 min at 11 000 g. The filter was then discarded and the RNA binding conditions were adjusted by adding

molecular grade ethanol to the filtrate. The preparation was applied onto a Nucelospin® column (blue ring), and centrifuged for 30 sec at 11 000 g. The membrane on the column was then desalted by washing with Membrane Desalting Buffer and centrifuged at 11 000 g for 1 min. Next, rDNase was added onto the membrane to digest any remaining DNA and incubated for 15 min at room temperature. The rDNase was then deactivated by adding 200 µl of RA2 buffer and any remaining impurities from the isolation were washed twice with RA3 buffer. Bound RNA was eluted by adding 60 µl DEPC-treated dH_2O, preheated at 65°C, onto the membrane and centrifuged at 11 000 g for 1 min. The RNA was collected in sterile 1.5 ml RNase-free microcentrifuge tubes and kept at -80°C.

2. 2. 16 RNA Quality Control

It is important for any downstream experiments to ensure consistent quantity and quality of RNA between the samples. Poor approach to quality control can compromise the entire experiment and may have a large impact on the results. Furthermore, differences in quality between two samples can lead to misinterpretation of gene expression differences. The quality and quantity of isolated RNA was examined by UV spectrophotometry (Section 2. 2. 17. 1) and gel electrophoresis (Section 2. 2. 17. 2).

2. 2. 17. 1 **RNA Quantification by UV Spectrophotometry**

The RNA was quantified using the NanoDrop ND-1000 spectrophotometer. Also, the quality of the isolated nucleic acid was assessed by $A_{260/A280}$ ratio and $A_{260/A230}$ ratio. The $A_{260/A280}$ ratio is used to assess the purity of RNA, generally a ratio of ~2.0 is accepted. If the ratio is appreciably lower in either case, it may indicate the

presence of protein or other contaminants that absorb strongly at 280 nm. The $A_{260/A230}$ ratio is used as a secondary measure of nucleic acid purity and the ratio is usually in the range of 2.0-2.2. If the ratio is lower than the recommended range it may indicate the presence of contaminants which absorb at 230 nm, such as EDTA or carbohydrates. Interestingly, phenol (used in traditional RNA isolation protocols) can absorb at 270 nm and 230 nm and might affect the reading of both ratios. Briefly, 1.2 µl of RNase-free water was used to blank the instrument and 1.2 µl of sample was loaded to read the absorbance spectra from 230 nm to 600 nm.

2. 2. 17. 2 RNA Integrity Analysis by Gel Electrophoresis

To assess the integrity of the RNA, 1 µg of total RNA from each sample was used for visualisation. Briefly, 1% agarose gel was prepared in 100 ml of 1X TAE buffer. To visualise the RNA, 10 µl of SYBR Safe was added to cooled agarose solution and poured into gel rig and left to set in the dark. Samples were reduced by addition of buffer containing formamide and heated to 65°C for 10 min. Samples along with 100 bp ladder were resolved on a gel at 150 V for ~30 min. The gel was then visualised using the G-Box Gel Imagine System. Intact total RNA has two clear bands, corresponding to 28S and 18S subunits. The ratio of intensity of 28S to 18S should be 2:1.

2. 2. 17 Reverse Transcription of RNA to Complementary DNA (cDNA)

Transcription is the synthesis of RNA from a DNA template, while reverse transcription is referred to as the process of synthesis of DNA from a RNA template. The conversion from RNA to DNA is essential as PCR uses only DNA-dependent polymerases. The complementary DNA (cDNA) to isolated RNA was synthesised

using High Capacity cDNA Reverse Transcription kit. During the reverse transcription, single-stranded mRNA is reversely transcribed into cDNA. The reaction mixture is composed of a normalised amount of total RNA, a MultiScribe™ Reverse Transcriptase enzyme, random primers, dNTPs and enzyme buffer (Table 2.19).

Table 2. 19 RNA and DNA integrity by gel electrophoresis

Components	**Volume**
10x Reverse Transcriptase Buffer	2 µl
10x Random Primers	2 µl
25X dNTP (100 mM)	0.8 µl
MultiScribe™ Reverse Transcriptase	1 µl
Total RNA mixed with Nuclease Free H_20	14.2 µl
Total	**20 µl**

The reaction was gently mixed, spun and placed in a Thermocycler and run according to settings recommended by the manufacturer, outlined in Table 2. 20. The reaction generates a cDNA suitable for use in quantitative PCR.

Table 2. 20 Thermocycler settings for generation of cDNA

Step	Temperature	Duration
1	25°C	10 min
2	37°C	120 min
3	85°C	5 min
4	4°C	∞

2. 2. 18 Primer Efficiency

The efficiency of the qPCR reaction is an important factor in data analysis. Efficiency of qPCR can be influenced by many factors including target length, target

sequence, primer sequence, buffer conditions, impurities in the sample cycling conditions and enzyme used. The efficiency of a successful assay will be between 90% and 110%. Amplification efficiency can be calculated by analysing the slope of the log-linear portion of the standard curve. When the template concentrations are plotted onto the X axis and Cq values are on the Y axis, the PCR efficiency equals $10^{(-1/slope)} - 1$. Theoretical maximum efficiency of 1.00 (100%) indicates doubling of a product with each cycle. However, the efficiencies derived from the plots are not exact values but estimates, therefore, it explains the efficiencies < or > 100%.

Relative standard curves were set up to determine the efficiency of the primers in the assay performance and were used as quality control for the qPCR reaction. Relative standard curves were generated using s serial dilution of a neat sample down to 10^{-4}. The log of dilutions was plotted against Cq values. The PCR efficiency is close to 100% when the slope of the amplification curve is close to -3.32. The R^2 value of the line was also taken into account and values of >0.95 were deemed acceptable.

Efficiency of the qPCR reaction was carried out for every primer pair used in this study (as summarised in Table A2, Appendix C) and only primers that demonstrated efficiency between 90-110% were used.

2. 2. 19 Normalisation

In order to ensure the consistency during the qPCR, several normalising steps were introduced. This included normalising sample size by weighing it before tissue processing. All tissue samples used in this project (ie. *in vivo* and *ex vivo*) were cut to weigh approximately 30 mg, as this was the capacity of the RNA isolation kit. Also, only one type of isolation kit was applied to all samples. Furthermore, upon isolation, each sample was quantified using the NanoDrop and the amount of total

RNA was normalised to the sample with the lowest concentration (usually 1 µg/ml) to ensure that the same amount is used for each reverse transcription reaction. Finally, in order to carry out analysis, a PCR-dependent reference was applied in form of reference genes. This strategy targets the RNAs that are universally and constitutively expressed, and whose expression does not differ between the experimental and control groups. It is recommended to screen for multiple reference genes, as the most appropriate normalising genes to use will depend on the tissue source. The best practise it to include at least two or three normalisation genes to determine which expression levels fluctuate the least. The reference genes screened for the purpose of this project are outlined in Table 2. 21.

Table 2. 21 Reference Genes Screened for Normalisation of RT qPCR

Gene ID	Description
B2M	Beta-2-microglobulin
GUSB	Glucuronidase, beta
PPIA	Peptidylpropyl isomerase A
RPS18	Ribosomal protein S18
TBP	TATA box binding protein

2. 2. 20 Data Analysis

The approach used to analyse RT qPCR data involved relative quantification. To determine levels of expression, the differences (Δ) between threshold cycle (Cq) were measured. Relative quantification determines the changes in steady-state mRNA levels of a gene across multiple samples and expresses it relative to the levels of another mRNA. Relative quantification does not require a calibration curve or standards with known concentration.

2. 2. 21 DNA Product Analysis by Gel Electrophoresis

To assess the specificity of the primers towards the DNA targets, the RT qPCR reactions were visualised on agarose gel. The RT qPCR product (20 µl) was mixed with DNA buffer in 6:1 ratio and resolved on 1% agarose gel in 1X TAE with SYBR Safe. Samples were run at 150 V for ~30 min along with 100 bp ladder. The gel was then visualised using the G-Box Gel Imagine System. One sharp band indicated the specificity of the primer towards the target.

2. 2. 22 Processing and Paraffin-Embedding of Colon Tissue

To embed the tissue, 1.5 cm of colon was rolled using Swiss Roll technique and stored in formaline at room temperature until processing (Moolenbeek & Ruitenberg 1981). Leica TP1020 Tissue Processor was used to treat the samples. Samples were initially stored in formaline for at least 24 h, followed by steps outlined in the Table 2. 22. The cassettes were then promptly removed and moved to the paraffin embedding station. Plastic moulds were used to position the tissue and tissue was overlaid with molten paraffin. When the paraffin solidified, the tissue blocks were stored at room temperature.

Tissue blocks were cut into 6 µm section using microtome and mounted onto Histobond microscope slides (slides are pre-coated with adhesive coating for mounting tissue sections).

Table 2. 22 Stages of Tissue Processing for Paraffin-embedding.

Stage	Solution	Duration
1	Formaline	At least 24 h
2	70% Ethanol	1 h
3	96% Ethanol	1 h
4	100% Ethanol	1 h
5	100% Ethanol	1 h
6	Xylene	1 h
7	Xylene	1 h
8	Paraffin	1 h
9	Paraffin	∞

2. 2. 23 Colonic Tissue Sectioning

Two types of tissue preservation were used in this study, OCT (low temperature) and paraffin-embedding. These techniques required a separate approach in tissue sectioning and storage of slides.

2. 2. 23. 1 OCT

Samples were stored at -80°C and were sectioned using cryostat. Cryostat was calibrated to ~-20°C. A drop of OCT medium was used to secure frozen roll of colon tissue on the metal mount. The thickness was initially set to 10 µm to expose the tissue surface, after which the sections were cut to 6 µm. Finally, the tissue was cut at 6 µm and sections were mounted onto slides. The superfrost slides were wrapped individually in tin foil and stored at -20°C.

2. 2. 23. 2 Paraffin-embedding

Unlike OCT-preserved tissue, paraffin-embedded blocks were stored at room temperature. Sections were cut using microtome. The thickness was initially set to 10 µm to expose the tissue surface, after which the sections were cut at 6 µm. Sections were then transferred onto the surface of water bath set to 50°C, to soften the wax surrounding the tissue, before being mounted onto the histobond slides. The slides were then stored at room temperature in a slide box.

2. 2. 24 Haematoxylin and Eosin Staining

To visualise the structure of the colon, slides were stained with Haematoxylin and Eosin (H&E). To remove paraffin, slides were soaked in Xylene for 15 min at room temperature (this step was omitted for OCT-mounted tissue). Slides were then washed in PBS for 5 min, followed by staining with Haematoxylin for 8 min. Excess of dye was washed off for 5 min with tap water. Sections were then differentiated in 1% acid/alcohol for 30 sec/3 dips. Tap water was used to wash sections for 1 min and before being placed in 0.1% sodium bicarbonate for 1 min. Slides were again washed under tap water for 5 min, followed by 10 dips in 95% Ethanol. Eosin was used to counter stain slides for 1 min (constant dipping). Sections were then dehydrated by dipping in 75% ethanol for 3 min, 95% ethanol for 3 min (two times), 100% ethanol for 3 min and Histoclear for 3 min (two times). Finally, slides were then secured with a coverslip and DPX mounting medium and stored at room temperature until required.

2. 2. 25 Fluorescent Lectin Staining of Colonic Tissue Sections

Tissue sections from the *in vivo* susceptibility and infection models were probed for the presence of various glycans with FITC-conjugated lectins (Table 2. 23). First, tissue sections were pre-treated as described in Section 2. 2. 24. Paraffin-embedded sections were soaked in Histoclear for 15 min to remove any paraffin, followed by rehydration steps, (2 min in 100% ethanol, 2 min in 70% ethanol, and 2 min in dH_2O). OCT-embedded sections were left to thaw for 5 min and soaked in acetone for 1 min. From this step, both methods of preserving tissue followed the same protocol. Briefly, slides were washed in Tris buffer for 30 s, followed by a wash in Tris buffer with 1 mM Mg^{2+}/Ca^{2+} for 30 s. FITC-conjugated lectin was diluted to 5 µg/ml in lectin buffer (Tris buffer with 1 mM Mg^{2+}/Ca^{2+} with 1% BSA). Slides were covered in lectin solution and kept at room temperature, in the dark for 20 min.

Following this, slides were washed to remove any excess of lectin. This comprised of three washes in Tris buffer with 1 mM Mg^{2+}/Ca^{2+} for 30 s (with vigorous agitation), followed by a soak in the same buffer for 4 min. Slides were then left to air-dry. To preserve the staining, slides were mounted by adding ~10 µl of Vectashield mounting media with DAPI (to visualise tissue structure) and covered with long cover slide. Slides were kept in the dark at 4°C and examined under fluorescent microscope within a week.

2. 2. 25. 1 Incubation with Monosaccharides to Confirm the Lectin Specificity

To confirm lectin binding specificity, lectins were pre-incubated with corresponding monosaccharide prior to tissue incubation. Slides were prepared as described in section 2. 2. 26. However, 0.5 M of monosaccharide was added to the FITC-conjugated lectin in lectin buffer and incubated at room temperature for 30 min. Pre-

incubated lectins were then added onto tissue sections as previously described in Section 2. 2. 25.

2. 2. 26 Fluorescence Microscope Examination and Analysis

Samples were visualised using the Olympus BX51 Fluorescent Microscope controlled by Cell^2 software. Images were analysed using the Image J software. Firstly, samples were blindly scored for the presence of the fluorescence signal. The part of the epithelium structure where the signal was obtained was noted (intestinal lumen, columnar surface epithelium, lamina propria, goblet cells, stem cells, crypt of Lieberkühn, muscularis mucosae or submucosa; Figure 2. 8). The intensity of such signal was also noted (+++ denoting extremely strong staining; ++ denoting strong staining; + some staining present; lack of signal was left blank). This analysis presented the distribution of glycosylation within the epithelial structure.

Furthermore, the total intensity of the slide was scored. Briefly, the image was split into separate channels (DAPI and FITC) and FITC channel was used further. Total intensity of the image was measured and normalised to background fluorescence. For each condition, at least five images were taken.

Table 2. 23 FITC-conjugated lectins used to examine glycans on the surface of the colonic epithelium. Table comprises the primary specificity of lectin and monosaccharide sugars used to inhibit the interaction between lectin and tissue, as recommended by manufacturer. All information sourced from www. vectorlabs.com.

Lectin	Abbreviation	Source	Specificity	Inhibiting sugar
Concanavalin A	ConA	*Canavalia ensiformis* (Jack Bean) seeds	Core Mannose	Methyl α-D-mannopyranoside
Aleuria aurantia	AAL	*Aleuria aurantia* mushrooms	Fucose-(α-1,6)-N-Acetylglucosamine	L-Fucose
***Ulex europaeus* I**	UEA I	*Ulex europaeus* (Furze Gorse) seeds	α-Fucose	L-Fucose
Dolichos biflorus	DBA	*Dolicos biflorus* (Horse Gram) seeds	α-N-Acetylgalactosamine	N-Acetyl-D-galactosamine
Peanut	PNA	*Arachis hypogaea* peanuts	Galactosyl-(β-1,3)-N-Acetylgalactosamine	N-Acetyl-D-galactosamine
Succinylated Wheat Germ	sWGA	*Triticum vulgaris* (wheat germ)	α/β-N-Acetylglucosamine	N-Acetyl-D-glucosamine
Griffonia simplicifolia II	GSL II	*Griffonia simplicifolia* seeds	α/β-N-Acetylglucosamine	N-Acetyl-D-glucosamine
Sambucus nigra	SNA	*Sambucus nigra* (Elderberry) bark	Galactosyl-(α-2,6)/(α-2,3)-Sialic Acid	N-Acetylneuraminic acid
Wheat Germ	WGA	*Triticum vulgaris* (wheat germ)	Sialic Acid	N-Acetylneuraminic acid
Maackia amurensis I	MAL I	*Maackia amurensis* seeds	Galactosyl-(α-2,3)-Sialic Acid	N-Acetylneuraminic acid

CHAPTER 3 *CLOSTRIDIUM DIFFICILE* GROWTH AND SURFACE LAYER PROTEINS ISOLATION

3. 1 INTRODUCTION

Surface Layer Proteins (SLPs) are the main components of the S-layer of *C. difficile*. There is high sequence variability of SLPs between different ribotypes (Mccoubrey & Poxton 2001; Calabi *et al.* 2001; Karjalainen *et al.* 2002). The differences in these surface antigens may contribute to immune evasion, resulting in some ribotypes causing more severe infection, while others are cleared efficiently by the immune system.

The colonisation of *C. difficile* is the primary step in the pathogenesis process. This includes adhesion to the host mucosal surface in the colon. However, the pathogen surface is also the first set of antigens that the host immune system encounters (Calabi & Fairweather 2002). The recognition of these antigens is crucial for eliciting an immune response and subsequent clearance of the bacterium. Strong serum IgG response to SLPs from *C. difficile* in patients' samples have indicated that SLPs are indeed recognised by the immune system (Eidhin *et al.* 2006) and therefore may be important in activating the immune response.

The surface of the *C. difficile* is covered by S-layer, regularly ordered planar array of proteins, located on the outside of the cell wall (Sleytr & Beveridge 1999). Proteins

of the S-layer are the most abundant of cellular proteins, suggesting their importance for the bacterium (Sára & Sleytr 2000). Unlike other S-layer proteins, SLPs of *C. difficile* are composed of two subunits, namely Low Molecular Weight (LMW) and High Molecular Weight (HMW) subunits (Calabi *et al.* 2001). These two biologically distinct entities are product of one gene product, *slpA*. The precursor protein is then cleaved into two mature subunits by Cwp84 (Bradshaw *et al.* 2014).

The LMW subunit appears to be the main immunogenic antigen with considerable sequence variability (Eidhin *et al.* 2006). The LWM subunit is positioned facing the outside environment and this likely affects its structure, as it is recognised by antibodies (Fagan *et al.* 2009). The sequence variability found in the LMW subunits of various ribotypes, was initially thought to reflect the pressure to evade the immune response. However, our group recently determined that the most virulent ribotypes with the most sequence variability in LMW subunit, are still recognised by the immune system and indeed elicit a more potent immune response (Lynch 2014, unpublished). This induces the inflammatory environment in the gut with neutrophil infiltration. This, altogether with toxin secretion, propagates colonic epithelium damage.

The HMW subunit is the anchor of the SLPs within the cell wall. The HMW subunit is relatively conserved and it is suspected to mediate the adhesion of the bacterium to host GI tissues (Calabi *et al.* 2002). While the S-layer plays an important role in protection of bacterium from outside factors, the SLPs from *C. difficile* have specifically been shown to be involved in adherence (Fagan & Fairweather 2014; Merrigan *et al.* 2013).

Additionally, the SLPs from *C. difficile* have been shown to elicit an immune response from immune cells such as macrophages (Collins *et al.* 2014), dendritic cells (Ryan *et al.* 2011) and monocytes (Ausiello *et al.* 2006). However, these studies focused on the effect of a single ribotype of *C. difficile* on these immune cells only. Given the sequence differences between strains of *C. difficile*, we aimed to assess the effects of SLPs isolated from multiple strains of *C. difficile* and determine these effects in colonic mucosal environment rather than the immune cells alone.

This chapter is comprised of two parts. First, the methods to isolate and purify the SLPs from *C. difficile* ribotypes 001, 002, 010, 014, 027, 046 and 078 needed to be developed and optimised as our group had only previously purified SLPs from *C. difficile* ribotype 001. These ribotypes were isolated from patients' samples by our collaborators at St. James's Hospital, in Sir Patrick Dunne Laboratory (Trinity College, Dublin).

The second part of this chapter investigated the colonic mucosal response *ex vivo* to two SLPs ribotypes. Here we aimed to demonstrate if SLPs from two clinically distant ribotypes, RT 001 and RT 027 were able to elicit different immune and mucosal response in colonic environment. In order to assess this, we examined expression of key inflammatory factors such as cytokines, chemokines and Toll-like receptors (TLRs), but also expression of mucosal integrity proteins such as tight junction and mucins.

3. 2 RESULTS

3. 2. 1 *Clostridium difficile* Growth

3. 2. 1. 1 Growth of *C. difficile* on the Surface of Blood Agar was Optimised.

The growth of *C. difficile* of ribotypes 001, 002, 010, 014, 027, 046 and 078 was observed only under strict anaerobic conditions, generated by use of the gas pack kit. Two setups of the anaerobic chamber were initially tested (first with the gas pack, which required the addition of 10 ml of water and a metal catalyst; second with the gas pack only). The second setup was found to be more reliable in generating anaerobic conditions. Removal of oxygen was monitored by the use of as anaerobe indicator test, which turned from pink to white in the absence of oxygen (under reducing conditions).

Upon streaking bacterial spores on the surface of blood agar, no growth was observed after 24 h or 48 h when anaerobic conditions were not maintained, as observed in Figure 3. 1 F. In this case, spores of RT 078 were streaked onto the surface of blood agar and the plate was placed in an anaerobic jar. However, the jar was not sealed properly and anaerobic conditions were not maintained.

Overall, spores from RT 001, RT 002, RT 010, RT 014, RT 017, RT 027, RT 046 and RT 078 were used in this study, and all ribotypes recovered well in anaerobic conditions (Figure 3. 1 A-E). Growing the bacterial culture on the surface of the blood agar plate was the first step of the SLP isolation. Initially three passages of bacterial streaking of 48 h were performed before proceeding to liquid culture. However, this was shortened to only one passage to avoid introducing any mutation that could have occurred during the extended period of incubation.

3. 2. 1. 2 Differences in Colony Morphologies were Observed Between *C. difficile* Ribotypes 001, 002, 014, 017, 027 and 078.

During the optimisation of *C. difficile* growth, we observed substantial differences in the colony morphology between different ribotypes. In order to compare the colony morphology between ribotypes, *C. difficile* RT 001, RT 002, RT 014, RT 017, RT 027 and RT 078 were streaked onto the surface of blood agar and were incubated for 48 h under previously described anaerobic conditions. The colony morphology is summarised in Table 3. 1 and described using the key in Figure 3. 2.

Ribotypes RT 001, RT 002, RT 017 and RT 027 appeared to have an irregular shape with undulate margins, while ribotype 014 was observed to have colonies of circular shape with an entire margin. Furthermore, RT 002, RT 014, RT 017 and RT 027 were observed to have flat elevation, rough texture and dull appearance, while RT 001 had slightly raised elevation, smooth texture and a glistening appearance. Colonies were either large (RT 002 or RT 017) or moderate (RT 001, RT 014 and RT 027) in size. All ribotypes had colonies of cream color and had opaque (RT 001 and RT 002) or translucent (RT 014, RT 017 and RT 027) optical properties.

3. 2. 1. 3 Growth of *C. difficile* in Liquid Broth Culture was Optimised.

To isolate SLPs, *C. difficile* was cultivated in liquid broth culture. The same anaerobic conditions as described in section 3. 2. 1 were applied (anaerobic jar and gas pack). The liquid broth culture required optimisation. Initially, a two-step culture was applied, in Fastidious Anaerobic Broth (FAB) to aid recovery of bacterial cells from solid medium to broth culture, followed by incubation in Brain Heart Infusion (BHI) to grow microbial cells in dense suspension. All ribotypes of *C. difficile* recovered well as suspended colonies after 24 h in FAB.

To aid removal of oxygen from BHI culture, the broth was freshly autoclaved, sodium thioglycolate was added, and finally the broth was incubated under anaerobic conditions for a minimum of 1 h. The growth in BHI broth depended on the ribotype. It was observed that RT 001, RT 002, RT 010, RT 014, RT 027 and RT 078 required an incubation time of 18 h to present turbid growth of OD ~0.8 to 1. In the case of RT 078, an 18 h incubation time caused the culture to precipitate into sediment. Therefore, the incubation time for this ribotype was shortened to 8 h (summarised in Table 3.2).

Furthermore, the total growth procedure (blood agar plate, FAB incubation and BHI incubation) was shortened by omitting the FAB culture. It was observed that all ribotypes recovered well upon inoculation from blood agar plate directly into BHI broth and it did not affect the growth rate, SLPs isolation, or final yield of SLPs of any ribotypes used in this study.

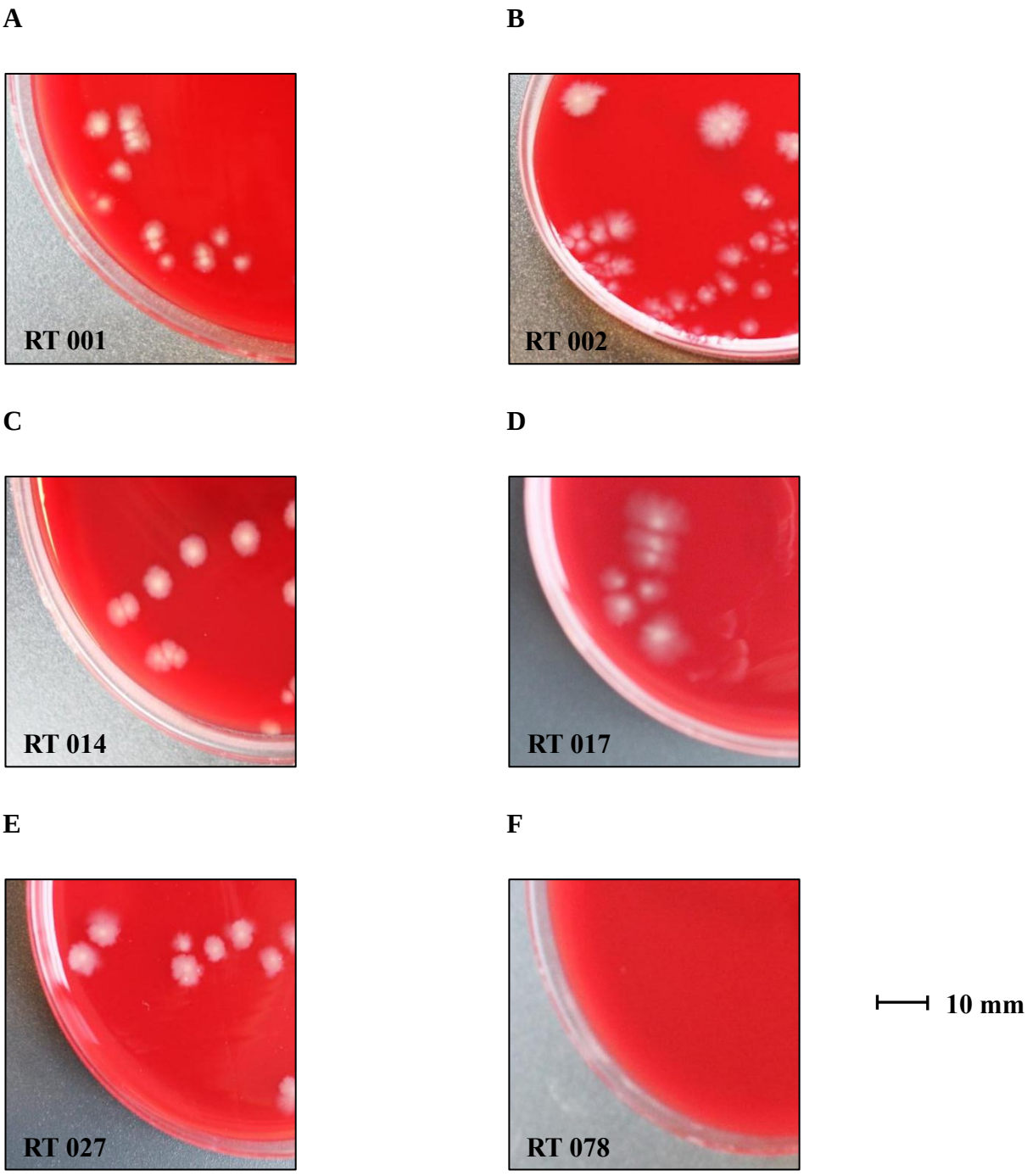

Figure 3. 1 Growth of RT 001, RT 002, RT 014, RT 017, RT 027 and RT 078 of *C. difficile* on the surface of blood agar plate. Bacterial spores were streaked on the surface of the blood agar and incubated in anaerobic conditions at 37°C for 48 h except for **F**, as this culture was maintained under aerobic conditions at 37°C for 48 h. Presented here are ribotype 001 (**A**), ribotype 002 (**B**), ribotype 014 (**C**), ribotype 017 (**D**), ribotype 027 and ribotype 078 (**F**). Differences in colony morphology are summarised in Table 3. 1.

Table 3. 1 Bacterial colony morphology of RT 001, RT 002, RT 014, RT 017, RT 027 and RT 078. Variations in bacterial morphology had been observed macroscopically. The general shape, margin, size, texture, appearance, pigmentation and optical property were determined by looking down at the top of the colony. The nature of colony elevation was determined when viewed from the side as the plate was held at the eye level.

Characteristics	001	002	014	017	027	078
Shape	Irregular	Irregular	Circular	Irregular	Irregular	Irregular
Margin	Undulate	Undulate	Entire	Undulate	Undulate	Undulate
Elevation	Raised	Flat	Flat	Flat	Flat	Flat
Size	Moderate	Large	Moderate	Large	Moderate	Moderate
Texture	Smooth	Rough	Rough	Rough	Rough	Rough
Appearance	Glistening	Dull	Dull	Dull	Dull	Dull
Pigmentation	Cream	Cream	Cream	Cream	Cream	Cream
Optical Property	Opaque	Opaque	Opaque	Translucent	Translucent	Translucent

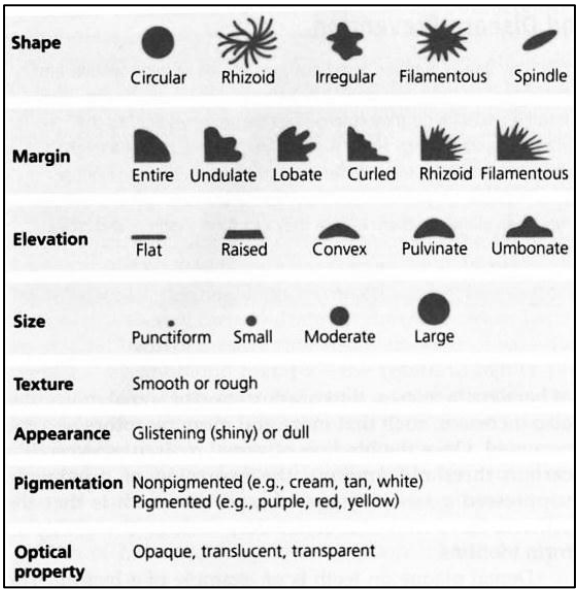

Figure 3. 2 Colony morphology key used to describe *C. difficile* ribotypes (adapted from Bauman 2012).

Table 3. 2 Time required for *C. difficile* BHI liquid culture incubation. All ribotypes required 18 h incubation to achieve OD of ~0.8 – 1, while RT 078 incubation was shortened to 8 h only, because of higher growth rate presented by this ribotype.

C. difficile Ribotype	Incubation Time
001	18 h
002	18 h
010	18 h
014	18 h
027	18 h
046	18 h
078	8 h

3. 2. 2 Crude SLPs RT 001, RT 002, RT 010, RT 014, RT 027 and RT 078 Were Purified by FPLC and Proteins Were Identified by SDS PAGE.

SLPs were isolated from the surface of *C. difficile* RT 001, RT 002, RT 010, RT 014, RT 027, RT 046 and RT 078 using an 8 M urea/20 mM Tris/HCl pH 8.5 method. Crude samples were dialysed to remove urea and were the subject of FPLC to isolate fractions containing SLPs. Proteins bound to the anion exchange chromatography column were washed off by an increasing NaCl gradient depending on the size and affinity of the column. To ensure maximum resolution of protein fractions in the crude sample and to prevent loss of the protein of interest, the slope of the NaCl gradient was optimised experimentally for each ribotype used in this study.

To confirm the protein identity, fractions collected during FPLC were run on SDS PAGE (10% w/v) and stained with Coomassie Brilliant Blue. SLPs are composed of two subunits, High Molecular Weight (HMW; approximately 55 kDa) and Lower Molecular Weight (LMW; approximately 35 kDa) and fractions containing both protein subunits were identified by the appearance of those two bands.

3. 2. 2. 1 Purification of RT 001.

Purification of crude SLPs RT 001 with FPLC was optimised to maximise the yield. Initially fractionation was carried out with two intervals of NaCl gradient, ten column volumes from 0% to 50% NaCl gradient, followed by four column volumes from 50% to 100% (Figure 3. 3). This resulted in good resolution between peaks as confirmed by SDS PAGE analysis (Figure 3. 5 A-B). However, fractions B2-B8 (corresponding to peak eluting at 37 min), contained only LMW subunit, while fractions containing both subunits eluted at 42 min (B10 – C5). To prevent subunit dissociation, the S-layer isolation procedure was changed. When whole microbial

cells were incubated with 8 M urea/20 mM Tris/HCl pH 8.5 in a shaking incubator, we suspected that LMW subunits dissociated on their own (as they are presented on the outermost on the surface). Therefore, the shaking incubator was avoided in favour of a steady incubator and dissociation of the LMW subunit was no longer observed in any isolation of SLPs from any ribotype. The same purification procedure (same NaCl gradient) was applied and SLPs eluted at 49 min (Figure 3. 4) and SDS PAGE analysis confirmed that those fractions contained both subunits (B8 – B14, Figure 3. 5 C).

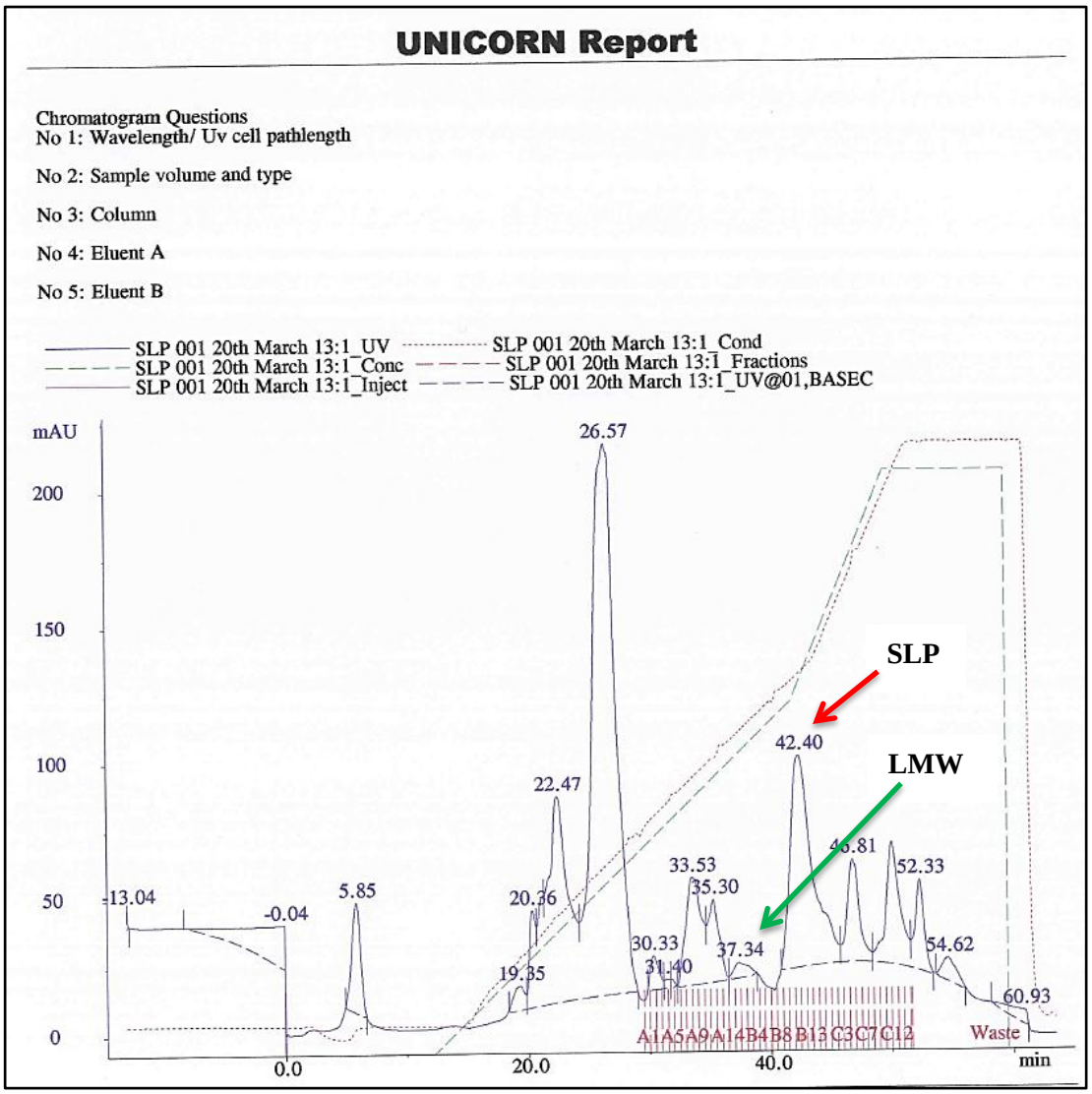

Figure 3. 3 Optimising FPLC purification of SLPs RT 001. The gradient of buffer B was set between two intervals, five column volumes at 0-50% NaCl and four column volumes at 50-100% NaCl. It resulted in steep gradient and low resolution between eluted peaks. First large peak had retention time of 26 min (not collected). Two peaks were eluted around 40 min, one at 37 min, corresponded to LMW subunit and second peak at 42 min corresponding to SLPs (confirmed by SDS PAGE analysis, Figure 3. 5 A–B), dissociation of subunits was caused by different incubation conditions during SLPs isolation. UNICORN™ 3.21v Chromatogram legend: Blue line: protein concentration measured by UV light absorption at 280 nm (mAU); Green dashed line: concentration of NaCl gradient (Buffer B), from 0% to 100%; Red dotted line: NaCl concentration measured by conductivity (mS/cm); Red dashed line (A1-C12): collected fractions.

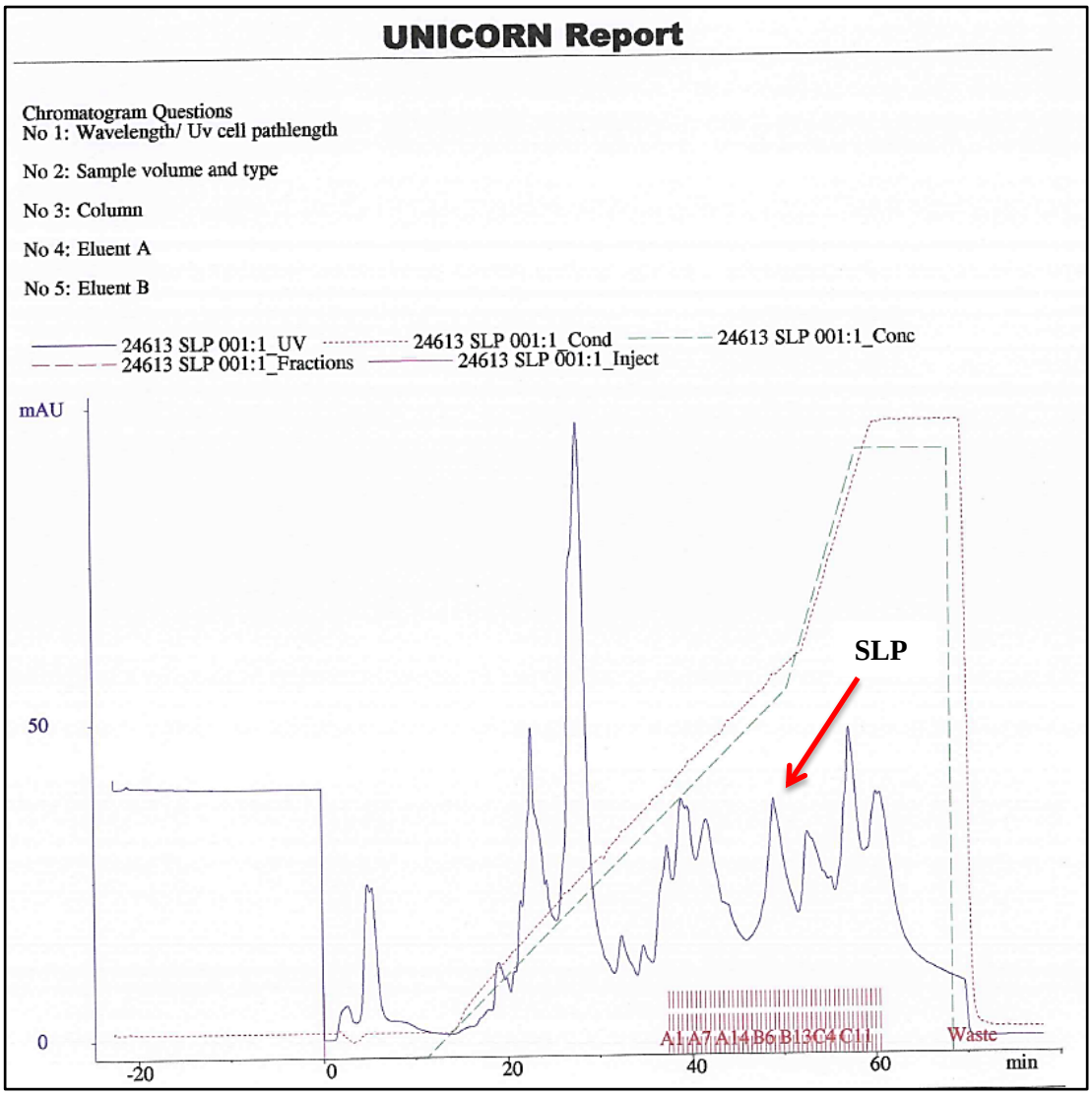

Figure 3. 4 FPLC purification of crude of SLPs RT 001. The gradient of buffer B was set between two intervals, twenty column volumes at 0-50% NaCl and four column volumes at 50-100% NaCl. It resulted in good resolution between the peaks, SLPs fraction eluted at 49 min. SDS PAGE analysis confirmed identity of SLPs and purity of the fraction collected (Figure 3. 5 C). UNICORN™ 3.21v Chromatogram legend: Blue line: protein concentration measured by UV light absorption at 280 nm (mAU); Green dashed line: concentration of NaCl gradient (Buffer B), from 0% to 100%; Red dotted line: NaCl concentration measured by conductivity (mS/cm); Red dashed line (A1-C11): collected fractions.

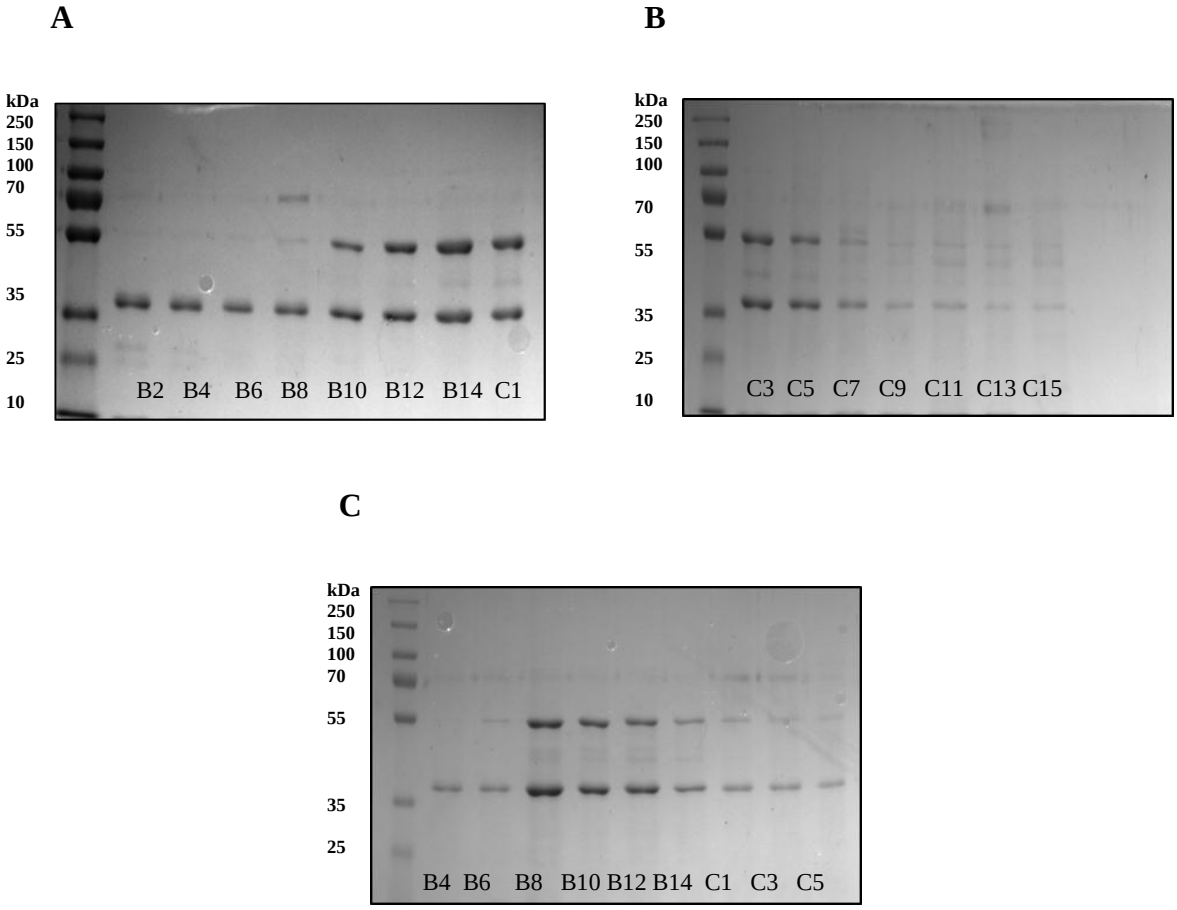

Figure 3. 5 SDS PAGE was used to confirm identity of SLPs RT 001. Isolated SLPs were purified using liquid chromatography. To confirm the identity of proteins isolated from the culture, fractions were run on 10% SDS polyacrylamide gels and stained with Coomassie Brilliant Blue. Two bands represent Higher Molecular Weight (HMW; top) and Lower Molecular Weight (LMW; bottom) subunits of SLPs, any other bands observed are considered impurities of surface isolation. Fractions containing two bands were processed further. Three figures above represent different purification approaches. **A and B**: Fractions B2-B8 contained only LMW subunit that dissociated separately during S-layer isolation on shaking incubator, SLPs fractions are easily identified (B10 – C15) however impurities are also observed due to steep NaCl gradient. **C**: Under optimised conditions of isolation and purification, high purity fractions are easily identified (B8 – B14).

3. 2. 2. 2 Purification of RT 002.

Purification of crude SLPs RT 002 with FPLC was experimentally optimised. Formerly, it was observed that initially detected proteins were just minor proteins and peptides. Therefore, 50% NaCl over ten column volumes was applied from the beginning of purification to wash off all the proteins that were not of interest and speed up the process. It was followed by steadily increasing the NaCl gradient from 50% to 100% NaCl over four column volumes (Figure 3. 6). This resulted in extremely low resolution between fractions as only two peaks were detected during purification. The first peak eluted at 5 min and was very large (70 mAU), indicating a high concentration of protein content was lost in waste effluent. However, this peak was not collected to confirm the identity of proteins. The second peak eluted at 37 min, however, the concentration was low as observed by FPLC (10 mAU) and confirmed by SDS PAGE, as very faint bands were observed (A8 – A10, Figure 3. 8 A).

During the optimised FPLC purification, 50% NaCl was applied over five column volumes, then changed to increase gradually to 60% NaCl over two column volumes and then to 100% over four column volumes (Figure 3. 7). As a result, good resolution between peaks was observed and the purity of SLP fractions was confirmed by SDS PAGE (A8 – B1, Figure 3. 8 B).

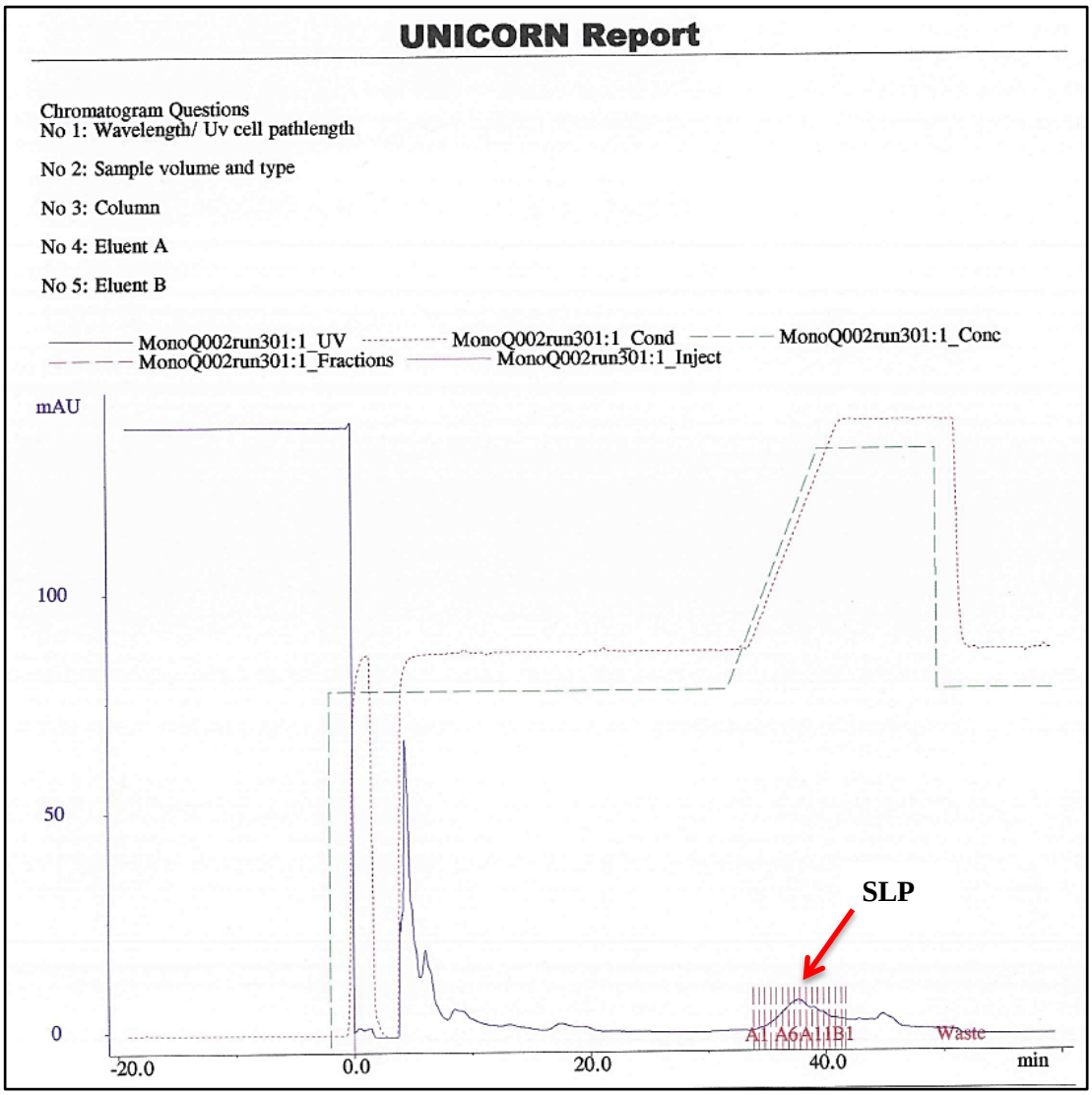

Figure 3. 6 Optimising FPLC purification of SLPs RT 002. The gradient of buffer B was set between two intervals, ten column volumes at 50% NaCl and four column volumes at 50-100% NaCl. It resulted in a large peak eluting at 5 min, while second peak had retention time of 37 min and very low protein concentration. Also, very small numbers of fractions were set to be collected (A1-B1). This chromatogram corresponds to SDS PAGE analysis (Figure 3. 8 A). UNICORN™ 3.21v Chromatogram legend: Blue line: protein concentration measured by UV light absorption at 280 nm (mAU); Green dashed line: concentration of NaCl gradient (Buffer B), from 0% to 100%; Red dotted line: NaCl concentration measured by conductivity (mS/cm); Red dashed line (A1 – B1): collected fractions.

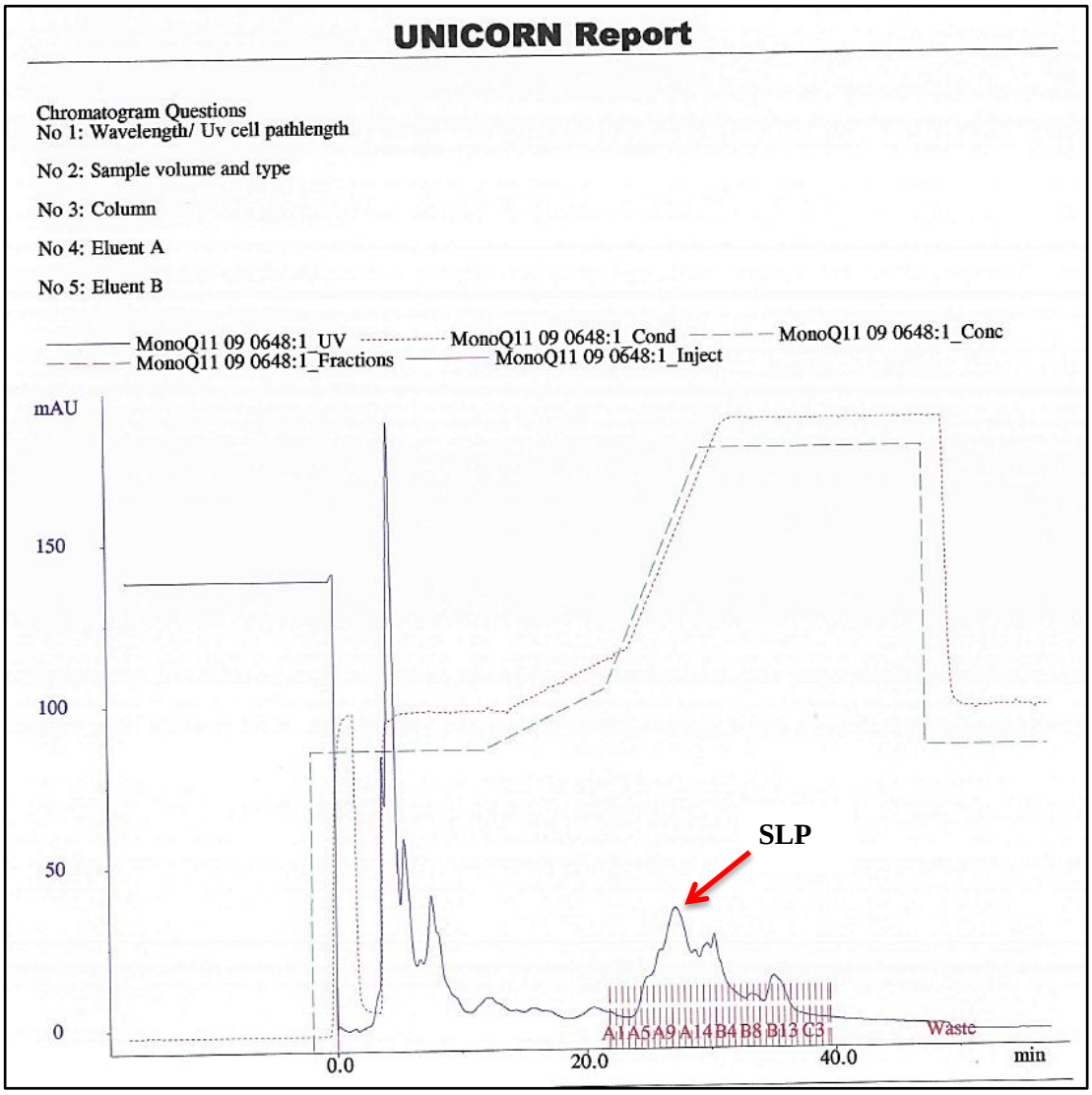

Figure 3. 7 FPLC purification of crude of SLPs RT 002. The gradient of buffer B was set between three intervals, five column volumes at 50% NaCl, two column volumes at 50-60% and four column volumes at 60-100% NaCl. It resulted in large peak eluting at 5 min. With this elution profile SLPs has retention time of 27 min. Identity of the protein was confirmed by SDS PAGE analysis (Figure 3. 8 B). UNICORN™ 3.21v Chromatogram legend: Blue line: protein concentration measured by UV light absorption at 280 nm (mAU); Green dashed line: concentration of NaCl gradient (Buffer B), from 0% to 100%; Red dotted line: NaCl concentration measured by conductivity (mS/cm); Red dashed line (A1 – C3): collected fractions.

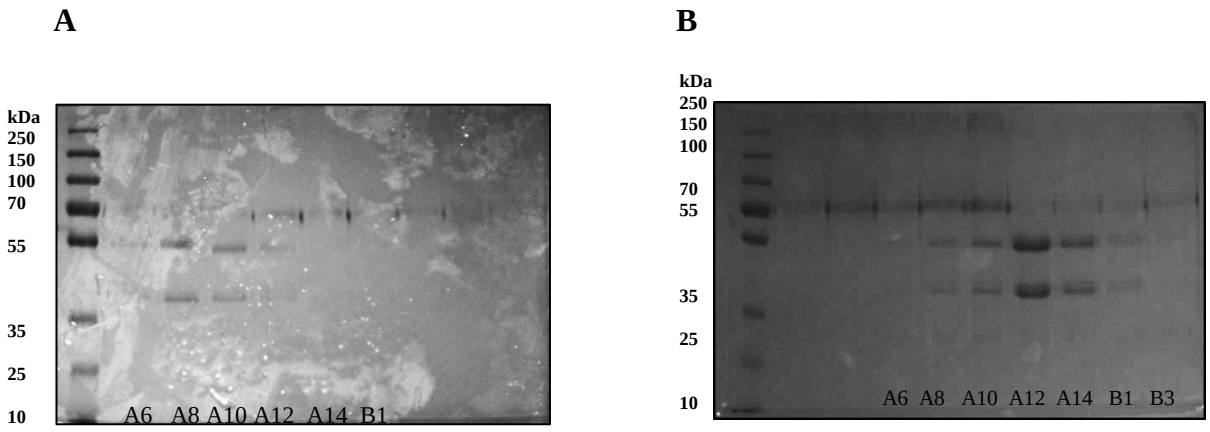

Figure 3. 8 SDS PAGE was used to confirm identity of SLPs RT 002. Isolated SLPs were purified using liquid chromatography. To confirm the identity of proteins isolated from the culture, fractions were run on 10% SDS polyacrylamide gels and stained with Coomassie Brilliant Blue. Two bands represent Higher Molecular Weight (HMW; top) and Lower Molecular Weight (LMW; bottom) subunits of SLPs, any other bands observed are considered impurities of surface extraction. Fractions containing two bands were processed further. Two figures above represent different purification approaches. **A**: Low concentration of protein was observed (B5 – B7); **B**: Under optimised conditions of isolation and purification, high purity fractions are easily identified (A8 – B1).

3. 2. 2. 3 Purification of RT 010.

The purification of crude SLPs RT 010 with FPLC was experimentally optimised. Formerly, it was determined that initially detected proteins are just minor proteins and peptides. Therefore, 50% NaCl over ten column volumes was applied from the beginning of the purification to wash off all the proteins that were not of interest. It was followed by steadily increasing the gradient from 50% to 100% NaCl over four column volumes (Figure 3. 9). This resulted in extremely low resolution between fractions as only two peaks were detected during purification. The first peak eluted at 5 min and was very large (200 mAU), indicating a high concentration of protein content was lost in the waste effluent. However, this peak was not collected to confirm the identity of proteins. The second peak eluted at 60 min, however the concentration was low as observed by FPLC (25 mAU) and confirmed by SDS PAGE, with very faint bands being observed (A13 – A15, Figure 3. 11 A). Furthermore, the software was set to collect only small number of fractions, which resulted in some of the SLPs peak to be eluted in waste effluent (Figure 3. 9, fractions eluting >60 min were not collected).

During optimised FPLC purification, the NaCl gradient was applied in two intervals, first from 0% to 50% over twenty column volumes and from 50% to 100% over four column volumes (Figure 3. 10). This resulted in high resolution between peaks and the purity of SLP fractions was confirmed by SDS PAGE analysis (A13 – B4, Figure 3. 11 B).

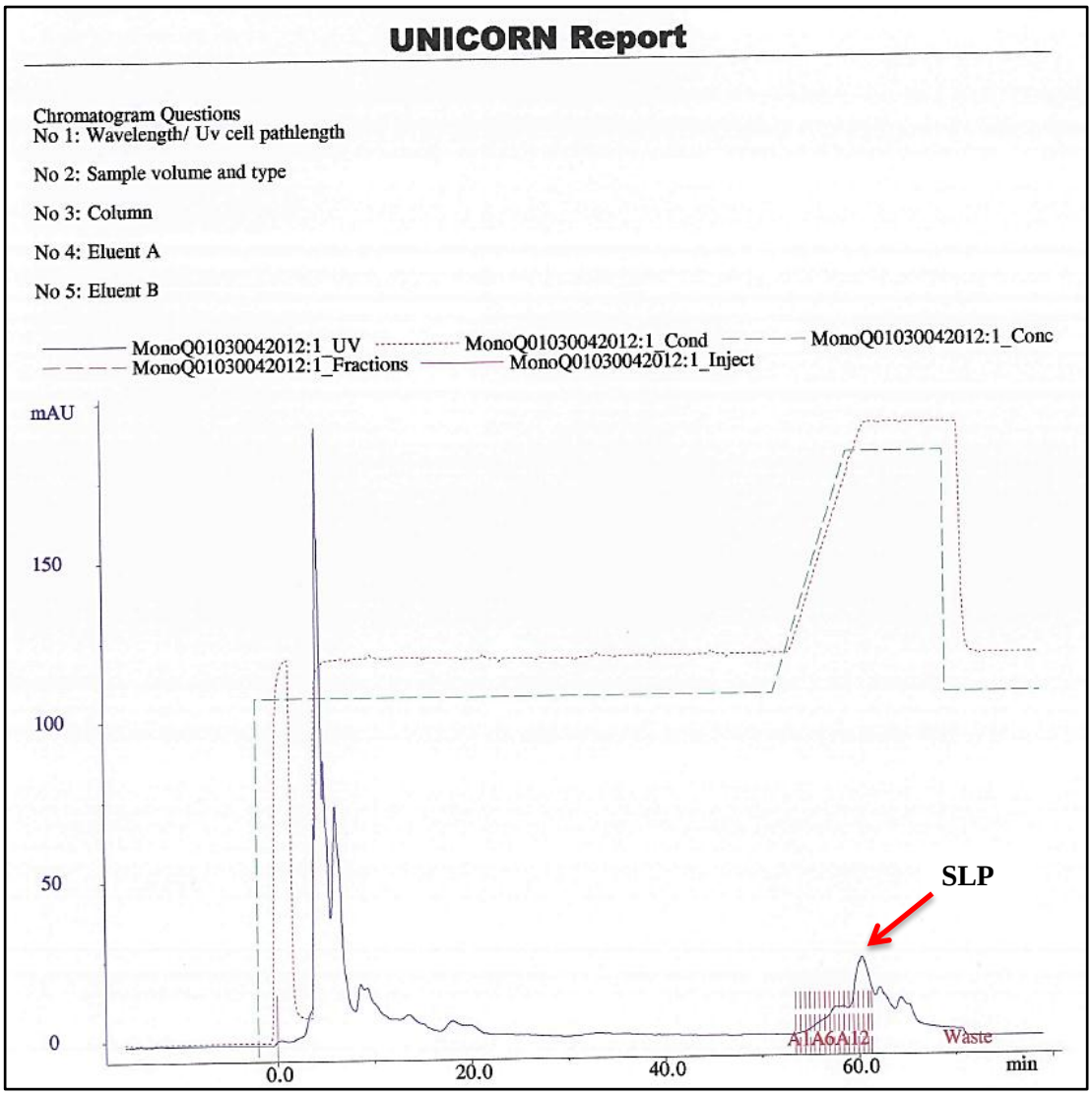

Figure 3. 9 Optimising FPLC purification of SLPs RT 010. The gradient of buffer B was set between two intervals, twenty column volumes at 50% NaCl and four column volumes at 50-100% NaCl. It resulted in large peak eluting at 5 min, while second peak had retention time of 60 min. Also, a very small number of fractions were set to be collected (A1-A12), resulting in some of the effluent being lost in waste. This chromatogram corresponds to SDS PAGE analysis (Figure 3. 11 A). UNICORN™ 3.21v Chromatogram legend: Blue line: protein concentration measured by UV light absorption at 280 nm (mAU); Green dashed line: concentration of NaCl gradient (Buffer B), from 0% to 100%; Red dotted line: NaCl concentration measured by conductivity (mS/cm); Red dashed line (A1 – A12): collected fractions.

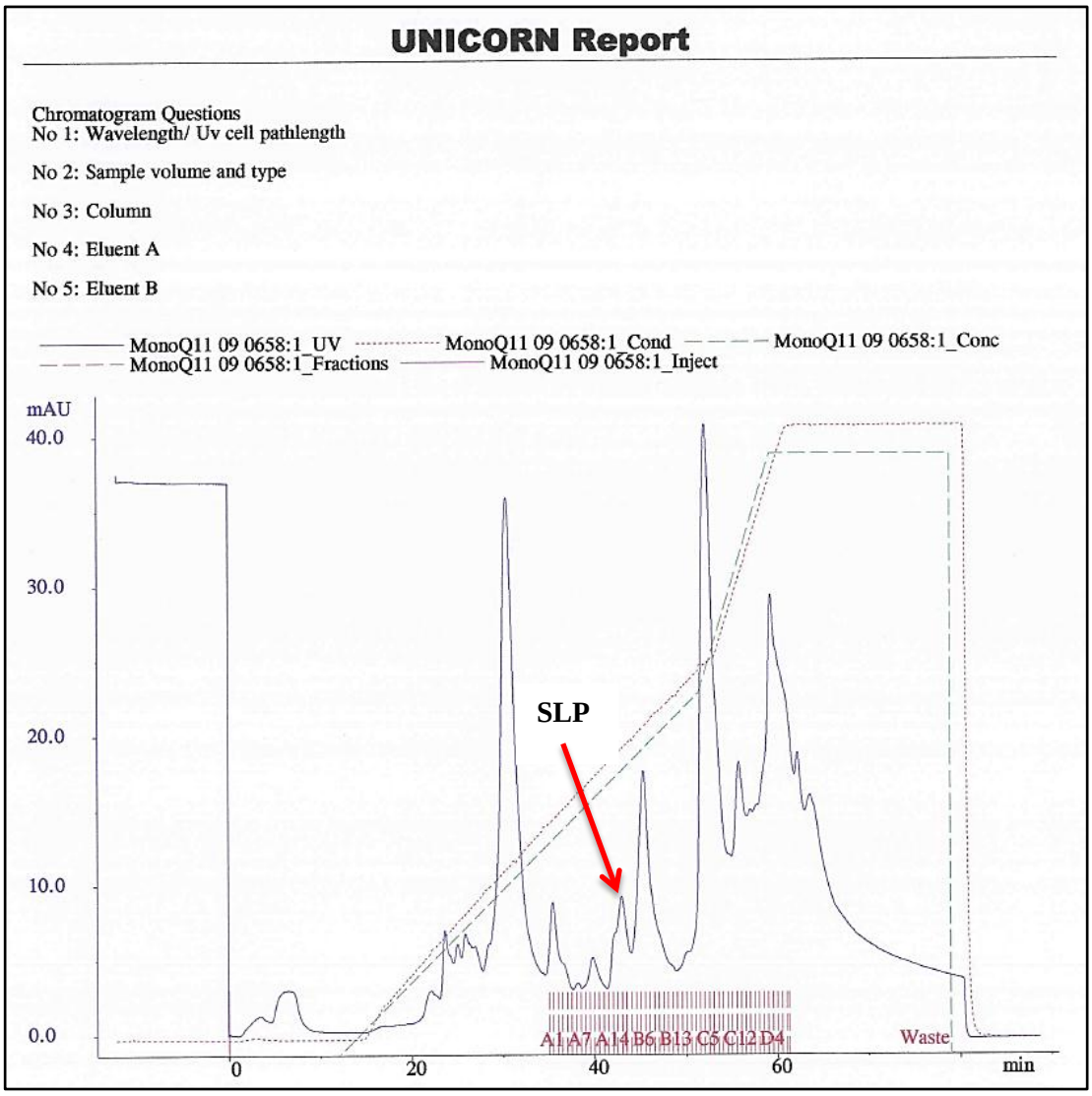

Figure 3. 10 FPLC purification of crude of SLPs RT 010. The gradient of buffer B was set between two intervals, twenty column volumes at 0-50% NaCl and four column volumes at 50-100% NaCl. It resulted in a large peak eluting at 30 min, which was not collected. With this elution profile SLPs has retention time of 43 min. Identity of the protein was confirmed by SDS PAGE analysis (Figure 3. 11 B). UNICORN™ 3.21v Chromatogram legend: Blue line: protein concentration measured by UV light absorption at 280 nm (mAU); Green dashed line: concentration of NaCl gradient (Buffer B), from 0% to 100%; Red dotted line: NaCl concentration measured by conductivity (mS/cm); Red dashed line (A1 – D4): collected fractions.

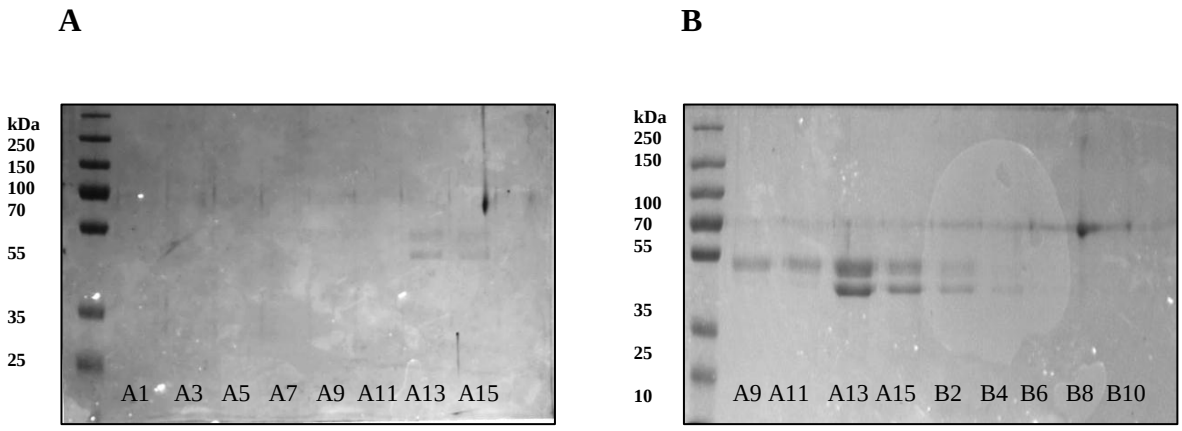

Figure 3. 11 SDS PAGE was used to confirm identity of SLPs RT 010. Isolated SLPs were purified using liquid chromatography. To confirm the identity of proteins isolated from the culture, fractions were run on 10% SDS polyacrylamide gels and stained with Coomassie Brilliant Blue. Two bands represent Higher Molecular Weight (HMW; top) and Lower Molecular Weight (LMW; bottom) subunits of SLPs, any other bands observed are considered impurities of surface extraction. Fractions containing two bands were processed further. Two figures above represent different purification approaches. **A**: Very low concentration of SLPs was observed (A13 – A15); **B**: Under optimised conditions of isolation and purification, high purity fractions are easily identified (A13 – B4).

3. 2. 2. 4 Purification of RT 014.

The purification of crude SLP RT 014 with FPLC was experimentally optimised. Initially fractionation was carried out with two intervals of NaCl gradient, ten column volumes from 0% to 50% NaCl gradient, followed by four column volumes from 50% to 100% (Figure 3. 12). This was sufficient to produce high resolution between peaks and SLPs eluted at 57 min. However, due to prolonged storage of the crude SLPs, concentration yielded was very low (20 mAU). High purity of fractions and low protein concentration was confirmed by SDS PAGE analysis (A5 – A9, Figure 3. 14 A).

During optimised FPLC purification, 50% NaCl was applied but only over five column volumes, then changed to increase gradually to 60% NaCl over two column volumes and then to 100% over four column volumes (Figure 3. 13). This produced sufficient resolution between peaks and resulted in high purity fractions with 27 min retention time for SLPs (70 mAU). Purity and high concentration was confirmed by SDS PAGE analysis (A9 – A13, Figure 3. 14 B).

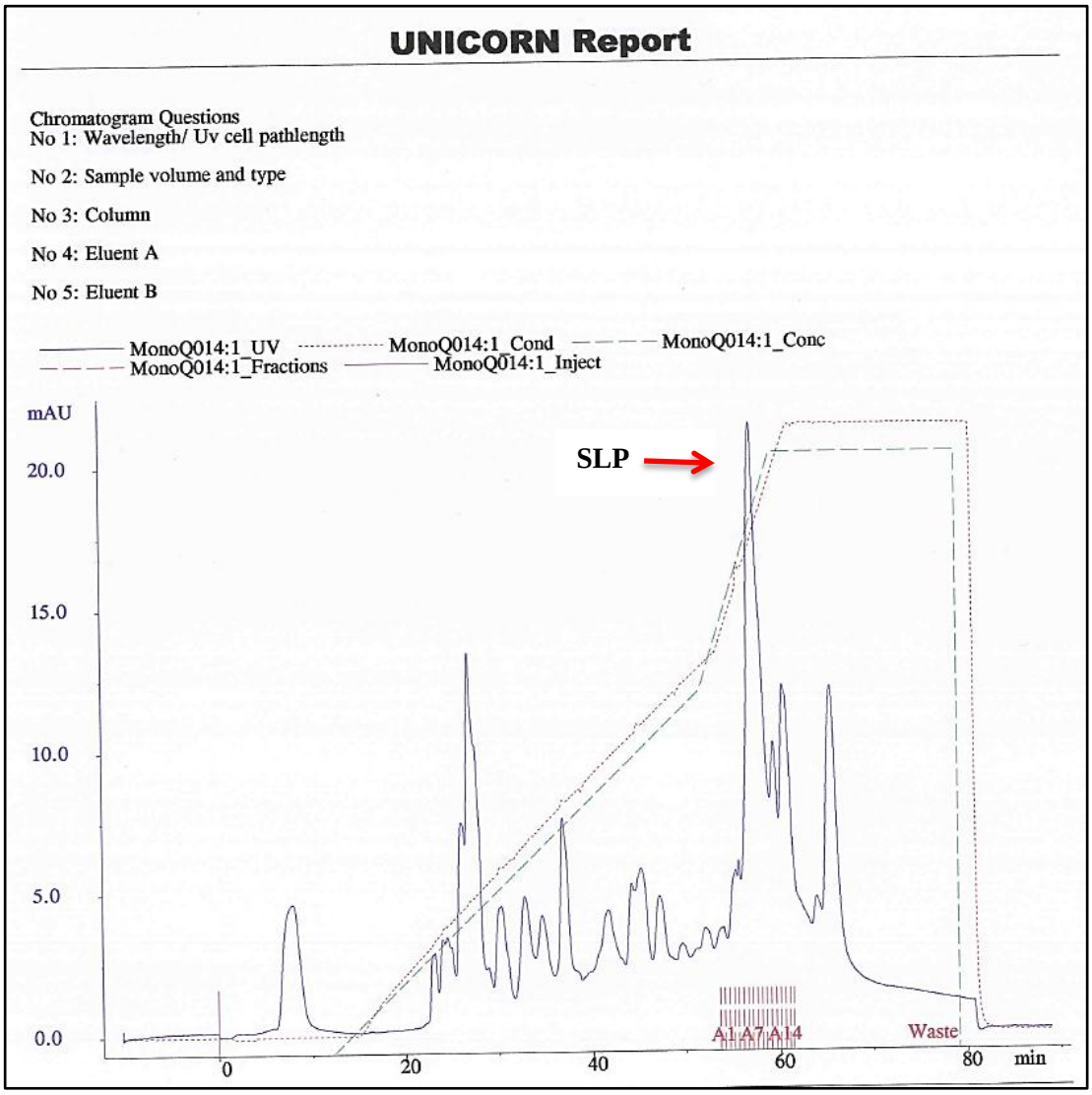

Figure 3. 12 Optimising FPLC purification of SLPs RT 014. The gradient of buffer B was set between two intervals, twenty column volumes at 0-50% NaCl and four column volumes at 50-100% NaCl. It resulted in multiple peaks eluting, SLPs had a retention time of 57 min. Overall protein concentration was very low due to prolonged storage. This chromatogram corresponds to SDS PAGE analysis (Figure 3. 14 A). UNICORN™ 3.21v Chromatogram legend: Blue line: protein concentration measured by UV light absorption at 280 nm (mAU); Green dashed line: concentration of NaCl gradient (Buffer B), from 0% to 100%; Red dotted line: NaCl concentration measured by conductivity (mS/cm); Red dashed line (A1 – A14): collected fractions.

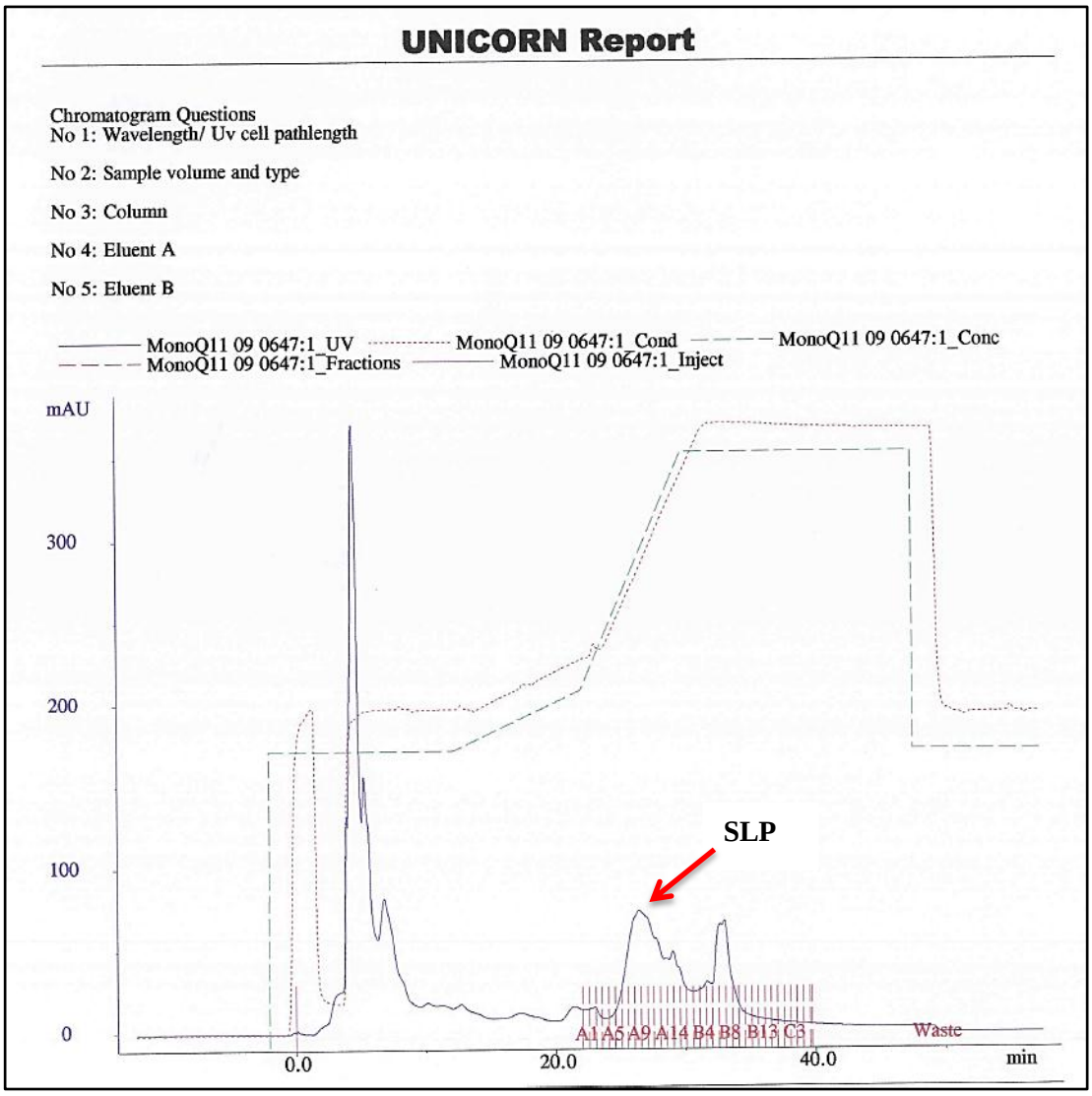

Figure 3. 13 FPLC purification of crude of SLPs RT 014. The gradient of buffer B was set with three intervals, five column volumes at 50% NaCl, two column volumes at 50-60% and four column volumes at 60-100% NaCl. It resulted in large peak eluting at 5 min, not collected. With this elution profile SLPs has retention time of 27 min. Identity of the protein was confirmed by SDS PAGE analysis (Figure 3. 14 A). UNICORN™ 3.21v Chromatogram legend: Blue line: protein concentration measured by UV light absorption at 280 nm (mAU); Green dashed line: concentration of NaCl gradient (Buffer B), from 0% to 100%; Red dotted line: NaCl concentration measured by conductivity (mS/cm); Red dashed line (A1 – C3): collected fractions.

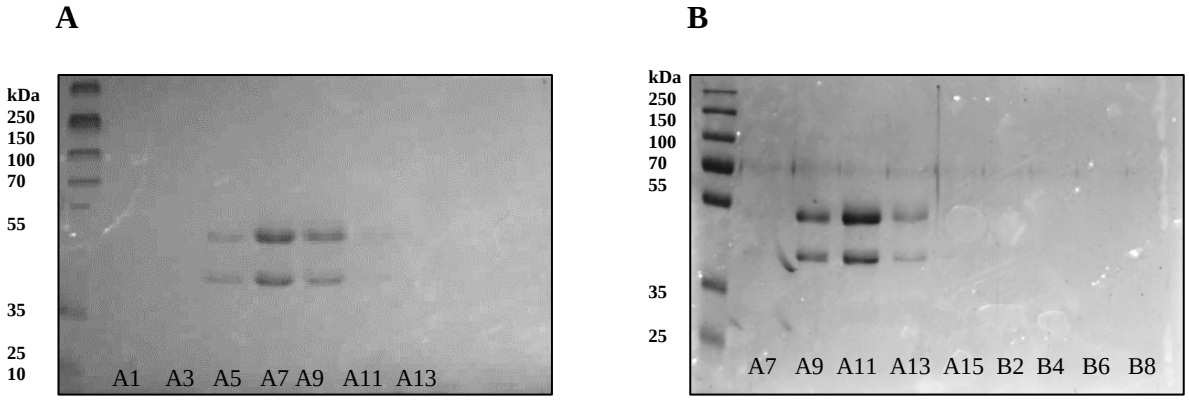

Figure 3. 14 SDS PAGE was used to confirm identity of SLPs RT 014. Isolated SLPs were purified using liquid chromatography. To confirm the identity of proteins isolated from the culture, fractions were run on 10% SDS polyacrylamide gels and stained with Coomassie Brilliant Blue. Two bands represent Higher Molecular Weight (HMW; top) and Lower Molecular Weight (LMW; bottom) subunits of SLPs, any other bands observed are considered impurities of surface extraction. Fractions containing two bands were processed further. Four figures above represent different purification approaches. **A**: Low concentration of protein was observed (A10-A14). **B**: Under optimised conditions of isolation and purification, high purity fractions are easily identified (A9 – A13).

3. 2. 2. 5 Purification of RT 027.

The purification of crude SLPs RT 027 with FPLC was experimentally optimised. Initially fractionation was carried out with two intervals of NaCl gradient, twenty column volumes from 0% to 50% NaCl, followed by four column volumes from 50% to 100% (Figure 3. 15). High resolution between fractions was achieved, however SDS PAGE analysis showed that SLP dissociated from the surface in two fractions, first peak eluting at 37 min and corresponding to LMW subunit (A11 – A13, Figure 3. 17 A) and second peak eluting at 39 min with whole SLP (A15 – B15, Figure 3. 17 A-B). When whole microbial cells were incubated with 8 M urea/20 mM Tris/HCl pH 8.5 in a shaking incubator, we suspect that LMW subunits dissociated on their own (as they are presented on the outermost on the surface). Therefore, the shaking incubator was avoided in favour of a steady incubator and dissociation of the LMW subunit was no longer observed in any isolation of SLPs from any ribotype. When the isolation procedure was changed, the same purification procedure was applied (same NaCl gradient), SLPs eluted at 40 min (Figure 3. 16) and SDS PAGE analysis confirmed that those fractions contained both subunits (A9 – A15, Figure 3. 17 C).

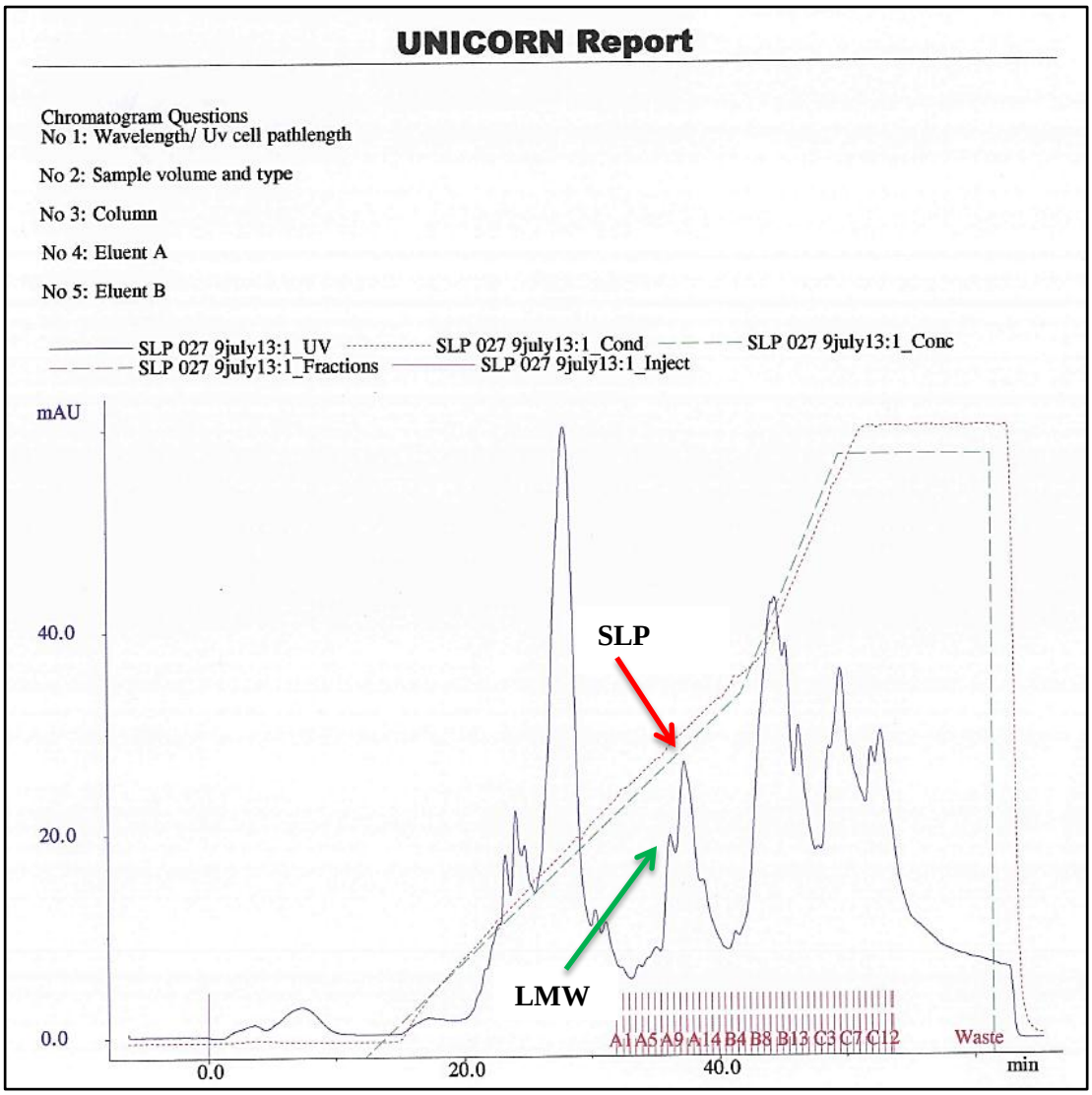

Figure 3. 15 Optimising FPLC purification of SLPs RT 027. The gradient of buffer B was set between two intervals, ten column volumes at 0-50% NaCl and four column volumes at 50-100% NaCl. It resulted in high resolution between the peaks. Large peak with retention time of 29 min was not collected. Two peaks were eluted around 40 min, one at 37 min, corresponded to LMW subunit and second peak at 39 min corresponding to SLPs (confirmed by SDS PAGE analysis, Figure 3. 17 A – B), dissociation of subunits was possibly caused by different incubation conditions during SLPs isolation. UNICORN™ 3.21v Chromatogram legend: Blue line: protein concentration measured by UV light absorption at 280 nm (mAU); Green dashed line: concentration of NaCl gradient (Buffer B), from 0% to 100%; Red dotted line: NaCl concentration measured by conductivity (mS/cm); Red dashed line (A1 – A12): collected fractions.

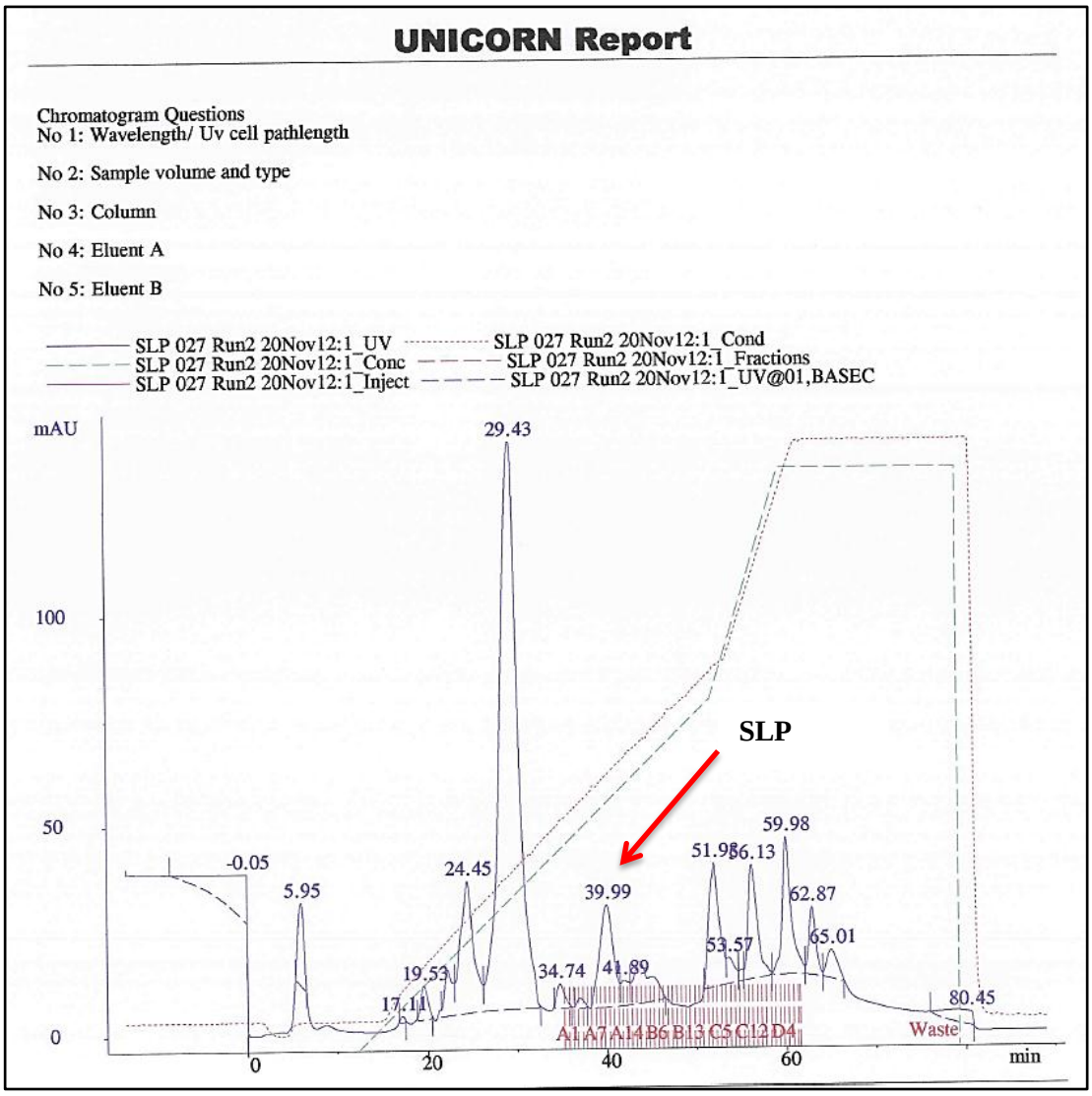

Figure 3. 16 FPLC purification of crude of SLPs RT 027. The gradient of buffer B was set between two intervals, twenty column volumes at 0-50% NaCl and four column volumes at 50-100% NaCl. It resulted in large peak eluting at 30 min, not collected. With this elution profile SLPs has retention time of 40 min. Identity of the protein was confirmed by SDS PAGE analysis (Figure 3.17 C). UNICORN™ 3.21v Chromatogram legend: Blue line: protein concentration measured by UV light absorption at 280 nm (mAU); Green dashed line: concentration of NaCl gradient (Buffer B), from 0% to 100%; Red dotted line: NaCl concentration measured by conductivity (mS/cm); Red dashed line (A1 – D4): collected fractions.

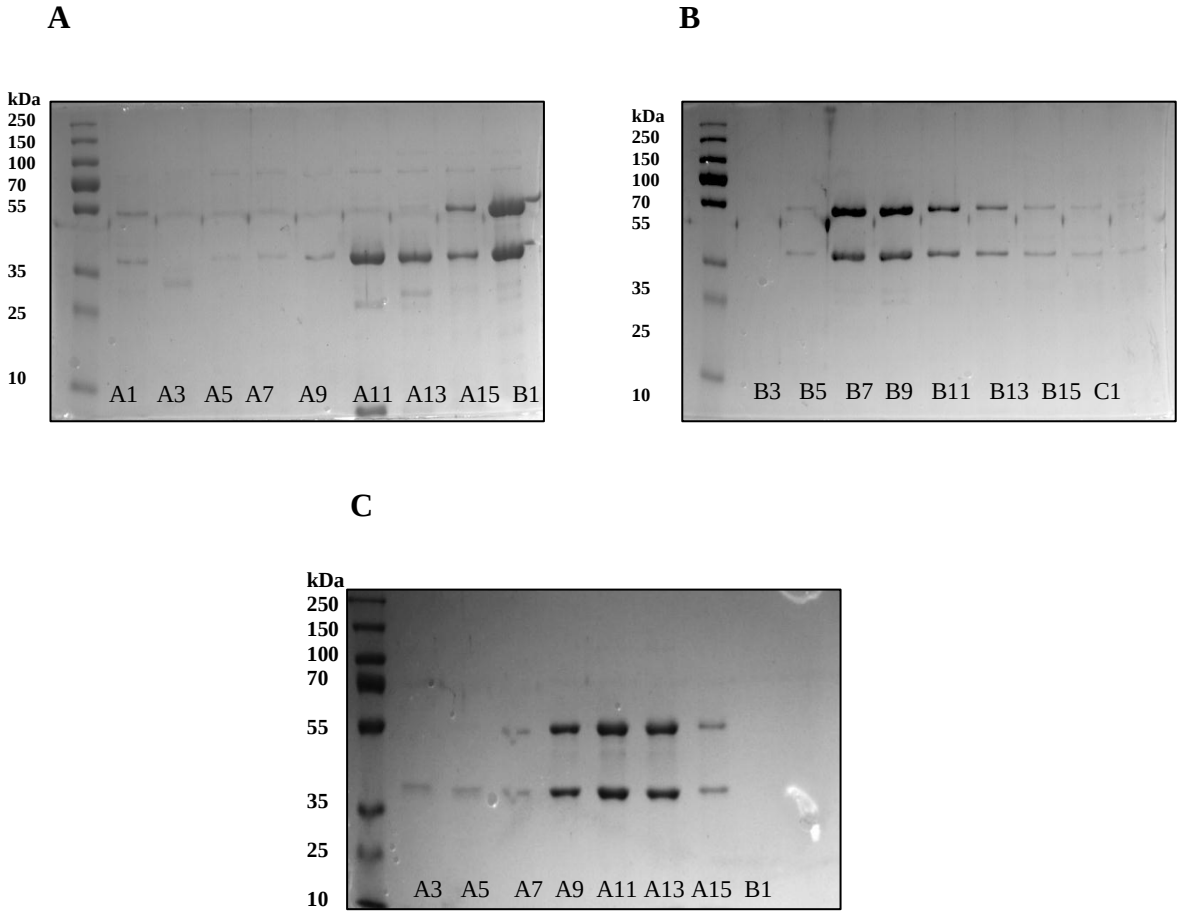

Figure 3. 17 SDS PAGE was used to confirm identity of SLPs RT 027. Isolated SLPs were purified using liquid chromatography. To confirm the identity of proteins isolated from the culture, fractions were run on 10% SDS polyacrylamide gels and stained with Coomassie Brilliant Blue. Two bands represent Higher Molecular Weight (HMW; top) and Lower Molecular Weight (LMW; bottom) subunits of SLPs, any other bands observed are considered impurities of surface extraction. Fractions containing two bands were processed further. Three figures above represent different purification approaches. **A** and **B**: Fractions A11 – A13 contained only LMW that dissociated separately during S-layer isolation on shaking incubator, but high purity fractions of SLPs can also be observed (A15 – B1; B3 – B15); **C**: Under optimised conditions of isolation and purification, high purity fractions are easily identified (A7 – A15).

3. 2. 2. 6 Purification of RT 046.

The purification of crude SLP RT 046 with FPLC was experimentally optimised. Initially fractionation was carried out with two intervals of NaCl gradient, ten column volumes from 0% to 50% NaCl, followed by four column volumes from 50% to 100% (Figure 3. 18). This resulted in a steep gradient of NaCl, which would be insufficient to separate fractions of proteins. However, due to prolonged storage, protein concentration was extremely low (all detected peaks <10mAU). Fractions containing SLPs were identified with SDS PAGE analysis however very faint bands confirmed very low protein concentration (A13 – B1, Figure 3. 20 A and B).

During optimised FPLC purification, 50% NaCl was applied but only over five column volumes, then changed to increase gradually to 60% NaCl over two column volumes and then to 100% over four column volumes (Figure 3. 19). This resulted in good resolution between peaks and retention time for SLP at 28 min. High protein concentration was detected (50 mAU) and was confirmed by SDS PAGE analysis (A15 – B11, Figure 3. 20 C and D).

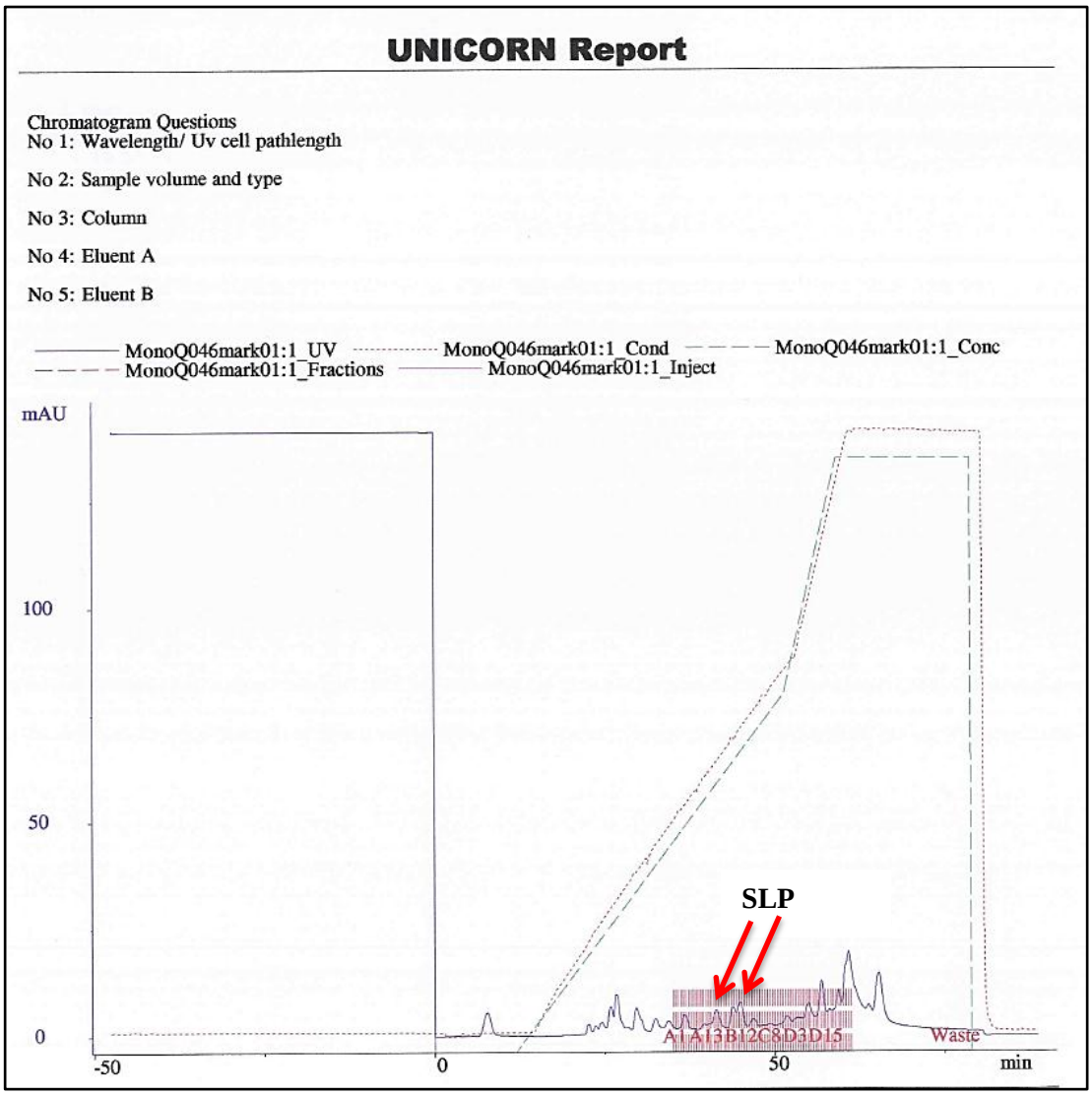

Figure 3. 18 Optimising FPLC purification of SLPs RT 046. The gradient of buffer B was set between two intervals, ten column volumes at 0-50% NaCl and four column volumes at 50-100% NaCl. It resulted in very low concentration of proteins, possibly due to prolonged storage at -20°C. This chromatogram corresponds to SDS PAGE analysis (Figure 3. 20 A – B). UNICORN™ 3.21v Chromatogram legend: Blue line: protein concentration measured by UV light absorption at 280 nm (mAU); Green dashed line: concentration of NaCl gradient (Buffer B), from 0% to 100%; Red dotted line: NaCl concentration measured by conductivity (mS/cm); Red dashed line (A1 – D15): collected fractions.

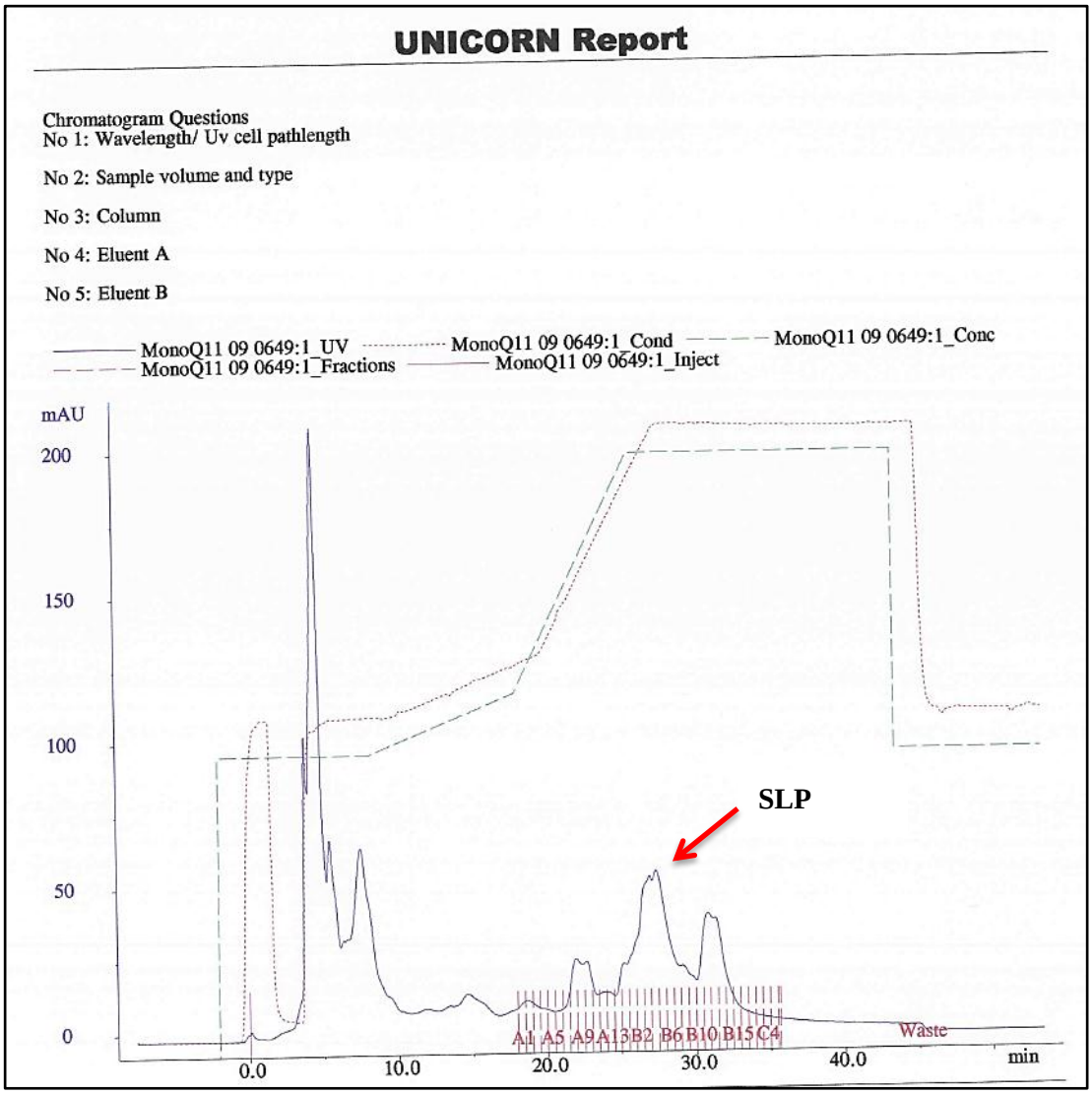

Figure 3. 19 FPLC purification of crude of SLPs RT 046. Gradient of buffer B was set between three intervals, five column volumes at 50% NaCl, five column volumes at 50-60% and four column volumes at 60-100% NaCl. It resulted in large peak eluting at 5 min, not collected. With this elution profile SLPs has retention time of 28 min. Identity of the protein was confirmed by SDS PAGE analysis (Figure 3. 20 C – D) UNICORN™ 3.21v Chromatogram legend: Blue line: protein concentration measured by UV light absorption at 280 nm (mAU); Green dashed line: concentration of NaCl gradient (Buffer B), from 0% to 100%; Red dotted line: NaCl concentration measured by conductivity (mS/cm); Red dashed line (A1 – C4): collected fractions.

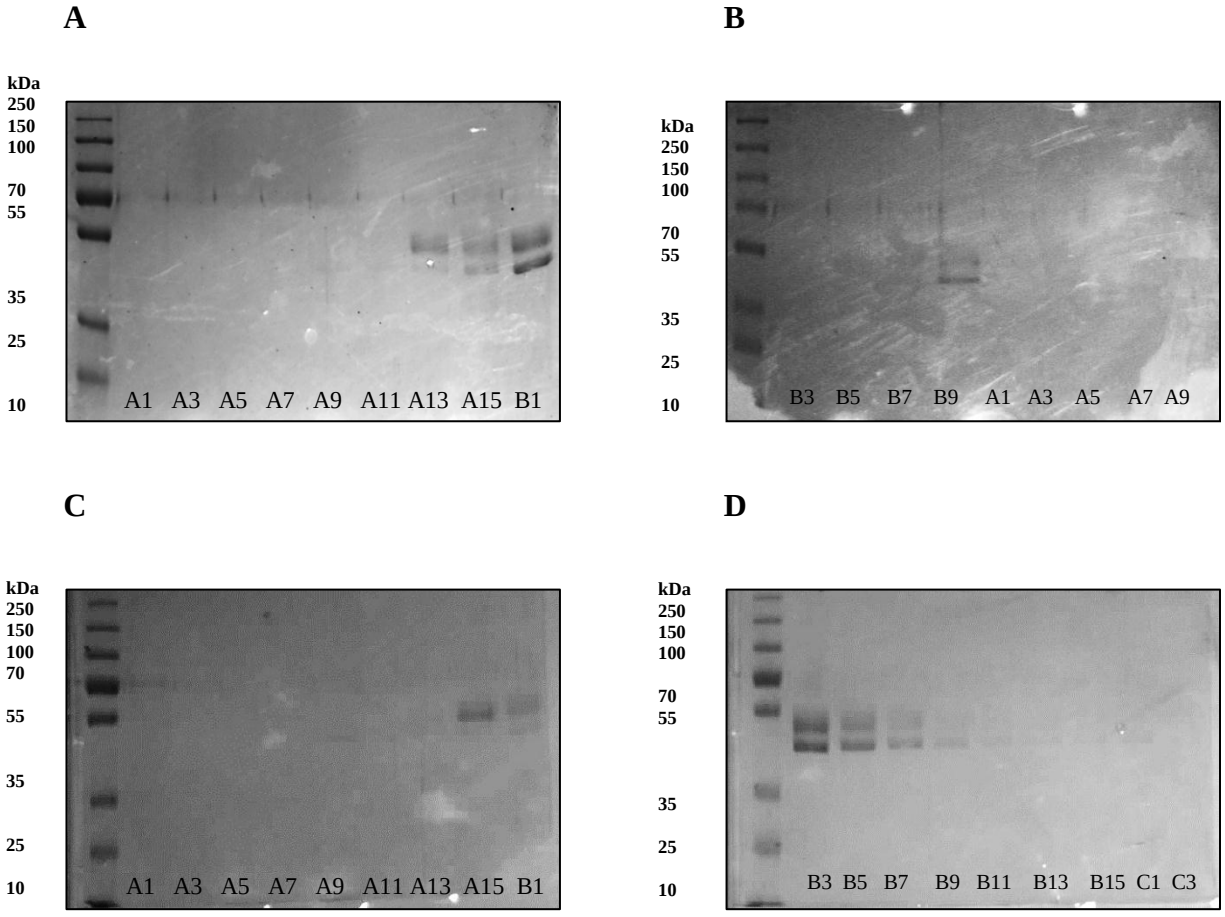

Figure 3. 20 SDS PAGE was used to confirm identity of SLPs RT 046. Isolated SLPs were purified using liquid chromatography. To confirm the identity of proteins isolated from the culture, fractions were run on 10% SDS polyacrylamide gels and stained with Coomassie Brilliant Blue. Two bands represent Higher Molecular Weight (HMW; top) and Lower Molecular Weight (LMW; bottom) subunits of SLPs, any other bands observed are considered impurities of surface extraction. Fractions containing two bands were processed further. Four figures above represent different purification approaches. **A and B**: Low concentration of SLPs was observed (A15-B1; B9); **C and D**: Under optimised conditions of isolation and purification, high purity fractions are easily identified (A15 – B7).

3. 2. 2. 7 Purification of RT 078.

The purification of crude SLP ribotype 078 with FPLC was experimentally optimised. A unique FPLC profile was observed when purifying crude preparation of RT 078 isolated from precipitated bacterial sediment. Two main peaks were observed, first at 30 min, the second peak eluted at 56 min (Figure 3. 21). Because this profile was not consistent with any other profile observed before, those samples were abandoned and not used for further analysis. Purification of crude preparation of RT 078 from optimised broth culture (BHI incubation for 8 h) is presented on Figure 3. 22. However, steep gradient from 0 to 100% NaCl over only ten column volumes caused low resolution between peaks. SDS PAGE analysis confirmed presence of impurities in fractions on interests (B1 – C3, Figure 3. 24 A – B).

During optimised FPLC purification, the NaCl gradient was applied in two intervals, first from 0% to 50% over twenty column volumes and from 50% to 100% over four column volumes (Figure 3. 23). This resulted in high resolution between peaks, SLP eluted at 49 min. The purity of SLP fractions was confirmed by SDS PAGE analysis (B12 – C5, Figure 3. 24 D).

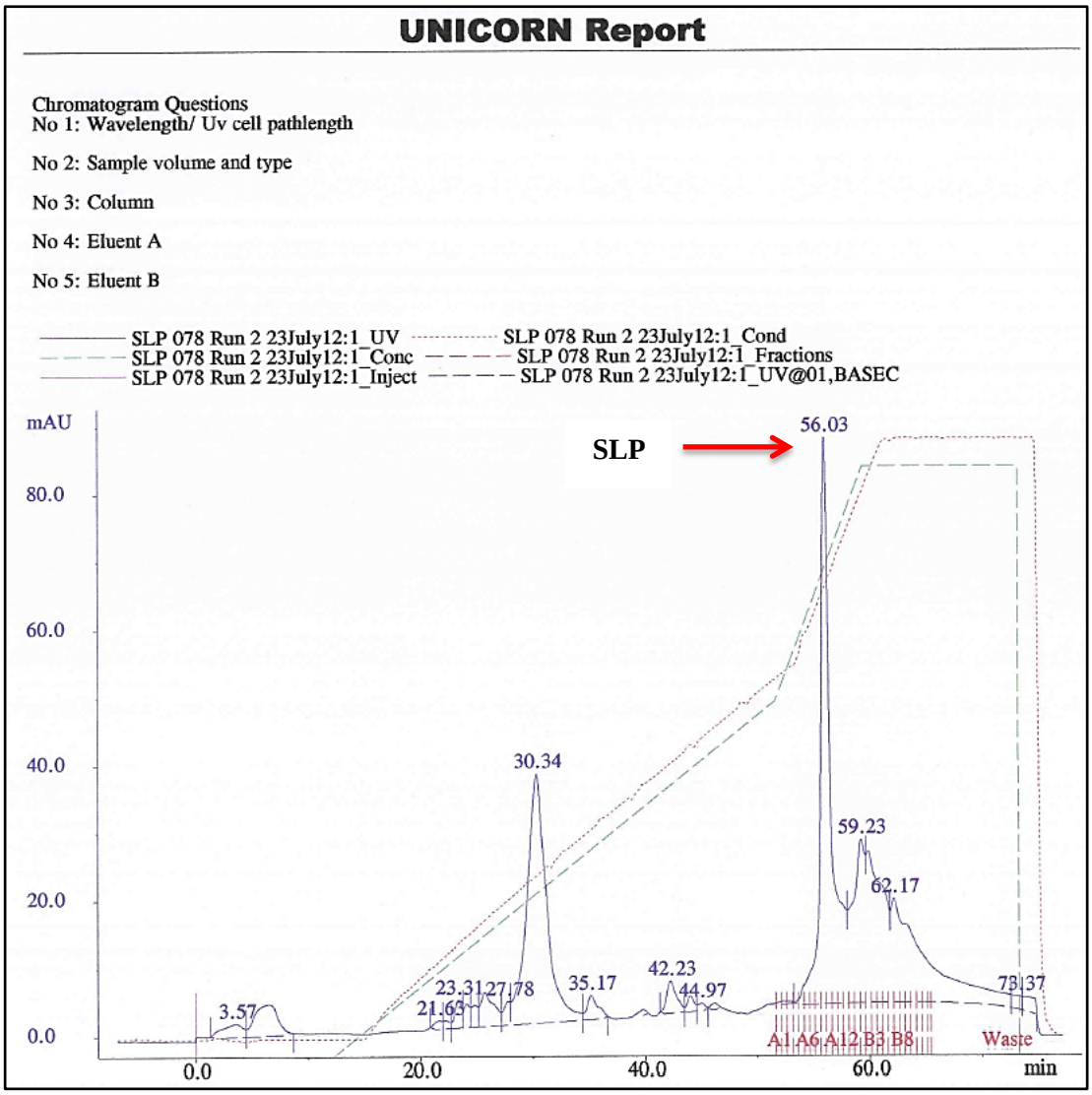

Figure 3. 21 Optimising FPLC purification of SLPs RT 078. The gradient of buffer B was set between two intervals, ten column volumes at 0-50% NaCl and four column volumes at 50-100% NaCl. Broth culture growth resulted in precipitated bacterial sediment, due to bacterial aggregation or death of bacterial culture. Characteristic FPLC profile was observed, two main peaks eluting, first with retention time of 30 min and second peak with retention time of 56 min. These SLPs were not used in this study and were disposed. UNICORN™ 3.21v Chromatogram legend: Blue line: protein concentration measured by UV light absorption at 280 nm (mAU); Green dashed line: concentration of NaCl gradient (Buffer B), from 0% to 100%; Red dotted line: NaCl concentration measured by conductivity (mS/cm); Red dashed line (A1 – B8): collected fractions.

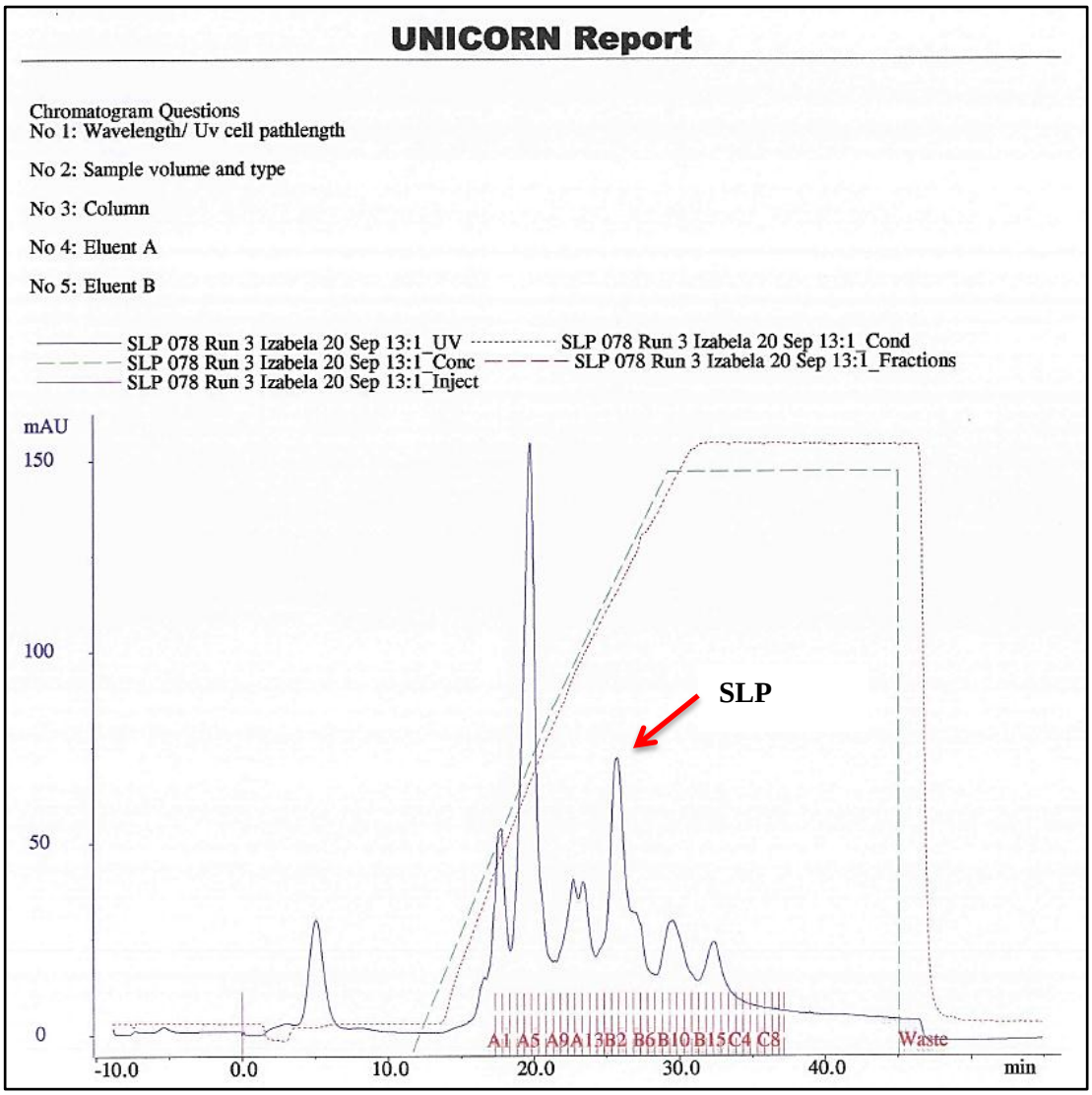

Figure 3. 22 Optimising FPLC purification of SLPs RT 078. The gradient of buffer B was set to one interval, ten column volumes at 0-100% NaCl. It resulted in multiple the peaks observed, however the resolution between fractions was not satisfactory and multiple bands were observed on SDS PAGE analysis (Figure 3. 24 A – B) UNICORN™ 3.21v Chromatogram legend: Blue line: protein concentration measured by UV light absorption at 280 nm (mAU); Green dashed line: concentration of NaCl gradient (Buffer B), from 0% to 100%; Red dotted line: NaCl concentration measured by conductivity (mS/cm); Red dashed line (A1 – C8): collected fractions.

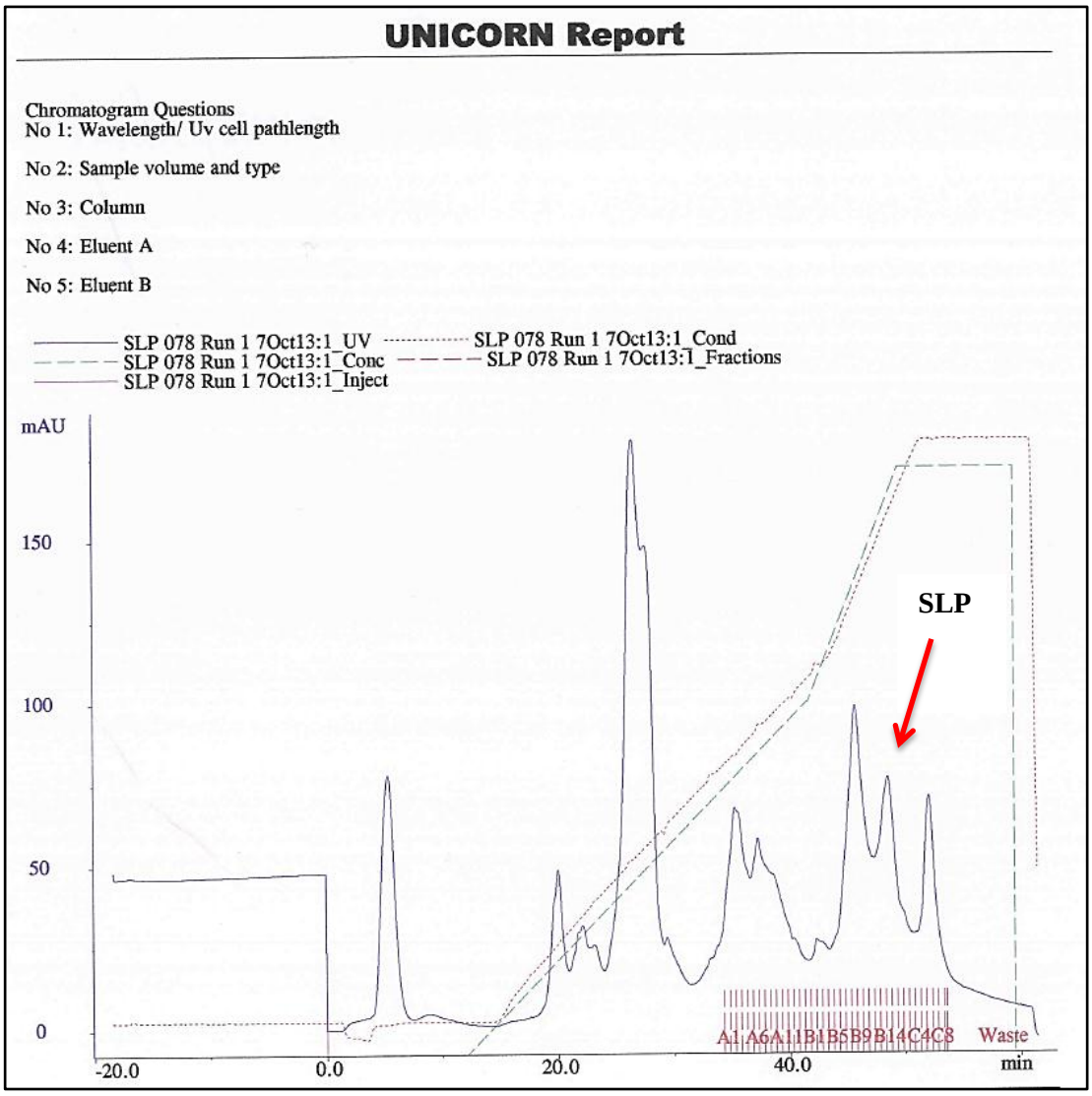

Figure 3. 23 FPLC purification of crude of SLPs RT 078. The gradient of buffer B was set between in one interval, ten column volumes at 0-100% NaCl. It resulted in multiple the peaks eluting, SLPs fraction eluted at 49 min. SDS PAGE analysis confirmed identity of SLPs and purity of the fraction collected (Figure 3. 24 D). UNICORN™ 3.21v Chromatogram legend: Blue line: protein concentration measured by UV light absorption at 280 nm (mAU); Green dashed line: concentration of NaCl gradient (Buffer B), from 0% to 100%; Red dotted line: NaCl concentration measured by conductivity (mS/cm); Red dashed line (A1 – C8): collected fractions.

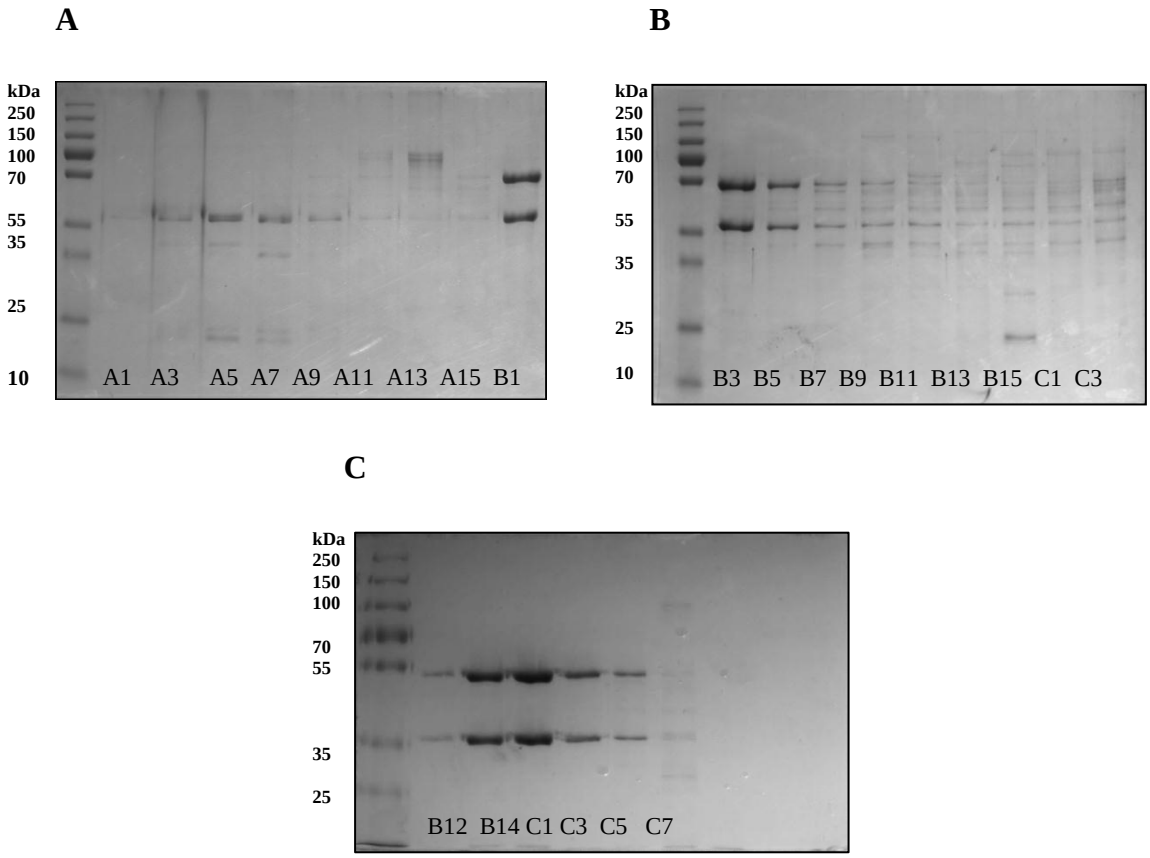

Figure 3. 24 SDS PAGE was used to confirm identity of SLPs RT 078. Isolated SLPs were purified using liquid chromatography. To confirm the identity of proteins isolated from the culture, fractions were run on 10% SDS polyacrylamide gels and stained with Coomassie Brilliant Blue. Two bands represent Higher Molecular Weight (HMW; top) and Lower Molecular Weight (LMW; bottom) subunits of SLPs, any other bands observed are considered impurities of surface extraction. Fractions containing two bands were processed further. Three figures above represent different purification approaches. **A** and **B**: High concentration of SLPs however impurities observed due to steep NaCl gradient applied during the purification (B1 – C3); **C**: Under optimised conditions of isolation and purification, high purity fractions are easily identified (B14 – C3).

3. 2. 2. 8 FPLC Purification Profile of SLPs Was Optimised.

Two methods of SLP purification were optimised experimentally; this included the adjustment of the NaCl gradient and volume of buffer B. This is summarised in Table 3. 2. The first method allowed for SLP fractions to elute at 27 min, while the second method allowed for SLPs to be eluted at 40 min. Both methods proved to be sufficient to purify SLPs from a crude sample and provided good resolution between eluting peaks. Also, it was noticed that both methods could be applied to all ribotypes used in this study. The second method was chosen for any future purification of all ribotypes to decrease any inconsistencies in the procedure.

Table 3. 3 Optimised SLPs purification methods. Two methods to purify SLPs with FPLC were identified. Both methods were identified as reliable to produce satisfactory yield and good resolution between fractions. Method 2 was choses for any future purifications of all ribotypes to omit any inconsistencies in the procedure.

Purification Method	NaCl Gradient (% Buffer B) and Column volumes (CV) applied			SLP Retention (min)
	Interval I	Interval II	Interval III	
Method 1	50%	50 – 60%	60 – 100%	27 min
	5 CV	2 CV	4 CV	
Method 2	0 – 50%	50 – 100%	-	40 min
	20 CV	4 CV	-	

3. 2. 3 SLPs From RT 001 and RT 027 Induced Different Responses from Colonic Tissue *Ex Vivo*.

To examine the mucosal immune response to SLPs of various ribotypes, colon explants were cultured *ex vivo* and stimulated with purified SLPs RT 001 and RT 027. Parameters measured included gene expression of inflammation and mucosal integrity markers. Colon was sourced from female C57BL/6J mice and cultured in the presence of LPS or SLPs from RT 001 and RT 027

3. 2. 3. 1 SLPs RT 001 and RT 027 Induced Changes in Expression of Inflammatory Markers *Ex Vivo*.

After 6 h incubation, total RNA was harvested from the tissue. RT qPCR was then carried out to examine the expression of genes involved in maintaining the colonic immune response, such as cytokines (Figure 3. 25), chemokines (Figure 3. 26), and TLRs (Figure 3. 27). It was determined that in cases of all inflammatory cytokines (Figure 3.25), RT 001 and RT 027 stimulated the gene expression differently. This included increased expression of proinflammatory cytokines *Il23*, *Il2*, *Il6* ($p<0.05$), and *Il17a* and anti-inflammatory cytokine *Il10* when stimulated with SLPs RT 027. The stimulation with RT 001 did not change expression of *Il23* and *Il6*, it also decreased expression *Il10* and *Il17a*. Only expression of *Il2* was induced by SLPs of both ribotypes. Expression of cytokines *Tnfa* ($p<0.05$) and *Tgfb* ($p<0.01$) was decreased significantly by stimulation in case of both RT 001 and RT 027. Responses to the LPS stimulation resulted in decrease of cytokines, except for the *Il2*, *Tnfa* and *Tgfb*, which were upregulated. In the case of chemokines (Figure 3.26), RT 001 and RT 027 also presented different profile of expression. *Ccl3* (MIP1α) was induced 3-fold by stimulation with SLP RT 027 ($p<0.05$), while

stimulation with SLP RT 001, presented 1.5-fold change. The increase induced by SLP RT 027 proved to be significant relative to control ($p<0.05$) and to SLP RT 001 ($p<0.05$). In the case of *Cxcl2* (MIP2α), there was 3-fold increase in expression when stimulated with SLP RT 027, while there was 0.2-fold decrease when stimulated with SLP RT 001. The increase induced by SLP RT 027 also proved to be significant relative to control ($p<0.05$) and to SLP RT 001 ($p<0.05$). Expression of *Ccl2* (MCP1) was decreased by stimulation with both SLPs, however significance was not observed. Expression of *Ccl5* (RANTES) was also decreased by both SLPs, 0.1-fold by SLP RT 001 and 0.75-fold by SLP RT 027. There was significance decrease of *Ccl5* (RANTES) relative to control ($p<0.05$), LPS ($p<0.05$) and RT 001 ($p<0.05$). The stimulation with LPS resulted in decrease of expression of all chemokine genes under investigation. Overall, the stimulation with RT 001 resulted in decreased expression relative to RT 027 and this difference was significant in expression of chemokines genes *Ccl3* (MIP1α), *Cxcl2* (MIP2α) and *Ccl5* (RANTES).

TLRs also presented different profiles of expression when stimulated with SLPs of the two ribotypes. The expression of *Tlr2*, *Tlr4*, *Tlr5* and *Tlr9* was induced when stimulated with SLP RT 027 (15-fold, 1.5-fold, 6-fold and 3-fold, respectively). In contrast, stimulation with SLP RT 001 resulted in relatively lower induction of *Tlr2* and *Tlr9* (1.5-fold in both cases) and decrease of expression of *Tlr4* and *Tlr5* (0.5-fold in both cases). This included significant difference in decrease between RT 001 and RT 027 in expression of *Tlr2* ($p<0.05$). LPS stimulation resulted in increase of expression of *Tlr2* and *Tlr9*, 2-fold and 3-fold respectively, and decrease of expression fo *Trl5* (0.1-fold). There was a minor change in expression of *Tlr4* when stimulated with LPS.

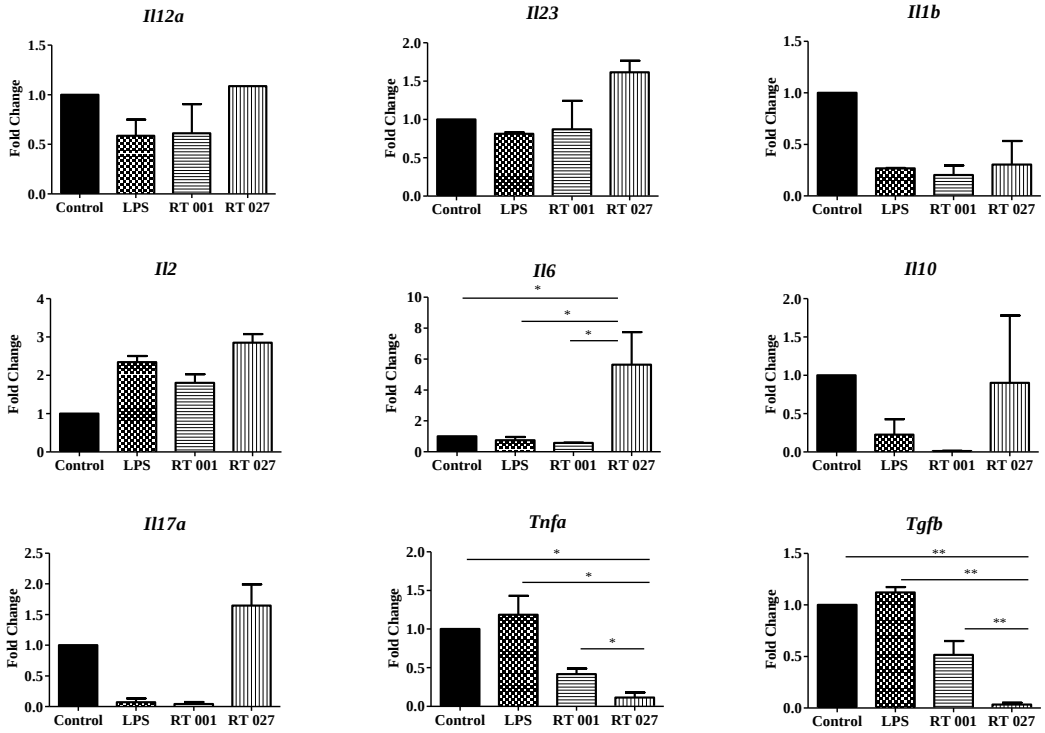

Figure 3. 25 SLPs from RT 001 and RT 027 induced inflammatory cytokines expression from colon *ex vivo*. Mice colon explants were stimulated for 6 h with 100 ng/ml of LPS or 20 µg/ml of SLPs RT 001 or RT 027, respectively. Tissue from each sample was homogenised and mRNA was extracted using Nucleospin RNA II kit and quantified. Normalised amounts of mRNA were converted into cDNA using a High Capacity cDNA Mastermix. The cDNA was mixed with primers for *Il12a*, *Il23*, *Il1b*, *Il2*, *Il6*, *Il10*, *Il17*, *Tnfa* and *Tgfb* and FAST SYBR Mastermix. Samples were assayed in triplicates and analysed on LightCycler®96. Groups were compared using relative quantitation. After normalising samples to geometric mean of two endogenous controls, *Ppia* and *B2m*, expression of control sample was normalised to 1, and expression in treatment group is shown relative to this value. Results are means ±SD of 3 biological replicates per group. One-way ANOVA, followed by Newman-Keuls Multiple Comparison test was carried out to search for statistical significance (*p<0.05, **p<0.01, ***p<0.001) (GraphPad Prism 5.01).

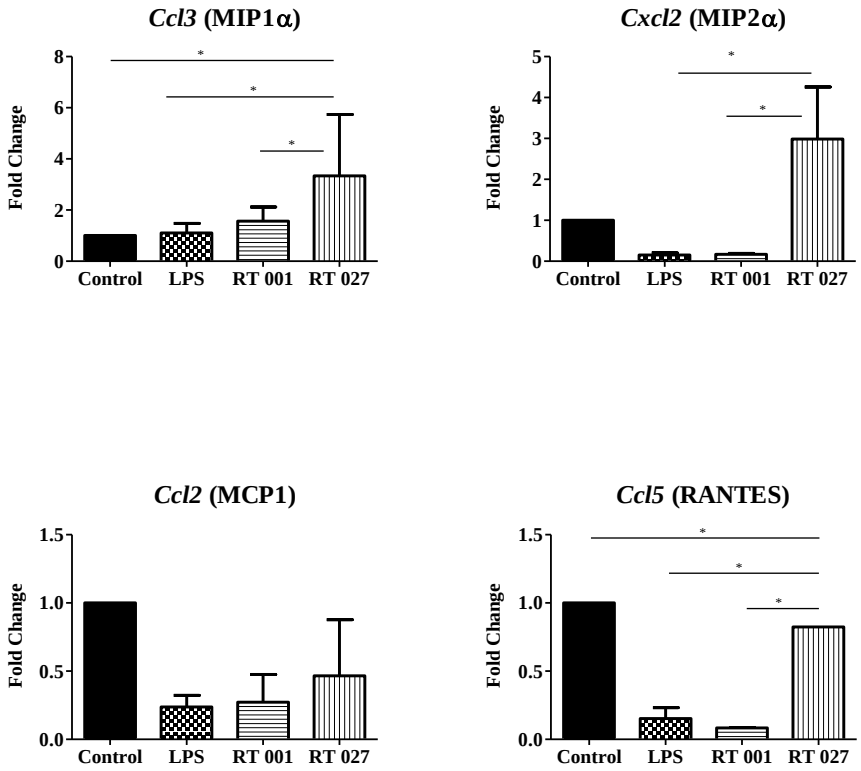

Figure 3. 26 SLPs from RT 001 and RT 027 induced chemokines expression from colon *ex vivo*. Mice colon explants were stimulated for 6 h with 100 ng/ml of LPS or 20 µg/ml of SLPs RT 001 or RT 027, respectively. Tissue from each sample was homogenised and mRNA was extracted using Nucleospin RNA II kit and quantified. Normalised amounts of mRNA were converted into cDNA using a High Capacity cDNA Mastermix. The cDNA was mixed with primers for *Ccl3* (MIP1α), *Cxcl2* (MIP2α), *Ccl2* (MCP1) and *Ccl5* (RANTES) and FAST SYBR Mastermix. Samples were assayed in triplicates and analysed on LightCycler®96. Groups were compared using relative quantitation. After normalising samples to geometric mean of two endogenous controls, *Ppia* and *B2m*, expression of control sample was normalised to 1, and expression in treatment group is shown relative to this value. Results are means ±SD of 3 biological replicates per group. One-way ANOVA, followed by Newman-Keuls Multiple Comparison test was carried out to search for statistical significance (*p<0.05, **p<0.01, ***p<0.001) (GraphPad Prism 5.01).

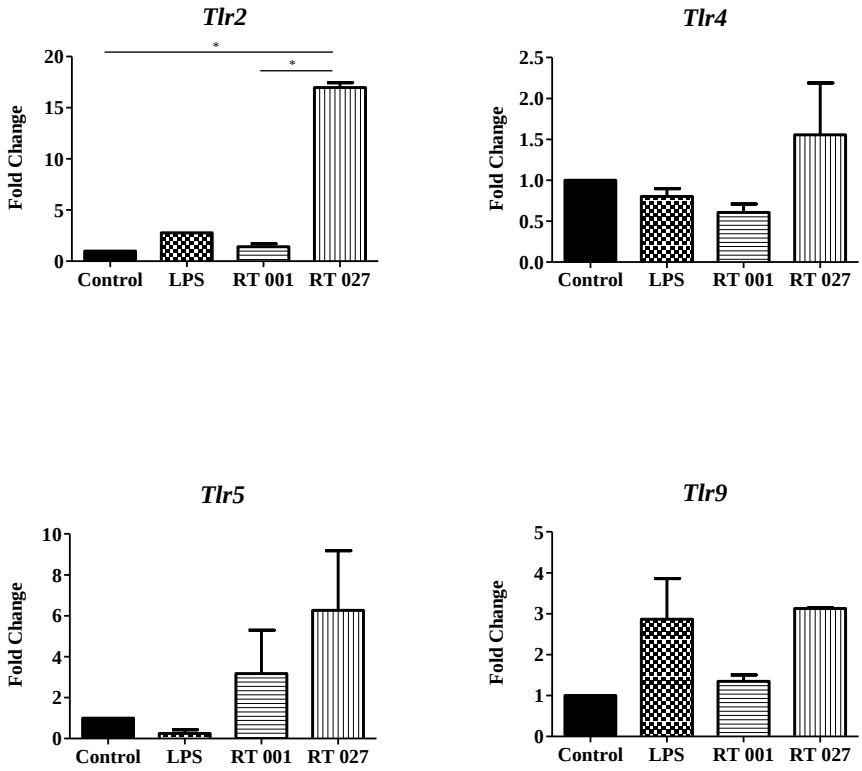

Figure 3. 27 SLPs from RT 001 and RT 027 induced TLRs expression from colon *ex vivo*. Mice colon explants were stimulated for 6 h with 100 ng/ml of LPS or 20 µg/ml of SLPs RT 001 or RT 027, respectively. Tissue from each sample was homogenised and mRNA was extracted using Nucleospin RNA II kit and quantified. Normalised amounts of mRNA were converted into cDNA using a High Capacity cDNA Mastermix. The cDNA was mixed with primers for *Tlr2*, *Tlr4*, *Tlr5* and *Tlr9* and FAST SYBR Mastermix. Samples were assayed in triplicates and analysed on LightCycler®96. Groups were compared using relative quantitation. After normalising samples to geometric mean of two endogenous controls, *Ppia* and *B2m*, expression of control sample was normalised to 1, and expression in treatment group is shown relative to this value. Results are means ±SD of 3 biological replicates per group. One-way ANOVA, followed by Newman-Keuls Multiple Comparison test was carried out to search for statistical significance (*$p<0.05$, **$p<0.01$, ***$p<0.001$) (GraphPad Prism 5.01).

3. 2. 3. 2 SLPs RT 001 and RT 027 Induced Changes in Expression of Mucosal Integrity Markers *Ex Vivo*.

After 6 h incubation, total RNA was harvested from the tissue. RT qPCR was then carried out to examine the expression of genes involved in maintaining the colonic immune response, such as mucins (Figure 3. 28) and tight junction proteins (Figure 3. 29). Mucin genes were expressed differently when stimulated with SLP RT 001 and RT 027 (Figure 3. 28). Expression of *Muc1*, *Muc3* and *Muc4* was decreased by SLPs of both ribotypes, however in all cases the decrease induced by RT 001 was relatively lower than RT 027. *Muc1* was decreased 0.5-fold and 0.25-fold, respectively ($p<0.05$), *Muc3* was decreased 0.5-fold and 0.1-fold, respectively (non-significant), and *Muc4* was decreased 0.25-fold and 0.1-fold, respectively (non-significant). SLPs RT 027 increased expression of *Muc2*, *Muc5ac* ($p<0.05$), *Muc6*, *Muc13* ($p<0.05$) and *Muc*20 ($p<0.05$) relative to stimulation of these genes by SLPs RT 001. Expression of *Muc15* was not detected in this tissue under these conditions. Stimulation with LPS resulted in increase of expression of *Muc2*, *Muc5ac*, *Muc6*, *Muc13* and *Muc20* (2-fold, 1.5-fold, 1.5-fold and 1.5 respectively). Decrease of expression was observed in the case of *Muc3* and *Muc4* (0.5-fold and 0.25-fold).

The expression of tight junction proteins of epithelial cells was different following stimulation with SLPs RT 001 and RT 027 (Figure 3.29). Stimulation with SLP RT 027 resulted in downregulation of expression of both e-cadherin *Cdh1* and occludin *Ocln*, 0.1-fold and 0.25-fold, respectively. Stimulation with RT 001 downregulated the expression of *Cdh1*0.5-fold, while it upregulated the expression of *Ocln* 2-fold. However these changes in the expression were not statistically significant. There was no change in expression in *Cdh1* and *Ocln* when stimulated with LPS.

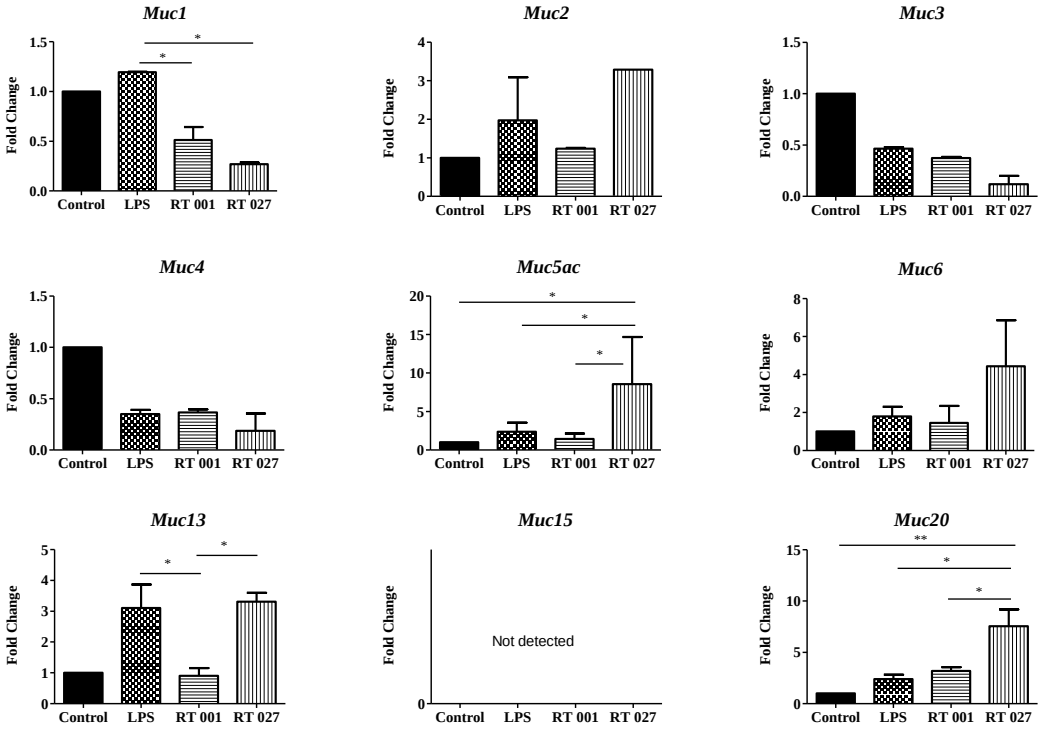

Figure 3. 28 SLPs from RT 001 and RT 027 induced mucin expression from colon *ex vivo*. Mice colon explants were stimulated for 6 h with 100 ng/ml of LPS or 20 µg/ml of SLPs RT 001 or RT 027, respectively. Tissue from each sample was homogenised and mRNA was extracted using Nucleospin RNA II kit and quantified. Normalised amounts of mRNA were converted into cDNA using a High Capacity cDNA Mastermix. The cDNA was mixed with primers for *Muc1*, *Muc2*, *Muc3*, *Muc4*, *Muc5ac*, *Muc6*, *Muc13*, *Muc15* and *Muc20* and FAST SYBR Mastermix. Samples were assayed in triplicates and analysed on LightCycler®96. Groups were compared using relative quantitation. After normalising samples to geometric mean of two endogenous controls, *Ppia* and *B2m*, expression of control sample was normalised to 1, and expression in treatment group is shown relative to this value. Results are means ±SD of 3 biological replicates per group. One-way ANOVA, followed by Newman-Keuls Multiple Comparison test was carried out to search for statistical significance (*p<0.05, **p<0.01, ***p<0.001) (GraphPad Prism 5.01).

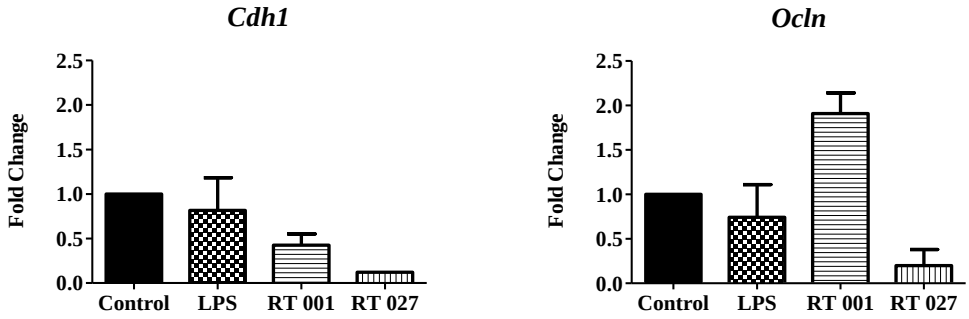

Figure 3. 29 SLPs from RT 001 and RT 027 induced tight junction protein expression from colon *ex vivo*. Mice colon explants were stimulated for 6 h with 100 ng/ml of LPS or 20 µg/ml of SLPs RT 001 or RT 027, respectively. Tissue from each sample was homogenised and mRNA was extracted using Nucleospin RNA II kit and quantified. Normalised amounts of mRNA were converted into cDNA using a High Capacity cDNA Mastermix. The cDNA was mixed with primers for e-cadherin, *Cdh1*, and occludin, *Ocln*, and FAST SYBR Mastermix. Samples were assayed in triplicates and analysed on LightCycler®96. Groups were compared using relative quantitation. After normalising samples to geometric mean of two endogenous controls, *Ppia* and *B2m*, expression of control sample was normalised to 1, and expression in treatment group is shown relative to this value. Results are means ±SD of 3 biological replicates per group. One-way ANOVA, followed by Newman-Keuls Multiple Comparison test was carried out to search for statistical significance (*$p<0.05$, **$p<0.01$, ***$p<0.001$) (GraphPad Prism 5.01).

3. 3 DISCUSSION

The focus of this chapter was to optimise the growth of *C. difficile* and the subsequent isolation and purification of SLPs. Furthermore, the effect of SLPs RT 001 and RT 027 on the mucosal immune response and mucosal integrity barrier was examined *ex vivo*.

The Latin name *C. difficile* was supposed to indicate the difficulty of culturing this microbe in the laboratory. Optimisation of growth included the liquid microbial culture. Initially a two-step culture was applied. FAB incubation is supposed to aid the recovery of bacterial cells from solid into broth culture. This step was followed by incubation in BHI broth, which is an ideal medium for growth of anaerobic fastidious microorganisms. To shorten the procedure, bacterial colonies were inoculated directly into BHI broth, omitting the FAB incubation. The microbial culture in BHI is well-established in *C. difficile* research (Wright *et al.* 2005; Emerson *et al.* 2008; Carlson *et al.* 2013; Drudy *et al.* 2004; Ausiello *et al.* 2006; Dapa *et al.* 2013). Other liquid media were considered, such as Tryptone Yeast growth media (TYG; Engevik *et al.* 2014; Janoir *et al.* 2013), Columbia broth (Theriot & Young 2014) or Protease Peptone Yeast Extract (PPYE) broth (Cerquetti *et al.* 2000). However, these media are used for various purposes such as isolation from human sample and differentiation from other bacteria. For example, the PPYE approach used by Cerquetti *et al.* aimed to recover *C. difficile* from patients' samples, as a selective type of media (Cerquetti *et al.* 2000). This was not necessary in this study, as the stocks of *C. difficile* were isolated and purified, and only required an enrichment medium.

The liquid culture of *C. difficile* in BHI broth was optimised to achieve recommended growth of OD 1.0. All ribotypes required 18 h to achieve turbid growth of OD 0.8-1, an incubation time which was comparable with other studies (Vohra & Poxton 2012). However, RT 078 presented the culture with sediment after this period of incubation, due to aggregation of microbial cells or the cell culture reaching the death phase and observed sediment was identified as cell debris. To support the growth of RT 078 and to enrich the medium, BHI broth was supplemented with vitamin K and hemin, nutritious supplements known to enhance the cultivation of anaerobes (MacFaddin 1985; Roe *et al.* 2002). Also, to adjust to the higher growth rate of RT 078, the culture of this ribotype was shortened to 8 h. This proved to be satisfactory to support the growth of RT 078.

Various bacterial species differ in their susceptibility to disrupt their S-layers, therefore there are numerous methods described to isolate S-layers (Sleytr & Beveridge 1999). Methods applied to isolate the S-layer from *C. difficile* include a low pH glycine method (Calabi *et al.* 2001), a cation substitution method (LiCl) (Koval & Murray 1984) and a hydrogen-bond-breaking method (8 M urea; Cerquetti *et al.* 2000). Cerquetti *et al.* reported the latter method was sufficient to completely remove the hexagonally arranged SLPs from the surface of *C. difficile* (Cerquetti *et al.* 2000). Furthermore, Wright *et al.* compared all the methods used to isolate S-layer from the surface of *C. difficile* and concluded that SLPs recovered in roughly equimolar amounts by both low pH glycine and 8 M urea treatments (Wright *et al.* 2005). Therefore, the latter method was used to isolate S-layer from *C. difficile* in this project.

Initially, isolation of the S-layer with 8 M urea was carried out with constant agitation during incubation, a technique used by other groups (Vohra & Poxton

2012). However, we observed that this caused the LMW to dissociate separately from the surface and appeared as separate bands eluted during FPLC. Therefore, the incubation was carried out without agitation, to prevent this from happening and this was no longer observed.

The SLPs make up to 99% of the surface of *C. difficile* (Calabi & Fairweather 2002), however there are other proteins presented on the surface. To remove additional surface proteins and debris, crude S-layer extract was purified using FPLC anion exchange chromatography. The FPLC purification approach (target NaCl concentration and the length of the purification) was determined experimentally, and it resulted in the identification of one method to purify SLPs from S-layer extract.

As mentioned beforehand, the surface of *C. difficile* is comprised of SLPs, therefore they are the predominant surface antigen and are recognised by the immune system. In this chapter, the colonic mucosal response *ex vivo* to two ribotypes, RT 001 and RT 027 was investigated. To our knowledge, such analysis has not been previously performed. These two ribotypes were chosen, as they present different clinical disease outcomes. RT 001 is associated with mild symptoms and prompt recovery, while infection with RT 027 is described as hypervirulent and causing a long-lasting infection (Archbald-Pannone *et al.* 2014). Both ribotypes also represent the most commonly isolated *C. difficile* ribotypes in Europe and Northern America (Barbut *et al.* 2007; Cheknis *et al.* 2009).

Furthermore, our group previously described that SLPs elicit an immune response (Collins *et al.* 2014; Ryan *et al.* 2011) and undergo evolutionary selection in a ribotype dependant-manner (Lynch 2014, unpublished). The SLPs RT 001 induced cytokine secretion from dendritic cells via activation of TLR4 (Ryan *et al.* 2011).

Also, stimulation with the same ribotype of SLPs resulted in activation of macrophages, observed as increase in phagocytosis, which is important in clearance (Collins *et al.* 2014). Other studies have demonstrated that human monocytes stimulated with SLPs RT 012 secreted elevated levels of proinflammatory IL-6 and IL-1β (Ausiello *et al.* 2006).

While these studies provided an important insight into how SLPs activate the immune system, they were based on interaction between one ribotype of SLPs with single type of immune cells. As already mentioned, *C. difficile* infection outcome varies between the ribotypes. Moreover, the sequence of SLPs is different between ribotypes. Therefore, there was need for study that incorporated various ribotypes of SLPs. Furthermore, the recognition by immune cells is crucial for clearance, however, *C. difficile* initially interacts with more dynamic environment of colonic mucosa. Hasegawa *et al.* demonstrated that chemokines secreted during *C. difficile* infection and essential for the recruitment of the neutrophils, were predominantly secreted by colonic epithelial cells (Hasegawa *et al.* 2011). Therefore, here we presented how SLPs from the two most common *C. difficile* ribotypes interacted with colonic tissue *ex vivo*. This allowed mimicking the actual environment in the gut, where *C. difficile* interacts not only with cells of the immune system but also the mucosal barriers.

We demonstrated that there was higher expression of the proinflammatory cytokines IL-23, IL-6 and IL-17 and the anti-inflammatory cytokine IL-10 by SLPs RT 027 relative to the expression induced by RT 001. Furthermore, we demonstrated that key chemokines, MIP1α and MIP2α were induced by SLPs RT027. MIP2α was shown to be a potent neutrophil chemoattractant and activator (Sadighi Akha *et al.* 2013). While switching on the immune response is essential for clearance, the

overproduction of chemokines and sudden influx of phagocyting cells may augment the infection site. Pender *et al.* demonstrated that elevated levels of MIP1α during intestinal infections (macrophage inflammatory protein 1α, MIP-1α) are responsible for exacerbated colitis in Inflammatory Bowel Disease (IBD) patients (Pender *et al.* 2005). We also observed decreased levels of MCP1 and RANTES. The MCP1 chemokine has previously been shown to be induced early during infection with enteric parasite *Trichuris muris*, however its expression was dependent on elevated expression of TNFα (DeSchoolmeester *et al.* 2006). We also observed decrease in TNFα expression, therefore we concluded that at this time point post-stimulation, this chemokine is not induced yet. Furthermore, Hasegawa *et al.* suggested that MCP1 is not essential for the initial recruitment of the neutrophils during infection with *C. difficile* (Hasegawa *et al.* 2011). Interestingly, we also observed the decrease of expression of RANTES when stimulated with RT 001 and RT 027. This chemokine has been shown to be upregulated when the gut microbiota was disturbed, leading to elevated IL-6 cytokine secretion and inflammatory state in the gut (Hu *et al.* 2013). While we observed that RANTES was downregulated significantly by RT 001, this decrease was less pronounced by RT 027. Overall, we demonstrated that SLP RT 027 can activate a more potent immune response or that it has a better adherence to the colonic epithelium, as evidenced by relatively higher expression of cytokines and chemokines when stimulated with RT 027 relative to RT 001. Additionally, we have noticed that *ex vivo* stimulation with LPS, which supposed to be a positive control for SLP stimulation, did not stimulate the expression of cytokines, chemokines and TLRs as anticipated. The stimulation of cells of immune system such as macrophages and dendritic cells usually results in increase of expression and secretion of cytokines and TLRs (Lynch 2014,

unpublished). This was not observed in the case of *ex vivo* stimulation of colonic tissue. This could be due to the fact that colonic environment is more complex than single immune cells, and furthermore there were no previous reports of stimulating *ex vivo* colon culture with LPS and measuring cytokine, chemokine and TLR expression that our results could be compared with.

Ausiello *et al.* indicated the host's immune recognition and excessive recruitment of key inflammatory cells actually results in exacerbated reaction and further epithelial damage and this could be an unexpected virulence strategy employed by *C. difficile* (Ausiello *et al.* 2006). This strategy may indeed be utilised by *C. difficile* RT 027, as indicated by a most recent study from our group (Lynch 2014, unpublished).

Our further analysis indicated that *ex vivo* stimulation with SLPs RT 001 and RT 027, resulted in different level of expression of key mucosal integrity proteins, mucins and tight junction proteins. The mucins are secretory proteins, which are highly glycosylated and hydrophilic (Bansil & Turner 2006). They are important components of GI tract homeostasis, as disruption or inappropriate expression could predispose to infectious disease (McGuckin *et al.* 2011).

The expression of mucins and secretion of mucus from goblet cells is a tightly regulated process, largely influenced by the composition of commensals (Kamada *et al.* 2013). It is a great example of how GI microbiota and host cooperate in symbiotic relationship in order to fend off invading pathogens. For example, short-chain fatty acids (SCFA), the by-products of commensal metabolism, signal through the colonic epithelium to increase the mucus secretion (Xu *et al.* 2013). In our study, we observed upregulation of MUC2, MUC5AC, MUC6 and MUC13 and MUC20 when stimulated with SLP RT 027. This indicates a potent response from host mucosal

barriers and to our knowledge, the effect of SLPs on the expression of mucins has not yet been investigated.

Some previous studies reported the role that *C. difficile* may play in mucus composition, however it involved the infection with whole pathogen. *C. difficile* infection have been shown to induce MUC1 secretion in humans, presumably as a protective measure (Linden *et al.* 2008). Branka *et al.* demonstrated that toxins actually reduce the mucin secretion and this, altogether with increased neutrophil recruitment by elevated IL-8, directly contributes to exacerbated epithelial inflammation (Branka *et al.* 1997). Furthermore, *C. difficile* has been shown to utilise the glycans sourced from mucins as energy source, which indicated that this pathogen may directly influence the composition of mucus (Ng *et al.* 2013). This correlates with previous studies presenting the evidence that enteric pathogens actively influence the secretion of mucins. MUC1 secretion was increased by *Citrobacter rododentium* infection in mice (Linden *et al.* 2008). This is supposed to be a host reaction to increase the thickness of the mucus to trap the pathogens and exclude them from interaction with epithelium and immune receptors such as TLRs. On the other hand, *Vibrio cholera* induces the mucin expression in order to increase the binding surface for its mucin adhesins, to aid the colonisation (Juge 2012).

Furthermore, mucins play immunomodulatory functions. Shen *et al.* demonstrated that MUC1 has an anti-inflammatory role in gut homeostasis, while MUC13 resulted in proinflammatory reactions and both of these mucins regulated the chemokine MIP2α secretion (Sheng *et al.* 2013). In this chapter we presented that SLPs RT 027 significantly reduced MUC1 expression and significantly upregulated the expression of MUC13. Moreover, the observed that MIP2α is significantly upregulated when stimulated with SLP RT 027. Therefore, we propose that SLPs RT 027 may actively

modulates the mucosal environment by downregulating the anti-inflammatory factors such MUC1 and elevating proinflammatory MUC1 and MIP2α.

The downregulation of MUC1 has further consequences, as MUC1 has been shown to supress the expression of TLRs such as TLR2, TLR3, TLR4, TLR5, TLR7 and TLR9 (Ueno *et al.* 2008). In this study, we observed that expression of TLR2, TLR4, TLR5 and TLR9 was upregulated by the stimulation with RT 001 and RT 027. However, this upregulation was more pronounced with RT 027, again indicating more potent response of the immune system to this ribotype. The increase in these receptors on the surface of the colonic epithelium may result in exacerbated immune response and cell recruitment. The activation of TLR2 is important for the maturation of Tregs and IL-10 cytokine secretion (Round *et al.* 2011). In recent study conducted by our group, we observed that infection with RT 027 resulted in upregulation of anti-inflammatory IL-10, in order to dampen the host's clearance mechanisms (Lynch 2014, unpublished). In this study, we observed upregulation of both TLR2 and IL-10 expression in response to SLP RT 027 *ex vivo.* This may suggest that early on during the infection the pathogen may switch on the mechanism that delays the clearance.

Finally, we examined the expression of tight junction genes. The formation of tight junction proteins between cells of the epithelial layer of the GI tract provide the protective barrier from pathogens, while allowing the basic function of nutrient absorption via pores (Knoop *et al.* 2015). It is well-established that *C. difficile* toxins affect the cell actin cytoskeleton and tight junction proteins, in order to induce apoptosis, fluid accommodation and destruction of the colonic epithelium (Voth & Ballard 2005). Adhesion of *C. difficile* to Caco-2 cells was significantly increased when tight junction proteins were disrupted by chemical treatment, indicating the

importance of the integrity of the epithelium in the process of colonisation (Cerquetti 2002). On the other hand, *Shigella* toxin was demonstrated to directly decrease the expression of tight junction proteins (Sakaguchi *et al.* 2002). This evidence indicates that enteric pathogens directly target not only the integrity of the epithelium by destroying it, but also by modulating the key proteins at the expression level.

However, little is known about the effect of other clostridial virulence factors such as SLPs on expression of tight junction proteins during the early stage of colonisation and induction of the immune response. We observed that stimulation with SLP RT 027 downregulated the expression of tight junction proteins *ex vivo*, occludin and e-cadherin. Kucharzik *et al.* suggested that decreased expression of tight junction genes may play a role in enhanced permeability of colonic mucosal barriers in IBD patients (Kucharzik *et al.* 2001). We again observed that RT 027 induced the downregulation of both tight junction genes, suggesting that this may be an additional mechanism employed by the pathogen to invade the host. The increased permeability of the mucosal barriers allows for influx of inflammatory cells but also allows pathogen to breach the mucosal barriers and enter the blood system (Ng *et al.* 2010). Other enteric pathogens also actively modulate the expression of tight junction proteins. During infection with *H. pylori*, tight junction proteins expression was found to be decreased, which further contributed to disease pathogenesis by increased permeability at the epithelial barrier, however the exact mechanism was not revealed in this study (Zhang *et al.* 2014). In contrast, we observed that SLP RT 001 induced occludin, but not e-cadherin. Increased expression of tight junction genes could be interpreted as a host protective response to defend from the pathogen invasion. Pott & Hornef indicated that innate immune stimulation at the mucosal surfaces leads to reinforcement of tight junction proteins, along with increased

expression of antimicrobial peptides (Pott & Hornef 2012). Therefore, we propose that SLP RT 001 induced the host protective response, as observed by the induction of occludin.

Previous studies by Bianco *et al.* and Vohra and Poxton suggested that ribotype and SLP recognition by immune system was not linked to the severity of the infection (Bianco *et al.* 2011; Vohra & Poxton 2012). However, in this chapter we demonstrated that SLPs of two ribotypes elicit different immune and mucosal response. Furthermore, the observed immune expression pattern presented more pronounced response to SLP RT 027. This correlates with clinical symptoms elicited by hypervirulent RT 027 (Rao *et al.* 2014).

The exact role of SLPs in modulating the mucus composition is yet to be determined, as there is a dynamic network of interactions between the immune and mucosal components. However, we demonstrated that SLPs RT 027 induce the more potent immune and mucosal response. More proinflammatory tone of the response is supposed to aid the pathogen invasion in the gut. This immediately suggests that the interaction between the host epithelium and SLP RT 027 is more efficient. This could be influenced by the prompt recognition of SLPs by immune system or more successful adherence of this ribotype.

Therefore next it is important to examine the factors that may influence the interaction of SLPs with colonic epithelium. While SLPs have been shown to be essential for the adherence of the pathogen to the colonic epithelium (Merrigan *et al.* 2013), the exact mechanism remains unclear. As it is evident that the SLPs from various strains differ in sequence and molecular weight, we would like to examine next whether the SLPs are glycosylated. The differences in glycosylation patterns

between different ribotypes could account for the different responses from the colonic tissue *ex vivo*, presented in this chapter.

CHAPTER 4 GLYCOSYLATION OF SURFACE LAYER PROTEINS

4. 1 INTRODUCTION

CDI is associated with several virulence factors (Borriello *et al.* 1990). As already mentioned, toxins contribute to epithelial damage (Rupnik 2005), however they are not secreted until the late phase of growth (Hundsberger *et al.* 1997), furthermore, not all toxigenic ribotypes result in disease (Kuehne *et al.* 2010). Consequently, toxins alone cannot fully explain *C. difficile* pathogenesis.

This has prompted the search for additional virulence factors that provide *C. difficile* with colonisation advantage. This includes enhanced germination of spores of hypervirulent strains (Carlson *et al.* 2015), and their use of secondary bile acids (Buffie *et al.* 2014; Merrigan *et al.* 2010). Conversely, the surface of the bacterium is covered with various proteins that may facilitate binding to the host epithelium and evading the immune response. The exact mechanism of adhesion remains unknown despite very active research in the area of *C. difficile* physiology.

To date, several surface-associated proteins have been investigated as adherence factors, such as flagella (Tasteyre *et al.* 2001; Twine *et al.* 2009; Janoir *et al.* 2013), protease Cwp84 (Bradshaw *et al.* 2014; Chapetón Montes *et al.* 2013) and Cwp66

(Waligora *et al.* 1999), the fibronectin binding protein Fbp68 (Waligora *et al.* 2001; Barketi-Klai *et al.* 2011) and the GroEL heat-shock protein (Hennequin *et al.* 2001; Péchiné *et al.* 2013).

Our research is focused on SLPs, which have been previously shown to be implicated in the adhesion of *C. difficile* to GI tissues, but exact mechanism remains unknown (Calabi *et al.* 2002; Spigaglia *et al.* 2013). Furthermore, Merrigan *et al.* has demonstrated that SLPs are essential for *C. difficile* binding to host (Merrigan *et al.* 2013). S-layers are very important features that are evolved in some Eubacteria and Archaea. Interestingly, the S-layer is ubiquitous and occurs on both Gram-positive and Gram-negative bacteria, indicating the evolutionary need for this surface feature (Sleytr & Beveridge 1999). The proteins that constitute the S-layer are often the most abundant of the cellular proteins, indicating the importance of the S-layer for the function of the bacterium (Fagan & Fairweather 2014). In *Bacillus stearothermophilus*, S-layer proteins constitute up to 15% of the total protein secretion (Kuen *et al.* 1994). The fact that the S-layer is often lost during laboratory cultivation, when no growth pressure is applied or nutrient competition, demonstrates the importance of S-layer to withstand the harsh environmental conditions (Debabov 2004).

Several functions for the S-layer have been described, including serving as a protective coat, molecular sieve or scaffolding for enzymes, but also it may be involved in the cell adhesion and surface recognition, and therefore serve as virulence factor (Sára & Sleytr 2000). Indeed our group has already demonstrated a role for SLPs in pathogen recognition (Ryan *et al.* 2011). Fagan and Fairweather indicated that S-layer of *C. difficile* is essential for cell growth of this pathogen (Fagan & Fairweather 2014).

Today we know that glycosylation occurs in all three domains of life, Archeae, Bacteria and Eukaryota (Eichler 2013; Nothaft & Szymanski 2010). Remarkably, it was the investigation of human pathogens that led to the discovery that prokaryotic cells also utilise glycosylation to enrich their protein structures. Specifically, it was the surface appendages, such as pili or flagella that have been shown to be glycosylated (Schäffer & Messner 2004). It soon led to the discovery that S-layer proteins are the main class of prokaryotic glycoproteins (Messner *et al.* 2008; Schäffer *et al.* 2001; Wang *et al.* 2012). S-layers may be modified with glycan chains reaching up to 150 sugar subunits, as opposed to glycan chains of non-S-layer proteins, which were built with up to 20 glycans (Messner *et al.* 2008; Ristl *et al.* 2011).

It is evident that glycosylation on the cell surface or the S-layer, which represent the contact zone of pathogen with host environment, may contribute to bacterial colonisation, and possible immune evasion. Human pathogens, such *E. coli* recognise and adhere to the surface of the intestinal epithelium via specific glycoproteins (Wang *et al.* 2012). Other human pathogen, *Tannerella forsythia* actively modify the glycosylation of its cell surface to suit the pathogenic strategy (Posch *et al.* 2011). Furthermore, glycosylation on the surface of *C. jejuni* protects the pathogen from proteases present in the GI tract (Alemka *et al.* 2013). Glycosylation of SLPs is very common among other species of bacteria, including *Paenibacillus alvei*. This bacterial species used glycosylation of SLPs to anchor the S-layer within the cell wall (Janesch *et al.* 2013).

In the previous chapter we demonstrated that SLPs were able to elicit mucosal immune response *ex vivo*. Furthermore, the ability to affect the magnitude and polarisation of the response depended on the ribotype of *C. difficile*. It has previously

been demonstrated that molecular weights of both SLPs subunits greatly differ between different ribotypes (Calabi *et al.* 2001; Karjalainen *et al.* 2002). Knowing this, we next wanted to examine whether there are any post-translational modifications to SLPs, such as glycosylation. This may explain the difference in molecular weights between the ribotypes, while also possibly the differences in adherence to host tissue and recognition by host's immune system. Differences in glycosylation could contribute to immune evasion of certain ribotypes and could contribute to the disease outcome.

SLPs of *C. difficile* were previously investigated for the presence of glycosylation, however the studies only included one strain (Cerquetti *et al.* 1992), four ribotypes (Calabi *et al.* 2001) or seven ribotypes (Qazi *et al.* 2009). The results from these studies were contradicting. Here we investigate SLPs from ribotypes RT 001, RT 002, RT 014, RT 027, RT 046 and RT 078 for the presence of glycosylation.

4. 2 RESULTS

4. 2. 1. LMW and HMW Subunits of SLPs RT 001, RT 002, RT 027 and RT 078 Differ in Molecular Weights.

Crude and purified samples of SLP RT 001, RT 002, RT 027 and RT 078, total 10µg, were run on 10% (w/v) polyacrylamide gels and stained with Commassie Brilliant Blue. Purification efficiency between crude preparation and purified samples is observed in the case of all ribotypes. Furthermore, sizes of High Molecular Weight (HMW) and Low Molecular Weight (LMW) subunits of SLP differ between the ribotypes. The LMW Subunit of ribotype 001 weighs 35 kDa, while the HMW subunit had an estimated weight of 54 kDa. In the case of ribotype 002, the LMW subunit showed an estimated weight of 40 kDa, while the HMW subunit weighed 56kDa. The LMW subunit of ribotype 027 weighed 37 kDa, while The HMW subunit weighed 55 kDa. In the case of ribotype 078, the LMW subunit weighed 36 kDa, while the HMW subunit was the heaviest of all ribotype subunits, with estimated weight of 70 kDa (Figure 4. 1).

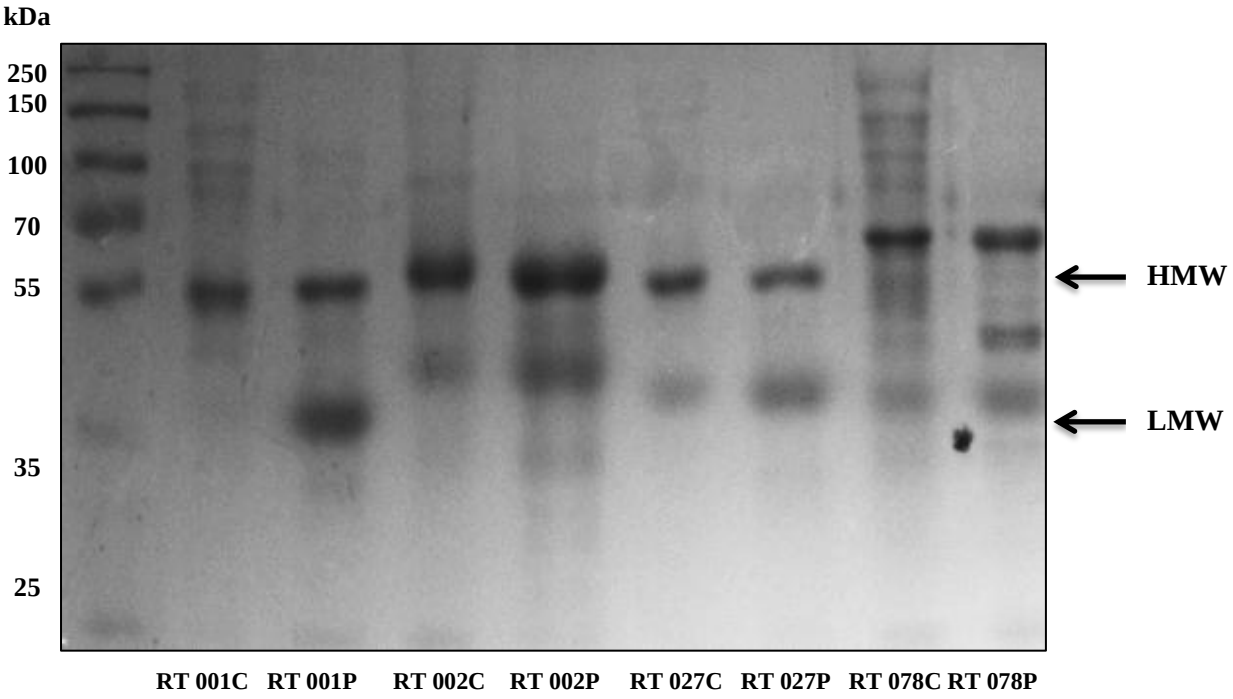

Figure 4. 1 Comparison of SLPs RT 001, RT 002, RT 027 and RT 078 ribotypes of *C. difficile.* 10µg of crude and purified samples of SLP (ribotype 001, 027 and 078) were run on 10% (w/v) SDS polyacrylamide gel and stained with Coomassie Brilliant Blue. Purification efficiency between crude and pure samples is easily observed. Furthermore, the difference in molecular weights between different ribotypes is also recognised. Red arrow indicates estimated weight of High Molecular Weight Subunit (~55 kDa); green arrow indicates estimated weight of Low Molecular Weight Subunit (~35 kDa).

4. 2. 2 SLPs from RT 001, RT 002, RT 027 and RT 078 Demonstrated Absence of Glycosylation When Stained with Periodic Acid-Schiff Staining.

The SLPs from major pathogenic ribotypes of *C. difficile* differ in molecular weights. Post-translational modifications, such as glycosylation, could be contributing to differences in molecular weights. Purified samples of SLPs from RT 001, RT 002, RT 027, and RT 078 were resolved on SDS PAGE and stained with periodic acid-Schiff reagent.

Two bands corresponding to the LMW subunit and the HMW subunit were detected in the case of all examined ribotypes, as expected at approximately 35 kDa and 55 kDa, respectively. None of the SLPs subunits demonstrated the change of colour to purple when stained with Schiff reagent, as opposed to positive control, horseradish peroxidase (HRP) (Figure 4. 2). This indicated that SLPs subunits of RT 001, RT 002 RT 027 and RT 078 may not be modified with sugar residues that are in cis-diol confirmation.

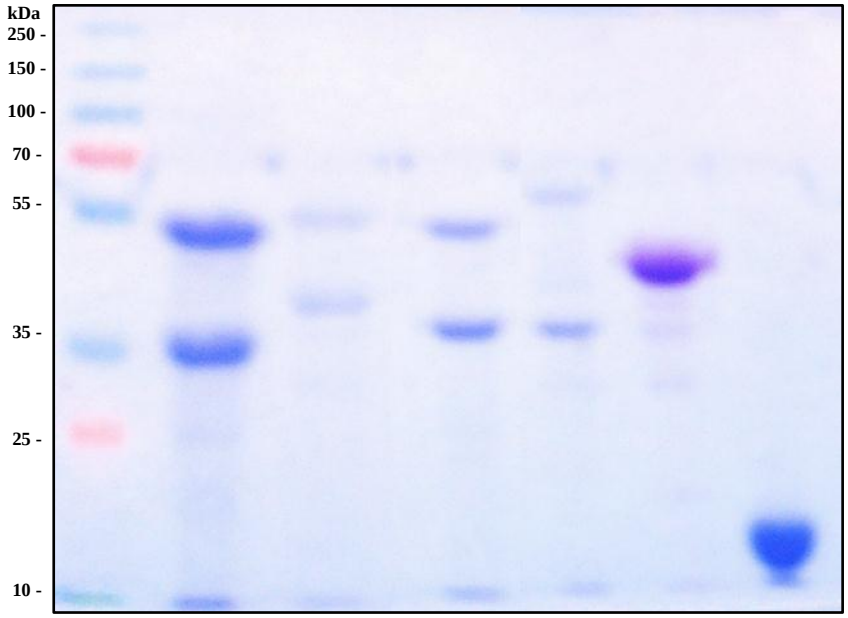

Figure 4. 2 SLPs from RT 001, RT 002, RT 027 and RT 078 demonstrated absence of glycosylation with periodic acid-Schiff staining. SLPs from RT 001, RT 002, RT 027 and RT 078 (10 µg total of purified protein samples) were separated on 15% (w/v) SDS polyacrylamide gels and stained with Commassie Brilliant Blue. Gels were stained with Periodic Acid-Schiff Staining kit. Soybean Trypsin Inhibitor (SBT) was used as a negative control (remained blue) and Horseradish Peroxidase (HRP) was used as a positive control (stained magenta). None of the crude and purified SLP ribotypes indicated presence of glycosylation.

4. 2. 3 Crude S-layer and Purified SLPs from RT 001, RT 002, RT 027 and RT 078 Were Blotted and Probed With Lectins for Various Glycosylation Patterns.

Lectins are specific carbohydrate-binding proteins. We used a range of plant lectins to explore glycosylation patterns on the SLPs from ribotypes used in this study. We searched for the most common carbohydrate structures found on bacterial proteins, mannose (ConA, NPL and LCA), N-Acetylglucosamine (AAL, GSL II and ECL), N-Acetylgalactosamine (PNA, Jacalin, GSL I and DBA) and sialic acid (SNA). Using multiple lectins for each of these carbohydrate structures was essential, as carbohydrates form unique and extensive chain structures. We included crude samples of S-layer extract (RT 001C, RT 002C, RT 027C and RT 078C) but also as the purified proteins (RT 001P, RT 002P, RT 027P and RT 078P).

4. 2. 3. 1 Crude S-layer and Purified SLPs from RT 001, RT 002, RT 027 and RT 078 Were Probed for Mannose with ConA, NPL, LCA and GNL Lectins.

Mannose residues were probed with ConA (Figure 4. 3 A), NPL (Figure 4. 3 B), LCA (Figure 4. 3 C) and GNL (Figure 4. 3 D).

Mannose signal was detected from all crude S-layer samples in the form of core mannose when probed with ConA (Figure 4. 3 A), terminal or high mannose probed with NPL (Figure 4. 3 B), α-mannose probed with LCA (Figure 4. 3 C) and (α-1,3)-mannose when probed with GNL (Figure 4. 3 D). However, none of the detected bands was identified as SLP subunit. Interestingly, a >250kDa protein detected in RT 078C was demonstrated to be a heavily mannose-glycosylated, developing signal from all mannose-specific lectins used.

In the case of purified samples, a weak signal was detected for ribotype RT 002P and RT 078P when probed for core mannose with ConA (Figure 4. 3 A) and ribotype RT 002P, RT 027P and RT 078P when probed for α-mannose with LCA (Figure 4. 3 C). In each case, these bands correspond to both SLP subunits. Purified ribotypes RT 001, RT 002, RT 027 and RT 078 demonstrated a lack of glycosylation signal when probed for terminal or high mannose probed with NPL (Figure 4. 3 B) and (α-1,3)-mannose when probed with GNL (Figure 4. 3 D). RT 001 was the only ribotype that consistently presented no mannose residues when probed by ConA, NPL, LCA and GNL.

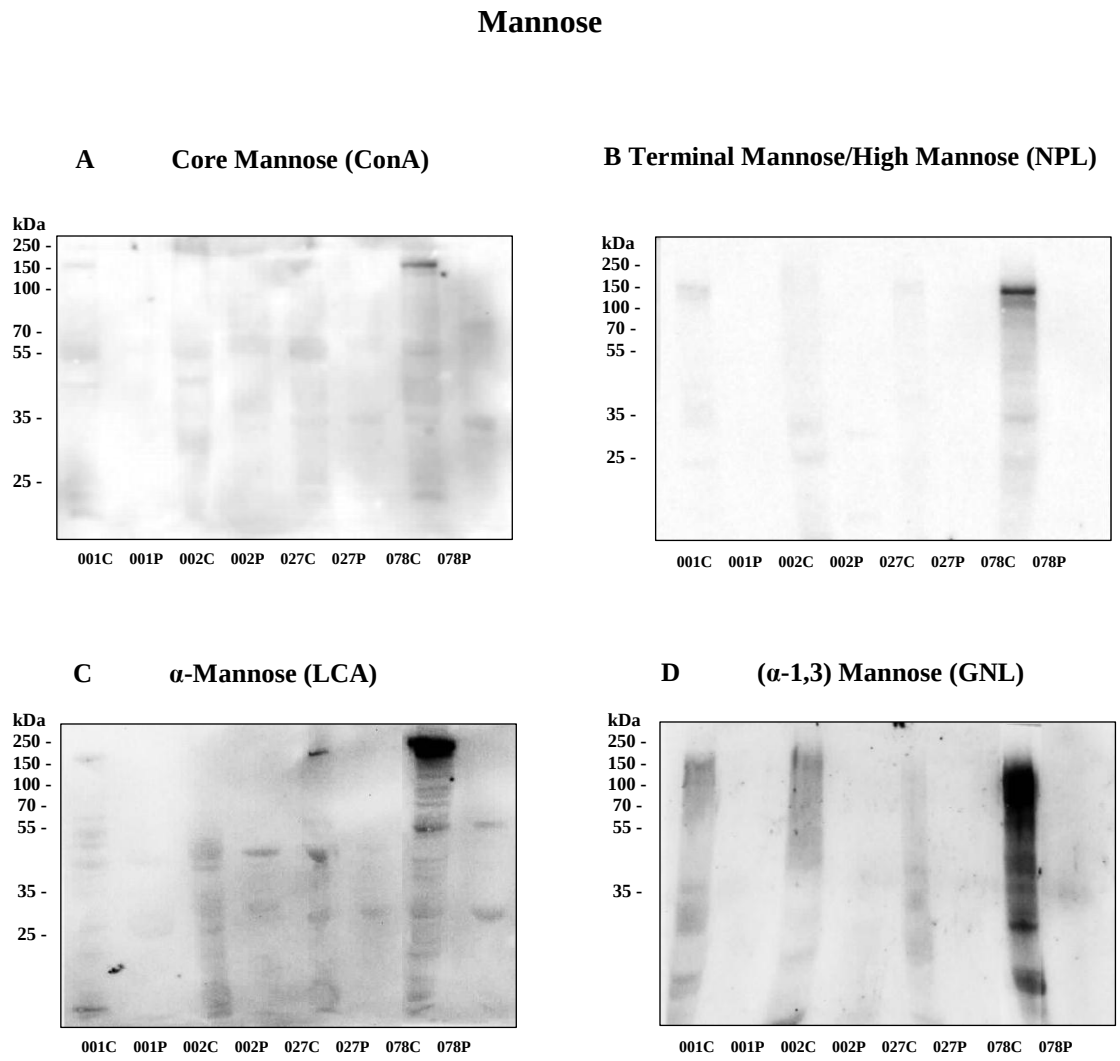

Figure 4. 3 Lectin blotting examination of SLPs isolated from RT 001, RT 002, RT 027 and RT 078 demonstrated presence of mannose. SLPs from ribotype RT 001, RT 002, RT 027 and RT 078 were resolved on SDS PAGE (10 µg of crude S-layer isolation and purified) and probed for presence of core mannose residues with ConA (**A**), high or terminal mannose with NPL (**B**), α-mannose with LCA (**C**) or (α-1-3) mannose with GNL (**D**) by lectin blotting (1 in 2000 dilution of biotinylated lectin in lectin buffer). In all cases, crude sample demonstrated glycosylation signal, while purified samples presented very light or no signal. Abbreviations: 001C: RT 001 crude; 001P: RT 001 purified; 002C: RT 002 crude; 002P: RT 002 purified; 027C: RT 027 crude; 027P: RT 027 purified; 078C: RT 078 crude; 078P: RT 078 purified.

4. 2. 3. 2 Crude S-layer and Purified SLPs from RT 001, RT 002, RT 027 and RT 078 were Probed for N-Acetylgalactosamine with PNA, Jacalin, GSL I, DBA and SBA Lectins.

N-Acetylgalactosamine residues were examined by PNA, Jacalin, GSL I, DBA and SBA lectins (Figure 4. 4).

Crude SLP extract of all ribotypes demonstrated a glycosylation signal for Galactosyl-(β-1,3)-N-Acetylgalactosamine when probed with PNA (Figure 4. 4 A) or Jacalin (Figure 4. 4 B), α-N-Acetylgalactosamine or α-Galactose when probed with GSL I (Figure 4. 4 C), α-N-Acetylgalactosamine when probed with DBA (Figure 4. 4 D) and α-/β-N-Acetylgalactosamine with SBA (Figure 4. 4 E). None of the detected bands was identified as SLP subunit.

Purified proteins of RT 001P, RT 002P, RT 027P and RT 078P demonstrated lack of Galactosyl-(β-1,3)-N-Acetylgalactosamine when probed with PNA (Figure 4. 4 A) and Jacalin (Figure 4. 4 B). However, all those ribotypes produced faint signals when probed for α-N-Acetylgalactosamine or α-galactose with GSL I (Figure 4. 4 C) and α-N-Acetylgalactosamine with DBA (Figure 4. 4 D). Faint bands corresponding to subunits of RT 001P and RT 002P were detected when probed for α-/β-N-Acetylgalactosamine with SBA (Figure 4. 4 E). No glycosylation was detected in the case of RT 027P and RT 078P.

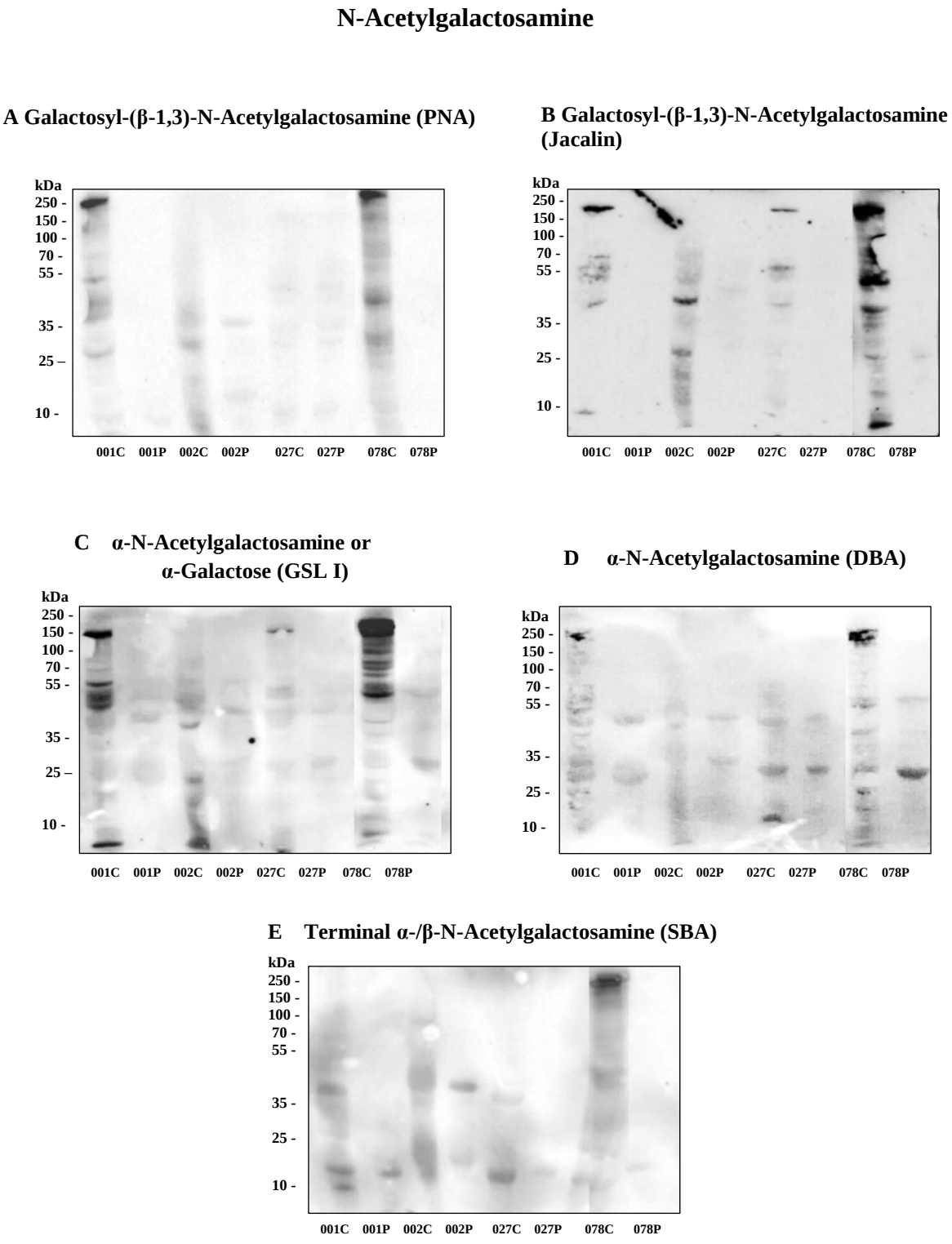

Figure 4. 4 Lectin blotting examination of SLPs isolated from RT 001, RT 002, RT 027 and RT 078 demonstrated presence of N-Acetylgalactosamine. SLPs from RT 001, RT 002, RT 027 and RT 078 were resolved on SDS PAGE (10 µg of crude S-layer isolation and purified) and probed for presence of Galactosyl-(β-1,3)-N-Acetylgalactosamine with PNA (**A**) and with Jacalin (**B**), α-N-Acetylgalactosamine or α-galactose with GSL I (**C**) and α-N-

Acetylgalactosamine with DBA (**D**) and terminal α-/β-N-Acetylgalactosamine with SBA by lectin blotting (**E**) (1 in 2000 dilution of biotinylated lectin in lectin buffer). In all cases, crude sample demonstrated glycosylation signal, while purified samples presented very light or no signal. Abbreviations: 001C: RT 001 crude; 001P: RT 001 purified; 002C: RT 002 crude; 002P: RT 002 purified; 027C: RT 027 crude; 027P: RT 027 purified; 078C: RT 078 crude; 078P: RT 078 purified.

4. 2. 3. 3. Crude S-layer and Purified SLPs from RT 001, RT 002, RT 027 and RT 078 Were Probed for N-Acetylglucosamine with AAL, GSL II and ECL Lectins.

N-Acetylglucosamine residues were examined by probing with AAL (Figure 4. 5 A), GSL II (Figure 4. 5 B) and ECL (Figure 4. 5 C). The crude S-layer extract demonstrated signal for all ribotypes when probed for Fucose-(α-1,6)-N-Acetylglucosamine with AAL (Figure 4. 5 A), α- or β-N-Acetylglucosamine when probed with GSL II (Figure 4. 5 B) and Galactosyl-(β-1,4)-N-Acetylglucosamine when probed with ECL (Figure 4. 5 C). None of the detected bands was identified as either SLP subunit. A heavily glycosylated protein, >250 kDa in size, appeared in RT 078C samples when probed with all these lectins.

In the case of purified samples, very faint signals developed when probed for Fucose-(α-1,6)-N-Acetylglucosamine with AAL (all ribotypes) (Figure 4. 5 A), α- or β-N-Acetylglucosamine when probed with GSL II (RT 001P and RT 002P) (Figure 4. 5 B) and Galactosyl-(β-1,4)-N-Acetylglucosamine when probed with ECL (RT 027P and RT 078P) (Figure 4. 5 C). These bands corresponded to both SLP subunits. Purified RT 027P and RT 078P demonstrated lack of this type of glycosylation when probed with GSL II while RT 001P and RT 002P demonstrated a lack of this type of glycosylation when probed with ECL.

N-Acetylglucosamine

A Fucose-(α-1,6)-N-Acetylglucosamine (AAL)

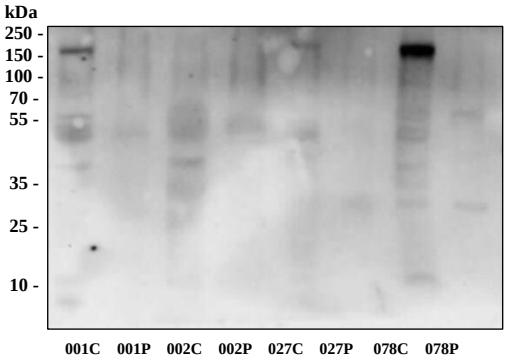

B α/β-N-Acetylglucosamine (GSL II)

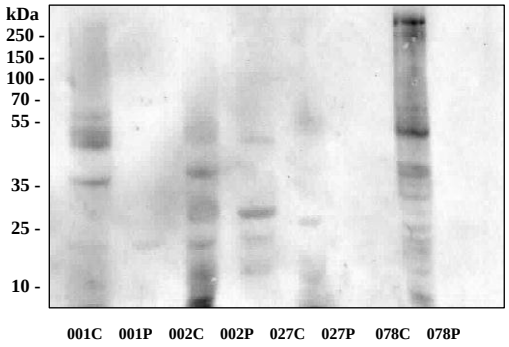

C Galactosyl-(β-1,4)-N-Acetylglucosamine (ECL)

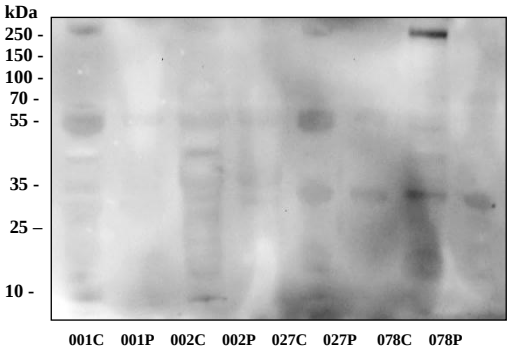

Figure 4. 5 Lectin blotting examination of SLPs isolated from RT 001, RT 002, RT 027 and RT 078 demonstrated presence of N-Acetylglucosamine. SLPs from RT 001, RT 002, RT 027 and RT 078 were resolved on SDS PAGE (10 µg of crude S-layer isolation and purified) and probed for presence of and probed for presence of Fucose-(α-1,6)-N-Acetylglucosamine with AAL (**A**), α/β-N-Acetylglucosamine with GSL II (**B**) or Galactosyl-(β-1,4)-N-Acetylglucosamine with ECL (**C**) by lectin blotting (1 in 2000 dilution of biotinylated lectin in lectin buffer). In all cases, crude sample demonstrated glycosylation signal, while purified samples presented very light or no signal. Abbreviations: 001C: RT 001 crude; 001P: RT 001 purified; 002C: RT 002 crude; 002P: RT 002 purified; 027C: RT 027 crude; 027P: RT 027 purified; 078C: RT 078 crude; 078P: RT 078 purified.

4. 2. 3. 4 Crude S-layer and Purified SLPs from RT 001, RT 002, RT 027 and RT 078 were Probed for Sialic Acid with SNA and MAL II Lectins.

Sialic acid was probed with SNA (Figure 4. 6 A) and MAL II lectins (Figure 4. 6 B).

All crude S-layer samples demonstrated heavy glycosylation when probed for Galactosyl-(α-2,6)/(α-2,3)-Sialic Acid with SNA (Figure 4. 6 A) and Galactosyl-(α-2,6)/(α-2,3)-Sialic Acid-(β-1,4)-N-Acetylgalactosamine with MAL II (Figure 4. 6 B). However, none of the detected bands could be identified as SLP subunit. Again, >250 kDa protein was detected in RT 078C sample.

None of the examined ribotypes demonstrated sialic acid glycosylation in purified samples (Figure 4. 6 A and B).

Sialic Acid

A Galactosyl-(α-2,6)/(α-2,3)-Sialic Acid (SNA)

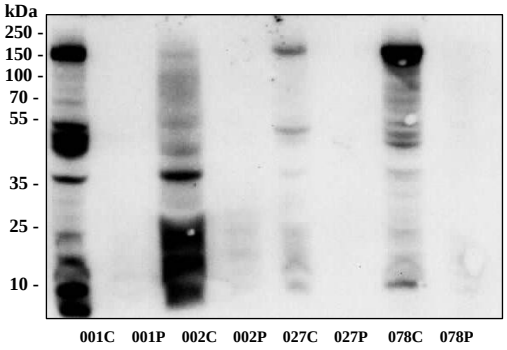

B Galactosyl-(α-2,6)/(α-2,3)-Sialic Acid-(β-1,4)-N-Acetylgalactosamine (MAL II)

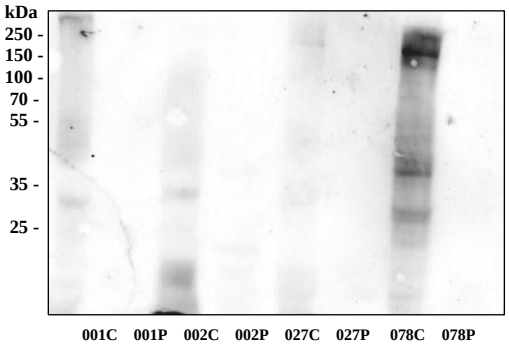

Figure 4. 6 Lectin blotting examination of SLPs isolated from RT 001, RT 002, RT 027 and RT 078 demonstrated presence of sialic acid. SLPs from RT 001, RT 002, RT 027 and RT 078 were resolved on SDS PAGE (10 µg of crude S-layer isolation and purified) and probed for presence of Galactosyl-(α-2,6)/(α-2,3)-Sialic Acid with SNA (**A**) and Galactosyl-(α-2,6)/(α-2,3)-Sialic Acid-(β-1,4)-N-Acetylgalactosamine with MAL II (**B**) by lectin blotting (1 in 2000 dilution of biotinylated lectin in lectin buffer). In all cases, crude sample demonstrated glycosylation signal, while purified samples presented very light or no signal. Abbreviations: 001C: RT 001 crude; 001P: RT 001 purified; 002C: RT 002 crude; 002P: RT 002 purified; 027C: RT 027 crude; 027P: RT 027 purified; 078C: RT 078 crude; 078P: RT 078 purified.

4. 2. 4 Purified SLPs RT 001, RT 002, RT 027 and RT 078 Were Probed for Glycosylation Using Enzyme-Linked Lectin Assay (ELLA).

To confirm the identity of the signal from lectin blotting, purified samples of all ribotypes were examined by ELLA.

4. 2. 4. 1 ELLA Conditions for Probing for Mannose with ConA and NPL Lectins.

SLPs RT 001, RT 002, RT 014, RT 027, RT 046 and RT 078 were probed for mannose residues with ConA and NPL lectins (Figure 4. 7 and Figure 4. 8). Initial assays (Figure 4. 7 A and Figure 4. 8 A) presented high background reading when probed with TBST buffer only, especially from HRP.

This invalidated the signals detected from actual lectin probing. Optimisation of the assay included washing technique, addition of $Ca^{2+}/Mg^{2+}/Mn^{2+}$ ions for lectin stability and use of synthetic blocking solution with no carbohydrate residues. The signal for the proteins probed with TBST was below the threshold (shaded bars) (Figure 4. 7 B and Figure 4. 8 B). However, the signal from HRP as positive control was not detected in any case, and this invalidated the potential signals from lectins.

A

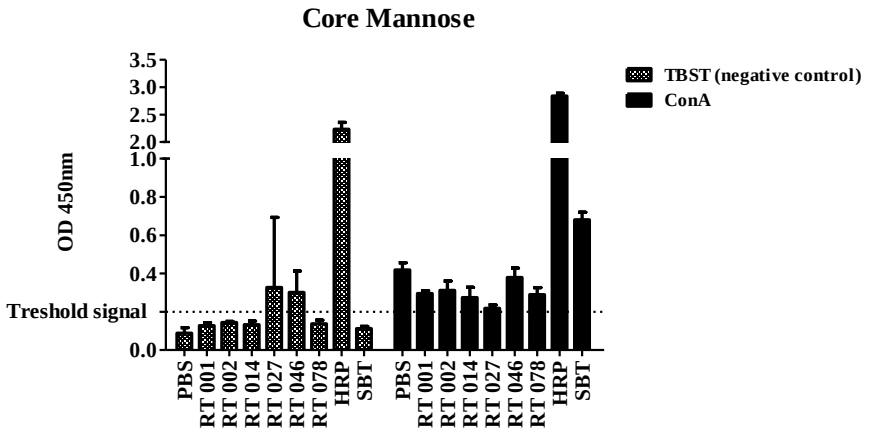

B

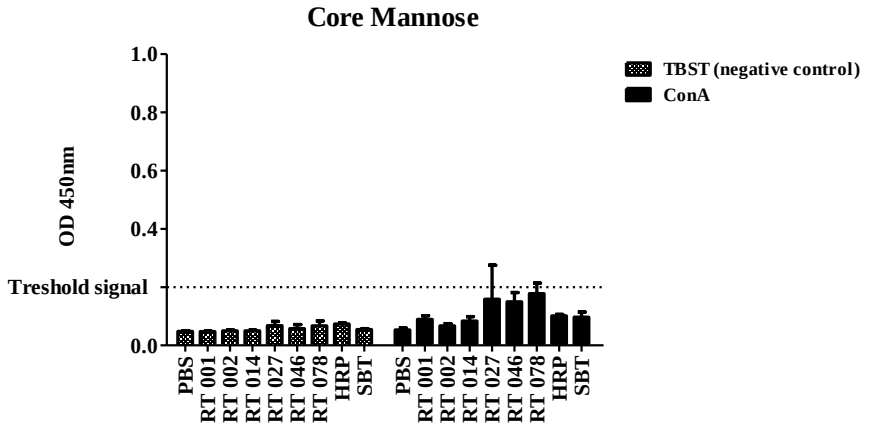

Figure 4. 7 ELLA conditions were optimised for probing SLPs with ConA lectin. SLP RT 001, RT 002, RT 014, RT 027, RT 046 and RT 078 were analysed for presence of core mannose residues using ELLA with biotinylated ConA. Horseradish Peroxidase protein (HRP) was used as positive control, while Soybean trypsin (SBT) and PBS were used as negative controls. Samples were probed with TBST as negative control for lectin specificity. Threshold signal was considered at 0.2 OD. **A**: Initial screening showed a very high background reading for TBST-probed samples. **B**: Optimised assay demonstrated TBST-probed samples below threshold signal, while none of SLP ribotypes demonstrated core mannose glycosylation.

A

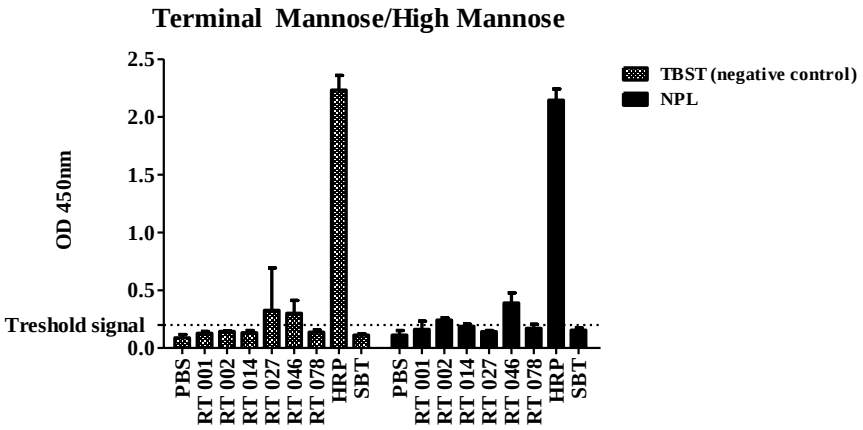

B

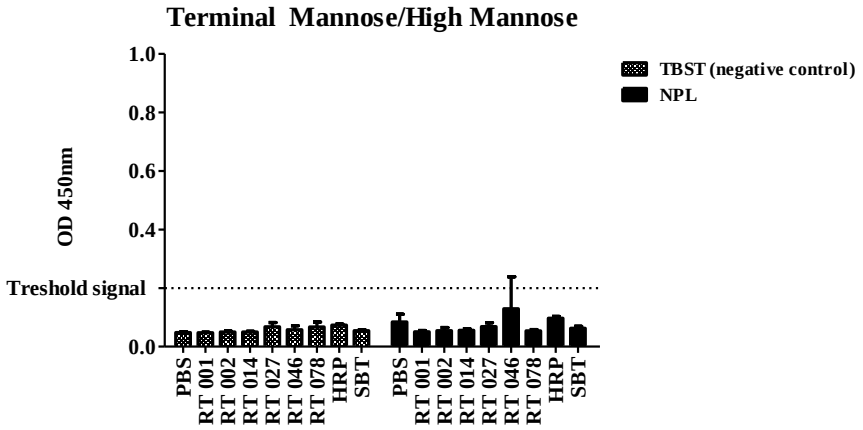

Figure 4. 8 ELLA conditions were optimised for probing SLPs with NPL lectin. SLP RT 001, RT 002, RT 014, RT 027, RT 046 and RT 078 were analysed for presence of terminal or high mannose residues using ELLA with biotinylated NPL. Horseradish Peroxidase protein (HRP) was used as positive control, while Soybean trypsin (SBT) and PBS were used as negative controls. Samples were probed with TBST as negative control for lectin specificity. Threshold signal was considered at 0.2 OD. **A**: Initial screening showed a very high background reading for TBST-probed samples. **B**: Optimised assay demonstrated TBST-probed samples below threshold signal, while none of SLP ribotypes demonstrated terminal or high mannose glycosylation.

4. 2. 4. 2 ELLA Conditions for Probing for N-Acetylgalactosamine With Jacalin and SBA Lectins.

SLPs RT 001, RT 002, RT 014, RT 027, RT 046 and RT 078 were probed for N-Acetylgalactosamine residues with Jacalin and SBA lectins (Figure 4. 9 and Figure 4. 10). Initial assays (Figure 4. 9 A and Figure 4. 10 A) presented high background reading when probed with TBST buffer only, especially from HRP. Optimisation of the assay included washing technique, addition of Ca^{2+}/Mg^{2+}/Mn^{2+} ions for lectin stability and use of synthetic blocking solution with no carbohydrate residues. The signal for the proteins probed with TBST was below the threshold (shaded bars) (Figure 4. 9 B and Figure 4. 11 B). However, the signal from HRP as positive control was only detected when probed with Jacalin and not with SBA lectin, therefore the assay required further optimisation. Negative control for the assay was above the threshold (Figure 4.9 A and B).

A

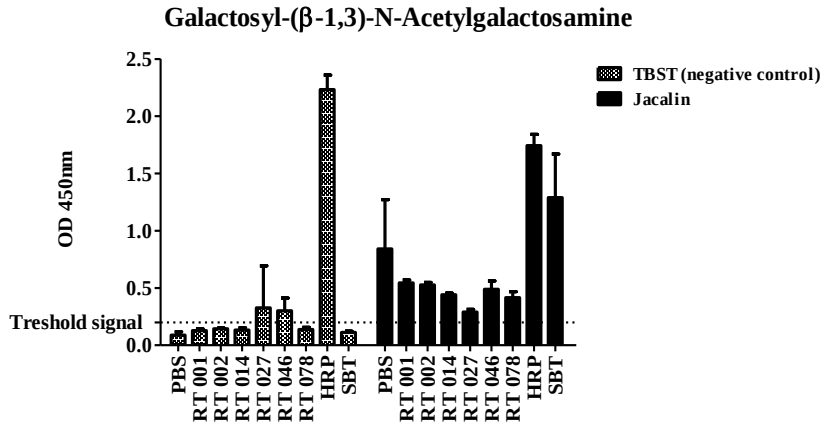

B

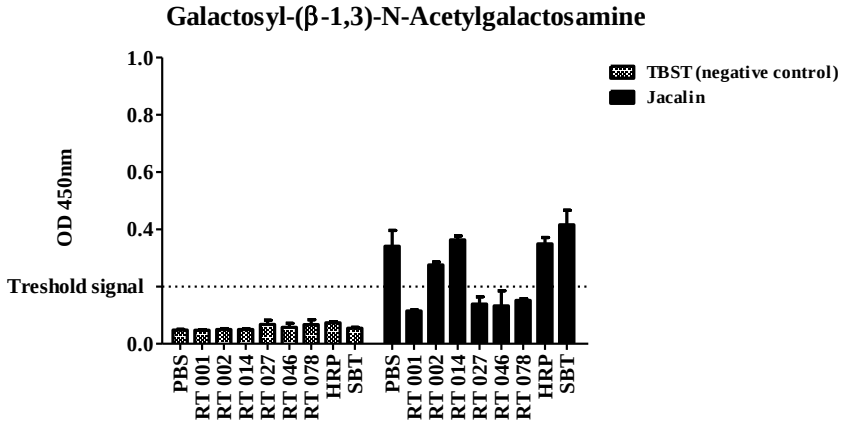

Figure 4. 9 ELLA conditions were optimised for probing SLPs with Jacalin lectin. SLP RT 001, RT 002, RT 014, RT 027, RT 046 and RT 078 were analysed for presence of Galactosyl-(β-1,3)-N-Acetylgalactosamine using ELLA with biotinylated Jacalin. Horseradish Peroxidase protein (HRP) was used as positive control, while Soybean trypsin (SBT) and PBS were used as negative controls. Samples were probed with TBST as negative control for lectin specificity. Threshold signal was considered at 0.2 OD. **A**: Initial screening showed a very high background reading for TBST-probed samples. **B**: Optimised assay demonstrated TBST-probed samples below threshold signal, while none of SLP ribotypes demonstrated Galactosyl-(β-1,3)-N-Acetylgalactosamine glycosylation.

A

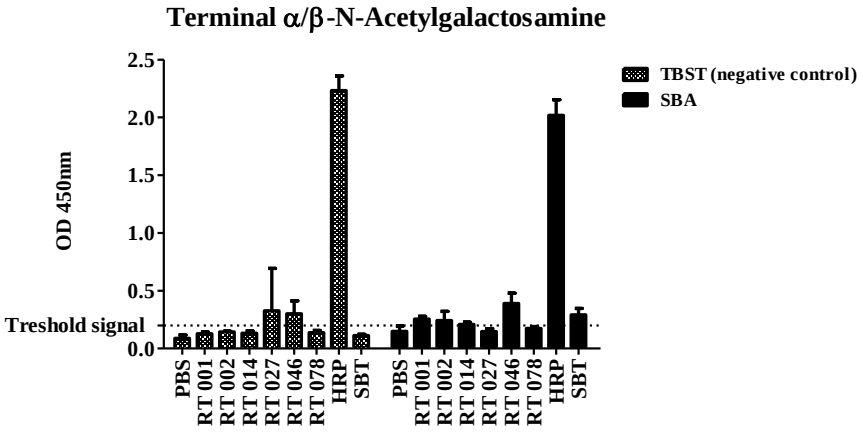

B

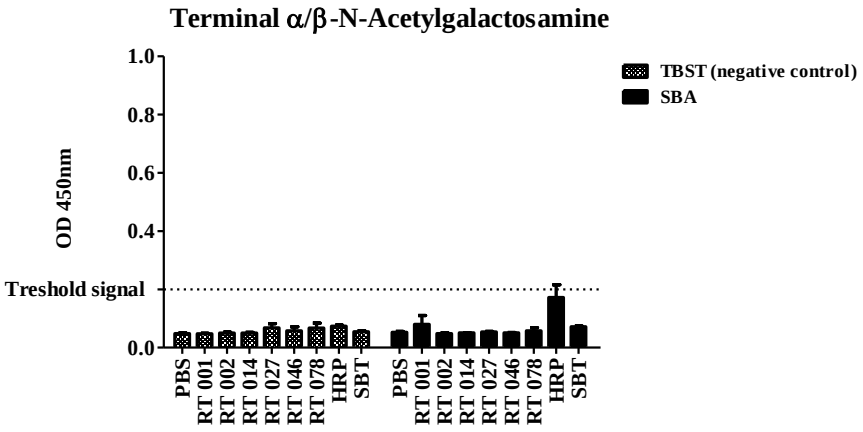

Figure 4. 10 ELLA conditions were optimised for probing SLPs with SBA lectin. SLP RT 001, RT 002, RT 014, RT 027, RT 046 and RT 078 were analysed for presence of terminal α/β-N-Acetylgalactosamine using ELLA with biotinylated SBA. Horseradish Peroxidase protein (HRP) was used as positive control, while Soybean trypsin (SBT) and PBS were used as negative controls. Samples were probed with TBST as negative control for lectin specificity. Threshold signal was considered at 0.2 OD. **A**: Initial screening showed a very high background reading for TBST-probed samples. **B**: Optimised assay demonstrated TBST-probed samples below threshold signal, while none of SLP ribotypes demonstrated terminal α/β-N-Acetylgalactosamine glycosylation.

4. 2. 4. 3 ELLA Conditions for Probing for N-Acetylglucosamine With AAL, GSL II and ECL Lectins.

SLPs RT 001, RT 002, RT 014, RT 027, RT 046 and RT 078 were probed for N-Acetylglucosamine residues with AAL, GSL II and ECL lectins (Figure 4. 11, Figure 4. 12 and Figure 4. 13). Initial assays (Figure 4. 11 A, Figure 4. 12 A and Figure 4. 13 A) presented high background reading when probed with TBST buffer only, especially from HRP. Also negative controls presented signal above the threshold initially (Figure 4. 11 A). Optimisation of the assay included washing technique, addition of $Ca^{2+}/Mg^{2+}/Mn^{2+}$ ions for lectin stability and use of synthetic blocking solution with no carbohydrate residues. The signal for the proteins probed with TBST was below the threshold (shaded bars) (Figure 4. 11 B, Figure 4. 12 B and Figure 4. 13 B). However, the signal from HRP as positive control was only detected when probed with ECL and not with AA or GSL II lectin, therefore the assay required further optimisation.

A

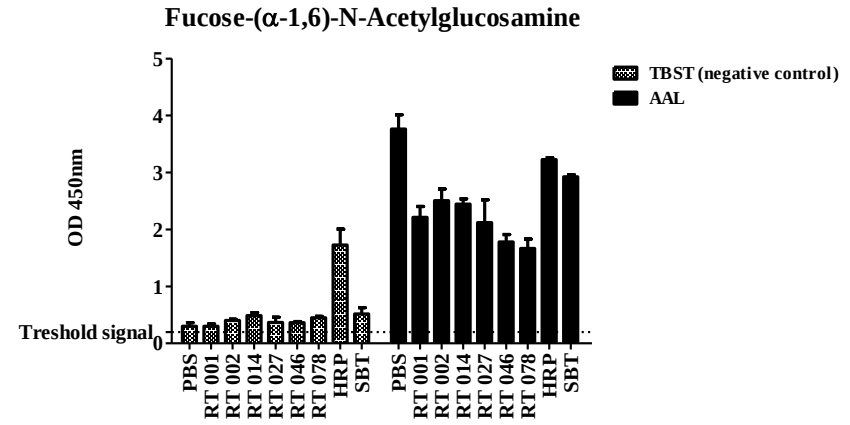

B

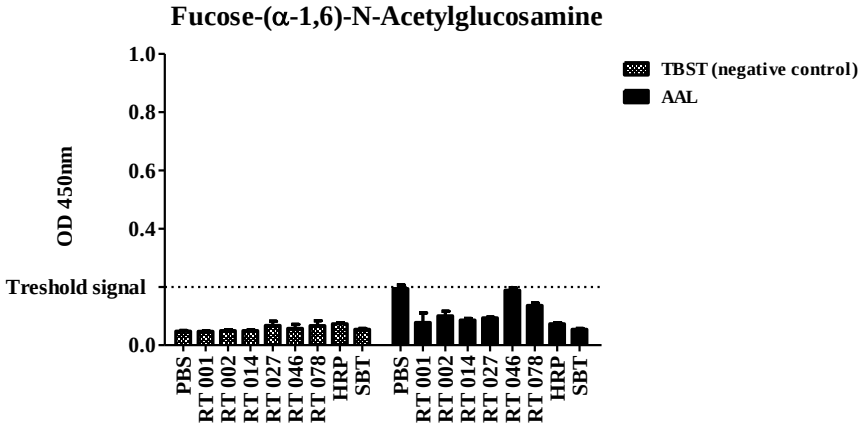

Figure 4. 11 ELLA conditions were optimised for probing SLPs with AAL lectin. SLP RT 001, RT 002, RT 014, RT 027, RT 046 and RT 078 were analysed for presence of Fucose-(α-1,6)-N-Acetylglucosamine using ELLA with biotinylated ALL. Horseradish Peroxidase protein (HRP) was used as positive control, while Soybean trypsin (SBT) and PBS were used as negative controls. Samples were probed with TBST as negative control for lectin specificity. Threshold signal was considered at 0.2 OD. **A**: Initial screening showed a very high background reading for TBST-probed samples. **B**: Optimised assay demonstrated TBST-probed samples below threshold signal, while none of SLP ribotypes demonstrated Fucose-(α-1,6)-N-Acetylglucosamine.

A

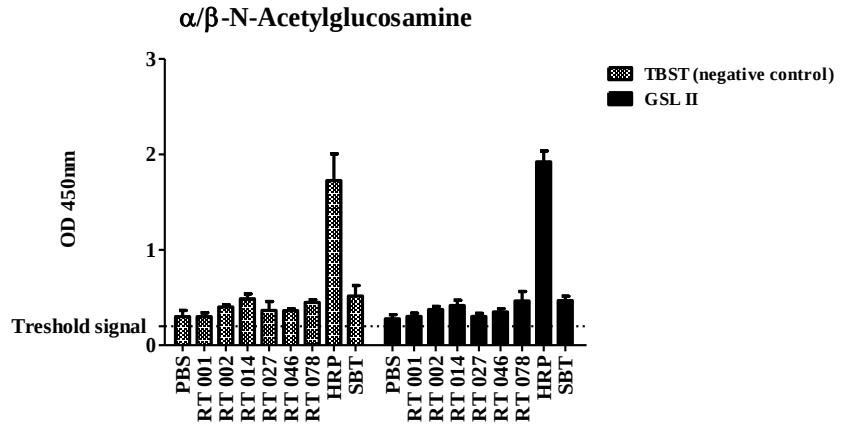

B

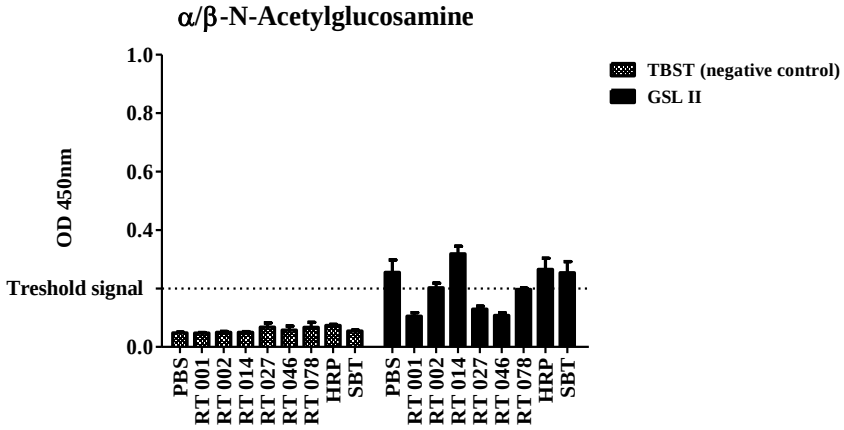

Figure 4. 12 ELLA conditions were optimised for probing SLPs with GSL II lectin. SLP RT 001, RT 002, RT 014, RT 027, RT 046 and RT 078 were analysed for presence of α/β-N-Acetylglucosamine using ELLA with biotinylated GSL II. Horseradish Peroxidase protein (HRP) was used as positive control, while Soybean trypsin (SBT) and PBS were used as negative controls. Samples were probed with TBST as negative control for lectin specificity. Threshold signal was considered at 0.2 OD. **A**: Initial screening showed a very high background reading for TBST-probed samples. **B**: Optimised assay demonstrated TBST-probed samples below threshold signal, while none of SLP ribotypes demonstrated α/β-N-Acetylglucosamine glycosylation.

A

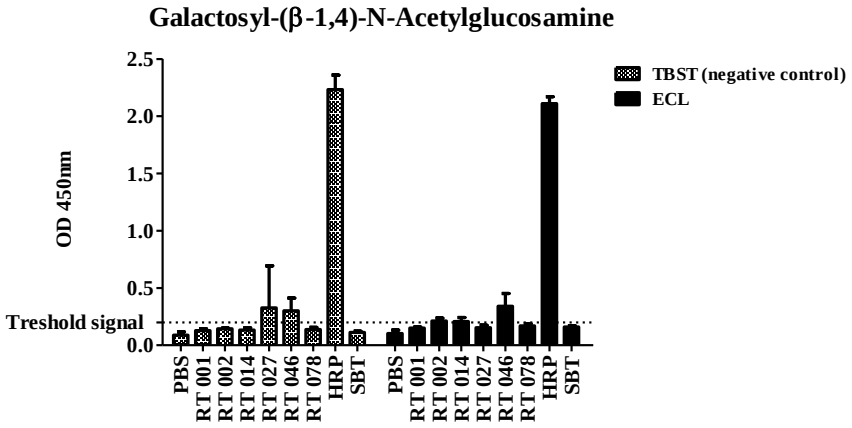

B

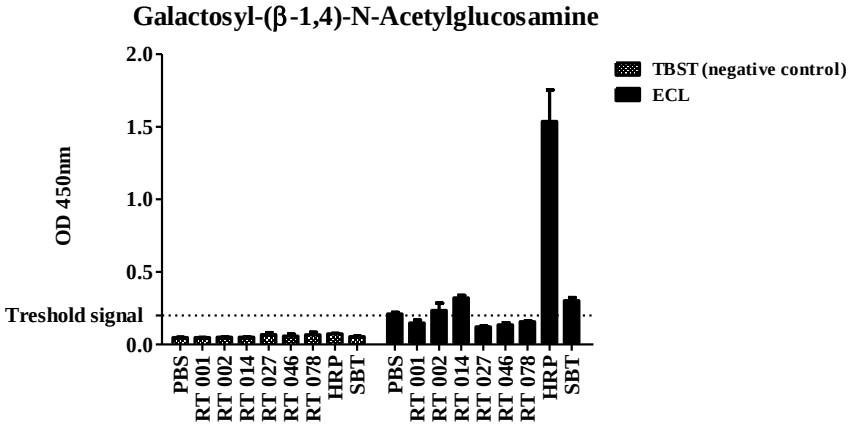

Figure 4. 13 ELLA conditions were optimised for probing SLPs with ECL lectin. SLP RT 001, RT 002, RT 014, RT 027, RT 046 and RT 078 were analysed for presence of Galactosyl-(β-1,4)-N-Acetylglucosamine using ELLA with biotinylated ECL. Horseradish Peroxidase protein (HRP) was used as positive control, while Soybean trypsin (SBT) and PBS were used as negative controls. Samples were probed with TBST as negative control for lectin specificity. Threshold signal was considered at 0.2 OD. **A**: Initial screening showed a very high background reading for TBST-probed samples. **B**: Optimised assay demonstrated TBST-probed samples below threshold signal, while none of SLP ribotypes demonstrated Galactosyl-(β-1,4)-N-Acetylglucosamine glycosylation.

4. 2. 4. 4 ELLA Conditions for Probing for Sialic Acid with SNA Lectin.

SLPs RT 001, RT 002, RT 014, RT 027, RT 046 and RT 078 were probed for sialic acid residues with SNA lectin (Figure 4. 14). Initial assay (Figure 4. 14 A) presented high background reading when probed with TBST buffer only, especially from HRP. Optimisation of the assay included washing technique, addition of Ca^{2+}/Mg^{2+}/Mn^{2+} ions for lectin stability and use of synthetic blocking solution with no carbohydrate residues. The signal for the proteins probed with TBST was below the threshold (shaded bars) (Figure 4. 14 B). However, the signal from HRP as positive control was not detected and therefore the assay required further optimisation.

A

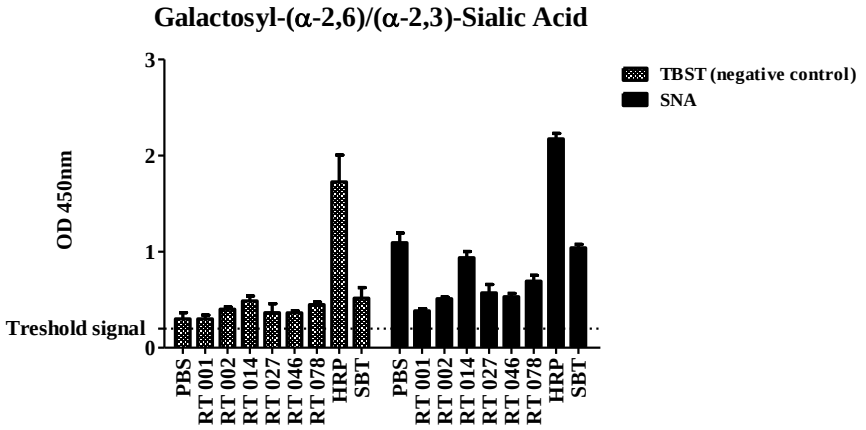

B

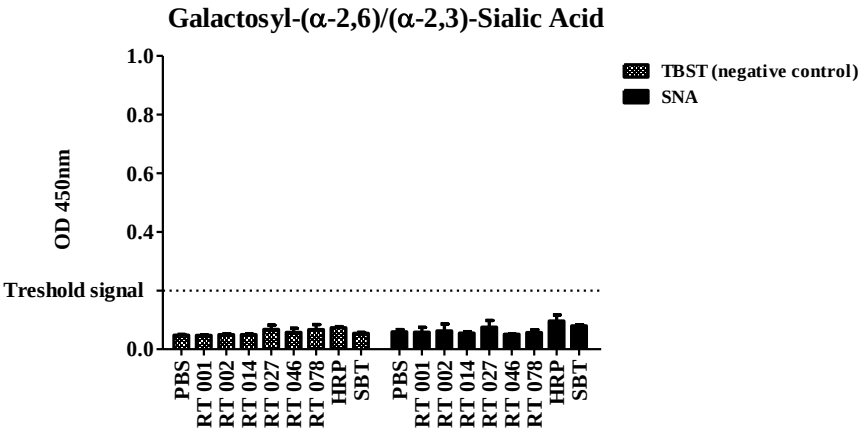

Figure 4. 14 ELLA conditions were optimised for probing SLPs with SNA lectin. SLP RT 001, RT 002, RT 014, RT 027, RT 046 and RT 078 were analysed for presence of Galactosyl-(α-2,6)/(α-2,3)-Sialic Acid using ELLA with biotinylated SNA. Horseradish Peroxidase protein (HRP) was used as positive control, while Soybean trypsin (SBT) and PBS were used as negative controls. Samples were probed with TBST as negative control for lectin specificity. Threshold signal was considered at 0.2 OD. **A**: Initial screening showed a very high background reading for TBST-probed samples. **B**: Optimised assay demonstrated TBST-probed samples below threshold signal, while none of SLP ribotypes demonstrated Galactosyl-(α-2,6)/(α-2,3)-Sialic Acid glycosylation.

4. 2. 4. 5 Positive Controls for ELLA.

Positive controls are an essential part of every assay. HRP did not prove to be a universal positive control for all previous ELLA assays when probed with various lectins for different glycosylation patterns. Additionally, HRP was included in PAS glycoprotein staining kit, however it was not a suitable positive control for ELLA, as it may interfere with the ELLA detection system that utilises the active form of HRP. Therefore, we examined various glycoproteins as potential positive controls for different lectins (Figure 4. 15). Asialofetuin, fetuin, invertase and transferrin were investigated as positive controls for the individual lectins used to examine the glycosylation patterns of SLP. Only SLPs RT 001 and RT 027 were used, as these samples were available in abundance.

Asialofetuin produced signal above threshold for Galactosyl-(α-2,6)/(α-2,3)-Sialic Acid when probed with SNA, additionally, this assay produced signal for PBS (Figure 4. 15 A). Asialofetuin did not demonstrate presence of Galactosyl-(α-2,3)/(α-2,6)-Sialic Acid or Galactosyl-(α-2,6)/(α-2,3)-Sialic Acid-(β-1,4)-N-Acetylgalactosamine when probed with MAL II (Figure 4. 15 B). Fetuin proved to be sufficient positive control for NPL probing for terminal or high mannose (Figure 4. 15 C), however it did not demonstrate presence of (α-1,3)-mannose when probed with GNL (Figure 4. 15 D). Invertase was examined as positive control for Galactosyl-(β-1,4)-N-Acetylglucosamine, however it did not demonstrate this type of glycosylation when examined with ECL (Figure 4. 15 E). Finally transferrin was examined as potential positive control for core mannose residues and probed with ConA and it produced sufficient signal to be considered suitable control for this type of glycosylation (Figure 4. 15 F).

Overall, this part of the optimisation aimed to match a potential control with suitable lectin. This proved to be very time-consuming and therefore we decided to examine glycosylation of four positive controls along with each assay for any further analysis.

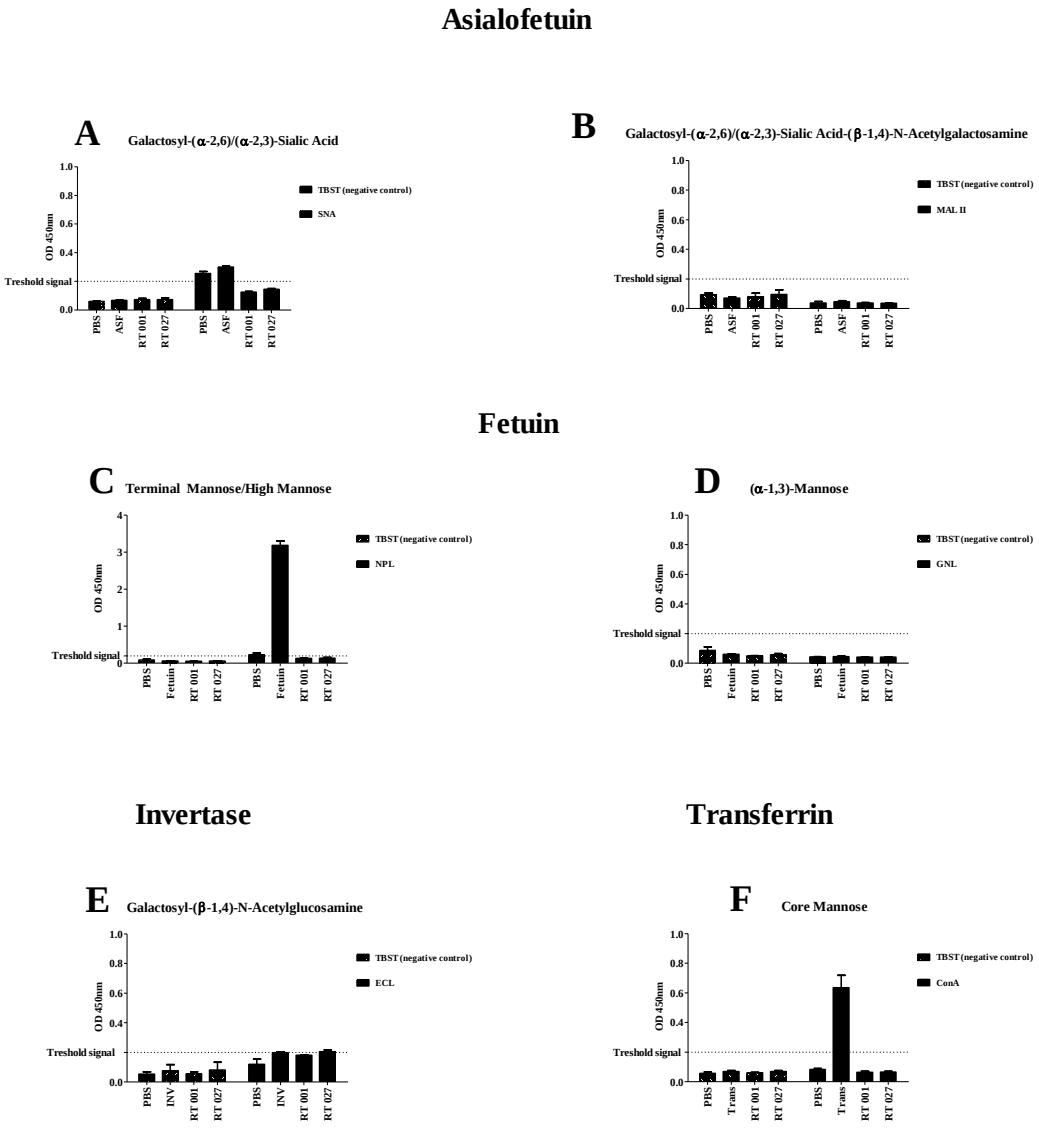

Figure 4. 15 Asialofetuin, fetuin, invertase and transferrin were examined as positive controls for ELLA. Asialofetuin was examined as positive control for sialic residues and it probed with biotinylated SNA (**A**) and MAL II (**B**). Fetuin was examined as positive control for detection of mannose residues and it was probed by NPL (**C**) and GNL (**D**). Invertase was examined as positive control for N-Acetylglucosamine and it was probed with ECL (**E**). Transferrin was examined as positive control for core mannose residues and it was probed with ConA (**F**). All positive controls were probed along with two SLPs, RT 001 and RT 027. PBS was used as negative control; samples were probed with TBST as negative control for lectin specificity. Threshold signal was considered at 0.2 OD.

4. 2. 4. 6 TBST is Sufficient Negative Control for ELLA.

Also, when all the assay preparation techniques were verified such as washing and blocking buffer, we examined again the background signal produced by TBST buffer probing only. We determined that TBST is suitable negative control for the assay as the reading was below threshold (Figure 4. 16). For any analysis, the total ELLA reading was corrected for the background signal by deducting the reading of TBST buffer probing from the reading of each of other ELLA assays.

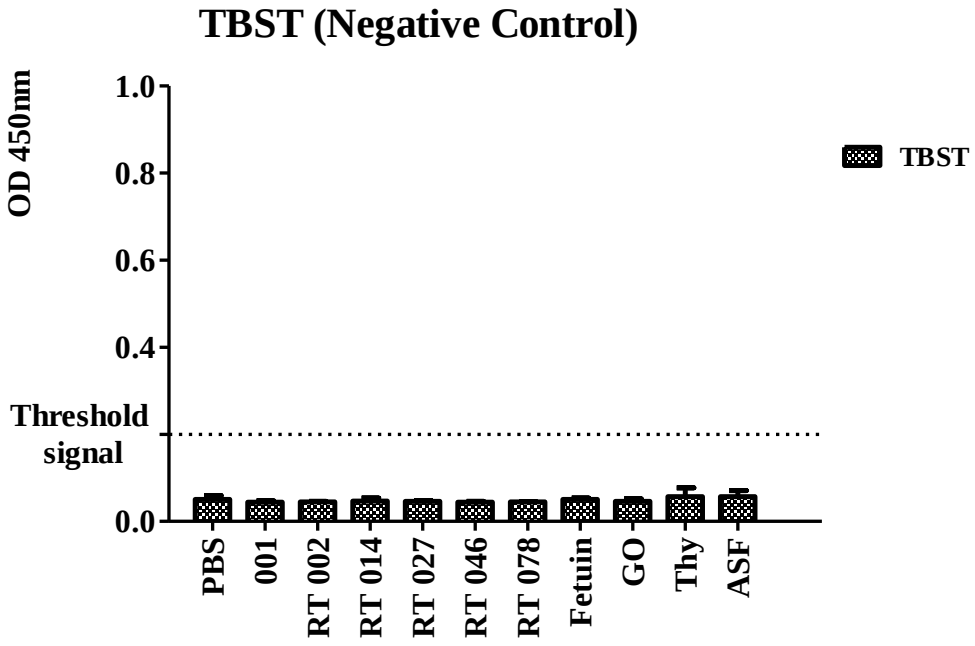

Figure 4. 16 TBST buffer was used as negative control for probing SLPs and positive controls in ELLA. SLP RT 001, RT 002, RT 014, RT 027, RT 046 and RT 078, along with four positive controls were probed with TBST buffer only. Minimal signal was detected, consistent with background reading. Threshold signal was considered at 0.2 OD.

4. 2. 4. 7 SLPs Did Not Demonstrate Presence of Mannose When Probed with ConA, NPL and LCA.

SLPs RT 001, RT 002, RT 014, RT 027, RT 046 and RT 078 were probed for presence of core mannose with ConA (Figure 4. 17), high or terminal mannose with NPL (Figure 4. 18) and α-mannose with LCA (Figure 4. 19).

Probing for core mannose with ConA presented threshold signal for presence of this type of glycosylation in RT 046 and RT 078, however since the signal from PBS (negative control) was also close to threshold, it was concluded that SLP RT 046 and RT 078 does not present this type of glycosylation.

None of the other ribotypes under investigation demonstrated signal required to confirm presence of glycosylation, and therefore we concluded that SLPs RT 001, RT 002, RT 014, RT 027, RT 046 and RT 078 are not modified with mannose.

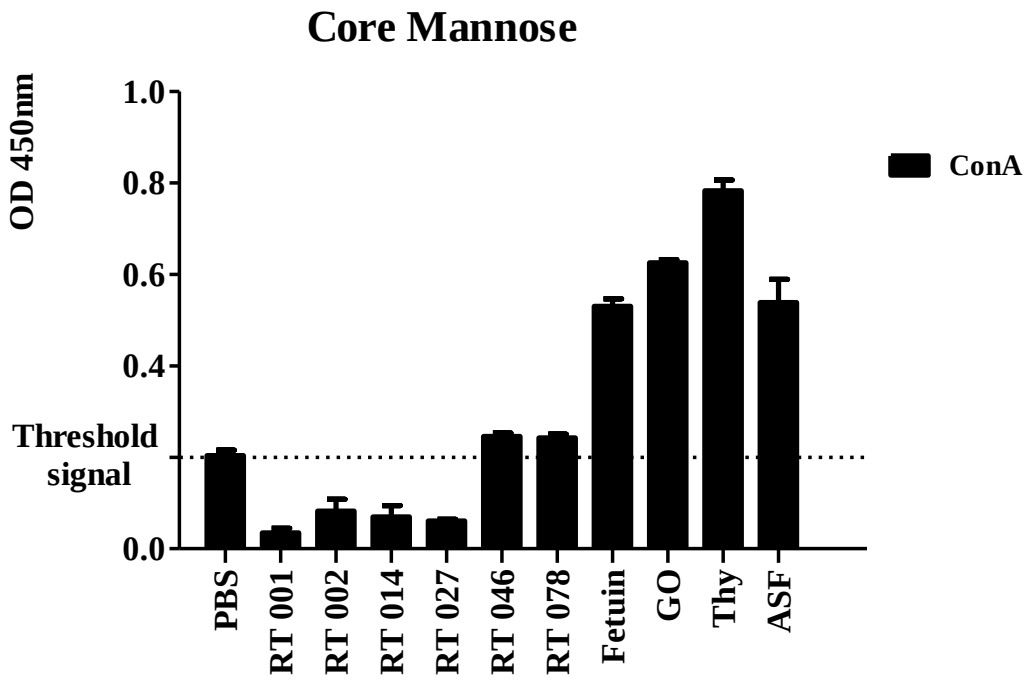

Figure 4. 17 SLPs were probed for core mannose with ConA lectin. SLP RT 001, RT 002, RT 014, RT 027, RT 046 and RT 078 were analysed for presence of core mannose using ELLA with biotinylated ConA. Four positive controls with known glycosylation patterns were used fetuin, glucose oxidase, thyroglobulin and asialofetuin and these interacted with lectins in a manner that was consistent with the glycan structures expected to be present on the surface of each glycoprotein. PBS and TBST were used as negative controls and the readings were corrected for background reading with TBST. Threshold signal was considered at 0.2 OD. None of SLPs ribotypes demonstrated presence of core mannose.

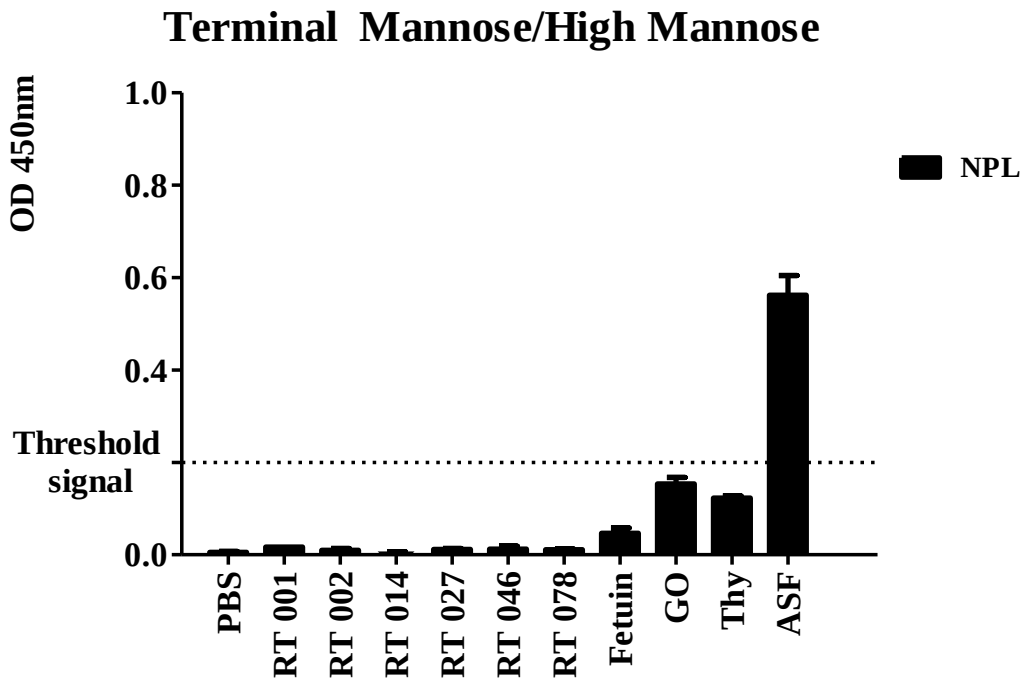

Figure 4. 17 SLPs were probed for terminal and high mannose with NPL lectin. SLP RT 001, RT 002, RT 014, RT 027, RT 046 and RT 078 were analysed for presence of terminal or high mannose using ELLA with biotinylated NPL. Four positive controls with known glycosylation patterns were used fetuin, glucose oxidase, thyroglobulin and asialofetuin and these interacted with lectins in a manner that was consistent with the glycan structures expected to be present on the surface of each glycoprotein. PBS and TBST were used as negative controls. Threshold signal was considered at 0.2 OD. None of the ribotypes demonstrated presence of terminal or high mannose.

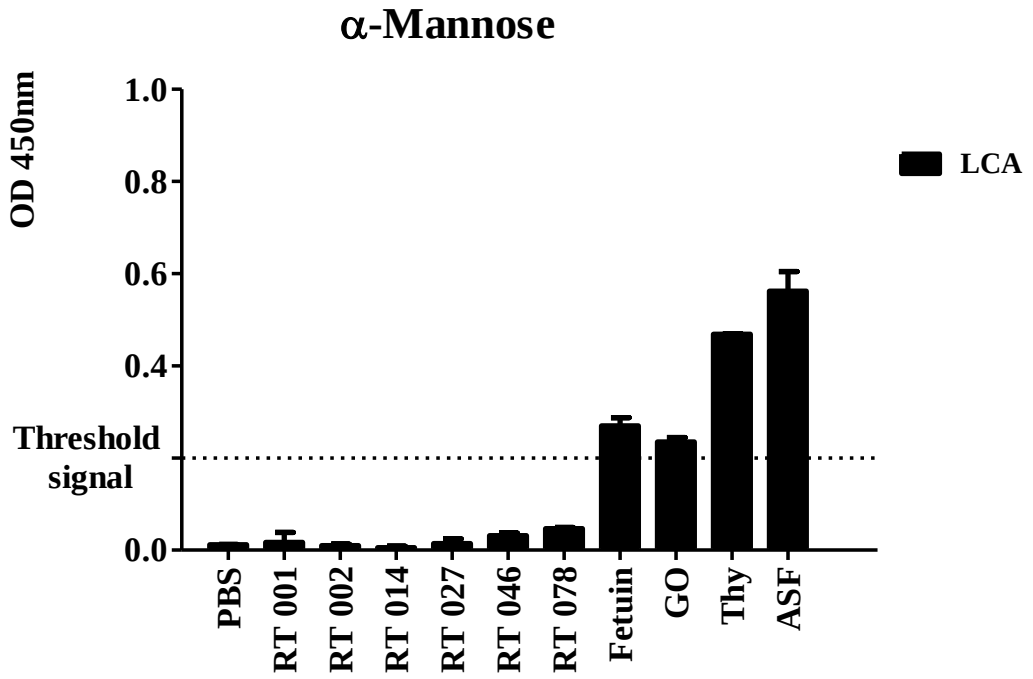

Figure 4. 18 SLPs were probed for α-mannose with LCA lectin. SLP RT 001, RT 002, RT 014, RT 027, RT 046 and RT 078 were analysed for presence of α-mannose using ELLA with biotinylated LCA. Four positive controls with known glycosylation patterns were used fetuin, glucose oxidase, thyroglobulin and asialofetuin and these interacted with lectins in a manner that was consistent with the glycan structures expected to be present on the surface of each glycoprotein. PBS and TBST were used as negative controls. Threshold signal was considered at 0.2 OD. None of the ribotypes demonstrated presence of α-mannose.

4. 2. 4. 8 SLPs Did Not Demonstrate Presence of N-Acetylgalactosamine When Probed with PNA, Jacalin, SBA, GSL I and DBA.

SLPs RTs 001, 002, 014, 027, 046 and 078 were probed for presence of Galactosyl-(β-1,3)-N-Acetylgalactosamine with PNA (Figure 4. 20), for Galactosyl-(β-1,3)-N-Acetylgalactosamine with Jacalin (Figure 4. 21), α-N-Acetylgalactosamine or α-galactose with GSL I (Figure 4. 22) and α-N-Acetylgalactosamine with DBA (Figure 4. 23).

Probing for Galactosyl-(β-1,3)-N-Acetylgalactosamine with Jacalin presented threshold signal for presence of this type of glycosylation in RT 046 and RT 078, however since the signal from PBS (negative control) was also close to threshold, it was concluded that SLP RT 046 and RT 078 does not present this type of glycosylation.

None of the other ribotypes under investigation demonstrated signal required to confirm presence of glycosylation, and therefore we concluded that SLPs RT 001, RT 002, RT 014, RT 027, RT 046 and RT 078 are not modified with N-Acetylgalactosamine.

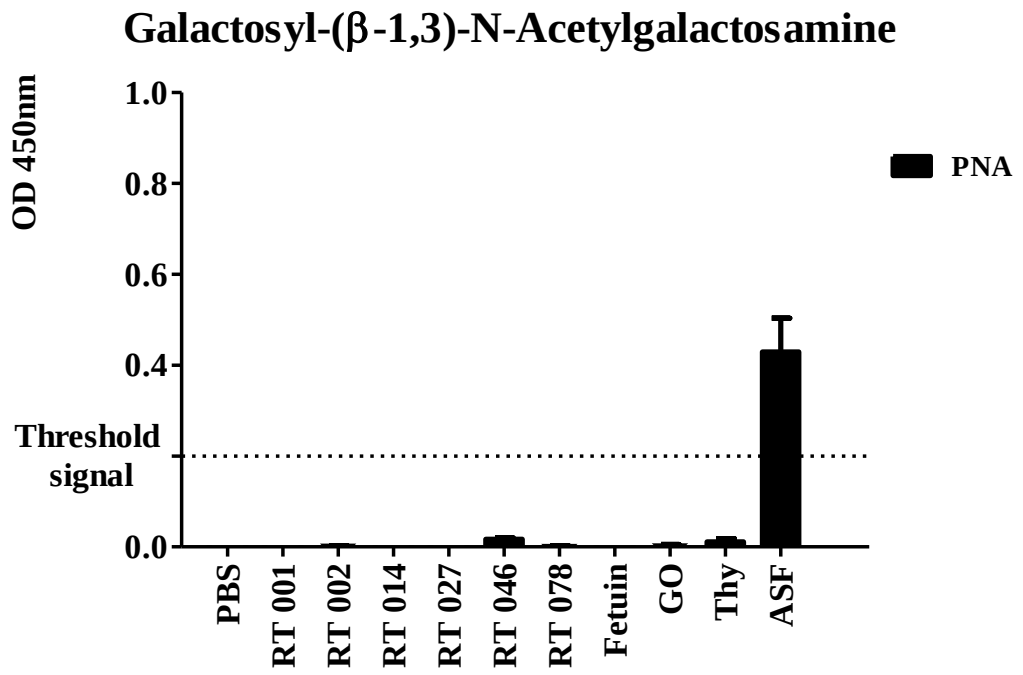

Figure 4. 20 SLPs were probed for Galactosyl-(β-1,3)-N-Acetylgalactosamine with PNA lectin. SLP RT 001, RT 002, RT 014, RT 027, RT 046 and RT 078 were analysed for presence of Galactosyl-(β-1,3)-N-Acetylgalactosamine using ELLA with biotinylated PNA. Four positive controls with known glycosylation patterns were used fetuin, glucose oxidase, thyroglobulin and asialofetuin and these interacted with lectins in a manner that was consistent with the glycan structures expected to be present on the surface of each glycoprotein. PBS and TBST were used as negative controls and the readings were corrected for background reading with TBST. Threshold signal was considered at 0.2 OD. None of the ribotypes demonstrated presence of Galactosyl-(β-1,3)-N-Acetylgalactosamine.

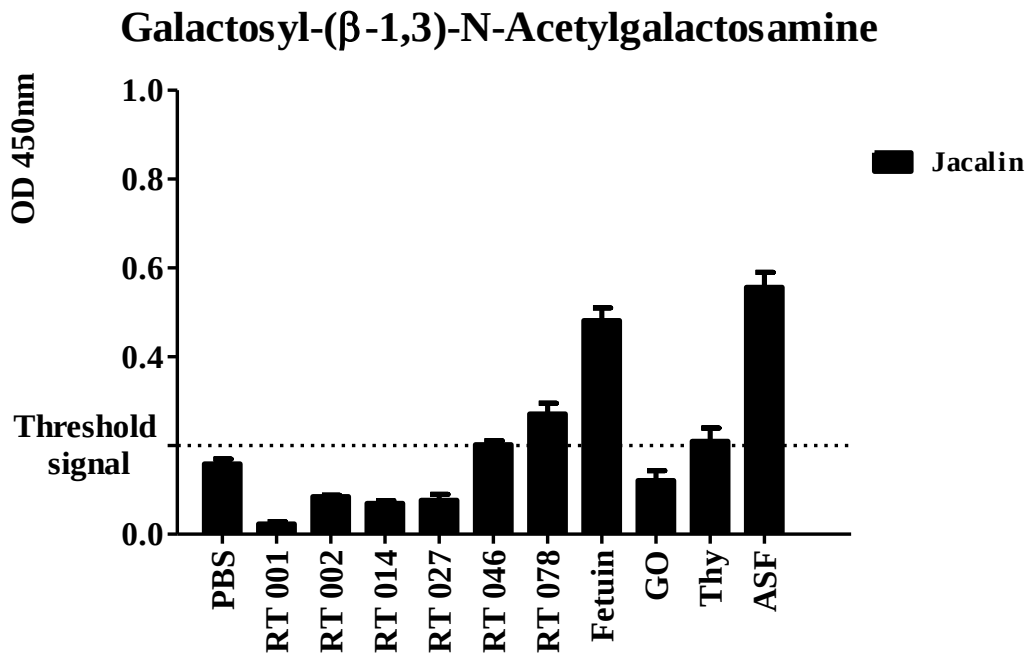

Figure 4. 21 SLPs were probed for Galactosyl-(β-1,3)-N-Acetylgalactosamine with Jacalin lectin. SLP RT 001, RT 002, RT 014, RT 027, RT 046 and RT 078 were analysed for presence of Galactosyl-(β-1,3)-N-Acetylgalactosamine using ELLA with biotinylated Jacalin. Four positive controls with known glycosylation patterns were used fetuin, glucose oxidase, thyroglobulin and asialofetuin and these interacted with lectins in a manner that was consistent with the glycan structures expected to be present on the surface of each glycoprotein. PBS and TBST were used as negative controls. Threshold signal was considered at 0.2 OD. None of the ribotypes demonstrated presence of Galactosyl-(β-1,3)-N-Acetylgalactosamine.

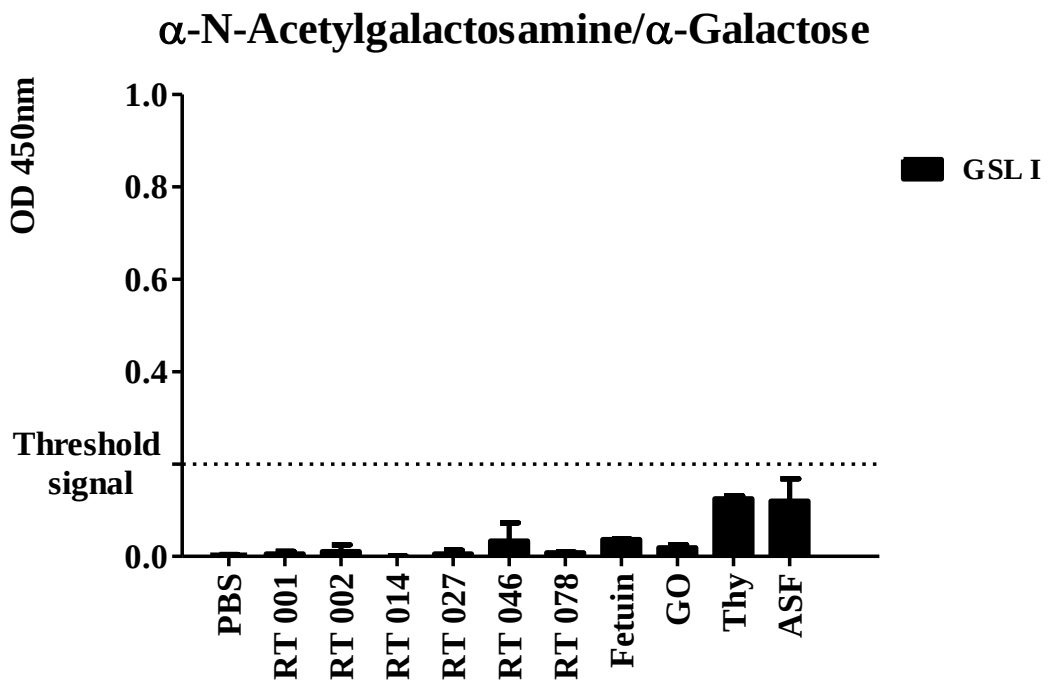

Figure 4. 22 SLPs were probed for α-N-Acetylgalactosamine or α-galactose with GSL I lectin. SLP RT 001, RT 002, RT 014, RT 027, RT 046 and RT 078 were analysed for presence of α-N-Acetylgalactosamine and α-Galactose using ELLA with biotinylated GSL I. Four positive controls with known glycosylation patterns were used fetuin, glucose oxidase, thyroglobulin and asialofetuin and these interacted with lectins in a manner that was consistent with the glycan structures expected to be present on the surface of each glycoprotein. PBS and TBST were used as negative controls. Threshold signal was considered at 0.2 OD. None of the ribotypes demonstrated presence of α-N-Acetylgalactosamine or α-Galactose.

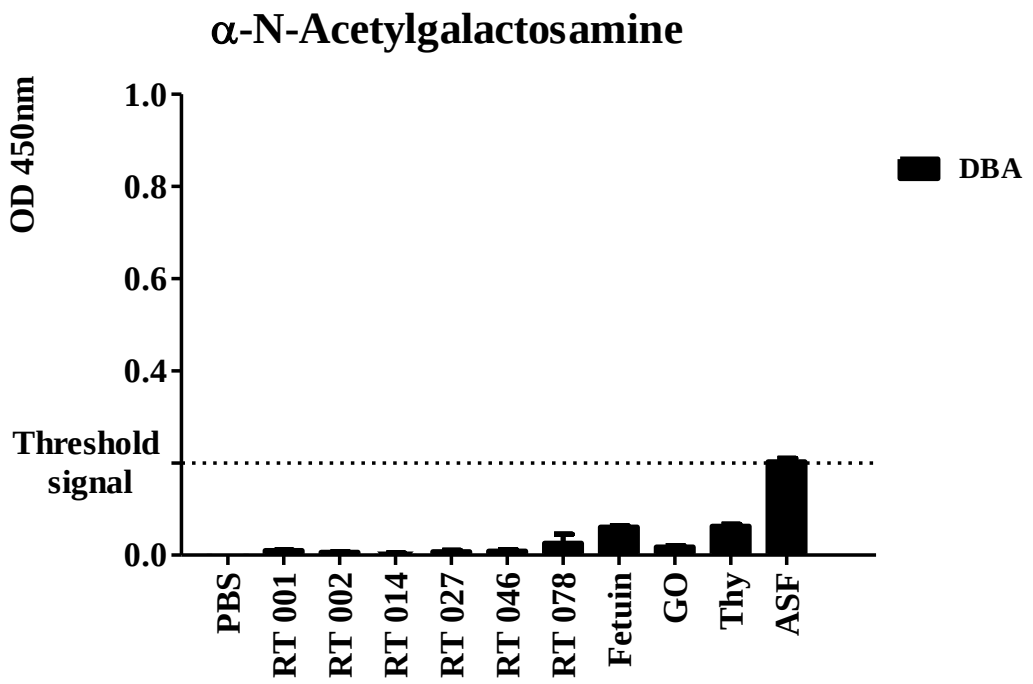

Figure 4. 23 SLPs were probed for α-N-Acetylgalactosamine with DBA lectin. SLP RT 001, RT 002, RT 014, RT 027, RT 046 and RT 078 were analysed for presence of α-N-Acetylgalactosamine using ELLA with biotinylated DBA. Four positive controls with known glycosylation patterns were used fetuin, glucose oxidase, thyroglobulin and asialofetuin and these interacted with lectins in a manner that was consistent with the glycan structures expected to be present on the surface of each glycoprotein. PBS and TBST were used as negative controls. Threshold signal was considered at 0.2 OD. None of the ribotypes demonstrated presence of α-N-Acetylgalactosamine.

4. 2. 4. 9 SLPs Did Not Demonstrate Presence of N-Acetylglucosamine When Probed With AAL, GSL II and ECL.

SLPs RT 001, RT 002, RT 014, RT 027, RT 046 and RT 078 were probed for presence of Fucose-(α-1,6)-N-Acetylglucosamine with AAL (Figure 4. 24), α- or β-N-Acetylglucosamine with GSL II (Figure 4. 25) and Galactosyl-(β-1,4)-N-Acetylglucosamine with ECL (Figure 4. 26).

Probing for Fucose-(α-1,6)-N-Acetylglucosamine with AAL presented threshold signal for presence of this type of glycosylation in RT 046 and RT 078, however since the signal from PBS (negative control) was also close to threshold, it was concluded that SLP RT 046 and RT 078 does not present this type of glycosylation.

None of the other ribotypes under investigation demonstrated signal required to confirm presence of glycosylation, and therefore we concluded that SLPs RT 001, RT 002, RT 014, RT 027, RT 046 and RT 078 are not modified with N-Acetylglucosamine.

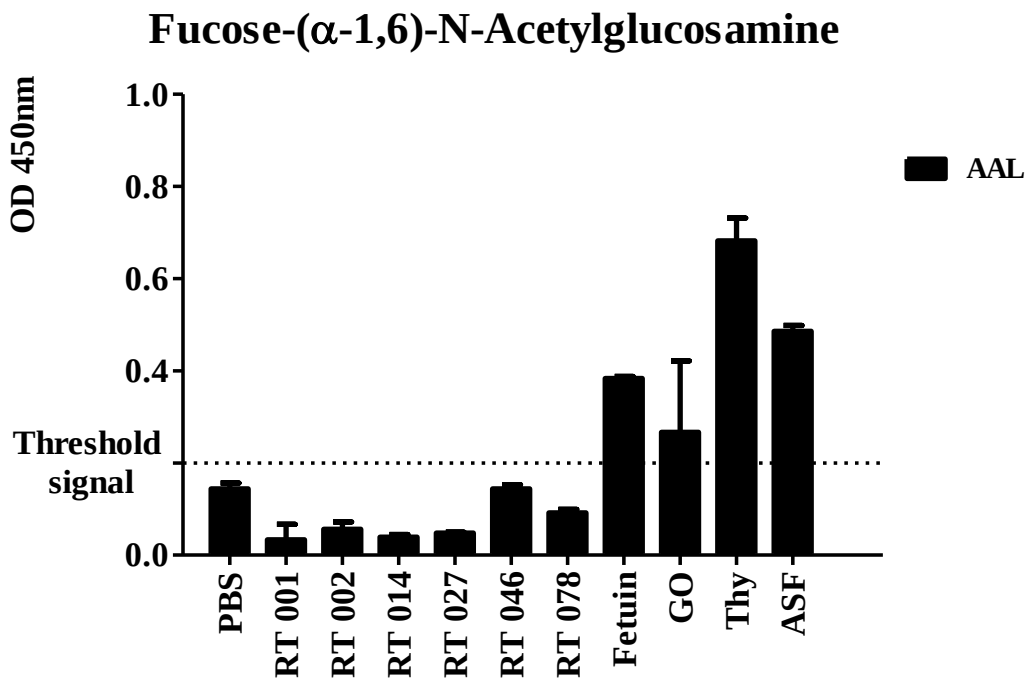

Figure 4. 24 SLPs were probed for (α-1,6)-Fucose-N-Acetylglucosamine with AAL lectin. SLP RT 001, RT 002, RT 014, RT 027, RT 046 and RT 078 were analysed for presence of Fucose-(α-1,6)-N-Acetylglucosamine using ELLA with biotinylated AAL. Four positive controls with known glycosylation patterns were used fetuin, glucose oxidase, thyroglobulin and asialofetuin and these interacted with lectins in a manner that was consistent with the glycan structures expected to be present on the surface of each glycoprotein. PBS and TBST were used as negative controls and the readings were corrected for background reading with TBST. Threshold signal was considered at 0.2 OD. None of the ribotypes demonstrated presence of Fucose-(α-1,6)-N-Acetylglucosamine.

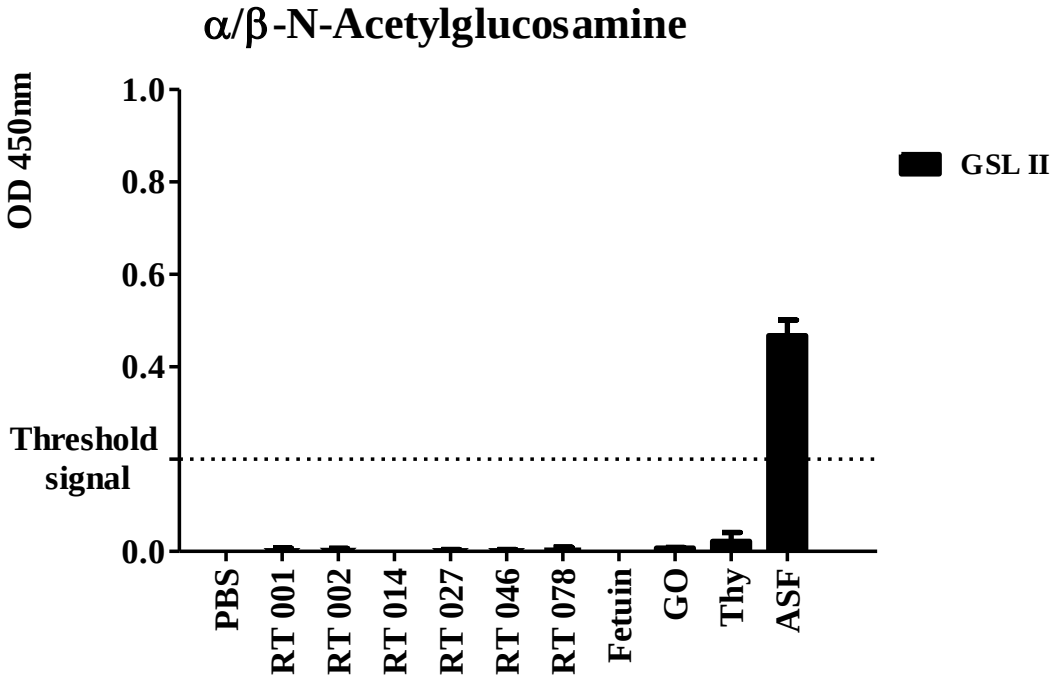

Figure 4. 25 SLPs were probed for α- or β-N-Acetylglucosamine with GSL II lectin. SLP RT 001, RT 002, RT 014, RT 027, RT 046 and RT 078 were analysed for presence of α- or β-N-Acetylglucosamine using ELLA with biotinylated GSL II. Four positive controls with known glycosylation patterns were used fetuin, glucose oxidase, thyroglobulin and asialofetuin and these interacted with lectins in a manner that was consistent with the glycan structures expected to be present on the surface of each glycoprotein. PBS and TBST were used as negative controls. Threshold signal was considered at 0.2 OD. None of the ribotypes demonstrated presence of α- or β-N-Acetylglucosamine.

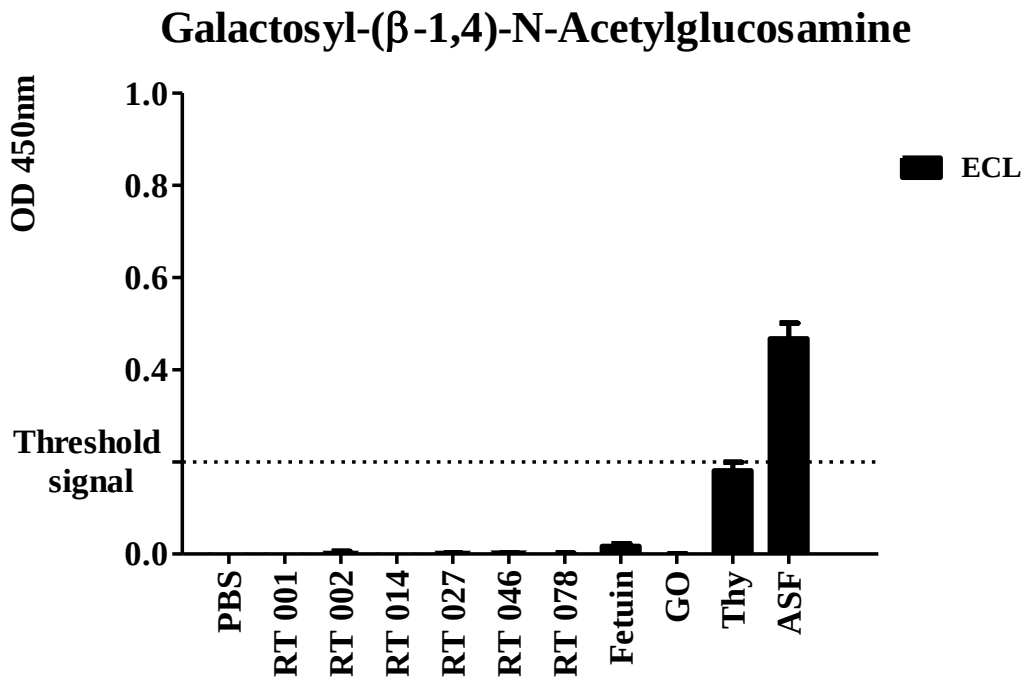

Figure 4. 26 SLPs were probed for Galactosyl-(β-1,4)-N-Acetylglucosamine with ECL lectin. SLP RT 001, RT 002, RT 014, RT 027, RT 046 and RT 078 were analysed for presence of Galactosyl-(β-1,4)-N-Acetylglucosamine using ELLA with biotinylated ECL. Four positive controls with known glycosylation patterns were used fetuin, glucose oxidase, thyroglobulin and asialofetuin and these interacted with lectins in a manner that was consistent with the glycan structures expected to be present on the surface of each glycoprotein. PBS and TBST were used as negative controls. Threshold signal was considered at 0.2 OD. None of the ribotypes demonstrated presence of Galactosyl-(β-1,4)-N-Acetylglucosamine.

4. 2. 4. 10 SLPs Did Not Demonstrate Presence of Sialic Acid When Probed with SNA.

SLPs RT 001, RT 002, RT 014, RT 027, RT 046 and RT 078 were probed for presence of Galactosyl-(α-2,6)/(α-2,3)-Sialic Acid with SNA (Figure 4. 27).

Probing for Galactosyl-(α-2,6)/(α-2,3)-Sialic Acid with SNA presented threshold signal for presence of this type of glycosylation in RT 046 and RT 078, however since the signal from PBS (negative control) was also close to threshold, it was concluded that SLP RT 046 and RT 078 does not present this type of glycosylation.

None of the other ribotypes under investigation demonstrated a signal required confirming presence of glycosylation, and therefore we concluded that SLPs RT 001, RT 002, RT 014, RT 027, RT 046 and RT 078 are not modified with Galactosyl-(α-2,6)/(α-2,3)-Sialic Acid.

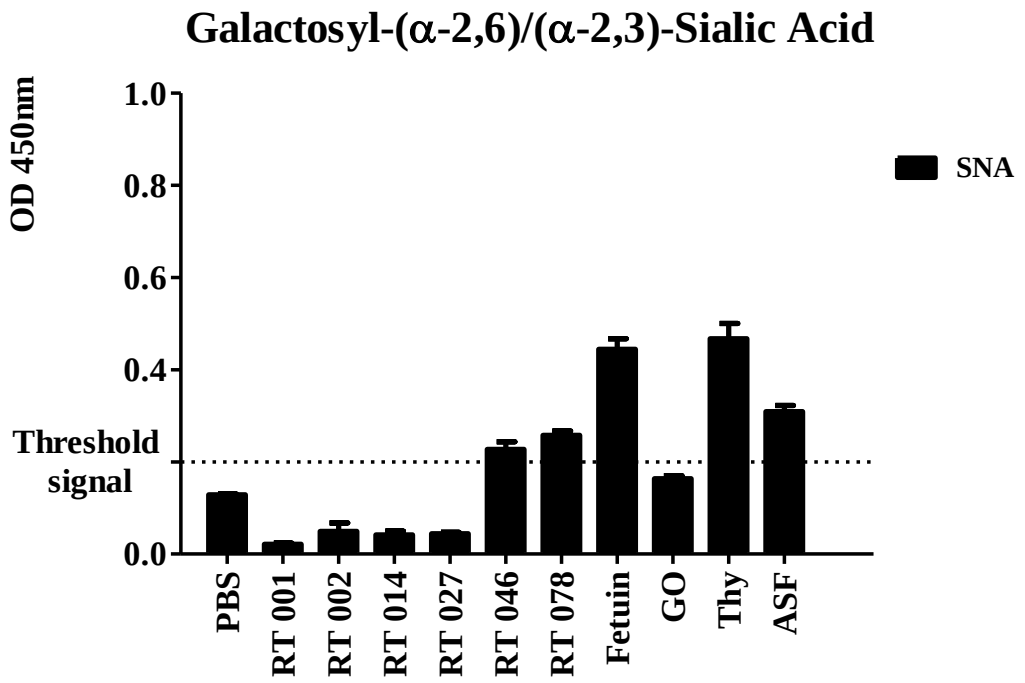

Figure 4. 25 SLPs were probed for Galactosyl-(α-2,6)/(α-2,3)-Sialic Acid with SNA lectin. SLP RT 001, RT 002, RT 014, RT 027, RT 046 and RT 078 were analysed for presence of Galactosyl-(α-2,6)/(α-2,3)-Sialic Acid using ELLA with biotinylated SNA. Four positive controls with known glycosylation patterns were used fetuin, glucose oxidase, thyroglobulin and asialofetuin and these interacted with lectins in a manner that was consistent with the glycan structures expected to be present on the surface of each glycoprotein. PBS and TBST were used as negative controls and the readings were corrected for background reading with TBST. Threshold signal was considered at 0.2 OD. None of the ribotypes demonstrated presence of Galactosyl-(α-2,6)/(α-2,3)-Sialic Acid.

4. 3 DISCUSSION

There has been enormous progress in CDI research in recent years and this has contributed to a better understanding of the disease mechanisms, as presented in multiple reviews (Sun & Hirota 2015; Solomon 2013; Madan & Petri Jr 2012). However, the steps involving adherence of *C. difficile* and subsequent colonisation still remain unclear.

In this chapter, we aimed to determine whether SLPs from RT 001, RT 002, RT 014, RT 027, RT 046 and RT 078 are glycosylated, as we wanted to determine whether any glycosylation differences may have implications for adherence and virulence.

We were able to show that SLPs derived from various ribotypes have different molecular weights subunits, which correlates with other studies (Calabi *et al.* 2001; Karjalainen *et al.* 2002; Eidhin *et al.* 2006). Also, Mauri *et al.* proposed that predicted molecular weights may differ from molecular weights estimated by SDS PAGE, which suggested post-translational modification, such as glycosylation (Mauri *et al.* 1999).

Previous research indicated that the S-layer of *C. difficile* isolated with EDTA contained up to 9% glycan moieties (Cerquetti *et al.* 1992). However, this study only involved one ribotype of SLP. Therefore, we proceeded with PAS staining for an initial screening of four SLPs ribotypes, RT 001, RT 002, RT 027 and RT 078. We observed no colour change in SLPs, as opposed to the positive control, HRP. Qazi *et al.* indicated that commercial glycosylation detection kits may be unreliable (Qazi *et al.* 2009). However, the lack of glycosylation signal in our experiment does not entirely rule out the possibility of glycosylation, as PAS staining does not engage

with carbohydrates with carbons that are not directly involved in glycosidic linkages or carbohydrate link closure (Mantle & Allen 1978).

Qazi *et al.* also suggested that the previous positive detection of glycans in SLPs was in fact due to contamination from cell wall peptidoglycan during the isolation and purification procedure (Qazi *et al.* 2009). Qazi *et al.* have used low pH glycine, while Cerquetti *et al.* used 8 M urea in Tris/HCl to extract the S-layer(Qazi *et al.* 2009; Cerquetti *et al.* 1992). We have used the same approach in an isolation of the S-layer as Cerquetti *et al.*, but these authors do not specify the purification procedure. Therefore we suggest that our FPLC protocol with 0.3 M NaCl gradient optimised for each ribotype was sufficient to remove any impurities and cell wall contaminants from isolation procedure. This was confirmed by two clear bands corresponding to HMW and LMW subunits of SLPs on SDS PAGE, as presented in Chapter 3.

The initial experiments did not confirm the presence of glycosylation on SLPs, however PAS staining did not eliminate the possibility of the glycan moieties on SLPs. Therefore we proceeded to examine SLPs with range of plant lectins, which were used for lectin blotting and ELLA.

Lectins are specific carbohydrate binding proteins, each lectin has from two to multiple carbohydrate recognition sites (Berg *et al.* 2002). The single interaction between lectins binding site and carbohydrate is relatively weak but the sum of the total interactions is extremely strong (Weis & Drickamer 1996).

Lectins selected for the screening included plant lectins that are specific for glycans presented on the bacterial surface (Leriche *et al.* 2000). This included group of mannose-specific lectins (ConA, NPL, LCA and GNL), N-Acetylgalactosamine-

specific lectins (PNA, Jacalin, GSL I, SBA and DBA), N-Acetylglucosamine-specific lectins (AAL, GSL II and ECL) and sialic acid-specific lectin (SNA and MAL II). To our knowledge, there was no previous research carried out on SLPs RT 001, RT 002, RT 014, RT 027, RT 046 and RT 078 with use of these lectins.

Initially, we examined RT 001, RT 002, RT 027 and RT 078, and we used crude S-layer extract and purified SLPs. The samples were separated on SDS PAGE and blotted onto nitrocellulose membrane. We wanted to determine whether there are differences in glycosylation between the total S-layer (which comprises SLPs and other surface-associated proteins) and purified SLPs.

These four ribotypes were chosen, as they represent the wide spectrum of virulence, from mild RT 001 to hypervirulent RT 027. SDS PAGE separated various fractions and subunits of proteins found in the samples, while denaturing conditions allowed presenting these proteins in non-native confirmation, exposing any potential glycosylation sites.

Crude samples of all the ribotypes demonstrated glycosylation when probed with all 14 lectins. However, none of the signals was identified as either subunit of SLPs. Similar approach was used by Cerquetti *et al.* (2000), where these authors used commercially available kit with four lectins and probed SLPs of six strains. These authors also confirmed the presence of glycosylation on total S-layer extract, which is consistent with our results.

In the case of purified SLPs, lectin blotting presented inconclusive results, indicating the possibility of glycosylation in some of the ribotypes. However, there was also a possibility of insufficient lectin washing, as lectins are known for their adhesive

properties and extensive washing is important for the lectin binding in blotting (Cao *et al.* 2013).

As we reached an inconclusive result whether SLPs present glycosylation, this was opposed to observations made by Cerquetti *et al.*, which confirmed at all six strains of SLPs were glycosylated (Cerquetti *et al.* 2000).

Since the lectin blotting experiments were inconclusive, we decided to employ an additional analytical method, ELLA, to verify the potential glycosylation signals. We proceeded with purified SLPs probing in native confirmation (two subunits associated together). This technique is high throughput, which allowed us to include more ribotypes of SLPs.

The initial screening included optimisation of washing techniques, as lectins are known to be very difficult to wash off. Therefore, probing of proteins with plant lectins is also known to be difficult, as the lectins require individual optimised blocking and washing techniques (Brooks & Hall 2012). Furthermore, it was important to adjust the blocking solution. Carbohydrate-free solution was used, as recommended by other groups (Thompson *et al.* 2011). This allowed us to reduce the background signal from TBST buffer probing below the threshold signal. Also, initially HRP was used in all assays as a positive control. However, the exact composition of HRP glycosylation was unknown and in the case of some lectin probing there was no signal from HRP, which invalidated the results. Therefore, HRP could not be considered a universal positive control for ELLA. Additionally, HRP and SBT were initially proposed as positive control for ELLA experiments to keep it consistent with positive controls used for Periodic-Schiff Staining. However, this may interfere with ELLA assay as HRP is used as an enzyme in the colorimetric

reaction used for detection. For this reason, other glycoproteins were matched for ELLA in these experiments.

Other glycoproteins were considered as positive controls, and we aimed to optimise a positive control for each lectin used. Four glycoproteins with known glycosylation patterns were initially selected, as recommended by the previous research (Thompson *et al.* 2011; Cerquetti *et al.* 2000; Lee *et al.* 2013) and were screened along with SLPs RT 001 and 027. In the case of some lectins it was possible to match specific glycoproteins, however other were unsuccessful. The lack of detection of glycosylation signal from glycoproteins with known glycan composition may be due to nature of the glycosidic linkages might introduce some steric hindrance, or one may need a larger concentration of glycan structures on the protein to detect binding (Larrgy 2011). For this reason and additionally, due to low stock of SLPs (no sufficient amount to carry out optimisation of matching lectin with glycoprotein positive control, we decided to include four glycoproteins with known glycosylation patterns, in order to ensure the variety of glycan structures when probing with each lectin. This proved to be successful approach, as in the most cases at least one glycoprotein showed signal for glycosylation, except for DBA and GSL I lectins, which validated the ELLA assays.

Overall, none of the ribotypes presented a glycosylation signal when examined by ELLA. This led us to the conclusion that SLPs RT 001, RT 002, RT 014, RT 027, RT 026 and RT 078 of *C. difficile* are not glycosylated. This is consistent with the conclusions reached by Qazi *et al.* (2009). These authors carried out mass spectroscopy analysis on SLPs from six ribotypes, including RT 001, RT 010, RT 012, RT 016, RT 017, RT 027 and RT 053 and did not determine the presence of any glycans.

Moreover, Qazi *et al.* determined that predicted molecular weights are equal to observed molecular weights when measured by mass spectroscopy. These authors suggested that possible differences between the predicted molecular weights and differences observed on SDS PAGE are due to aberrant migration of proteins through the gel matrix rather than presence of post-translational modification (Qazi *et al.* 2009). However, this study did not include SLPs RT 002, RT 014, RT 046 or RT 078, which were examined in this chapter.

Also, Calabi *et al.* carried out the enzymatic digestion of SLPs from four strains in order to remove potential glycosylation, however that did not change the mobility of the SLPs, indicating that SLPs were not glycosylated (Calabi *et al.* 2001).

While SLPs were demonstrated not to present glycosylation, other features on the surface of *C. difficile* have been previously shown to be glycosylated, with suspected implications for virulence of this pathogen.

This included the glycosylation of flagellum. Twine *et al.* determined that mutations leading to a change in flagellar glycosylation lead to loss of mobility by *C. difficile* (Twine *et al.* 2009). Furthermore, other studies concluded that the flagellar glycosylation evolved with virulence and aimed to subvert the host immune response (Stabler *et al.* 2009). However, Stevenson *et al.* determined that glycosylation of the flagella is not necessary for virulence, but it may have implications in adherence (Stevenson *et al.* 2015).

Reid *et al.* determined the presence of highly conserved surface polysaccharides among studied strains (Reid *et al.* 2012). However, these glycans were shown to be associated with lipids. Furthermore, *C. difficile* toxins were shown to be glycosylated and this allows them to modulate host physiology (Voth & Ballard 2005).

The glycosylation of the pathogen might also be utilised for therapeutic purposes. Bertolo *et al.* explored the surface polysaccharide PSII as an potent immunogenic adjuvant for the *C. difficile* toxin vaccine (Bertolo *et al.* 2012). Also, Dingle *et al.* discovered a new insertion in the S-layer genome cassette, that turned out to be a novel S-layer glycosylation cluster (Dingle *et al.* 2013). These authors suggested that this cluster codes for rhamnose biosynthesis pathway. However, we did not test the SLPs for the presence of rhamnose because from all the lectins available for us in ELLA assay or lectin blotting, rhamnose-binding lectin was not available at the time. Nonetheless, as this sugar is unique to bacteria, it represents an attractive drug target.

Glycosylation of *C. difficile* is a very dynamic evolutionary process that involves several virulence factors and the understanding of these evolutionary processes can contribute to our knowledge of temporal changes and geographical differences in the epidemiology of CDI.

There was potential for the glycosylation of SLPs from ribotypes examined in this chapter, as indicated by literature review carried out prior to this study. This post-translational modification could account for the observed differences between predicted and observed molecular weights, but also the differences in molecular weights of subunits of different ribotypes. Furthermore, we hypothesised that the various glycosylation patterns on SLPs from different ribotypes may contribute to virulence, understood here as adhesion to host mucosal surfaces, recognition by immune system and evading the clearance mechanisms.

In this chapter, we determined that the SLPs from ribotypes used in this study are not glycosylated. However, the question remains about how the differences in SLPs sequences contribute to initial colonisation of the pathogen and infection outcome.

The glycosylation still remains important for the host-pathogen interactions as there is evidence in the literature that the glycosylation state of the gut changes during the susceptibility and infection. Therefore, next, we would like to investigate the glycosylation patterns on the mucosal surface of the colonic epithelium to search for factors that may have implications for *C. difficile* adherence and colonisation.

CHAPTER 5 THE ROLE OF GLYCOSYLATION IN *CLOSTRIDIUM DIFFICILE* INFECTION

5. 1 INTRODUCTION

The GI tract is an example of an interface of dynamic interactions between the host and commensal microbiota cooperating together to keep pathogens at bay. This complex network requires a balanced system to be ready to destroy any potential threats. This process, known as colonisation resistance, is a key to maintain the integrity of the mucosal epithelium (Britton & Young 2012). Simultaneously, it does not augment an immune response when recognising self or commensal antigens.

Host and commensals employ several mechanisms to prevent infection at the colonic mucosal surface. This includes production of a mucus layer that prevents microbes from interacting with the epithelial barrier. While mucus is produced by epithelial cells, it is the commensals that influence the composition of mucus, often in response to invading pathogens (Jakobsson *et al.* 2015). Furthermore, commensals regulate antimicrobial peptide secretion into the inner layer of mucus (Littman & Pamer 2011). This renders the zone sterile from both commensals and pathogens and prevents both from interacting with TLRs and avoiding the unnecessary activation of the immune system (Johansson *et al.* 2008; McGuckin *et al.* 2011).

In the previous chapter we examined the surface proteins, SLPs, from various strains of *C. difficile* for the presence of glycosylation. The differences in the glycosylation may have accounted for the differences in the molecular weights of SLPs of various strains. Also, this could have contributed to the initial colonisation and adherence, and subsequent severity of infection. However, we determined that the SLPs of *C. difficile* lack glycosylation patterns, therefore the glycosylation does not contribute to the initial adhesion and colonisation of the pathogen in this context. Nevertheless, we came to appreciate the importance of glycosylation in the host-pathogen interactions. Therefore next, we wanted to explore whether glycosylation on the surface of the colon contributes to the susceptibility to infection with *C. difficile*. Specifically, we wanted to correlate any differences in glycosylation patterns on the colonic epithelium with the initial pathogen adherence, colonisation, and subsequent disease severity.

As already mentioned, commensals play a major role in maintaining the homeostasis in the gut, therefore, it is important for the host to support these commensals (Ubeda & Pamer 2013). The host fulfils this role by supplying the nutrients for the commensals, namely, sugars utilised for the energy purposes. However, the commensals also actively modulate the host metabolism to produce glycans that benefit the microbiota (Freitas & Chantal 2000). Specifically, the glycans are displayed on the mucus layer that covers the epithelium. Mucus is composed of heavily glycosylated proteins called mucins, and commensals remove the glycans from the surface of the mucus by enzymatic digestion (Jakobsson *et al.* 2015).

As already described above, the host and microbiota maintain mutualistic relationship that both parties benefit from. This host-microbiota system is a tightly regulated network of interactions, and when this balance is perturbed due a

disturbance of the microbiota, it may have a detrimental effect on the health of the host (Min & Rhee 2015).

Most commonly, the commensal microbiota is disturbed by the antibiotic treatment. While administration of antibiotics facilitates the clearance of invading pathogens, it also causes long-term shifts in the microbial community of the gut (Sekirov *et al.* 2008; Robinson & Young 2010; Antonopoulos *et al.* 2009). Also, the disturbance in microbiota has an effect on host's inability to clear any invading pathogens. For instance, microbial disruption with metronidazole, neomycin and vancomycin increased the colonisation rate of vancomycin-resistant *Enterococcus* (VRE) due to decreased secretion of antimicrobial peptide RegIIIγ by the host (Brandl *et al.* 2008). Antibiotic-induced disturbance in microbiota and subsequent lack of colonisation resistance is a key step in establishing *C. difficile* infection (Britton & Young 2014; Theriot *et al.* 2014). This mechanism is illustrated by the fact that hospital patients undergoing the antibiotic treatment are the major group at risk of developing the CDI (Huang *et al.* 2009).

While most of the reports about *C. difficile* infection attribute the susceptibility to the lack of colonisation resistance, antibiotic treatment, and presumably eradication of microbiota, has some further implications. For instance, this includes the glycans availability as nutrient sources. Due to low numbers of commensal microbes, surface glycans become available for energy utilisation by opportunistic pathogens such as *Salmonella typhimurium* (Ng *et al.* 2013). Furthermore, lack of stimulation from microbiota may influence the composition of glycans (Jakobsson *et al.* 2015).

We wanted to examine this well-defined "susceptibility state" to infection with *C. difficile*, specifically, whether the lack of commensals and their homeostatic effect

may influence the glycosylation state of the host. Specifically, we wanted to determine whether the glycosylation patterns on the surface of the colonic tissue may contribute to *C. difficile* adherence and subsequent colonisation if the nutrient niche was beneficial for the pathogen.

We developed an animal model of *in vivo* susceptibility to *C. difficile* infection. It was based on previous studies, including our own, where animals were treated with antibiotics to eradicate the microbiota, and then challenged with *C. difficile* (Chen *et al.* 2008; Lynch 2014, unpublished). This treatment was proven to be sufficient to render the animals susceptible in studies carried out by Chen *et al.* (2008) and Lynch (2014, unpublished), as mice succumbed to infection and developed all clinical symptoms of the disease. However, in our study, we treated animals with the antibiotics and we ceased the model at the susceptibility state, rather than challenging the animals with the pathogen. The aim was to understand and define the factors that render the animals susceptible to the pathogen. To our knowledge, no previous *C. difficile* susceptibility studies have been reported in the literature.

First, we examined the glycosylation status of the gut in the susceptibility state to infection with *C. difficile*. The aim was to correlate any changes in the glycosylation on the surface of the epithelium with an environment that benefits the pathogen during initial stages of invasion.

Furthermore, knowing the role commensals play in maintaining the homeostasis in the gut, we examined how the disturbance in the microbiota influences the expression of mucosal immune response such as expression of cytokines, chemokines and TLRs as well as epithelial integrity barrier, including expression of

mucins, tight junction proteins and antimicrobial peptides. The aim was to determine if these factors further contribute to pathogen invasion.

The susceptibility model allowed us to identify key factors that despite their protective properties may have benefited the pathogen in the susceptibility state. Therefore, we next used an *in vivo* infection model to examine if these factors play a role in resolving this infection. For this we used *in vivo* infection with *C. difficile* RT 001. This ribotype of *C. difficile* is characterised by the mild outcome of infection and we have demonstrated previously that animals infected with this pathogen resolve infection by the end of the study at day 7 (Lynch 2014, unpublished; Ryan *et al.* 2011). We examined the glycosylation patterns on the surface of the colonic epithelium during infection. Specifically, we examined the terminal glycans, fucose and sialic acid, as they have been previously shown to be important nutrients for *C. difficile* (Ng *et al.* 2013) and commensal recovery (Chow & Lee 2008). Furthermore, we examined the expression of IL-22 cytokine, as it is known to be essential for the epithelial barrier recovery.

5. 2 RESULTS

5. 2. 1 Susceptibility to *C. difficile in vivo* Induces an Environment That Supposed to be Protective for the Host in the Colon.

Mice underwent antibiotic treatment to render them susceptible to *C. difficile*. However, rather than challenging them with the pathogen, animals were sacrificed and examined for the factors that may contribute to the state of susceptibility of the host to the pathogen. We examined the effect of antibiotic-induced disturbance of microbiota on the glycosylation presented on the surface of the colonic epithelium.

Furthermore, we examined the expression of inflammatory markers such as cytokines, chemokines and TLRs but also key mucosal integrity proteins such as mucins, tight junction proteins and antimicrobial peptides. Also, the signalling pathway of key mucosal cytokine IL-22 was examined.

5. 2. 1. 1 The Efficacy of the Animal Model of *C. difficile* Susceptibility Was Monitored.

In order to confirm consumption of the relevant antibiotic concentrations required to induce the susceptibility to *C. difficile*, water intake was monitored daily. The average water consumption per animal was then normalised to 30 g body weight (BW) and was used to convert the dosage into the actual consumption of the antibiotic (Figure 5. 1 A). All animals in the study consumed above the minimum recommended dose of antibiotics, as per outlined in Table 2. 16 (Figure 5. 1 B – F).

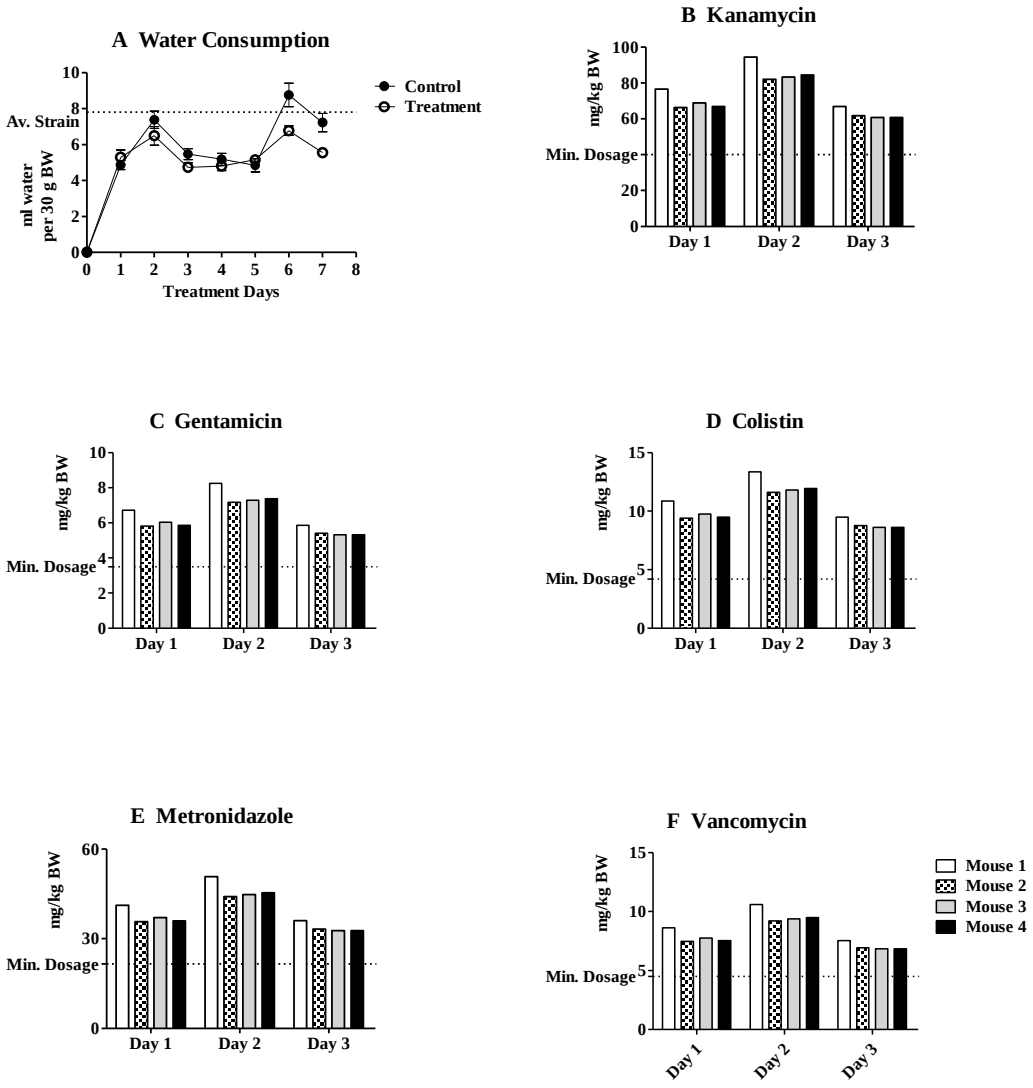

Figure 5. 1 Efficacy of the *in vivo* susceptibility model was ensured by monitoring water intake and corresponding antibiotic dosage. Female C57BL/6J mice had *ad libitum* access to water with antibiotics from day 0 to day 3. Water intake (**A**) was calculated as consumption per day per 30 g of body weight (BW). No significant difference was seen between two groups as determined by Repeated Measures ANOVA with Bonferroni post-test. Next, the volume of water was correlated with antibiotic dosage ingested, kanamycin (**B**), gentamicin (**C**), colistin (**D**), metronidazole MANAGEMENT and vancomycin (**F**). All animals under investigation ingested the dosage of all antibiotics recommended to eradicate the microbiota.

5. 2. 1. 2 Mice Treated With Antibiotics Experienced Significant Loss of Weight.

Animals under investigation were weighed daily at approximately the same time, to monitor any adverse effects that the treatment could have induced (severe diarrhea etc.). A weight loss above 15% was considered a threat for animal welfare and if reached, animals were to be sacrificed immediately. However, no animals in this study reached this state.

Day 0 weight was considered as 100% for each animal in the study and any weight change was converted into % of initial weight (Figure 5. 2). The antibiotic treatment group reached significant weight loss on day 3 of the antibiotic treatment, which was also the lowest average weight this group had reached ($p \leq 0.001$). The significant weight loss was maintained between the groups until the end of the study ($p \leq 0.001$).

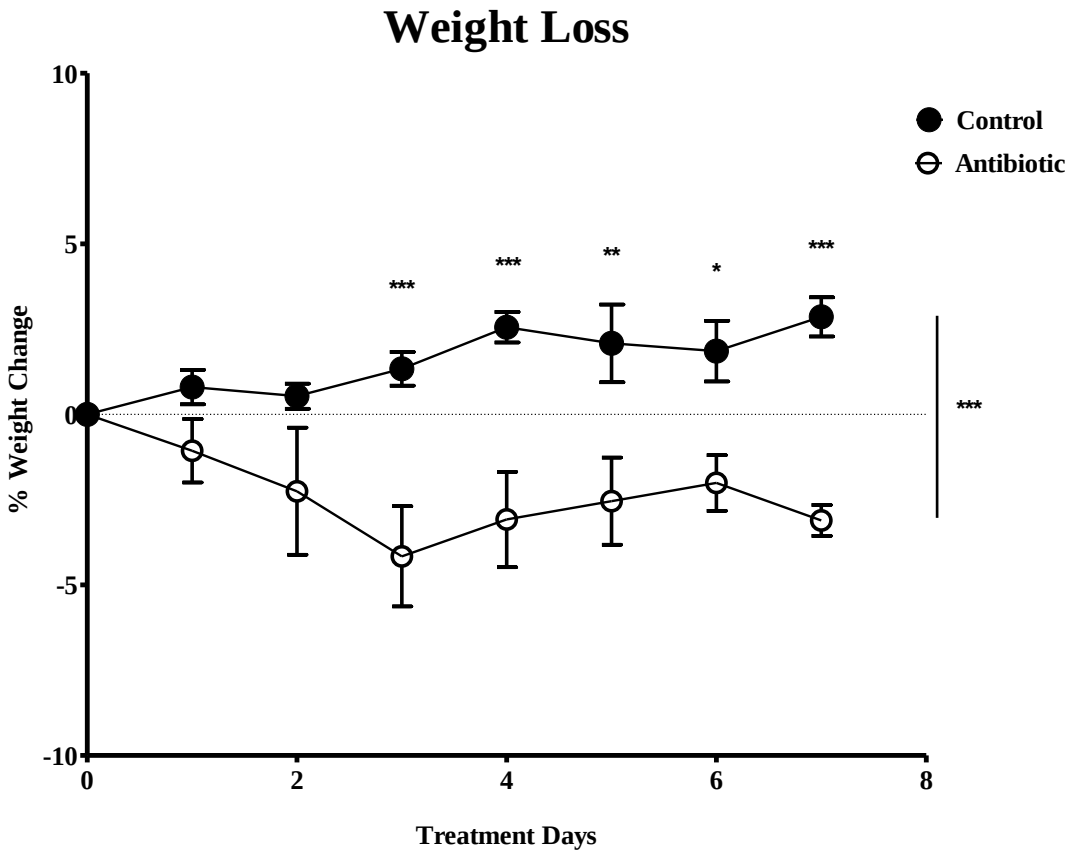

Figure 5. 2 Animals treated with antibiotics experienced significant weight loss from day 3 to day 7. Female C57BL/6J mice were weighed daily and weight change was expressed as % of total weight relative to day 0. Results for each day are then mean of control group (*n*=4) and treatment group (*n*=4). Repeated Measures ANOVA with Bonferroni post-test was used to determine the significance between the groups on given day and the overall significance between control and treatment groups (*p≤0.05, **p≤0.01 and ***p≤0.001).

5. 2. 1. 3 Mice Treated with Antibiotics Experienced Significant Increase in Daily Disease Index.

Animals under investigation were scored on a daily disease index, at approximately the same time each day, to monitor any adverse effects that the treatment could have induced. The factors measured on this index included appearance, behaviour, water intake and weight change (Appendix D) (Wolfensohn & Lloyd 2012).

The animals in the antibiotic treatment group had a significant increase in their daily disease index from day 3 ($p \leq 0.001$). This increase peaked at day 4, and it was maintained until the end of the study (Figure 5. 3). Furthermore, the difference between control and antibiotic-treated groups was shown to be extremely significant ($p \leq 0.001$). None of the animals was scored above 9 points, which was considered as adverse reaction with recommendation for removing from the study.

Additionally, we observed some heterobarbering among C57BL/6J mice. It was observed that animals over the age of 15 weeks were more prone to barbering. There was one severe case of heterobarbering among animals prior to this study. The barbered animal experienced severe wounds. There was a possibility that this could have induced the inflammatory reaction and this animal was removed from the group before the study. For that reason, we did not include any animals over the age of 15 weeks in our studies, to avoid any discrepancies.

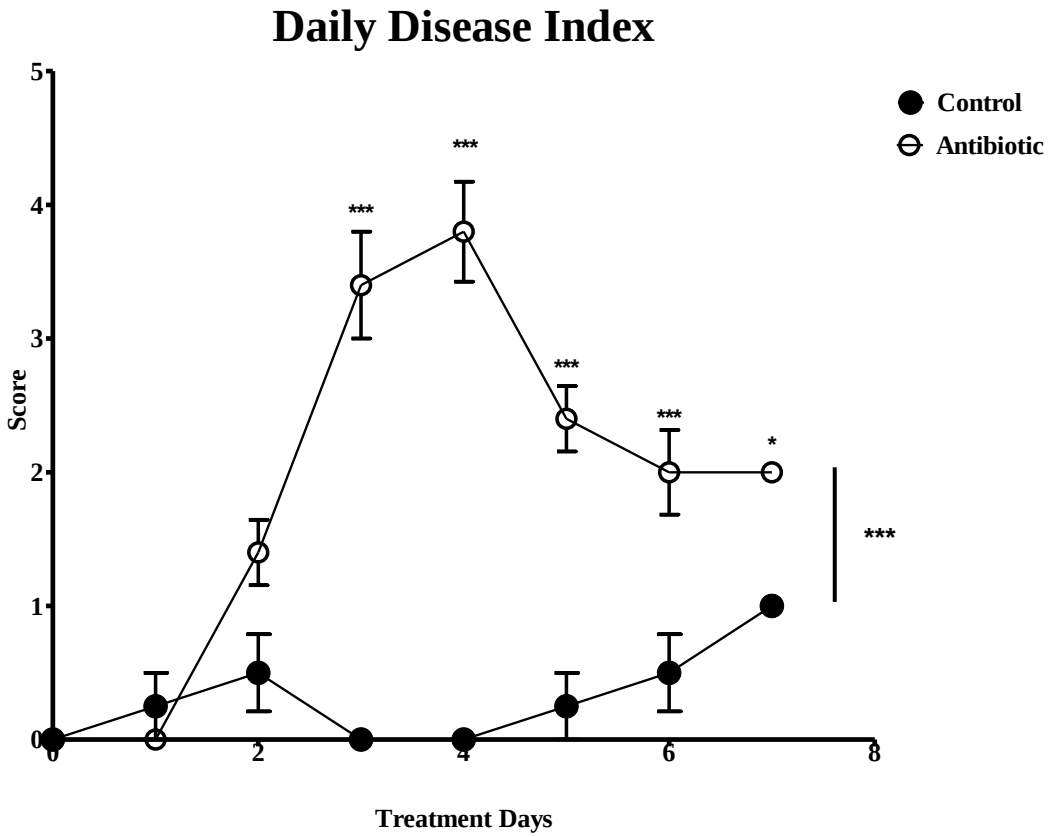

Figure 5. 3 Animals treated with antibiotics experienced significant increase in Daily Disease Index. Female C57BL/6J mice were scored daily for the behaviour, appearance, water intake, weight loss and stool consistency. Results for each day are mean of control group (n=4) and treatment group (n=4). Repeated Measures ANOVA with Bonferroni post-test was used to determine the significance between the groups on given day and the overall significance between control and treatment groups (*$p \leq 0.05$, **$p \leq 0.01$ and ***$p \leq 0.001$).

5. 2. 1. 4 Antibiotic Treatment Does Not Induce Colitis in Mice.

Mice were sacrificed after 7 days of the antibiotic regiment and the tissue was harvested. The colon was weighed (Figure 5. 4 A) and measured (Figure 5. 4 B – C). There was no significant difference in weight or length of the colon, as determined by Student's t-test. However, the macroscopic examination of the harvested colon led us to the conclusion that the structure of the colons from the antibiotic treatment group was less coiled and tense.

Finally, the structure of the epithelium was examined by H&E staining and no differences between two groups was determined (Figure 5. 4 D). This led us to the conclusion that antibiotic treatment does not induce colitis in mice.

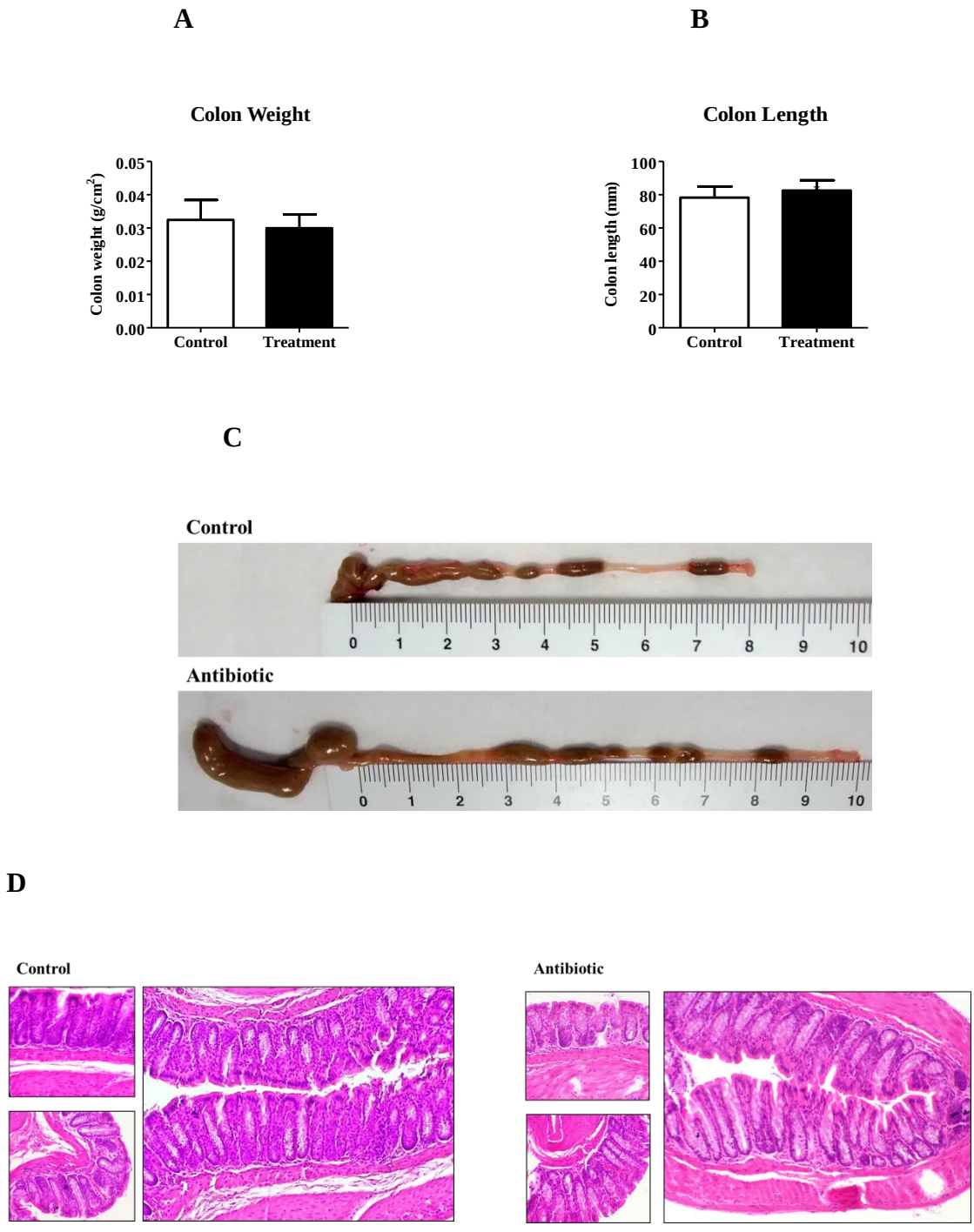

Figure 5. 4 Disturbance of microbiota due to antibiotic treatment does not induce colitis. Female C57BL/6J mice were treated with cocktail of antibiotics for 3 days, followed by IP injection of clindamycin on day 5. Animals were sacrificed on day 7 and colitis-associated factors were investigated (control group *n*=4 and treatment group *n*=4), colon weight (**A**), colon length (**B**) and (**C**), and H&E staining of colon structure (**D**). Student's t-test was used to determine significance. No significant changes between the groups were determined.

5. 2. 1. 5 Distribution of Fucose Glycosylation on the Surface of Colonic Tissue Changes Upon Antibiotic Treatment.

The surface of the colonic tissue was examined for fucose glycosylation with use of fluorescently-labelled lectins, as this is a glycan commonly present on the outermost of the glycan chains.

Fucose residues were examined by AAL which is specific for fucose-(α-1,6)-N-Acetylglucosamine and by UEA I specific for α-Fucose (Figure 5. 5). Both lectins were tagged with FITC, presented in green. To visualise the structure of the colon, DNA of the epithelial cells was stained with DAPI, presented in red. The staining with AAL is visualised in Figure 5. 5 A and B, and the distribution of the glycosylation summarised in Table 1. Fucose glycosylation was upregulated upon antibiotic treatment, specifically, fucose glycosylation signal was upregulated in intestinal lumen and in the middle and upper crypts. This glycosylation diminished from the lamina propria and stem cells and it was not changed on the surface epithelium.

Furthermore, fucose glycosylation was probed with UEA I, as visualised in Figure 5. 5 C and D, while the distribution of glycosylation is summarised in Table 1. Fucose glycosylation was upregulated upon antibiotic treatment, as the goblet cells and all parts of the crypts presented glycosylation signals compared to control. The fucose signal diminished from the lamina propria and stem cells, and it had not changed in the intestinal lumen and surface epithelium.

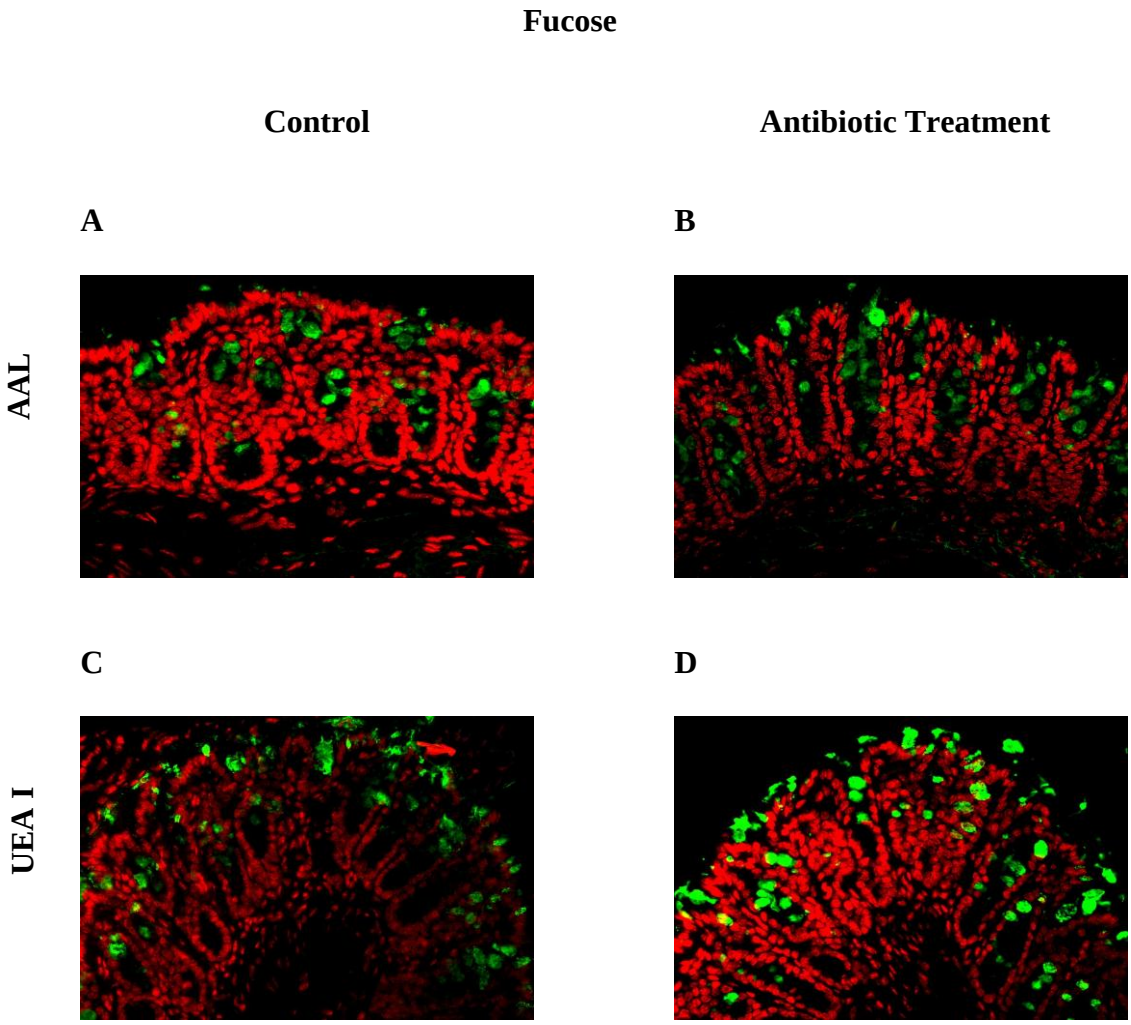

Figure 5. 5 Fucose residues on the surface of the intestinal epithelium were probed with AAL and UEA I lectins. Mice were treated with autoclaved water (control group) or antibiotic cocktail (treatment group) for 7 days and sacrificed. Colon was removed, rolled using Swiss roll technique, preserved in formaline and embedded in paraffin. Tissue was cut into 6 µm sections and probed with 5 µg/ml of lectin conjugated with FITC tag, AAL (**A** and **B**) and UEA I (**C** and **D**). Samples were mounted with VECTASHIELD® HardSet Mounting Medium with DAPI (to visualise epithelial structure). Samples were visualised using Olympus BX51 Fluorescent Microscope (FITC: green; DAPI: red).

5. 2. 1. 6 Distribution of Sialic Acid Glycosylation on the Surface of Colonic Tissue Changes Upon Antibiotic Treatment.

The surface of the colonic tissue was examined for sialic acid glycosylation with the use of fluorescently-labelled lectins, as this is a glycan commonly present on the outermost of the glycan chains.

Surface sialic acid glycosylation was measured with SNA specific for Galactosyl-(α-2,6)/(α-2,3)-Sialic Acid, MAL I specific for Galactosyl-(α-2,3)-Sialic Acid and WGA specific for all forms of sialic acid (Figure 5. 6). The staining with SNA is visualised in Figure 5. 6 A and B, and it is summarised in Table 1. The glycosylation signal upregulated in lower crypts and submucosa, while it was presented at the same level on surface epithelium, lamina propria, stem cells, middle and upper crypts and its intensity lowered its intensity in muscular mucosae.

When stained with MAL I (presented in Figure 5. 6 C and D), the glycosylation signal diminished from the surface epithelium, lamina propria and stem cells. Only goblet cells presented higher glycosylation signal compared to controls.

Glycosylation probing with WGA (visualised in Figure 5. 6 E and F, and summarised in Table 1) presented the same level on the surface epithelium, however, the glycosylation signal diminished in the crypts when compared treatment group to the control group. There was increase in signal from stem cell and submucosa, when probed with this lectin.

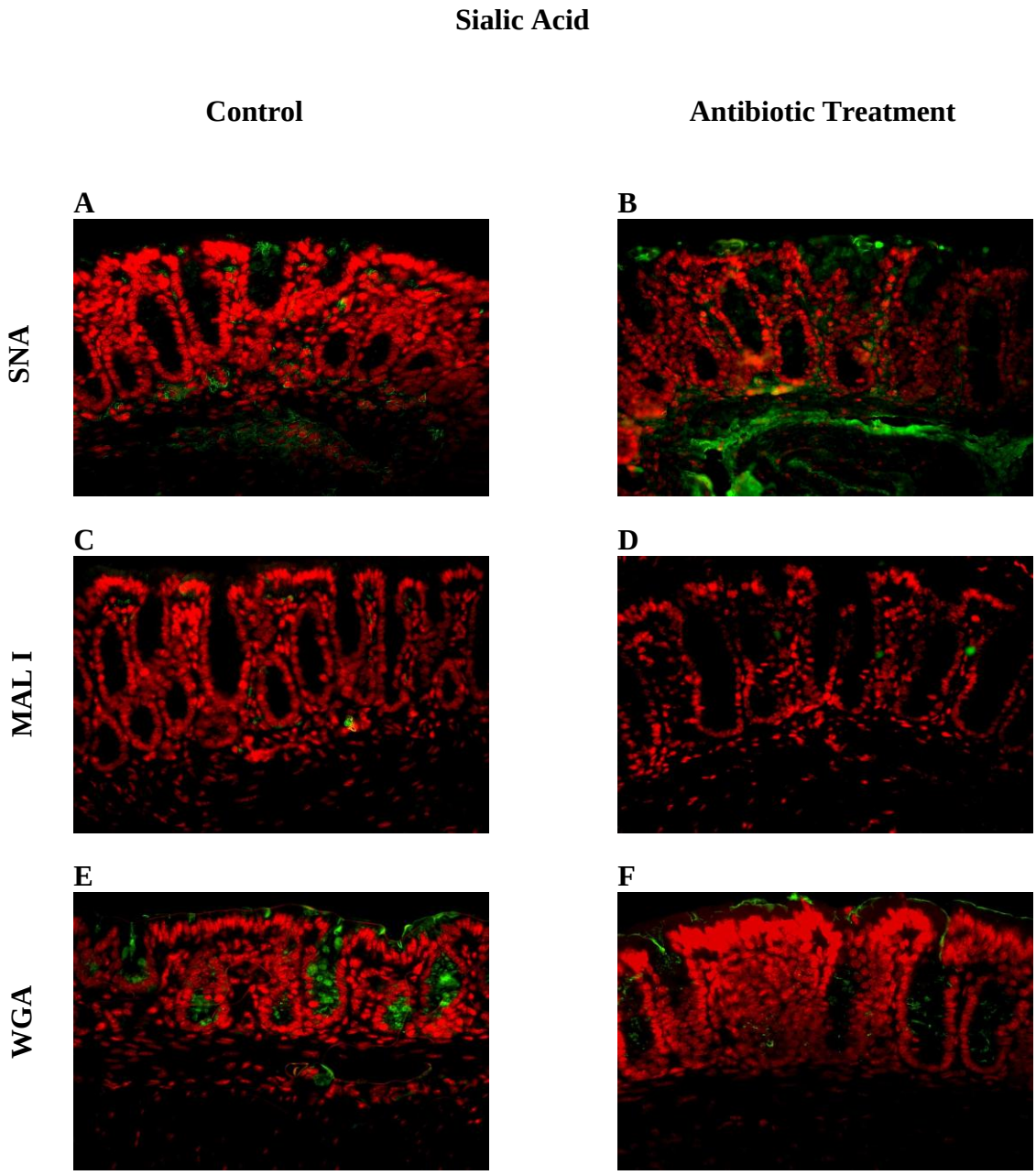

Figure 5. 6 Sialic Acid residues on the surface of the intestinal epithelium were probed with SNA, MAL I and WGA lectins. Mice were treated with autoclaved water (control group) or antibiotic cocktail (treatment group) for 7 days and sacrificed. The colon was removed, rolled using the Swiss roll technique, preserved in formaline and embedded in paraffin. Tissue was cut into 6 µm sections and probed with 5 µg/ml of lectin conjugated with FITC tag, SNA (**A** and **B**), MAL I (**C** and **D**) and WGA (**E** and **F**). Samples were mounted with VECTASHIELD® HardSet Mounting Medium with DAPI (to visualise epithelial structure). Samples were visualised using Olympus BX51 Fluorescent Microscope (FITC: green; DAPI: red).

5. 2. 1. 7 Fucose Presented on the Colonic Surface is Upregulated by the Antibiotic Treatment, While Sialic Acid is Downregulated.

In order to quantify the glycosylation signal, the total fluorescence of the images presented in the previous two sections was measured. This was possible because all the images taken for a given lectin were captured under the same conditions and comparable surface of the tissue section (FITC and DAPI exposure, and magnification). A total of five images per condition were measured.

As presented in Figure 5. 7, there was a significant increase in fucose glycosylation upon antibiotic treatment when probed with AAL ($p \leq 0.05$) and UEA I ($p \leq 0.05$). Sialic acid residues were decreased upon antibiotic treatment when measured with SNA, MAL I and WGA. This included a significant downregulation in sialic acid measured by MAL I ($p \leq 0.01$) and WGA ($p \leq 0.01$).

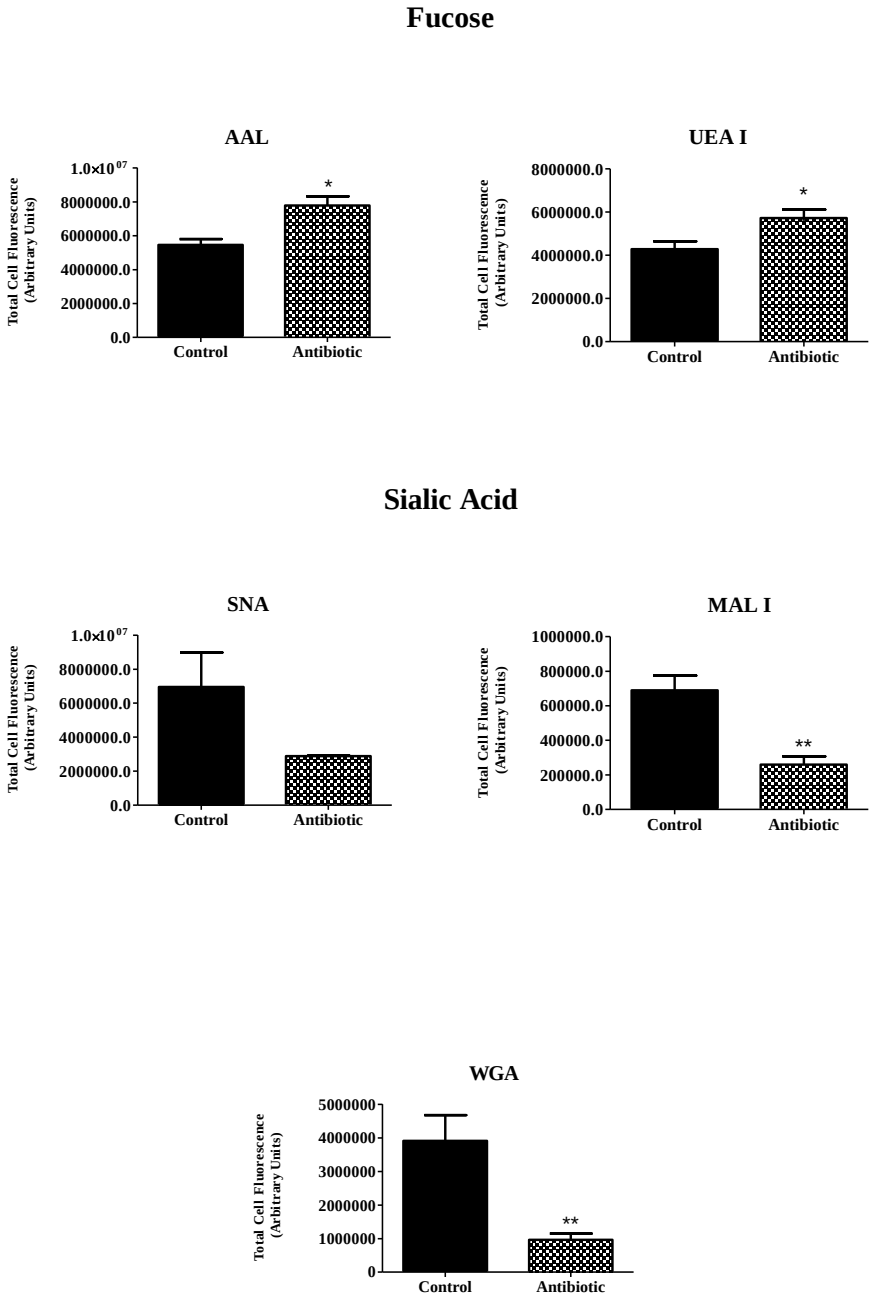

Figure 5. 7 Terminal fucose is upregulated in susceptibility state, while terminal sialic acid is downregulated. Terminal glycans on the surface of colonic epithelium from mice treated with antibiotic cocktail were examined using FITC-labelled lectins, fucose specific lectins, AAL and UEA I and sialic specific lectins, SNA, MAL I and WGA. Total fluorescence signal was measured using Image J and corrected for the background fluorescence. A minimum of five images were taken for given condition, control group n=4 and treatment group n=4. Results are mean ±SD and Student's two-tailed t test with Mann-Whitney U post-test was carried out to search for statistical significance (*p≤0.05, **p≤0.01, ***p≤0.001).

5. 2. 1. 8 Distribution of N-Acetylgalactosamine Glycosylation on the Surface of Colonic Tissue Changes Upon Antibiotic Treatment.

The surface of the colonic tissue was examined for N-Acetylgalactosamine glycosylation with the use of fluorescently-labelled lectins, as this type of glycosylation comprises the core glycosylation.

N-Acetylgalactosamine were examined by DBA specific for α-N-Acetylgalactosamine and PNA specific for Galactosyl-(β-1,3)-N-Acetylgalactosamine (Figure 5. 8).

Glycosylation staining with DBA is visualised in Figure 5. 8 A and B, and distribution of glycosylation within the epithelial structure is summarised in Table 1. The glycosylation signal increased on the surface epithelium, within goblet cells, and all the parts of the crypts. The signal remained the same within the intestinal lumen.

Furthermore, when stained with PNA (Figure 5. 8 C and D), the signal was upregulated on the surface epithelium, stem cells, while it remained the same in the lamina propria. Glycosylation signal diminished from goblet cells and submucosa.

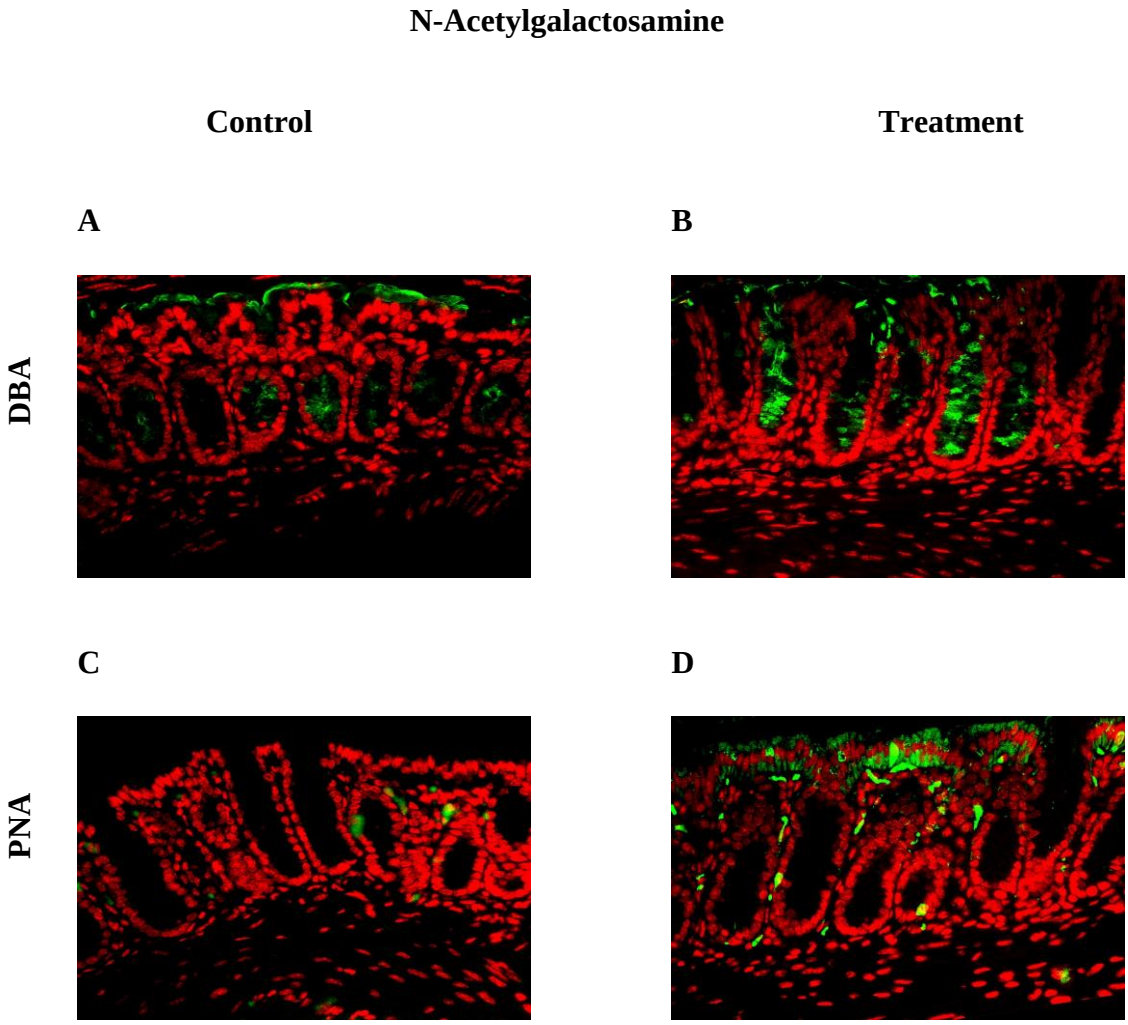

Figure 5. 8 N-Acetylgalactosamine residues on the surface of the intestinal epithelium were probed with DBA and PNA lectins. Mice were treated with autoclaved water (control group) or antibiotic cocktail (treatment group) for 7 days and sacrificed. Colon was removed, rolled using Swiss roll technique, preserved in formaline and embedded in paraffin. Tissue was cut into 6 µm sections and probed with 5 µg/ml of lectin conjugated with FITC tag, DBA (**A** and **B**) and PNA (**C** and **D**). Samples were mounted with VECTASHIELD® HardSet Mounting Medium with DAPI (to visualise epithelial structure). Samples were visualised using Olympus BX51 Fluorescent Microscope (FITC: green; DAPI: red).

5. 2. 1. 9 Distribution of N-Acetylglucosamine Glycosylation on the Surface of Colonic Tissue Changes Upon Antibiotic Treatment.

The surface of the colonic tissue was examined for N-Acetylglucosamine glycosylation with the use of fluorescently-labelled lectins, as this type of glycosylation comprises the core glycosylation.

N-Acetylglucosamine residues were examined by GSL II and sWGA specific for α- or β-N-Acetylglucosamine (Figure 5. 9).

Glycosylation staining with GSL II is visualised in Figure 5. 9 A and B, and distribution of glycosylation within the epithelial structure is summarised in Table 1. The glycosylation signal increased on the surface epithelium, within goblet cells, and lower crypts, while the glycosylation signal diminished from the middle crypts.

Furthermore, when stained with sWGA, the signal remained the same, but only the glycosylation within the middle crypts has changed from strong staining to a low level of signal (Figure 5. 9 C and D).

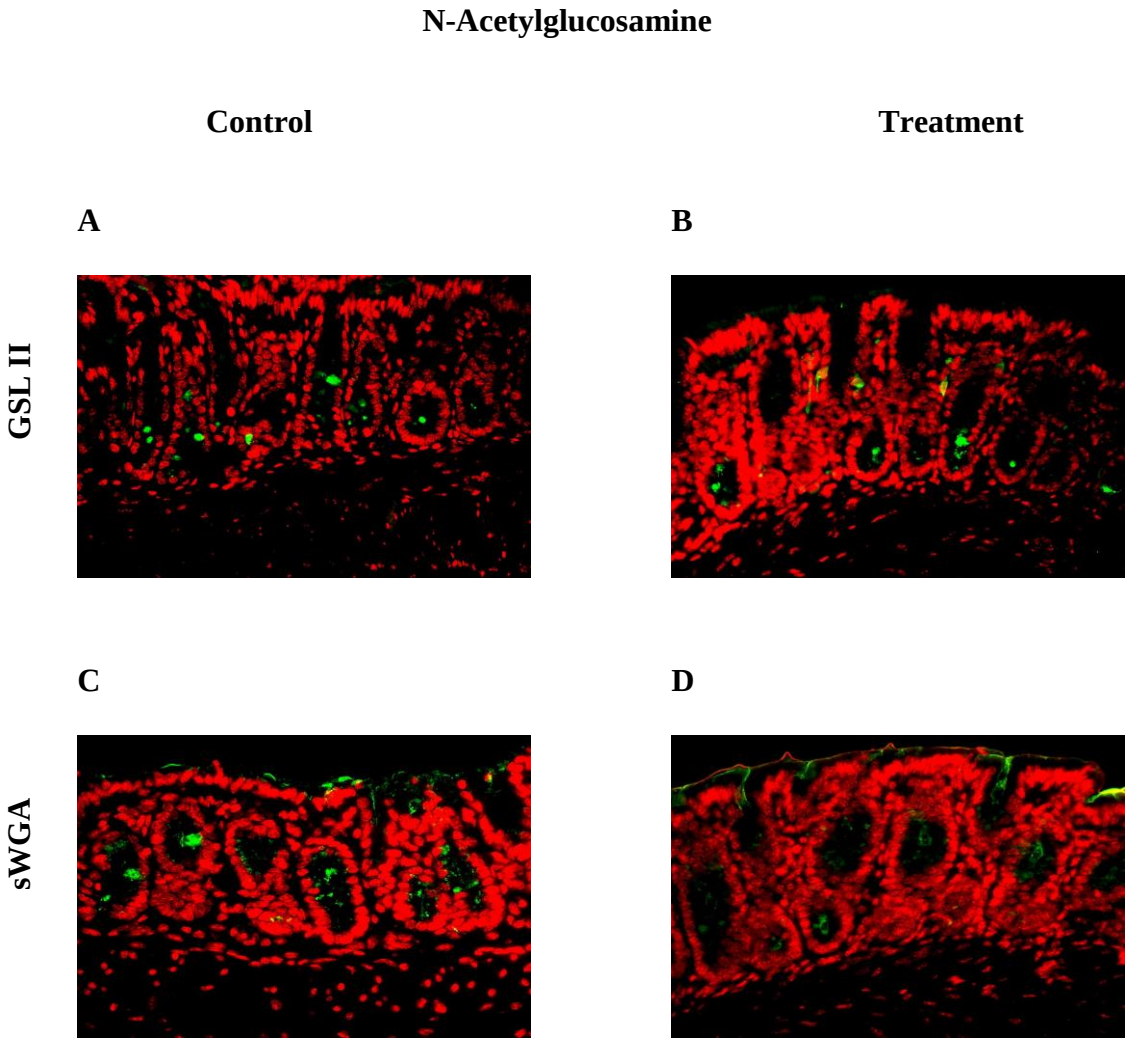

Figure 5. 9 N-Acetylglucosamine residues on the surface of the intestinal epithelium were probed with GSL II and sWGA lectins. Mice were treated with autoclaved water (control group) or antibiotic cocktail (treatment group) for 7 days and sacrificed. Colon was removed, rolled using Swiss roll technique, preserved in formaline and embedded in paraffin. Tissue was cut into 6 µm sections and probed with 5 µg/ml of lectin conjugated with FITC tag, GSL II (**A** and **B**) and PNA (**C** and **D**). Samples were mounted with VECTASHIELD® HardSet Mounting Medium with DAPI (to visualise epithelial structure). Samples were visualised using Olympus BX51 Fluorescent Microscope (FITC: green; DAPI: red).

5. 2. 1. 10 Distribution of Mannose Glycosylation on the Surface of Colonic Tissue Changes Upon Antibiotic Treatment.

The surface of the colonic tissue was examined for mannose glycosylation with use of fluorescently-labelled lectins, as this type of glycosylation is found within the core and terminal glycosylation.

Mannose was examined by ConA specific core mannose (Figure 5. 10). Glycosylation staining with ConA was visualised in Figure 5. 10 A and B, and distribution of glycosylation within the epithelial structure is summarised in Table 1. The glycosylation signal was upregulated in the muscular mucosae and submucosa, while it diminished from the middle and upper crypts. The mannose glycosylation signal remained at the same level on the surface epithelium, lamina propria, stem cells and lower crypts.

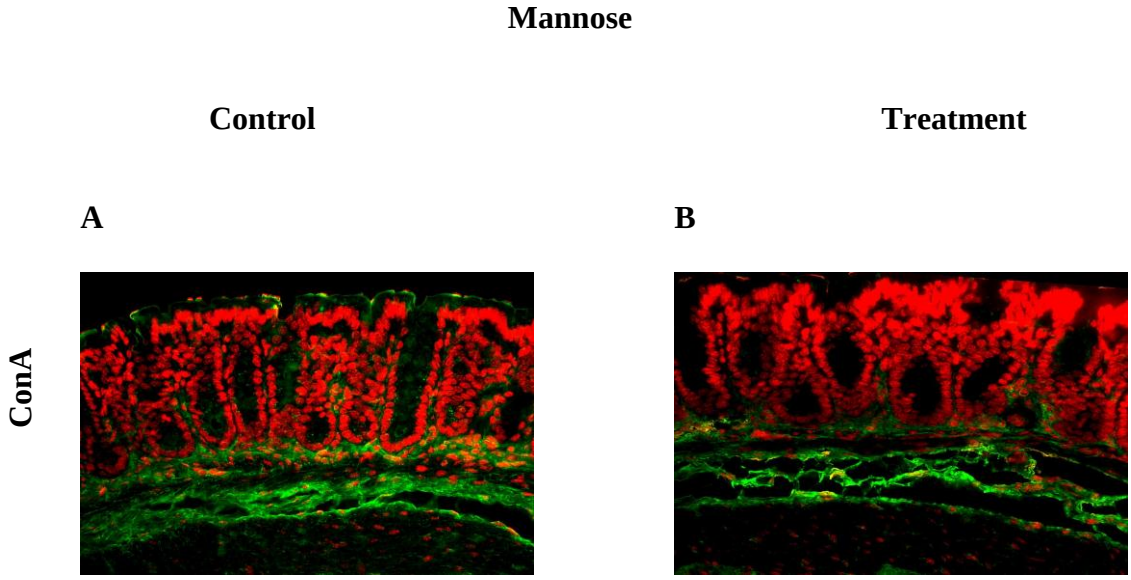

Figure 5. 10 Mannose residues on the surface of the intestinal epithelium were probed with ConA lectin. Mice were treated with autoclaved water (control group) or antibiotic cocktail (treatment group) for 7 days and sacrificed. Colon was removed, rolled using Swiss roll technique, preserved in formaline and embedded in paraffin. Tissue was cut into 6 µm sections and probed with 5 µg/ml of ConA lectin conjugated with FITC tag. Samples were mounted with VECTASHIELD® HardSet Mounting Medium with DAPI (to visualise epithelial structure). Samples were visualised using Olympus BX51 Fluorescent Microscope (FITC: green; DAPI: red).

5. 2. 1. 11 N-Acetylgalactosamine, N-Acetylglucosamine and Mannose Presented on the Colonic Surface are Changed by the Antibiotic Treatment.

In order to quantify the glycosylation signal, total fluorescence of the images presented in previous sections was measured. This was possible because all the images taken for a given lectin were captured under the same conditions and comparable surface of the tissue section (FITC and DAPI exposure, and magnification). A total of five images per condition were measured.

As presented in Figure 5. 11, there was a significant increase in α-N-Acetylgalactosamine upon antibiotic treatment when measured by DBA ($p \leq 0.05$) and significant decrease in Galactosyl-(β-1,3)-N-Acetylgalactosamine when probed by PNA ($p \leq 0.05$). Furthermore, there was upregulation of N-Acetylglucosamine glycosylation upon antibiotic treatment when probed by GSL II and sWGA, and this included a significant increase of glycosylation when probed with GSL II ($p \leq 0.05$). Finally, there was significant downregulation in the mannose residues on the surface of colonic epithelium upon antibiotic treatment ($p \leq 0.05$).

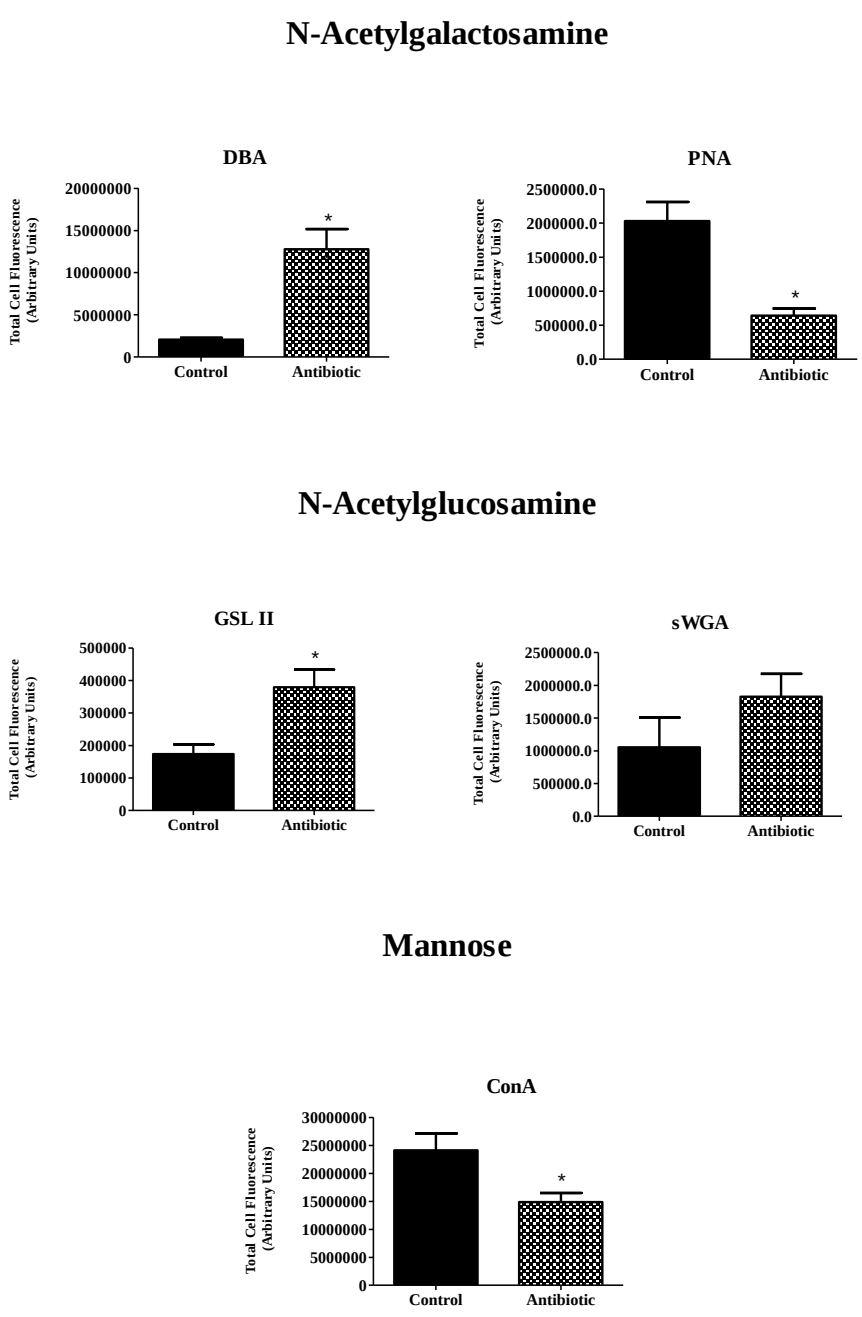

Figure 5. 11 Core glycans of the colonic epithelium are changed upon antibiotic treatment. Core glycans on the surface of the colonic epithelium from mice treated with antibiotic cocktail were examined using FITC-labelled lectins, N-Acetylgalactosamine specific lectins DBA and PNA, N-Acetylglucosamine specific lectins GSL II and sWGA, and core mannose-specific lectin ConA. Total fluorescence signal was measured using Image J and corrected for the background fluorescence. A minimum of five images were taken for a given condition, control group n=4 and antibiotic group n=4. Results are the mean ±SD and Student's two-tailed t test with Mann-Whitney U post-test was carried out to search for statistical significance (*p≤0.05, **p≤0.01, ***p≤0.001).

Table 5. 1 Distribution of glycosylation on colonic surface epithelium observed during susceptibility state. Susceptibility was induced in mice upon antibiotic treatment (Anti.). Glycosylation structures commonly observed on the colonic epithelium were examined by several lectins. Distribution of glycosylation signal within colon structure and its intensity was scored as +++ denoting extremely strong staining; ++ denoting strong staining; + some staining present; lack of signal was left blank.

Lectin binding site of the structure of colonic epithelium		Sialic Acid						Fucose				N-Acetylgalactosamine				N-Acetylglucosamine				Mannose	
		SNA		MAL I		WGA		AAL		UEA I		DBA		PNA		GSL II		sWGA		ConA	
		Control	Anti.	Control	Anti.	Control	Anti.	Control	Anti.	Control	Anti.	Control	Anti.	Control	Anti.	Control	Anti.	Control	Anti.	Control	Anti.
Intestinal lumen									+	+	+	+	+					+	+		
Surface epithelium		+	+	+		+	+	+	+	+	+		+		+		++			+	+
Lamina propria		+	+	+		+		+		+				+	+					+	+
Goblet cells					+						+		+	+			+				
Stem cells		+	+	+			++	+		+					+					++	++
Crypt of Lieberkühn	Lower		+			+++	++				+	+	+++			+	++	+	+	+	+
	Middle	+	+			++	+		+		+		++			+		++	+	+	
	Upper	+	+			+			+		++		+					+	+	+	
Muscular mucosae		++	+																		++
Submucosa			+				+							+							+

5. 2. 1. 12 Antibiotic-Induced Disturbance of the Microbiota Leads to a Mild Proinflammatory Profile in the Colon as Determined by Cytokine, Chemokine And TLRs Expression.

In order to determine how antibiotic treatment and disturbance in the microbiota affected the colon, expression of key inflammatory markers, such as cytokines (Figure 5. 12), chemokines (Figure 5. 13) and TLRs expression (Figure 5. 14) were examined by RT qPCR

The expression of the proinflammatory cytokines IL-12, IL-23, IL-1β and TGFβ were upregulated upon antibiotic treatment, while there was a minor increase in expression of IL-17 (4-fold, 5-fold, 15-fold, 5-fold and 12-fold, respectively), including a significant increase in expression of IL-1β ($p<0.001$). Expression of IL-6 was significantly decreased to 0.25-fold. Notably, antibiotic treatment significantly increased expression of the anti-inflammatory cytokine IL-10 6-fold ($p<0.001$). There was also a decrease in the expression of IL-2 and TNFα, 0.25-fold and 0.5-fold, respectively (Figure 5. 5).

Furthermore, expression of the chemokines MIP1α and MIP2α were downregulated (0.25-fold, both), including a significant decrease in MIP2α ($p<0.001$). There was a minor change in expression of MCP1. Only RANTES was shown to be increased in its expression (6-fold) (Figure 5. 6).

The expression of TLRs was also affected by the disturbance in the microbiota. The expression of TLR5 was downregulated 0.5-fold and TLR9 was also downregulated 0.5 fold, while there was a minor change in expression of TLR4. Only expression of TLR2 was increased (15-fold) (Figure 5. 7). However, none of these changes in expression were significant.

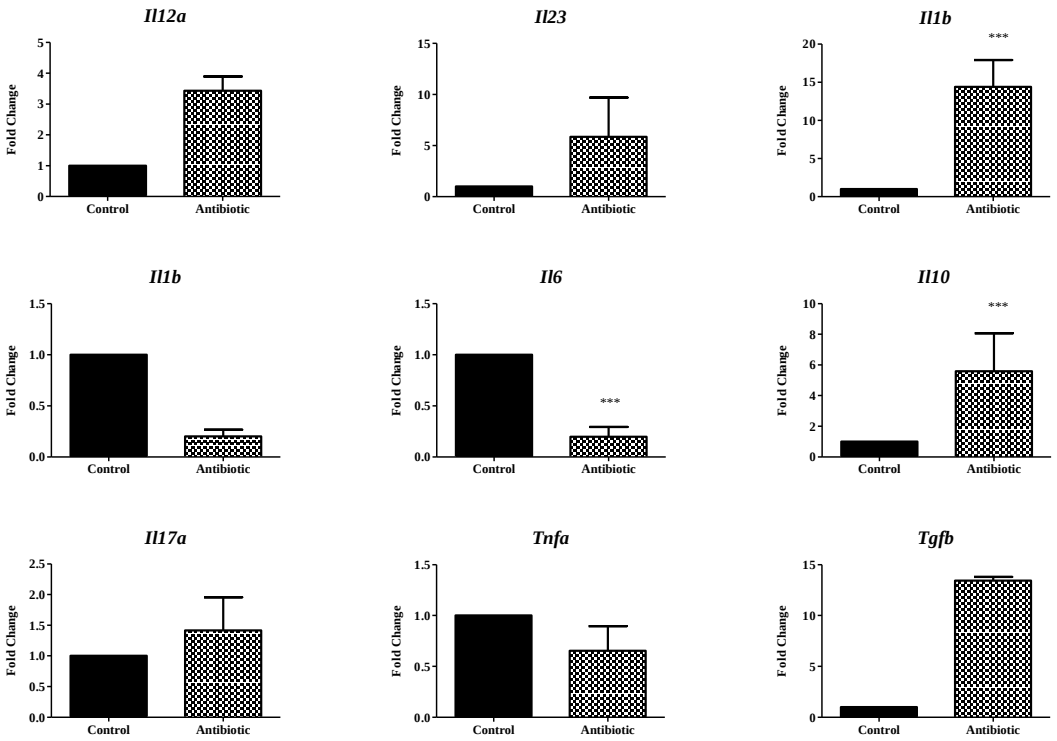

Figure 5. 12 Antibiotic treatment leads to a mild proinflammatory profile in the colon. Female C57BL/6J mice were treated with antibiotic cocktail for 3 days, followed by IP injection of clindamycin on day 5. Mice were sacrificed on day 7 and colons were removed. Tissue from each sample was homogenised, mRNA was extracted and normalised amounts of mRNA were converted into cDNA. The cDNA was mixed with primers for *Il12a*, *Il23*, *Il1b*, *Il2*, *Il6*, *Il10*, *Il17*, *Tnfa* and *Tgfb* and FAST SYBR Mastermix. Samples were assayed in triplicate and analysed on LightCycler®96. Groups were compared using relative quantitation. After normalising samples to geometric mean of two endogenous controls, *Ppia* and *B2m*, expression of control sample was normalised to 1, and expression in treatment group is shown relative to this value. Results are means ±SD of 4 mice/control and 4 mice/antibiotic. Mann-Whitney U test was carried out to search for statistical significance (*p<0.05, **p<0.01, ***p<0.001).

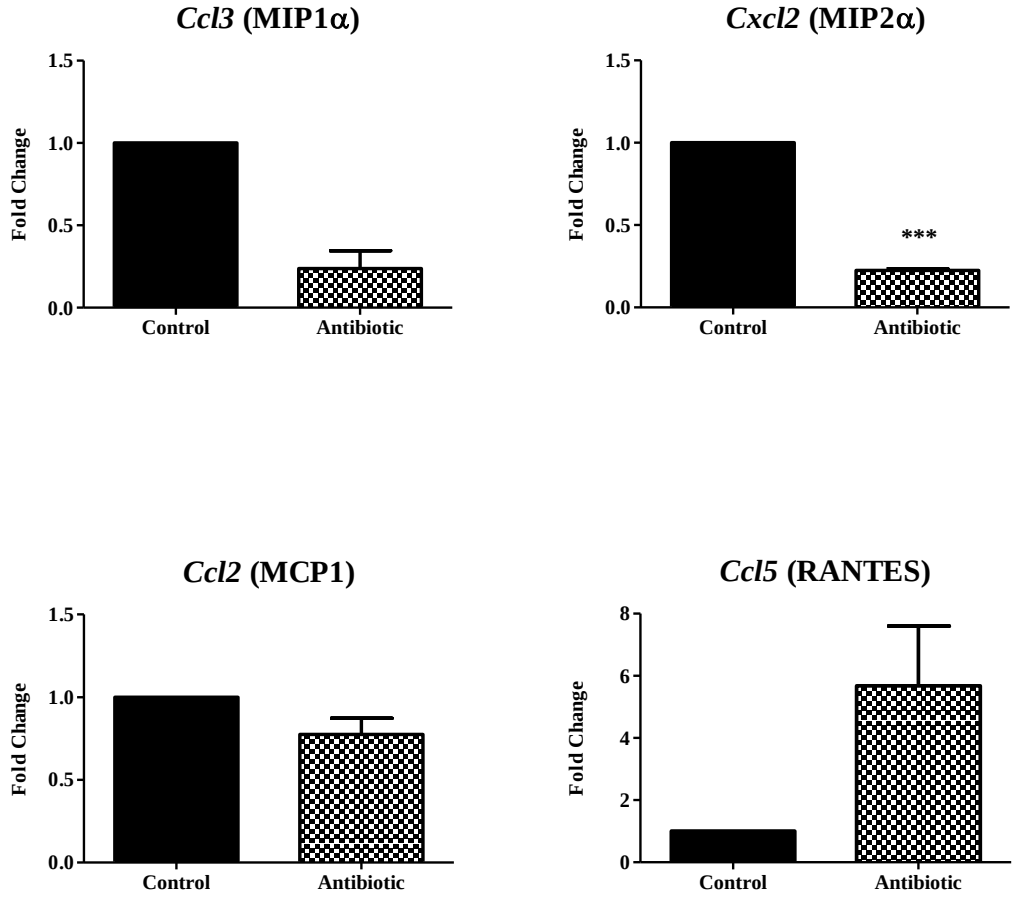

Figure 5. 13 Antibiotic treatment leads to changes in chemokine expression in the colon. Female C57BL/6J mice were treated with antibiotic cocktail for 3 days, followed by IP injection of clindamycin on day 5. Mice were sacrificed on day 7 and colons were removed. Tissue from each sample was homogenised, mRNA was extracted and normalised amounts of mRNA were converted into cDNA. The cDNA was mixed with primers for *Ccl3* (MIP1α), *Cxcl2* (MIP2α), *Ccl2* (MCP1) and *Ccl5* (RANTES) and FAST SYBR Mastermix. Samples were assayed in triplicate and analysed on LightCycler®96. Groups were compared using relative quantitation. After normalising samples to geometric mean of two endogenous controls, *Ppia* and *B2m*, expression of control sample was normalised to 1, and expression in treatment group is shown relative to this value. Results are means ±SD of 4 mice/control and 4 mice/antibiotic. Mann-Whitney U test was carried out to search for statistical significance (*p<0.05, **p<0.01, ***p<0.001).

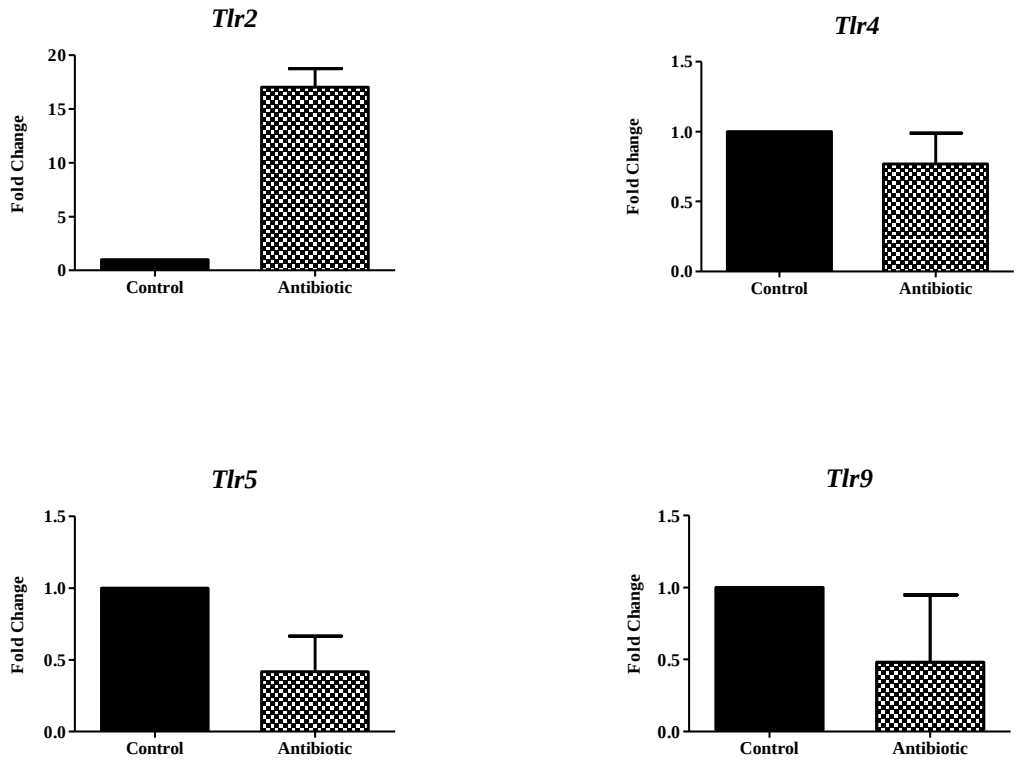

Figure 5. 14 Antibiotic treatment leads to changes in expression of TLRs in the colon. Female C57BL/6J mice were treated with antibiotic cocktail for 3 days, followed by IP injection of clindamycin on day 5. Mice were sacrificed on day 7 and colons were removed. Tissue from each sample was homogenised, mRNA was extracted and normalised amounts of mRNA were converted into cDNA. The cDNA was mixed with primers for *Tlr2*, *Tlr4*, *Tlr5* and *Tlr9* and FAST SYBR Mastermix. Samples were assayed in triplicate and analysed on LightCycler®96. Groups were compared using relative quantitation. After normalising samples to geometric mean of two endogenous controls, *Ppia* and *B2m*, expression of control sample was normalised to 1, and expression in treatment group is shown relative to this value. Results are means ±SD of 4 mice/control and 4 mice/antibiotic. Mann-Whitney U test was carried out to search for statistical significance (*$p<0.05$, **$p<0.01$, ***$p<0.001$).

5. 2. 1. 13 Antibiotic Treatment Alters the Expression of Mucins, Tight Junction Proteins and Antimicrobial Peptides in the Colon.

We investigated the effects of antibiotic treatment and microbiota disruption on the mucosal integrity markers by examining the expression of mucins (Figure 5. 15), tight junction proteins and antimicrobial peptides (Figure 5. 16).

Nine mucin genes were investigated. *Muc1*, *Muc2*, *Muc3*, *Muc4*, *Muc4* and *Muc15* were upregulated expression upon antibiotic treatment (7.5-fold, 10-fold, 10-fold, 25-fold, 4-fold and 5-fold, respectively). There was a minor change in expression of *Muc20*. This included a significant increase in the most abundant colonic mucin, *Muc2* ($p<0.05$). The expression of *Muc5ac* and *Muc6* were decreased, 0.1-fold and 0.2-fold, respectively (Figure 5. 16 A).

In order to determine the most prevalently expressed mucins, we carried out a relative expression study with mucin genes (Figure 5. 16 B). Expression of all the mucins was presented relative to *Muc1*, in the control group and antibiotic treatment group. We determined that *Muc1*, *Muc2*, *Muc3*, *Muc4* and *Muc13* are the most prevalently expressed in colon, before and after antibiotic treatment.

Furthermore, the expression of tight junction proteins were also examined. The expression of both, *Cdh1* and *Ocln* was upregulated upon the antibiotic treatment, 5-fold and 1.5-fold, respectively (Figure 5. 16). However, this increase is expression was not significant.

Finally, the expression of the antimicrobial peptide gene, *Reg3g* was decreased and this change was also non-significant (Figure 5. 16).

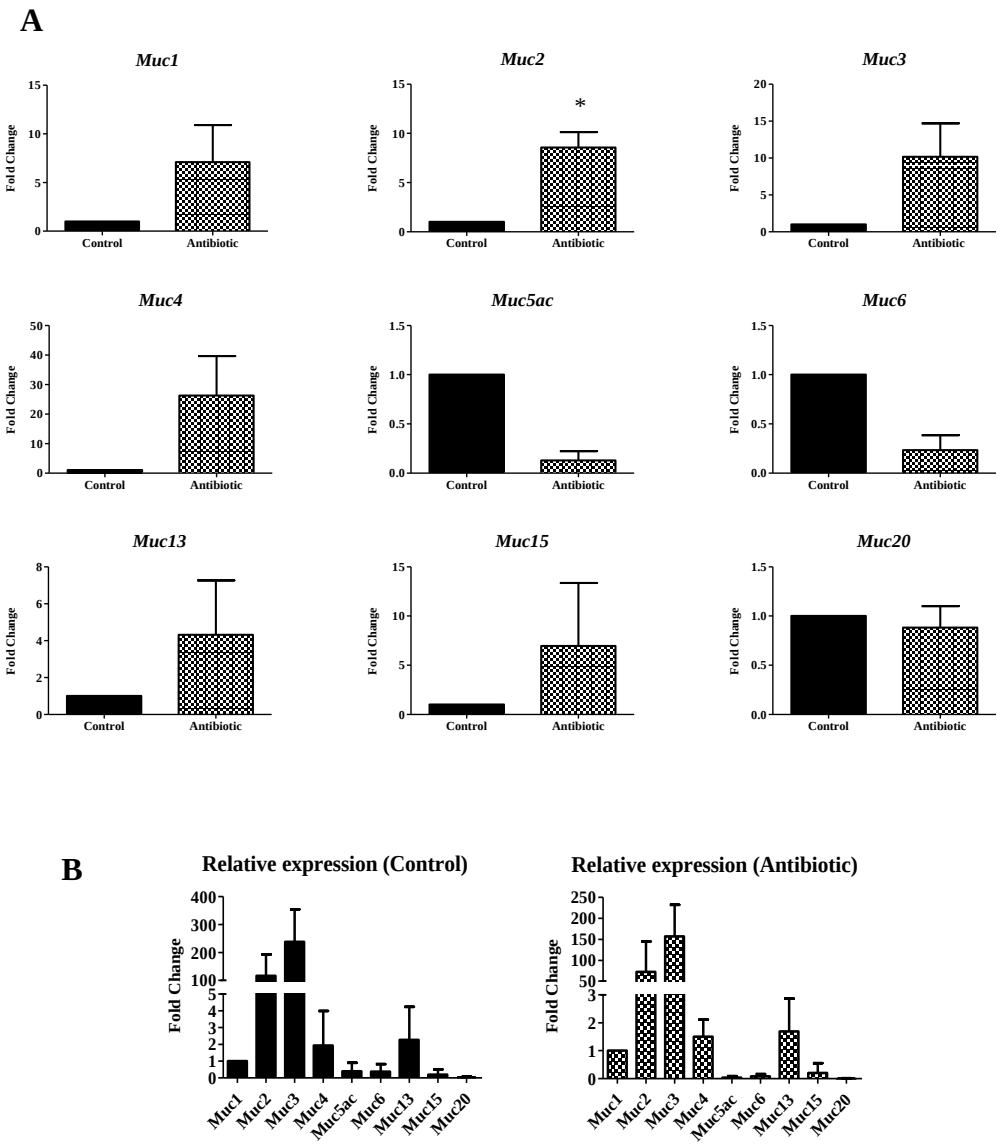

Figure 5. 15 Antibiotic treatment affected the expression of mucins in colonic tissue. Female C57BL/6J mice were treated with antibiotic cocktail for 3 days, followed by IP injection of clindamycin on day 5. Mice were sacrificed on day 7 and colons were removed. Tissue from each sample was homogenised, mRNA was extracted and normalised amounts of mRNA were converted into cDNA. The cDNA was mixed with primers for *Muc1*, *Muc2*, *Muc3*, *Muc4*, *Muc5ac*, *Muc6*, *Muc13*, *Muc15* and *Muc20* and FAST SYBR Mastermix. Samples were assayed in triplicate and analysed on LightCycler®96. Groups were compared using relative quantitation. After normalising samples to geometric mean of two endogenous controls, *Ppia* and *B2m*, expression of control sample was normalised to 1, and expression in treatment group is shown relative to this value (**A**). Relative levels of mucin expression were analysed with same approach but expression of all mucins was presented relative to *Muc1* (**B**). Results are means ±SD of 4 mice/control and 4 mice/antibiotic. Mann-Whitney U test was carried out to search for statistical significance (*p<0.05, **p<0.01, ***p<0.001).

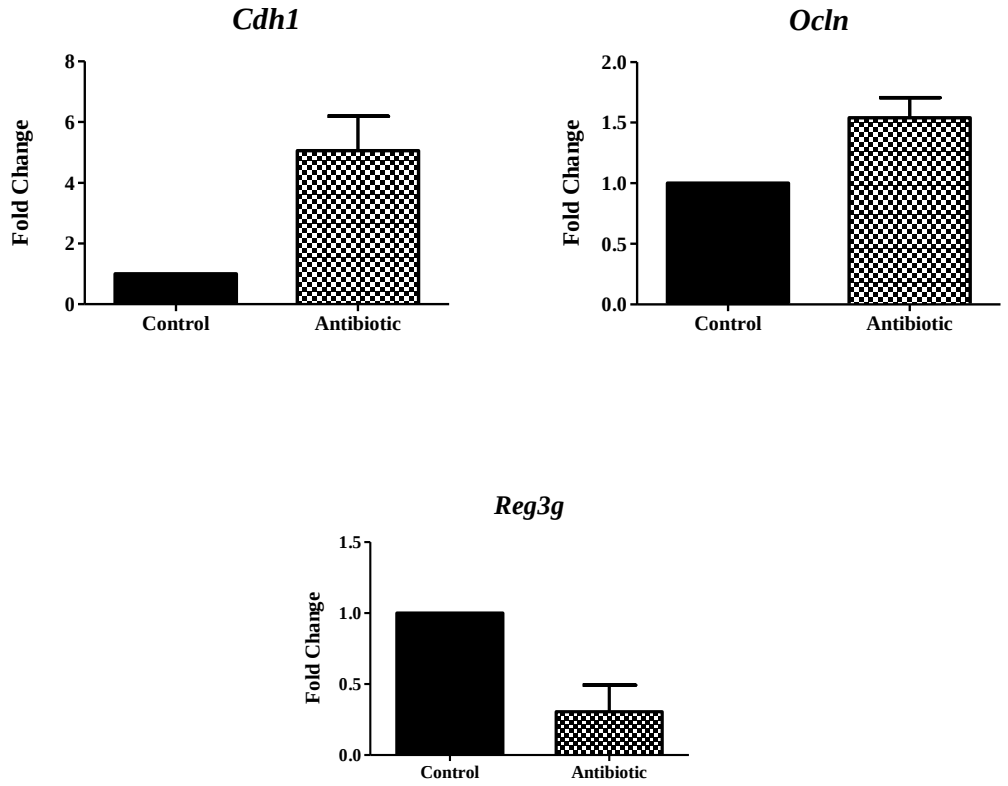

Figure 5. 16 Antibiotic treatment upregulated the expression of tight junction proteins CDH1 and OCLN and downregulated the expression of antimicrobial peptide REGIIIγ in colon. Female C57BL/6J mice were treated with antibiotic cocktail for 3 days, followed by IP injection of clindamycin on day 5. Mice were sacrificed on day 7 and colons were removed. Tissue from each sample was homogenised, mRNA was extracted and normalised amounts of mRNA were converted into cDNA. The cDNA was mixed with primers for *Cdh1*, *Ocln* and *Reg3g* and FAST SYBR Mastermix. Samples were assayed in triplicate and analysed on LightCycler®96. Groups were compared using relative quantitation. After normalising samples to geometric mean of two endogenous controls, *Ppia* and *B2m*, expression of control sample was normalised to 1, and expression in treatment group is shown relative to this value. Results are means ±SD of 4 mice/control and 4 mice/antibiotic. Mann-Whitney U test was carried out to search for statistical significance (*$p<0.05$, **$p<0.01$, ***$p<0.001$).

5. 2. 1. 14 Antibiotic Treatment Induces the Expression of Enzymes Involved in Fucose and Sialic Acid Glycosylation.

Next, we investigated the effects of antibiotic treatment and microbiota disruption on the expression of two glycosylating enzymes, fucose glycosylating enzyme *Fut2* (fucosyltransferase 2,) and sialic acid glycosylating enzyme *Nans* (sialic acid synthase enzyme) (Figure 5. 17). The expression of *Fut2* was increased 3.5-fold upon antibiotic treatment. Also the expression of *Nans* increased 3.5-fold upon antibiotic treatment. Both changes were shown to be non-significant.

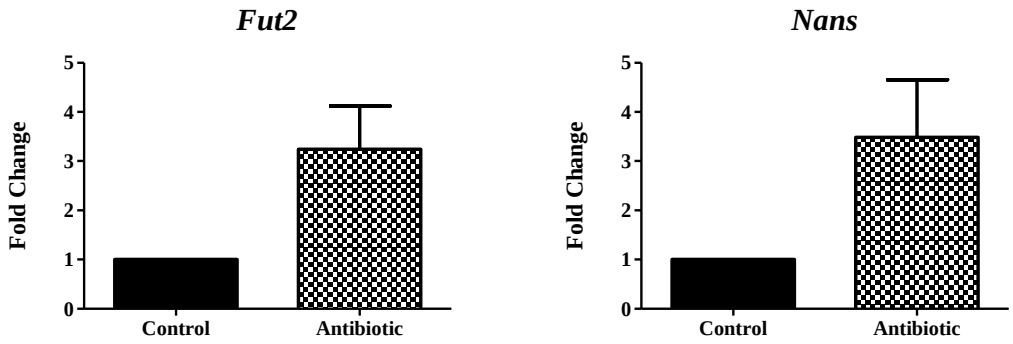

Figure 5. 17 Antibiotic treatment increases expression of fucose and sialic acid glycosylation genes *Fut2* and *Nans*. Female C57BL/6J mice were treated with antibiotic cocktail for 3 days, followed by IP injection of clindamycin on day 5. Mice were sacrificed on day 7 and colons were removed. Tissue from each sample was homogenised, mRNA was extracted and normalised amounts of mRNA were converted into cDNA. The cDNA was mixed with primers for *Fut2* and *Nans* and FAST SYBR Mastermix. Samples were assayed in triplicate and analysed on LightCycler®96. Groups were compared using relative quantitation. After normalising samples to geometric mean of two endogenous controls, *Ppia* and *B2m*, expression of control sample was normalised to 1, and expression in treatment group is shown relative to this value. Results are means ±SD of 4 mice/control and 4 mice/antibiotic. Mann-Whitney U test was carried out to search for statistical significance (*$p<0.05$, **$p<0.01$, ***$p<0.001$).

5. 2. 1. 15 Antibiotic Treatment Alters the Expression of IL-22 Pathway in the Colon.

In order to investigate how the mucosal clearance pathway was affected by the antibiotic treatment, we examined the expression of *Il22b* and *Stat3*.

Expression of *Il22b* was downregulated to 0.1-fold. The expression of transcription factor *Stat3* was also downregulated (0.75-fold). Both results were shown to be non-significant (Figure 5. 18).

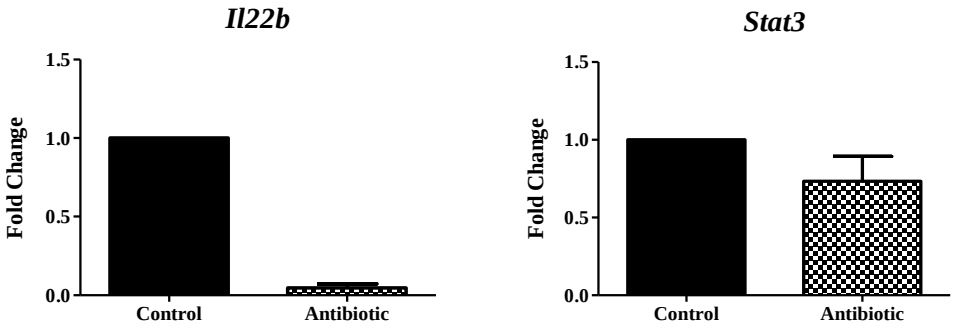

Figure 5. 18 Antibiotic treatment downregulated the expression of *Il22b* and *Stat3*. Female C57BL/6J mice were treated with antibiotic cocktail for 3 days, followed by IP injection of clindamycin on day 5. Mice were sacrificed on day 7 and colons were removed. Tissue from each sample was homogenised, mRNA was extracted and normalised amounts of mRNA were converted into cDNA. The cDNA was mixed with primers for *Il22b* and *Stat3* and FAST SYBR Mastermix. Samples were assayed in triplicate and analysed on LightCycler®96. Groups were compared using relative quantitation. After normalising samples to geometric mean of two endogenous controls, *Ppia* and *B2m*, expression of control sample was normalised to 1, and expression in treatment group is shown relative to this value. Results are means ±SD of 4 mice/control and 4 mice/antibiotic. Mann-Whitney U test was carried out to search for statistical significance (*$p<0.05$, **$p<0.01$, ***$p<0.001$).

5. 2. 2 *C. difficile* RT 001 Modulates the Intestinal Environment to Support Pathogenicity

Thus far we have demonstrated that the host employs several mechanisms to compensate for the lack of commensal microbiota and protect it from a potential invasion by a pathogen. Specifically, we demonstrated that fucose, a glycan preferred by the commensals and not available for *C. difficile*, was increased on the surface of the epithelium. Furthermore, the availability of sialic acid, the glycan of choice for *C. difficile*, was limited.

In this part of the study we next wanted to examine how the glycosylation on the surface of the surface of the epithelium is affected by infection with the *C. difficile* RT 001. This ribotype is known as a mild strain and in our previous study we were able to demonstrated that animals recovered from infection by the end of the study at day 7 (Lynch 2014, unpublished).

Two groups of mice underwent antibiotic treatment and then one group was challenged with *C. difficile* RT 001, respectively, while the control group was allowed to recover commensal microbiota. Colonic tissue was examined for the presence of fucose and sialic acid glycosylation, as well as the expression levels of glycosylation enzymes, FUT2 and NANS enzymes, and of IL-22 cytokine.

5. 2. 2. 1 Fucose Residues on the Surface of the Colonic Epithelium Did Not Change During Infection with *C. difficile* RT 001 and Increased Post-Infection.

Colonic tissue was harvested from mice infected with *C. difficile* RT 001 on day 3 and day 7 days post infection. The surface of the epithelium was examined for fucose glycosylation with use of fluorescently-labelled lectin UEA I, specific for α-Fucose (Figure 5. 19).

The staining with UEA I is visualised in Figure 5. 19 A – D, and the distribution of the glycosylation summarised in Table 2. On day 3 post–infection, fucose glycosylation diminished from goblet and stem cells and also lower crypts, when compared RT 001 to control group. On day 7 post-infection, the fucose glycosylation diminished slightly at the columnar surface epithelium, but also increased in goblet cells, when compared RT 001 to control group.

Fucose glycosylation did not change between control group and RT 001 group on day 3 post-infection when the total fluorescence was measured. By day 7 post-infection, the fucose glycosylation increased in both groups relative to day 3. This increase was higher in the RT 001 group relative to the control group (Figure 5. 19 E), however these changes were not significant.

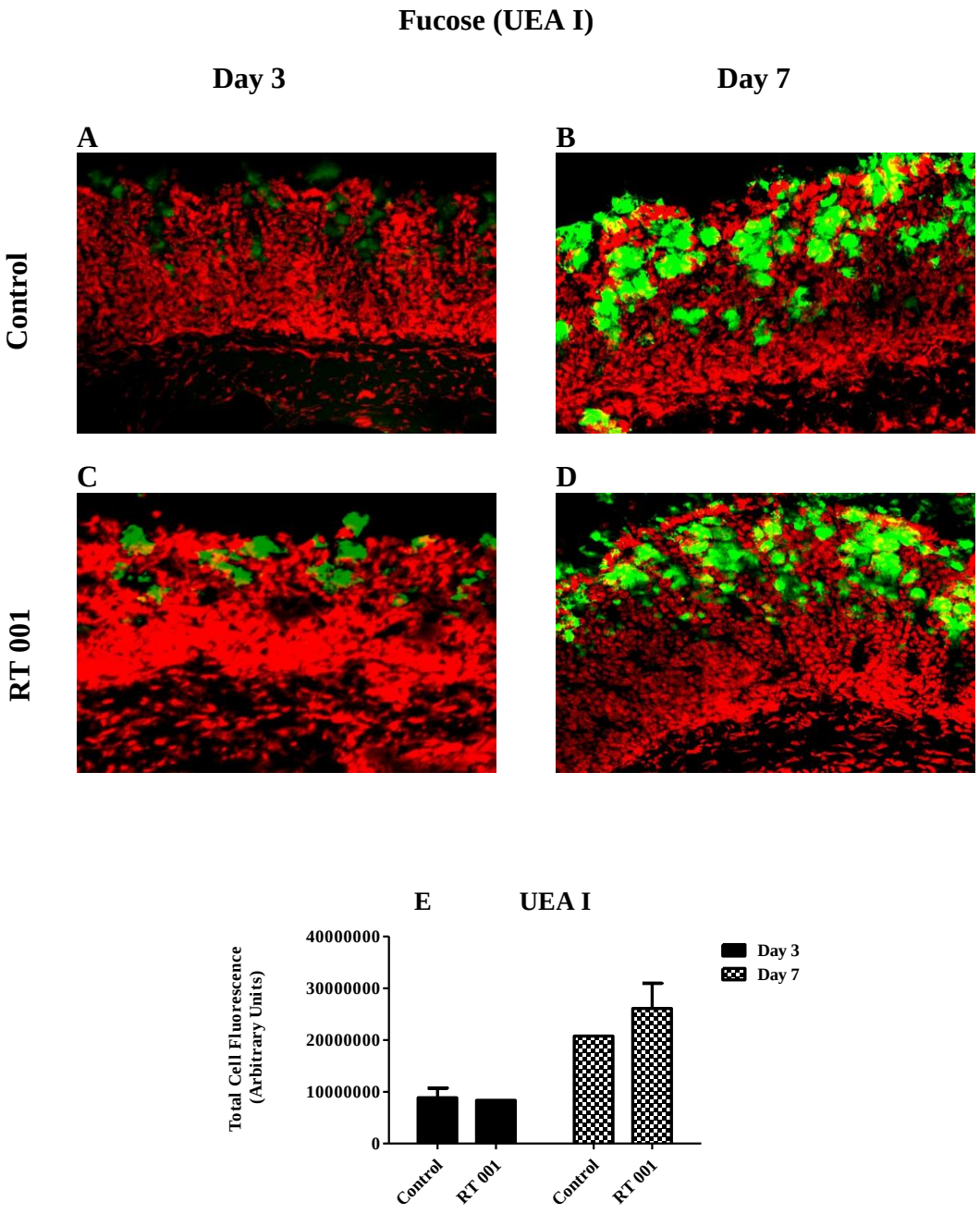

Figure 5. 19 Fucose residues on the surface of the colonic epithelium changed post-infection with *C. difficile* RT 001. C57BL/6J mice were pre-treated with antibiotic cocktail for 7 days. On day 7, mice were infected with *C. difficile* RT 001. Mice were sacrificed on day 3 or day 7 post-infection, and colon was removed, rolled using Swiss roll technique, and stored at -80°C. Tissue was cut into 6 µm sections and probed with 5 µg/ml of UEA I lectin conjugated with FITC tag. Samples were mounted with VECTASHIELD® HardSet Mounting Medium with DAPI. Samples were visualised using Olympus BX51 Fluorescent Microscope using FITC and DAPI filters (FITC: green; DAPI: red). Total fluorescence signal was measured using Image J and corrected for the background fluorescence. Student t-test was carried out to search for statistical significance (*$p<0.05$, **$p<0.01$, ***$p<0.001$).

5. 2. 5. 2 Sialic Acid Presented on the Surface of Colonic Tissue Was Increased Early During Infection with RT 001 and Decreased Post-Infection.

Colonic tissue was harvested from mice infected with *C. difficile* RT 001, on day 3 and day 7 post-infection. Surface sialic acid glycosylation was probed with WGA specific for all forms of sialic acid (Figure 5. 20).

The staining with WGA is visualised in Figure 5. 20 A – D, and the distribution of the glycosylation summarised in Table 2. On day 3 post-infection, the sialic acid glycosylation diminished from the most exposed parts of the epithelium, including the intestinal lumen and columnar surface epithelium, when compared RT 001 to control. However, the sialic acid increased in other parts of the epithelial structure such as lamina propria, goblet cells, stem cells, and middle and upper crypts, as wells as muscular mucosae. On day 7 post-infection, the sialic acid diminished from most of the epithelial structures, the glycosylation signal was only present at the columnar surface epithelium and muscular mucosae, when compared RT 001 to control.

In order to quantify the glycosylation signal, total fluorescence of the glycosylation signal was measured (Figure 5. 20 E). On day 3 post-infection, there was a significant increase in total fluorescence, when compared RT 001 to control ($p<0.001$). By day 7 post infection, the total fluorescence of the control increased (relative to day 3), while the total fluorescence of RT 001 group decreased (relative to day 3). The difference between control and RT 001 was shown to be significant ($p<0.001$).

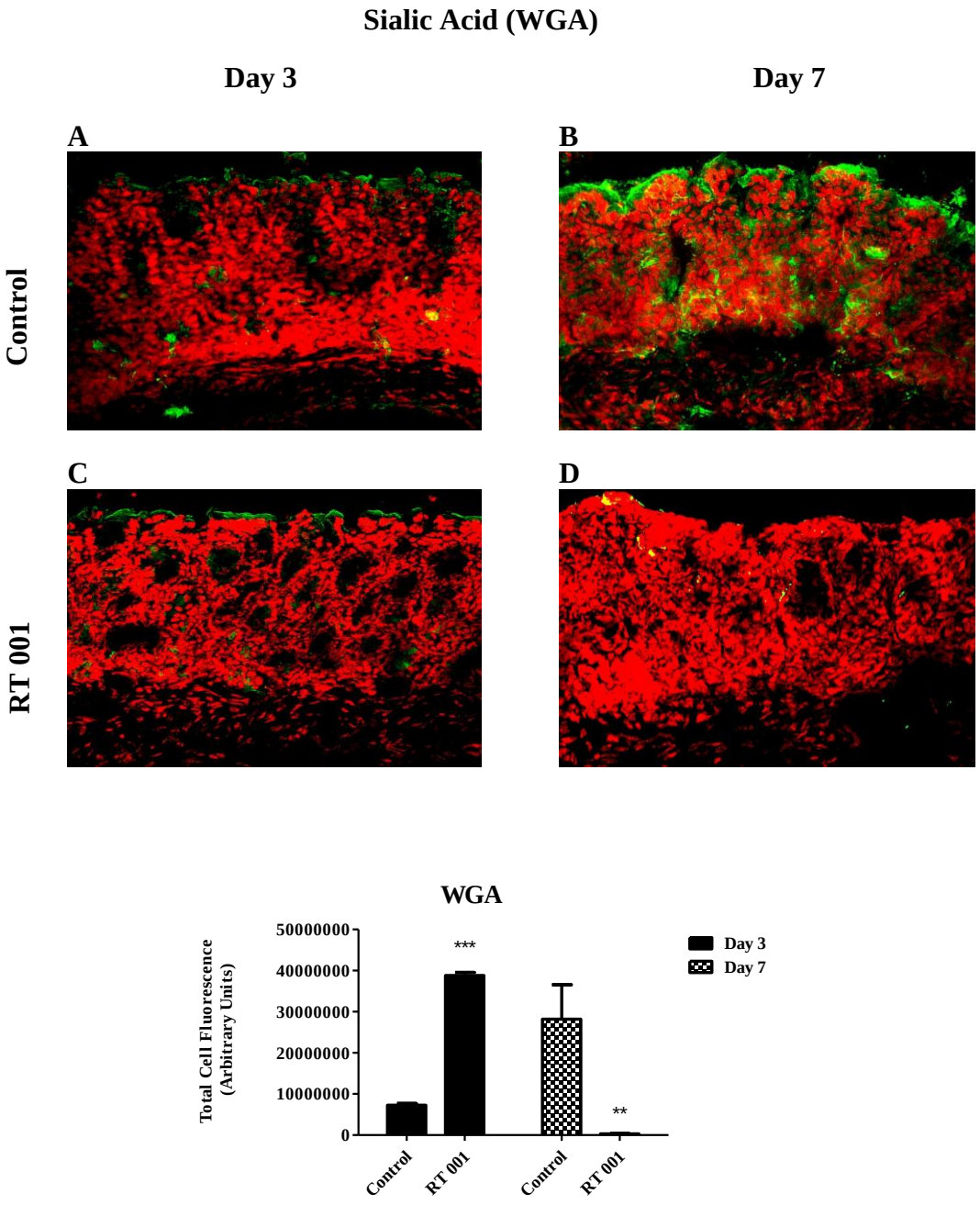

Figure 5. 20 Sialic acid residues on the surface of the colonic epithelium increased early during infection with *C. difficile* RT 001 and decreased post-infection. C57BL/6J mice were pre-treated with antibiotic cocktail for 7 days. On day 7, mice were infected with *C. difficile* RT 001. Mice were sacrificed on day 3 or day 7 post-infection, and colon was removed, and preserved in Optimum Cutting Medium and stored at -80°C. Tissue was cut into 6 µm sections and probed with 5 µg/ml of WGA lectin conjugated with FITC tag. Samples were mounted with VECTASHIELD® HardSet Mounting Medium with DAPI. Samples were visualised using Olympus BX51 Fluorescent Microscope using FITC and DAPI filters (FITC: green; DAPI: red). Total fluorescence signal was measured using Image J and corrected for the background fluorescence. Student t-test was carried out to search for statistical significance (*$p<0.05$, **$p<0.01$, ***$p<0.001$).

Table 5. 2 Fucose and sialic acid glycosylation profile of the colonic surface epithelium observed during infection with *C. difficile* RT 001. Glycosylation structures commonly observed on the colonic epithelium were examined by lectins, UEA I and WGA. Distribution within structure and its intensity was scored as +++ denoting extremely strong staining; ++ denoting strong staining; + some staining present; lack of signal was left blank.

Lectin binding site of the structure of colonic epithelium		**Sugar**							
		UEA I (Fucose)				**WGA (Sialic acid)**			
		Control Day 3	RT 001 Day 3	Control Day 7	RT 001 Day 7	Control Day 3	RT 001 Day 3	Control Day 7	RT 001 Day 7
Intestinal lumen		+		++	++	+			
Columnar surface epithelium			+	+++	++	++	+	+++	+
Lamina propria							+	++	
Goblet cells		+		++	+++		+	++	
Stem cells		+				+	++	+	
Crypt of Lieberkühn	Lower	+				+		++	
	Middle	+++	++	++	++	+	+	++	
	Upper	+++	+++	+++	+++	++	+	++	
Muscular mucosae							+	++	+
Submucosa						+	++	++	

5. 2. 2. 3 The Expression of *Il22b* and Glycosylation Enzymes *Fut2* and *Nans* in Colonic Tissue Was Altered 3 Days and 7 Days Post-Infection with *C. difficile* RT 001.

In order to examine how infection with RT 001 affects the mucosal barrier recovery and glycosylation activity, the expression of *Il22b*, *Fut2* and *Nans* was examined in colonic tissue (Figure 5. 21).

On day 3 post-infection, the expression of *Il22b* was decreased significantly during infection with RT 001 to less than 0.1-fold expression level, relative to the control group ($p \leq 0.001$). On day 7 post-infection, the expression of *Il22b* in RT 001 returned to the expression level compared with control group.

The fucosylation gene *Fut2*was significantly downregulated both on day 3 and day 7 post-infection, 0.75-fold and 0.25-fold, respectively ($p \leq 0.05$).

Furthermore, the sialic acid glycosylation gene *Nans* was shown to be significantly upregulated 4-fold on day 3 post-infection with RT 001 ($p \leq 0.05$). By day 7 post-infection, the expression of *Nans* during infection with RT 001 returned to the expression level compared with control group.

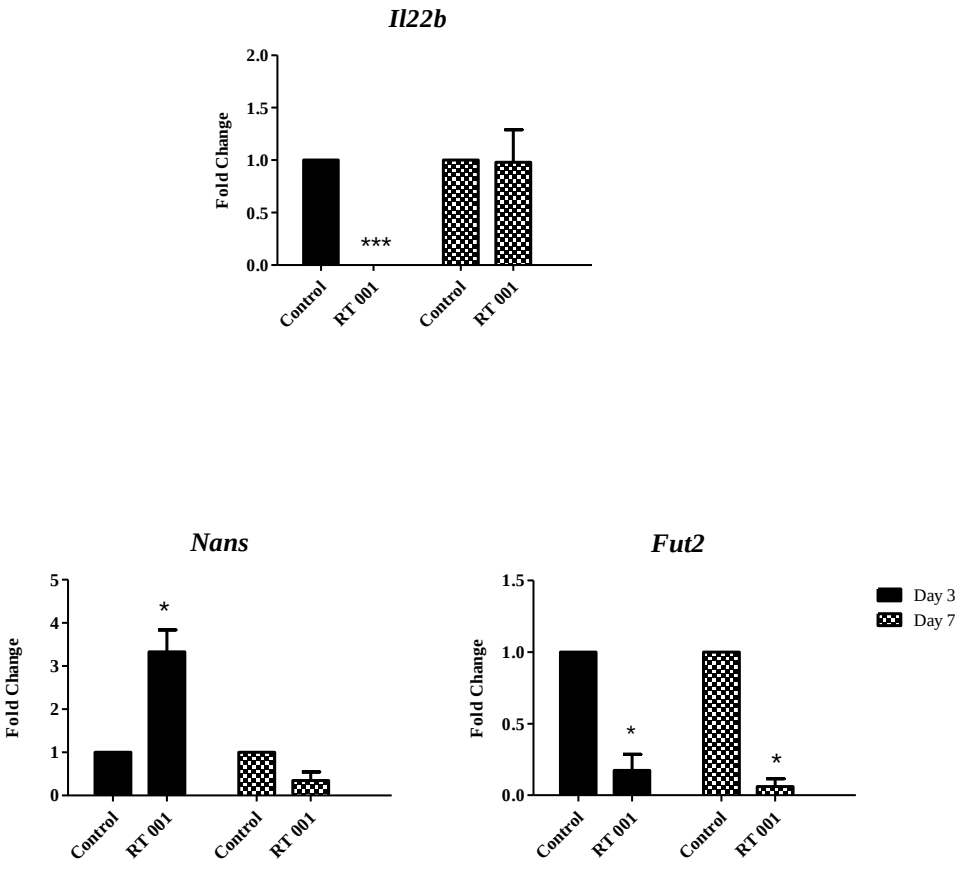

Figure 5. 21 The expression of *Il22b, Fut2* and *Nans* in colonic tissue is altered 3 days and 7 days post-infection with *C. difficile*. Female C57BL/6J mice were treated with antibiotic cocktail for 3 days, followed by IP injection of clindamycin on day 5. Mice were then challenged with *C. difficile* RT 001. Animals were sacrificed on day 3 and day 7 post-infection. Tissue from each sample was homogenised, mRNA was extracted and normalised amounts of mRNA were converted into cDNA. The cDNA was mixed with primers for *Il22b, Fut2* and *Nans* and FAST SYBR Mastermix. Samples were assayed in triplicate and analysed on LightCycler®96. Groups were compared using relative quantitation. After normalising samples to geometric mean of two endogenous controls, *Ppia* and *B2m*, expression of control sample was normalised to 1, and expression in treatment group is shown relative to this value. Results are means ±SD of 4 mice/control, 6 mice/RT 001, for day 3 and day 7. One-way ANOVA test with Newman-Keuls Multiple Comparison tests were carried out to search for statistical significance (*p≤0.05, **p≤0.01, ***p≤0.001).

5. 3 DISCUSSION

In this chapter, we examined the factors that may contribute to susceptibility to the infection with *C. difficile*. Specifically, we wanted to determine if glycosylation influences the colonisation with this pathogen or indeed its course of infection.

The susceptibility state to infection with *C. difficile* is attributed to antibiotic use and previous studies induced susceptibility in animals by antibiotic treatment, including our own (Chen *et al.* 2008; Theriot *et al.* 2015; Lynch 2014, unpublished; Ryan *et al.* 2011). However, there are no previous reports of studies that have examined the susceptibility state to *C. difficile* infection to define the factors that render the animals susceptible to the infection.

In a previous study in our laboratory, animals succumbed to infection with *C. difficile* RT 001 and RT 027 and developed full pathophysiological effects of colitis (Lynch 2014, unpublished). Antibiotics used in the *in vivo* model had a wide spectrum of action, and mimicked the immunocompromised state of patients by eradicating the majority of the commensal microbiome.

However, in the susceptibility model presented in this chapter the animals were not challenged with *C. difficile*. Therefore, in order to ensure that each mouse ingested the recommended amount of antibiotics to eradicate microbiota and induce the state of susceptibility, we monitored the water intake. Each animal under the study consumed less water than expected for C57BL/6J strain at this age (Bachmanov *et al.* 2002). However, all consumed at least the minimum recommended dosage of each of the antibiotics, therefore we consider these animals susceptible.

The animals from the susceptibility group presented with significant weight loss, which was an unexpected observation. The weight loss is usually observed when full

colitis is observed, either chemically induced with dextran sulphate sodium (DSS-induced colitis) (Melgar 2005) or due to infection with a pathogen such as *C. rodentium* (Bergstrom *et al.* 2010). None of the authors inducing susceptibility in mice with antibiotic treatment reported weight loss prior to infection with *C. difficile* (Chen *et al.* 2008; Akha *et al.* 2012; Bassis *et al.* 2014). The observed effect of weight loss could be due to increased levels of defecation and mild diarrhoea, which we observed in this group, however it could be also due to decreased level of feed consumption which we did not monitor in this study.

Furthermore, a significant increase in daily disease index was also observed. Again, this was unexpected, as the animals were not challenged with an infectious agent and we did not anticipate these symptoms. Using the same antibiotic regiment, Chen *et al.* monitored disease progression with a scoring system, however only after animals were inoculated with *C. difficile* and not during the antibiotic pre-treatment(Chen *et al.* 2008).

Due to significant weight loss and increase in daily disease index, the physiological symptoms of colitis were also examined. There was no change in the colon weight and length, as well as no change in the structure of colonic epithelium. This was anticipated, as only mice infected with infectious agents such as *C. rodentium* exhibit pathogenic structures and increased colon weight due to infiltration of immune cells (Koroleva *et al.* 2015).

Since we determined that antibiotic treatment did not induce colitis, we then moved next to examine the factors that may influence the susceptibility state. Overall, we determined that antibiotic treatment and presumably the eradication of microbiota

induced several changes in the host, most of them recognised as protective mechanisms.

Initially, we examined a range of glycans that are found on mucins. This included glycans that comprise the core in the glycan chains, N-Acetylglucosamine, N-Acetylgalactosamine and mannose (Liquori *et al.* 2012). The second group included glycans that are found in terminal positions in glycan chains, fucose and sialic acid and are important nutrient sources for commensals and pathogens (Varki 2008).

We demonstrated that the distribution of fucose on the epithelium shifted towards the surface and it significantly increased upon antibiotic treatment. The surface presentation of fucose is important in this context, as we proposed that increased levels of fucose may play an essential role for commensal recovery. The glycans have to be presented not only in the terminal sequences in order for commensal to remove the glycans from the glycosylation chain. The fact that the fucose shifts towards the surface in antibiotic-treated animals, may support the hypothesis that fucose is presented here for the commensal benefit. This increase correlated with the increased expression of fucosylation enzyme, FUT2. The increased fucosylation presented on the surface of the epithelium has an enormous impact on the recovery of compromised commensals because fucose is used by microbiota as a preferred energy source. Therefore, fucose-digesting enzymes are constitutively expressed and readily available in commensal bacteria, while pathogens have to switch the metabolism to fucose and express the appropriate enzymes (Hooper & Xu 1999). Pickard *et al.* has shown during infection with *C. rodentium* that the increase in fucose is a mechanism employed by the host to actively enhance the commensal recovery (Pickard *et al.* 2014). This profile correlates with our model, as antibiotic-treated mice try to support the microbiota and fucose may enhance this recovery.

Another terminal glycan, sialic acid, is an important energy supply for *C. difficile* during infection (Ng *et al.* 2013). Therefore, we anticipated that sialic acid may be upregulated in the susceptibility state, which could contribute to colonisation of *C. difficile*. To our surprise we observed a significant decreased in sialic acid residues upon antibiotic treatment. However, when we examined the expression levels of sialic acid synthase gene, NANS we found it to be upregulated in the susceptibility state. The lower levels of sialic acid on the surface of the epithelium, despite upregulation of NANS, may be explained by the lack of mannose that we also observed. As determined by the lectin probing, mannose residues decreased upon antibiotic treatment. Interestingly, mannose, in form of N-acetylmannosamine 6-phosphate is a substrate for NANS (sialic acid synthase) to form sialic acid (Hao *et al.* 2005; Tanner 2005). We observed that NANS expression was increased in the susceptibility state but there was no increase in sialic acid residues as determined by the lectin probing. We propose that the lack of sialic acid on the surface of the epithelium in the susceptibility state is due to the limited supply of mannose, despite the increased expression of sialic synthase enzyme.

Additionally, sialic acid has a reversible relationship with fucose. In the human GI tract, under healthy conditions, there is an increasing gradient of surface sialic acid from the ileum to the colon associated with a reversed gradient of fucose, both presented on mucins (Robbe *et al.* 2003). However, this ratio is inverted when the host is compromised, with high fucose and low sialic acid presented on the surface of colonic epithelium. This is the exact relationship that we observed in the susceptibility state, as there was a significant increase in fucose with significant downregulation of sialic acid. This suggests that antibiotic treatment induces a

profile of terminal glycans that is essential for the commensal recovery (high fucose) and disadvantages the growth of *C. difficile* (low sialic acid).

Core glycans are not essential for bacterial growth, as demonstrated by the lack of enzymes catabolising N-Acetylgalactosamine or N-Acetylglucosamine in a genome of pathogens such as *E. coli* (Fabich *et al.* 2008). In this study, we observed that antibiotic treatment increased the N-Acetylglucosamine when probed with both GSL II and sWGA. Tobisawa *et al.* demonstrated that increased N-Acetylglucosamine residues on mucins in the colon is correlated with a protective mechanism employed to prevent the massive leukocyte infiltration (Tobisawa *et al.* 2010). However, the increased levels of this glycan may benefit *C. difficile* during infection, as N-Acetylglucosamine has been shown to mediate binding of *C. difficile* toxin (Castagliuolo *et al.* 1998). Its position within the core of the glycan chain may aid the delivery of the toxin closer to the epithelial surface especially that the N-Acetylglucosamine residues increased in lower parts of the crypts of the epithelium.

Overall, here we show that the susceptibility state induced changes in the glycosylation present on the colonic surface. Specifically, we determined that the host presents the glycans that can promote the commensal recovery (fucose), and limit the glycans that could benefit the pathogen (sialic acid). This finding was unexpected, as we anticipated that the glycosylation profile may benefit the pathogen rather than the commensals. However, our further finding of an increase in A-Acetylglucosamine supports an environment that *C. difficile* may thrive in, through enhanced toxin binding.

Therefore, while our findings demonstrated that the glycosylation status of the gut may influence the susceptibility of the host to infection with *C. difficile*, it was clear

that other factors may also contribute. In particular, given that antibiotic-treated host becomes immunocompromised, as mice challenged with *C. difficile* succumb to infection unlike immunocompetent mice (Chen et al. 2008; Lynch 2014, unpublished), therefore we wanted the examine this immunocompromised state in order to determine the factors that may render these animals susceptible to the infection.

Commensals are actively involved in stimulating the immune response and mucosal integrity barrier, and this suggested that any change in microbiota due to antibiotic treatment may influence this balance (Min & Rhee 2015). Therefore, we next examined the expression of these factors to correlate any changes with susceptibility to the infection.

We determined that antibiotic treatment increased the inflammatory state presented in the colon, as evidenced by upregulated expression of proinflammatory cytokines IL-12, IL-23 and IL-1β. These cytokines are essential for initiating the immune response (Charo & Ransohoff 2006). The susceptibility state induced by the antibiotic treatment and anticipated lack of microbiota, may explain this proinflammatory tone. This is due to the lack of immunosuppressive effect that the microbiota has on the gut environment. Versalovic *et al.* suggested that commensal microbiota may have an anti-inflammatory effect on the GI tract, and therefore when this signal is eradicated, the proinflammatory pathways may be activated (Versalovic *et al.* 2008).

We also observed that chemokines, MCP1, MIP2α and MIP1α, were downregulated in the susceptibility state. These chemokines are essential for neutrophil recruitment (Fournier & Parkos 2012; Rydström & Wick 2009; Ohtsuka *et al.* 2001), and their

absence may suggest that the recruitment of the immune cells was repressed. Possibly it was a mechanism employed to prevent an augmented immune response to recovering microbiota. Interestingly, one of the chemokines, RANTES was upregulated in the susceptibility state. This chemokine is also essential for neutrophil recruitment and clearance of infection. However Hu *et al.* demonstrated that aberrant microbiota induced colitis in mice specifically via excessive induction of RANTES (Hu *et al.* 2013). While the upregulation of RANTES may not contribute to the infection, it may be detrimental during the early stage of the infection with *C. difficile*.

Possibly to counteract this proinflammatory effect, we observed an increase in expression of two major anti-inflammatory cytokines, IL-10 and TGFβ. These cytokines play key role in regulating and repressing expression of proinflammatory cytokines (Ouyang *et al.* 2011). Kang *et al.* reported that IL-10 and TGFβ synergise together to inhibit induction of proinflammatory cytokines when microbiota is disturbed (Kang *et al.* 2008). However the induction of these two cytokines may have a detrimental effect on the host. IL-10 and TGFβ may supress the normal host inflammatory responses, leading to persisting chronic infection via induction of an anergic state (Mege *et al.* 2006). Furthermore, induction of IL-10 by pathogens such as *Mycobacterium tuberculosis* or *Candida albicans*, followed by induction of Tregs is known as an immune evasion mechanism that impairs clearance (Ouyang *et al.* 2011). In our previous study, we also demonstrated that more persistent infection of *C. difficile* RT 027 was due to upregulated IL-10 expression, to dampen the clearance and maintain the infection (Lynch 2014, unpublished).

The protective environment induced in the colon upon the antibiotic treatment was further evidenced by downregulation of 3 out of 4 investigated TLRs. Intestinal

epithelial cells have very low basal expression of TLRs to tolerate the commensal antigens and the expression of TLRs is expected to increase upon stimulation with high loads of antigens in order to facilitate proinflammatory signalling (Moncada *et al.* 2003). We observed downregulated levels of TLR4, TLR5 and TLR9 in the susceptibility model. This could be a mechanism employed by host to dampen the immune response, as proinflammatory pathways were already induced and no further recognition by TLRs is required.

Furthermore, Ueno *et al.* suggested that the downregulation of TLR2, TLR4, TLR5 and TLR9 is a direct response to increased expression of MUC1 (Ueno *et al.* 2008). This is consistent with our observations as MUC1 expression in increased in the susceptibility state. However, TLR2 was increased in our study, contrary to Ueno *et al.* study. These authors carried out this investigation on cell line, while our *in vivo* study involved a dynamic environment.

Signalling via TLR2 is important for commensal recognition and Treg expansion to maintain the immunologic tolerance (Round *et al.* 2011). This includes the commensal *Bacillus fragilis* that require TLR2 signalling to promote regulatory T cell-mediated immune tolerance (Thaiss *et al.* 2014).

Furthermore, the upregulation in expression of TLR2 has been shown to be essential to strengthen the mucosal barriers by enhancing the tight junction expression (Yuki *et al.* 2011). Similarly, TLR2 knockout mice presented incompetent and permeable epithelial barrier due to downregulated tight junction genes (Kuo *et al.* 2013). In our study we observed that both tight junction genes were upregulated in the susceptibility state and we propose this is due to upregulated TRL2 expression. Therefore, the upregulation of TLR2 is a desirable mechanism in a situation where

the microbiota is compromised and the host employs mechanisms to recover the commensals. Along with tight junction proteins, we examined other factors contributing to the mucosal integrity barrier, namely mucin expression and antimicrobial peptide, REGIIIγ.

We determined that upon antibiotic treatment, MUC1, MUC2, MUC3, MUC4 and MUC13 were induced upon antibiotic treatment but also they were the most prevalently expressed. However, it may not be just the direct effect of antibiotics on the mucus-secreting epithelium but also the lack of the mucus-stimulating signal form commensal bacteria (Wlodarska et al. 2011). For example, probiotic microbes induce MUC3 transcription and extracellular secretion in order to reduce the adherence of a pathogenic strain of *E. coli* (Mack *et al.* 2003). Furthermore, two mice populations maintained under the same conditions, but with distinct microbiota compositions, displayed different compositions of mucus one group with an impenetrable barrier, while other group displayed easily penetrable mucus (Jakobsson *et al.* 2014). Also, MUC2-deficient mice presented a thinner mucus layer in the colon and were hypersensitive to DSS-induced colitis (Petersson *et al.* 2011).

Increased expression and secretion of mucins in infection is a desired host response to pathogen invasion, as a thicker mucus layer may act to exclude the invading bacteria from interacting with the epithelium. During infection with *C. rodentium*, there is increased expression of MUC1 in the colonic epithelium (Lindén *et al.* 2008). Also, *Salmonella* infection induces expression of MUC2 in the colon and MUC2-deficient mice demonstrated dramatic susceptibility to infection (Zarepour *et al.* 2013). Furthermore, Chu *et al.* has demonstrated that recognition of *Mycoplasma pneumoniae* via TLR2 directly stimulated mucus production (Chu *et al.* 2005). In our study, we observed the increased expression of key mucins, and we propose that

this is another protective mechanism employed by the host to defend from anticipated pathogen invasion. This mechanism may be largely influenced by the upregulated TLR2 expression.

RegIIIγ is an important antimicrobial peptide that is retained in the mucus upon its secretion and it generates the physical separation between the epithelium and microbiota. This antimicrobial peptide is constitutively expressed in the gut under healthy conditions (Hansson 2012). In our study we determined that in the susceptibility state, expression of RegIIIγ was decreased. This is consistent with the previous studies, as Brandl *et al.* also observed downregulation of RegIIIγ upon antibiotic treatment in mice (Brandl *et al.* 2008). This is a desirable response, as increased levels of antimicrobial peptide could impair recovering commensals. Furthermore, Kamada *et al.* determined that during infection, the expression of RegIIIγ is induced by IL-22 cytokine (Kamada *et al.* 2013). Therefore, the down regulated levels of REGIIIγ expression may be a direct result of downregulated expression of IL-22 we also observed in our susceptibility study.

Finally, we examined the expression of IL-22, an essential cytokine for maintaining homeostasis at the epithelial barrier in the gut. The ligation of IL-22 to its receptor in the intestine has been shown to induce a wide spectrum of action, including expression of antimicrobial peptides (Zheng *et al.* 2008) and mucins MUC1, MUC3, MUC10 and MUC13 (Sugimoto & Ogawa 2008), as well as the fucosylation genes FUT2 (Pham *et al.* 2014). Finally, it induces pathways involved in the proliferation and anti-apoptotic pathways (Sonnenberg *et al.* 2010).

In the susceptibility model, we determined that expression of IL-22 and its downstream signalling molecule STAT3 was downregulated. This was an

unexpected finding, as the mucosal barrier was compromised due to aberrant microbiota, and upregulation, rather than downregulation, of this cytokine in order to restore the balance was anticipated.

Overall, we demonstrated that the induction of susceptibility in the host resulted in triggering several protective mechanisms. These include an environment that promotes commensal recovery with fucose-rich glycans, increased TLR2 expression and repressed antimicrobial peptides. Furthermore, TLR2 enhances tight junction proteins and mucins production. Finally, we observed mild proinflammatory tone of the gut could promptly protect the host from anticipated pathogen invasion.

However, we also identified several mechanisms that are supposed to be protective to the host. Nevertheless, the pathogen may take advantage of them, and they may be key to explain what makes the animals susceptible. Specifically, it is the upregulation of IL-10 and TGFβ, cytokines known for their anti-inflammatory properties. Overexpression of these cytokines has been previous shown to be responsible for repressing the normal host inflammatory responses (Ouyang *et al.* 2011). In the context of *C. difficile* colonisation, this may suggest that the pathogen may successfully colonise the gut while evading immune response and clearance. Furthermore, IL-22 expression was downregulated; therefore, the epithelial barrier may be severely compromised at molecular level, despite the fact that no colitis was observed upon antibiotic treatment. Finally, the high expression levels of TLR2 and RANTES may support the development of colitis. The overexpression of TLR2 may contribute to the disease pathology as bacterial products may exacerbate acute inflammation via this receptor, also signalling thought TLR2 induces the secretion of IL-10 which may further induce the immunosuppressive environment which is beneficial for *C. difficile* (Zhang *et al.* 2015). Additionally, the excessive expression

of RANTES has been shown to specifically induce colitis in mice with aberrant microbiota (Hu *et al.* 2013) and this could also be beneficial for *C. difficile*.

Therefore next, we wanted to examine how these factors influence the course of *C. difficile* infection in order to correlate these factors with recovery and clearance. Specifically, we looked at the terminal glycan profile and their corresponding glycosylation enzyme expression but also the expression of IL-22.

We observed that 3 days post-infection, the expression of IL-22 is completely repressed. This correlates with the observations made by Lynch (2014, unpublished), 3 days post-infection the animals suffer from severe infection, epithelial damage and large bacterial load as determined by CFU counts. The lack of IL-22 expression may have an immediate implication for recovery of the epithelium, as its structure is collapsed and IL-22-induced proliferation signal are required to re-build the epithelium. As the lack of the recovery signals is beneficial for the pathogen, this possesses a question whether pathogen actively modulate the IL-22 signalling to repress this host protective mechanism. Alternatively, the lack of commensal-derived signal may explain the reduction of IL-22 expression. By day 7 post-infection, the pathogen is cleared and the epithelial barrier is recovered. This corresponds with expression of IL-22 that similar to the control group, which suggests that IL-22 may be important in restoring the epithelium. This commensal microbiota-IL-22 axis is largely unexplored and enhancing this signal may be an attractive therapeutic alternative in CDI.

IL-22 is known to regulate fucosylation by induction of FUT2 (Pham *et al.* 2014; Pickard *et al.* 2014) and we demonstrated that fucosylation is insignificantly decreased on day 3 post-infection when compared to control group and this

correlated with downregulation of FUT2 expression. As already mentioned, pathogen may actively repress IL-22 signalling, and one of the downstream factors affected by lack of IL-22 would be the lack of fucosylation signal, known to have a beneficial role in recovering commensals (Pham et al. 2014). The recovery of the commensals would be essential for recovering the colonisation resistance, therefore abolishing this IL-22-fucosyaltion-commensal axis is beneficial for *C. difficile*.

Finally, we show that sialic acid residues and NANS expression are upregulated on day 3 post-infection, the time point corresponding to the peak of the infection and pathogen count as demonstrated by Lynch (Lynch 2014, unpublished). By the end of the study (day 7 post-infection), as the animals recover from the infection, we also observe downregulation of sialic acid metabolism, both at glycan level, but also the expression level. This suggests that the pathogen may actively induce the sialic acid metabolism to maintain the infection. Overall, in the infection model, we observed that the glycans preferred by the commensals are actively repressed by the pathogen, while the sialic acid is induced.

To conclude, we determined that the glycosylation status in the gut did not fully explain how the host became susceptible to infection with *C. difficile*, as we show that the glycans displayed on the epithelial surface in fact aid the commensal recovery. However, it seems, that certain actions induced by the host to protect it from an anticipated invasion, such as high IL-10 and TLR2 expression, in fact may tip the balance over in favour of the pathogen. These factors may define the susceptibility of the animals to *C. difficile* infection.

The glycosylation environment becomes important during the infection, as demonstrated with the abundance of sialic acid that was observed, and this correlates

with high pathogen counts (Lynch 2014, unpublished). However, we observed the recovery of these animals and it may be due to delay action of IL-22 cytokine. Therefore, the exact role IL-22 in pathogenicity of *C. difficile* should be examined next.

CHAPTER 6 GENERAL DISCUSSION

The recent years brought have about remarkable advances in our understanding of the complexity of host-microbiota interactions, both in health and disease states. This has allowed for further elucidation of the mechanisms employed by opportunistic pathogens such as *C. difficile*. Due to the importance of commensals in colonisation resistance, disturbances in the normal microbiota, as is seen with antibiotic treatment, has an immediate effect on pathogen invasion (Zhang *et al.* 2015). This is due to the increased availability of nutrients and space and a relative lack of inhibitory metabolites (Britton & Young 2014).

C. difficile pathogenicity has largely been attributed to the actions of its toxins (Rupnik 2005; Genth *et al.* 2008; Voth & Ballard 2005; Young & Hanna 2014). Increased awareness of the role that the toxins play in damaging the epithelium led to the proposal of therapies involving immunisation against TcdA and TcdB, however to date, these vaccines have not proved effective in clinical settings (Mizrahi *et al.* 2014; Foglia *et al.* 2012). While toxins are known to play a detrimental role in damaging the epithelial barrier, they are not secreted until a later phase of infection (Hundsberger *et al.* 1997; Janoir *et al.* 2013). Furthermore, not all infectious ribotypes of *C. difficile* secrete toxins (Kuehne *et al.* 2010). Therefore, the pathogenesis of CDI cannot solely be attributed to toxins alone. This has prompted

the search for additional virulence factors, as the mechanisms of colonisation and adherence remain unknown.

We have previously shown that the surface of *C. difficile* is essential for the recognition of the pathogen by the host immune system. Specifically, SLPs are recognised by TLR4 (Ryan *et al.* 2011) and elicit an immune response that leads to the clearance of the pathogen (L. E. Collins *et al.* 2014). Given that these proteins coat up to 99% of the surface of *C. difficile* (Fagan *et al.* 2009; Calabi & Fairweather 2002), it is likely that SLPs are the first surface antigens that the host encounters. For this reason, we wanted to determine whether SLPs are essential for the *C. difficile* adherence and colonisation. In previous studies carried out in our laboratory only SLPs from one ribotype of *C. difficile* were used (Ryan *et al.* 2011; Collins *et al.* 2014). Therefore, our first objective was to develop methods to grow a range of clinically relevant ribotypes of *C. difficile* and to isolate their SLPs. This allowed us to build a library of SLP stocks used for various projects within our laboratory and by our collaborators.

Two *C. difficile* ribotypes used in this project, RT 001 and RT 027, are associated with two different clinical outcomes and are the most common isolated ribotypes from patients suffering from CDI in Europe and USA (Barbut *et al.* 2007; Cheknis *et al.* 2009). We showed that SLPs from these ribotypes, elicited distinct immune responses in colonic tissue *ex vivo*. This suggested that SLPs interact with the colonic tissue, but also that this interaction is ribotype-dependent.

Our findings prompted the question about the structure of SLPs and their role in mediating the interaction between the pathogen and colonic tissue. As evident from the literature, SLPs differ in the amino acid sequence between the ribotypes

(Mccoubrey & Poxton 2001) and also, the predicted molecular weights of SLPs are often different from molecular weights observed (Calabi *et al.* 2001). This suggested the possibility of post-translational modifications. Other enteric pathogens such as *H. pylori* and *E. coli* modify their surface proteins by addition of glycans and these glycosylated proteins are thought to enhance their pathogenicity (Champasa *et al.* 2013; Wang *et al.* 2012).

Glycosylation plays an important role in host-pathogen interactions, and glycosylated proteins and receptors often facilitate the interaction between both. Much of the knowledge regarding the prokaryotic glycosylation was derived from studies on S-layers of archaea and bacteria (Schäffer *et al.* 2001). *E. coli* does not not have S-layer, but surface adhesins have been shown to be glycosylated (Benz & Schmidt 2001). Also, the glycosylation of other surface appendages such as flagella, in enteric pathogens such as *C. jejuni* (Alemka *et al.* 2013) and *H. pylori* (Champasa *et al.* 2013), has been recently described. Most of the described bacterial glycoproteins are surface-associated, and this suggests that they may have an important role in pathogenicity including adhesion, protection from proteolytic cleavage, antigenic variation and immune evasion (Szymanski & Wren 2005). We suggested that differential glycosylation of SLPs from various ribotypes may account for the differences in molecular weights. This could also have implications for the initial interaction with the host surface and the subsequent immune response elicited, and may explain the differences in virulence between ribotypes.

In order to explore this hypothesis, we probed SLPs from a range of ribotypes for the presence of various glycan structures. However, even though we examined a range of ribotypes using different methods, we determined that SLPs were not glycosylated.

Therefore, the theory that the glycosylation on the surface of *C. difficile* may contribute to colonisation and immune evasion was no longer viable. However, this did not exclude the role of glycosylation in host-pathogen interaction and our focus switched to the glycosylation profile of the colonic environment and its role in pathogen colonisation. Specifically, we looked at the susceptibility state to *C. difficile* infection. Many *in vivo* studies of *C. difficile* infection have been reported in the literature (Chen *et al.* 2008; Seekatz *et al.* 2015; Abt *et al.* 2015; Ferreyra *et al.* 2014; Sun *et al.* 2011), but to our knowledge, there have been no studies focused on determining the factors that may contribute to the susceptibility to infection.

The antibiotic regiment administered to the mice in our study, previously has been shown to result in the eradication of the vast majority of the gut microbiota and we expected the similar shifts in the composition of commensals (Chen *et al.* 2008). Commensals present in the gut are responsible for actively shaping the intestinal environment. For instance, commensals have the ability to modulate the glycans presented on the surface of the epithelium to suit their nutritional requirements (Freitas *et al.* 2002). The absence of commensals and their stimulatory effects can therefore lead to changes in this environment. For that reason, we examined the glycosylation profile of the colonic epithelium. We wanted to explore whether this altered environment would benefit *C. difficile* during colonisation.

Sialic acid has been shown previously to be essential during the *C. difficile* infection as a source of energy for the pathogen (Ng *et al.* 2013; Ferreyra *et al.* 2014). With this in mind, we anticipated that antibiotic-treated mice would present with an abundance of sialic acid in the gut. As a result, *C. difficile* would be in an advantaged position to invade the host. Surprisingly, we determined that inducing the susceptibility state in mice by antibiotic treatment, results in decreased levels of

sialic acid with concurrent increase in the levels of fucose. This is similar to the profile presented in an immunocompromised state, where upregulated fucosylation is regarded as a protective mechanism to recover compromised microbiota (Pickard & Chervonsky 2015; Pham *et al.* 2014; Robbe *et al.* 2003). *C. difficile* lacks the enzymes essential for fucose digestion (Ng *et al.* 2013), therefore, the glycosylation profile observed in the susceptibility state was an unexpected finding. It seems that the glycosylation patterns on the surface of the epithelium aid in the commensal recovery and repress pathogen invasion, contrary to our predictions.

Considering that the glycosylation profile did not play a major role in the susceptibility, we also examined other factors that could have been affected by the antibiotic treatment and anticipated disturbance of the microbiota. Specifically, we looked at the host immune response and the integrity of mucosal barrier. Again, we found several changes that could be regarded as protective mechanisms. This included the mild proinflammatory profile of cytokines, together with downregulation of chemokines with the exception of the RANTES and TLRs with the exception of TLR2. The upregulation of TLR2 may have a protective effect as TLR2 is known for its role in supporting microbiota recovery and promoting gut homeostasis via induction of Tregs (Thaiss *et al*. 2014; Round *et al.* 2011). Also TLR2 has been shown to enhance the expression of tight junction proteins (Yuki *et al.* 2011; Frosali *et al.* 2015) and mucin secretion (Chu *et al.* 2005). The upregulation of tight junction proteins may lead to strengthening of the epithelial barrier, while the upregulation of mucin secretion allows for a thicker mucus layer, preventing the microbes from interacting with the epithelium. However, the upregulated levels of TLR2 may play a detrimental role for the host during the invasion by *C. difficile*, as high bacteria antigen load stimulates TLR2 signalling,

which contributes to exacerbated acute inflammation (Zhang *et al.* 2015). This may be one of the factors contributing to the acute colitis observed during *C. difficile* infection.

TLR2 may also influence the mucin secretion, as it has been previously reported that infection with *Haemophilus influenzae* results in increased expression of MUC2 via TLR2 and TGFβ signalling (Jono *et al.* 2002). This is consistent with our observation, as we determined that most prevalently expressed mucins, including MUC1, MUC2, MUC3, MUC4 and MUC13 were upregulated in susceptibility state, and this may be a direct result of the upregulated expression of TLR2 and TGFβ. In turn, the increased secretion of mucins may have a dampening effect on TLR expression. Ueno *et al.* have reported that increased expression of MUC1 correlated with decreased expression of TLR4, TLR5 and TLR9 (Ueno *et al.* 2008), which is consistent with our observations. MUC1 may repress the expression of these TLRs to dampen the immune response, as proinflammatory pathways are already activated. Suppression of the immune response during resolution of infection is essential to prevent over-stimulation of the immune system which can result in autoimmunity. Therefore the susceptibility model allowed us to identify a range of mechanisms that may be in place to protect the host from anticipated pathogen invasion, but also mechanisms that may directly contribute to the microbiota recovery.

However, among these protective mechanisms we identified several factors that may be utilised by *C. difficile* to take advantage and colonise the gut. This included the upregulated expression of IL-10 and TGFβ. These cytokines are essential for maintaining the balance in the immune response via their anti-inflammatory and regulatory properties (Kang *et al.* 2008). However, overexpression of these cytokines may in fact result in an overly immunosuppressive environment, where the host is

not able to mount an efficient immune response to invading pathogens (Mege *et al.* 2006). In our previous study we demonstrated that it is this upregulation of IL-10 that contributes to the prolonged infection seen with *C. difficile* RT 027 (Lynch 2014, unpublished). IL-10 has been shown to delay the immune response, enabling the pathogen to successfully colonise the colon and secrete toxins, causing the damage to the epithelium. In this study we demonstrated that levels of anti-inflammatory IL-10 and TGFβ may be increased at earlier stage, prior to infection, which contributes to the susceptibility of the host.

Furthermore, in our study we observed upregulated levels of the chemokine RANTES. This upregulation may contribute to disease progression and damage of the epithelial barrier. The primary function of chemokines is to orchestrate the recruitment of immune cells, such as neutrophils, to the site of infection (Charo & Ransohoff 2006). While the controlled recruitment of these cells is desirable for the clearance of pathogens, excessive presence of neutrophils may be detrimental for the host and result in colitis (Fournier & Parkos 2012). Large numbers of neutrophils are responsible for initiating a cascade of proinflammatory signalling that results in further recruitment of immune cells. The excessive proinflammatory signalling also results in damage to the epithelial structure (Hu *et al.* 2013). Despite the fact that antibiotic treatment does not induce colitis, the epithelial barrier may be compromised at the molecular level due to low expression of IL-22. This compromised epithelial barrier may be desirable for *C. difficile*, as this allows for delivery of the toxin directly to intestinal epithelial cells and subepithelial layer, resulting in further propagation of infection.

Another interesting observation in the susceptibility model was the upregulation of N-Acetylglucosamine in the core structures of the mucus. The increase of N-

Acetylglucosamine in intestinal mucins has been shown to have protective function in chemically-induced colitis in mice. In this model of chemically-induced colitis, the epithelial structure was not compromised and this was attributed to N-Acetylglucosamine preventing the excessive recruitment of immune cells to the site of inflammation (Tobisawa *et al.* 2010). Therefore, the abundance of N-Acetylglucosamine that we observed in susceptibility state may be a desired mechanism, as dampened infiltration of immune cells such as neutrophils may prevent excessive inflammation. However, the abundance of this glycan may in fact provide *C. difficile* with an additional advantage during invasion, as N-Acetylglucosamine is the main receptor for the *C. difficile* toxins (Castagliuolo *et al.* 1998). Due to its core position within the glycan chains, the toxins may adhere closely to the epithelium thus damaging the epithelium more effectively.

Finally, we examined the expression of IL-22, an essential cytokine for regulation of immunity, inflammation and the tissue homeostasis in the GI tract (Sonnenberg *et al.* 2011). IL-22 is expressed by immune cells such as neutrophils (Sadighi Akha *et al.* 2013) and Th17 cells (Min & Rhee 2015) but also epithelial cells (Pham *et al.* 2014) in response to trauma and epithelial damage. This cytokine is unusual among other interleukins, as it does not directly act on immune cells but rather it aids the recovery of the epithelial layer (Sabat *et al.* 2014). Its main role is to induce anti-apoptotic and proliferation pathways to restore the epithelial layer (Mühl 2013). Furthermore, it also induces the expression of antimicrobial peptides such as REGIIIγ (Zheng *et al.* 2008), fucosylation genes such as FUT2 (Pham *et al.* 2014; Pickard *et al.* 2014) and mucins such as MUC1, MUC3, MUC10 and MUC13 (Sonnenberg *et al.* 2010; Zenewicz *et al.* 2007; Radaeva *et al.* 2004). This wide spectrum of genes induced by IL-22 highlights its importance in restoring the epithelial barrier integrity (Hasegawa

et al. 2014). In our susceptibility study, we did not anticipate an increase in IL-22, as the antibiotic treatment did not breach the epithelial barrier and no infectious agent was introduced. Notably we observed downregulated IL-22 expression in susceptibility state, which was in agreement with the findings of Behnsen *et al.* (Behnsen *et al.* 2014). According to this study, the downregulation of IL-22 prevented antimicrobial peptide expression, which is thought to aid in commensal recovery. This correlates well with our observations, as concurrent with downregulation of IL-22 expression, we observed downregulation of REGIIIγ. However, this may be another protective mechanism utilised by *C. difficile* to its advantage to colonise the gut.

The susceptibility model allowed us to identify several factors that may predispose an individual to infection with *C. difficile*. Next, we wanted to examine these factors during the course of infection with *C. difficile* RT 001. Our study has highlighted the change of glycosylation during the *C. difficile* RT 001 infection. On day 3 post-infection with RT 001, there was a significant increase in sialic acid metabolism, as demonstrated by the increase of sialic acid on the surface of the epithelium and also by the increased expression of sialic acid synthase, NANS. This increase correlated with the peak of infection and pathogen load on day 3 (Lynch 2014, unpublished). By the end of the study, when the pathogen was cleared, both sialic acid and NANS were downregulated, relative to the control groups. While this correlates with the previous studies highlighting the importance of sialic acid in maintain CDI (Ng *et al.* 2013), it also possesses the question whether the pathogen actively modulate the sialic acid metabolism to suit its virulence during the infection and benefit from abundance of this nutrient.

Given that IL-22 plays an essential role in restoring the mucosal barrier, especially following pathogen invasion (Hasegawa *et al.* 2014), we also examined the expression of IL-22 during infection with *C. difficile* RT 001. IL-22 induces proliferation and anti-apoptotic pathways, antimicrobial peptides, mucin secretion and fucosylation (Sonnenberg *et al.* 2011), therefore its activity during recovery from pathogen-induced colitis is highly desirable. In our infection model, we observed downregulation of IL-22 expression during the initial stage of infection with *C. difficile* RT 001, which corresponds with the extensive epithelial damage observed during this stage of infection (Lynch 2014, unpublished). However, when the infection is resolved, and the recovery and restoration of the epithelial structure takes place, secretion of IL-22 returns to control levels. We propose that IL-22 may play an important role in recovery following infection with *C. difficile*. The role of IL-22 in the course of *C. difficile* infection has only recently been investigated. IL-22-deficient mice display increased mortality rates during *C. difficile* infection due to damage to the epithelium caused by excessive neutrophil recruitment (Jafari *et al.* 2013). This suggests that IL-22 may have anti-inflammatory properties in this context. Also, induction of the antimicrobial peptide REGIIIγ by IL-22 has been shown to be beneficial in clearance of *C. difficile* (A. A. Sadighi Akha *et al.* 2015). In depth investigation of the role of IL-22 in clearance of the pathogen and recovery of the intestinal epithelium is warranted. This is particularly important in the context of the *C. difficile* ribotypes that result in prolonged infection and excessive damage to the epithelium, as this suggests that the action of IL-22 may be impaired in this case. Better understanding of the role of IL-22 in *C. difficile* clearance may allow for design and development of both novel therapeutic targets and treatments.

Overall, in this study we have demonstrated how the susceptibility state induces changes in glycosylation patterns, immune responses, and the epithelial barrier integrity that may render the host vulnerable to invasion by *C. difficile*. Furthermore, we demonstrated that although the glycosylation may not contribute to susceptibility, however it plays pivotal role in maintaining the infection. Also, we have demonstrated that induction of IL-22 may be important for the clearance of the pathogen. These findings provide further insight into the mechanisms involved in CDI infection and may also contribute to future therapies designed for its treatment.

The main problem that CDI patients face currently is the lack of new therapies, high antibiotic resistance rates and high reoccurrence rate among patients. The main group at risk to develop CDI are elderly and immunocompromised patients admitted to hospitals (Rodriguez *et al.* 2014). Antibiotics that are effective against *C. difficile* have been discovered recently, however they have not been introduced into clinical application as of yet. These include thuricin CD (Rea *et al.* 2010) and teixobactin (Ling *et al.* 2015), both with a narrow specificity against *C. difficile.* While Ling *et al.* claims that there was no detectable resistance at the time of the study, it is a common knowledge that hospital-associated pathogens, including *C. difficile* RT 027, are exceptionally progressive in obtaining resistance against drugs (Cotter *et al.* 2013; Tenover *et al.* 2012). Therefore, there is an urgent need to design new, alternative approaches to treat CDI.

Faecal Microbiota Transplant (FMT) has proven to be the most effective therapy against CDI in recent years (Di Bella *et al.* 2015). This therapy is known to restore not only commensal microbiota but also the associated commensal-derived metabolites such as bile salts (Weingarden *et al.* 2014), short-chain fatty acids (SCFA) (Wlodarska *et al.* 2015) and the faecal microRNAs (Liu *et al.* 2015). The

recommended donor is usually a domestic partner; however the recent use of antibiotics or immunosuppressants, travel or disease may exclude this person as a suitable donor. Furthermore, there is a high risk of transmitting disease agents that are not currently screened for under laboratory conditions (Rohlke & Stollman 2012). Also, Weil & Hohmann highlighted the differences in composition in microbiota between lean and obese people and its possible effect on the recipient's health (Weil & Hohmann 2015). Ridaura *et al.* reported that mice harbouring microbiota from obese people gathered more adipose tissue, while the mice with microbiota from lean population maintained a healthy weight (Ridaura *et al.* 2013). These findings suggest that, while FMT proved to be effective in restoring the balance in the colon post-infection with *C. difficile*, we do not know the full effect that transferring microbiota from one person to another may have on the patients.

In a recent report Seekatz *et al.* suggested that the success of the FMT therapy is due to the restoration of a specific community structure, and not the whole microbiome of the donor (Seekatz *et al.* 2015). Similarly, Buffie *et al.* were able to identify a single strain of commensal bacteria, *Clostridium scindens* that has the ablity to restore the colonisation resistance against *C. difficile* in mice (Buffie *et al.* 2014). This bacterium restored the secondary bile acid balance, known to have an inhibitory effect on *C. difficile* vegetative cells. These authors proposed that the precise microbiome reconstitution may be an interesting alternative to FMT. The main advantage of this approach is that only defined and beneficial organisms are introduced to the recipient rather than an unknown mix of faecal matter. In other study, it has been demonstrated that co-administration of the antibiotics along with *Saccharomyces boulardii* yeast significantly reduced the occurrence of CDI disease among hospital patients (McFarland *et al.* 1994).

All of these studies point to a new direction that CDI treatment may take in the future. While there is still an urgent need for antibiotics to deal with outbreaks of the disease, future therapies may involve the use of CDI-tailored probiotics and prebiotics as a preventative measure against this disease. As mentioned previously, some beneficial organisms, such as *C. scindens*, have already been identified as efficient in outcompeting *C. difficile* (Buffie & Pamer 2013). Furthermore, the probiotic bacteria can also stimulate the mucosal barrier by inducing the secretion of mucus from intestinal epithelial cells (Mack *et al.* 2003).

In our study, but also in previous projects (Ng *et al.* 2013; Ferreyra *et al.* 2014), the importance of sialic acid as a nutrient source for *C. difficile* has been highlighted. We therefore suggest that commensals that utilise sialic acid as a nutrient source could represent a candidate probiotic bacteria. When introduced to the host, these probiotic bacteria would directly compete with *C. difficile* for nutrients and energy, which could contribute to resolving the infection.

Furthermore, recent advances in our understanding of the immune response in susceptibility state should be utilised to stimulate the immune system in immunocompromised patients. Our results now indicate that this may include the stimulation of IL-22 or counteracting the immunosuppressive actions of overexpressed IL-10 and TGFβ. Various therapies that involve modulation of these cytokines to treat inflammatory conditions have been reported in the literature (Sabat *et al.* 2014; Llorente *et al.* 2000; Marafini *et al.* 2013; Guo *et al.* 2014). Also, supplementing the diet with prebiotics that stimulate the expansion of commensals that may modulate these immune responses could be a viable therapeutic approach. Specifically, our study suggests an important role for fucose in supporting commensal microbiota and restoring colonisation resistance. This suggests a

possibility of formulating a prebiotic treatment that could be administrated to immunocompromised patients at risk of developing CDI. This supplementation with sugars such as fucose would promote an environment that supports commensals and prevent *C. difficile* from thriving. Ultimately, patients at risk of developing CDI may receive a preventative treatment upon admission to the hospital. It may be a tailored mix of ingredients that stimulates both the immune system and commensals, known as prebiotics, and a mix of probiotic bacteria that would challenge *C. difficile* at several metabolic and lifestyle levels.

Targeting the risk of CDI at an early stage of susceptibility may prove a more feasible method to eradicate this pathogen, rather than treating the fully manifested infection. The data presented in this thesis may aid the development of a novel therapeutic plan and provide alternatives to use of antibiotics.

CHAPTER 7 BIBLIOGRAPHY

Aas, J., Gessert, C.E. & Bakken, J.S., 2003. Recurrent Clostridium difficile colitis: case series involving 18 patients treated with donor stool administered via a nasogastric tube. *Clinical infectious diseases : an official publication of the Infectious Diseases Society of America*, 36(5), pp.580–5. Available at: http://cid.oxfordjournals.org/content/36/5/580 [Accessed June 3, 2015].

Abreu, M.T., 2010. Toll-like receptor signalling in the intestinal epithelium: how bacterial recognition shapes intestinal function. *Nature reviews. Immunology*, 10(2), pp.131–144. Available at: http://dx.doi.org/10.1038/nri2707.

Abt, M.C. et al., 2015. Innate Immune Defenses Mediated by Two ILC Subsets Are Critical for Protection against Acute Clostridium difficile Infection. *Cell Host & Microbe*, 18(1), pp.27–37. Available at: http://linkinghub.elsevier.com/retrieve/pii/S1931312815002590.

Akerlund, T. et al., 2008. Increased sporulation rate of epidemic Clostridium difficile Type 027/NAP1. *Journal of clinical microbiology*, 46(4), pp.1530–3. Available at: http://www.pubmedcentral.nih.gov/articlerender.fcgi?artid=2292905&tool=pmcentrez&rendertype=abstract [Accessed January 29, 2014].

Akha, A.S. et al., 2012. The local immune response in a mouse model of acute Clostridium difficile infection. In *The Journal of immunology*. p. 188. Available at: http://www.jimmunol.org/cgi/content/meeting_abstract/188/1_MeetingAbstracts/67.8 [Accessed March 19, 2014].

Alemka, A. et al., 2013. N-glycosylation of Campylobacter jejuni surface proteins promotes bacterial fitness. *Infection and immunity*, 81(5), pp.1674–82. Available at: http://www.pubmedcentral.nih.gov/articlerender.fcgi?artid=3648013&tool=pmcentrez&rendertype=abstract [Accessed December 6, 2014].

Alexopoulou, L. et al., 2001. Recognition of double-stranded RNA and activation of NF-kappaB by Toll-like receptor 3. *Nature*, 413(6857), pp.732–8. Available at: http://www.ncbi.nlm.nih.gov/pubmed/11607032 [Accessed December 30, 2014].

Altschul, S.F. et al., 1990. Basic local alignment search tool. *Journal of molecular biology*, 215(3), pp.403–10. Available at: http://www.ncbi.nlm.nih.gov/pubmed/2231712 [Accessed July 10, 2014].

Antonopoulos, D. a et al., 2009. Reproducible community dynamics of the gastrointestinal microbiota following antibiotic perturbation. *Infection and immunity*, 77(6), pp.2367–75. Available at: http://www.pubmedcentral.nih.gov/articlerender.fcgi?artid=2687343&tool=pmcentrez&rendertype=abstract [Accessed November 6, 2013].

Archbald-Pannone, L.R. et al., 2014. Clostridium difficile ribotype 027 is most prevalent among inpatients admitted from long-term care facilities. *Journal of Hospital Infection*. Available at: http://www.sciencedirect.com/science/article/pii/S0195670114002230 [Accessed July 31, 2014].

Aubry, A. et al., 2012. Modulation of toxin production by the flagellar regulon in Clostridium difficile. *Infection and immunity*, 80(10), pp.3521–32. Available at: http://iai.asm.org/content/80/10/3521 [Accessed June 4, 2015].

Ausiello, C.M. et al., 2006. Surface layer proteins from Clostridium difficile induce inflammatory and regulatory cytokines in human monocytes and dendritic cells. *Microbes and infection / Institut Pasteur*, 8(11), pp.2640–6. Available at: http://www.sciencedirect.com/science/article/pii/S128645790600270X [Accessed February 14, 2014].

Baban, S.T. et al., 2013. The role of flagella in Clostridium difficile pathogenesis: comparison between a non-epidemic and an epidemic strain. *PloS one*, 8(9), p.e73026. Available at: http://www.pubmedcentral.nih.gov/articlerender.fcgi?artid=3781105&tool=pmcentrez&rendertype=abstract [Accessed June 4, 2015].

Bachmanov, A.A. et al., 2002. Food intake, water intake, and drinking spout side preference of 28 mouse strains. *Behavior genetics*, 32(6), pp.435–43. Available at: http://www.pubmedcentral.nih.gov/articlerender.fcgi?artid=1397713&tool=pmcentrez&rendertype=abstract [Accessed April 29, 2014].

Bansil, R. & Turner, B.S., 2006. Mucin structure, aggregation, physiological functions and biomedical applications. *Current Opinion in Colloid & Interface Science*, 11(2-3), pp.164–170. Available at: http://linkinghub.elsevier.com/retrieve/pii/S1359029405001184 [Accessed March 21, 2014].

Barbut, F. et al., 2007. Prospective study of Clostridium difficile infections in Europe with phenotypic and genotypic characterisation of the isolates. *Clinical microbiology and infection: the official publication of the European Society of Clinical Microbiology and Infectious Diseases*, 13(11), pp.1048–57. Available at: http://www.ncbi.nlm.nih.gov/pubmed/17850341 [Accessed May 11, 2015].

Barketi-Klai, A. et al., 2011. Role of fibronectin-binding protein A in Clostridium difficile intestinal colonization. *Journal of Medical Microbiology*, 60(8), pp.1155–1161. Available at: http://jmm.sgmjournals.org/cgi/doi/10.1099/jmm.0.029553-0 [Accessed February 7, 2014].

Bartlett, J.G. et al., 1978. Antibiotic-Associated Pseudomembranous Colitis Due to Toxin-Producing Clostridia. *New England Journal of Medicine*, pp.531–534. Available at: http://www.nejm.org/doi/full/10.1056/NEJM197803092981003 [Accessed March 5, 2014].

Bassis, C.M., Theriot, C.M. & Young, V.B., 2014. Alteration of the Murine Gastrointestinal Microbiota by Tigecycline Leads to Increased Susceptibility to Clostridium difficile Infection. *Antimicrobial agents and chemotherapy*, 58(March), pp.2767–2774. Available at: http://www.ncbi.nlm.nih.gov/pubmed/24590475 [Accessed March 19, 2014].

Bauman, R.W., 2012. *Microbiology with Diseases by Body System* 3rd ed., Benjamin Cummings.

Behnsen, J. et al., 2014. The cytokine IL-22 promotes pathogen colonization by suppressing related commensal bacteria. *Immunity*, 40(2), pp.262–73. Available at: http://www.pubmedcentral.nih.gov/articlerender.fcgi?artid=3964146&tool=pmcentrez&rendertype=abstract [Accessed July 27, 2015].

Behroozian, A. a et al., 2013. Detection of mixed populations of Clostridium difficile from symptomatic patients using capillary-based polymerase chain reaction ribotyping. *Infection control and hospital epidemiology: the official journal of the Society of Hospital Epidemiologists of America*, 34(9), pp.961–6. Available at: http://www.pubmedcentral.nih.gov/articlerender.fcgi?artid=4016961&tool=pmcentrez&rendertype=abstract.

Di Bella, S., Gouliouris, T. & Petrosillo, N., 2015. Fecal Microbiota Transplantation (FMT) for Clostridium difficile infection: focus on immunocompromised patients. *Journal of Infection and Chemotherapy*. Available at: http://www.sciencedirect.com/science/article/pii/S1341321X15000306 [Accessed February 1, 2015].

Benz, I. & Schmidt, M.A., 2001. Glycosylation with heptose residues mediated by the aah gene product is essential for adherence of the AIDA-I adhesin. *Molecular microbiology*, 40(6), pp.1403–13. Available at: http://www.ncbi.nlm.nih.gov/pubmed/11442838 [Accessed August 11, 2015].

Berg, J.M., Tymoczko, J.L. & Stryer, L., 2002. *Biochemistry* 5th ed., New York, USA: W. H. Freeman.

Bergstrom, K.S.B. et al., 2010. Muc2 protects against lethal infectious colitis by disassociating pathogenic and commensal bacteria from the colonic mucosa. *PLoS pathogens*, 6(5), p.e1000902. Available at: http://www.pubmedcentral.nih.gov/articlerender.fcgi?artid=2869315&tool=pmcentrez&rendertype=abstract [Accessed September 17, 2014].

Bertolo, L. et al., 2012. Clostridium difficile carbohydrates: glucan in spores, PSII common antigen in cells, immunogenicity of PSII in swine and synthesis of a dual *C. difficile*-ETEC conjugate vaccine. *Carbohydrate research*, 354, pp.79–86. Available at: http://www.ncbi.nlm.nih.gov/pubmed/22533919 [Accessed January 16, 2014].

Bianco, M. et al., 2011. Immunomodulatory activities of surface-layer proteins obtained from epidemic and hypervirulent Clostridium difficile strains. *Journal of medical microbiology*, 60(Pt 8), pp.1162–7. Available at: http://www.ncbi.nlm.nih.gov/pubmed/21349985 [Accessed February 14, 2014].

Blair, J.M. a. et al., 2014. Molecular mechanisms of antibiotic resistance. *Nature Reviews Microbiology*, 13(1), pp.42–51. Available at: http://www.nature.com/doifinder/10.1038/nrmicro3380 [Accessed December 1, 2014].

Borriello, S.P. et al., 1990. Virulence factors of Clostridium difficile. *Reviews of infectious diseases*, 12 Suppl 2, pp.S185–91. Available at: http://www.ncbi.nlm.nih.gov/pubmed/2406871.

Van De Bovenkamp, J.H.B. et al., 2003. The MUC5AC Glycoprotein is the Primary Receptor for Helicobacter pylori in the Human Stomach. *Helicobacter*, 8(5).

Bradshaw, W.J. et al., 2014. The structure of the cysteine protease and lectin-like domains of Cwp84, a surface layer-associated protein from Clostridium difficile. *Acta crystallographica. Section D, Biological crystallography*, 70(Pt 7), pp.1983–93. Available at: http://www.pubmedcentral.nih.gov/articlerender.fcgi?artid=4089489&tool=pmcentrez&rendertype=abstract [Accessed August 21, 2014].

Brandl, K. et al., 2008. Vancomycin-resistant enterococci exploit antibiotic-induced innate immune deficits. *Nature*, 455(7214), pp.804–807. Available at: http://www.pubmedcentral.nih.gov/articlerender.fcgi?artid=2663337&tool=pmcentrez&rendertype=abstract [Accessed May 27, 2015].

Branka, J.E. et al., 1997. Early Functional Effects of Clostridium difficile Toxin A in Human Colonocytes. *Gastroenetrology*, (112), pp.1887–1894.

Brazier, J.S., 2001. Typing of Clostridium difficile. *Clinical microbiology and infection : the official publication of the European Society of Clinical Microbiology and Infectious Diseases*, 7(8), pp.428–31. Available at: http://www.ncbi.nlm.nih.gov/pubmed/11591206.

Britton, R. a & Young, V.B., 2012. Interaction between the intestinal microbiota and host in Clostridium difficile colonization resistance. *Trends in microbiology*, 20(7), pp.313–9. Available at: http://www.ncbi.nlm.nih.gov/pubmed/22595318 [Accessed June 7, 2013].

Britton, R. a & Young, V.B., 2014. Role of the Intestinal Microbiota in Resistance to Colonization by Clostridium difficile. *Gastroenterology*. Available at: http://www.ncbi.nlm.nih.gov/pubmed/24503131 [Accessed February 10, 2014].

Brooks, S.A. & Hall, D.M.S., 2012. Lectin histochemistry to detect altered glycolsyaltion in cell and tissues. In M. Dwek, S. A. Brooks, & U. Schumacher, eds. *Metastasis Research Protocols*. Methods in Molecular Biology. Totowa, NJ: Humana Press, pp. 31–50. Available at: http://link.springer.com/10.1007/978-1-61779-854-2 [Accessed July 14, 2014].

Brown, E.M., Sadarangani, M. & Finlay, B.B., 2013. The role of the immune system in governing host-microbe interactions in the intestine. *Nature immunology*, 14(7), pp.660–7. Available at: http://www.nature.com/ni/journal/v14/n7/full/ni.2611.html?elq=0f003c156d4a4efdafb874f6853c78b9 [Accessed January 21, 2014].

Brun, P. et al., 2008. Clostridium difficile TxAC314 and SLP-36kDa enhance the immune response toward a co-administered antigen. *Journal of medical microbiology*, 57(Pt 6), pp.725–31. Available at: http://www.ncbi.nlm.nih.gov/pubmed/18480329 [Accessed March 9, 2014].

Buffie, C.G. et al., 2014. Precision microbiome reconstitution restores bile acid mediated resistance to Clostridium difficile. *Nature*, 517(7533), pp.205–208. Available at: http://www.nature.com/doifinder/10.1038/nature13828 [Accessed October 22, 2014].

Buffie, C.G. & Pamer, E.G., 2013. Microbiota-mediated colonization resistance against intestinal pathogens. *Nature reviews. Immunology*, 13(11), pp.790–801. Available at: http://www.ncbi.nlm.nih.gov/pubmed/24096337 [Accessed November 9, 2013].

Burns, D.A. & Minton, N.P., 2011. Sporulation studies in Clostridium difficile. *Journal of microbiological methods*, 87(2), pp.133–8. Available at: http://www.ncbi.nlm.nih.gov/pubmed/21864584 [Accessed February 14, 2014].

Calabi, E. et al., 2002. Binding of Clostridium difficile Surface Layer Proteins to Gastrointestinal Tissues. *Infection and immunity*, 70(10), pp.5770–8. Available at: http://www.pubmedcentral.nih.gov/articlerender.fcgi?artid=128314&tool=pmcentrez&rendertype=abstract [Accessed February 14, 2014].

Calabi, E. et al., 2001. Molecular characterization of the surface layer proteins from Clostridium difficile. *Molecular Microbiology*, 40(5), pp.1187–1199. Available at: http://doi.wiley.com/10.1046/j.1365-2958.2001.02461.x [Accessed February 14, 2014].

Calabi, E. & Fairweather, N., 2002. Patterns of sequence conservation in the S-Layer proteins and related sequences in Clostridium difficile. *Journal of bacteriology*, 184(14), pp.3886–97. Available at: http://www.pubmedcentral.nih.gov/articlerender.fcgi?artid=135169&tool=pmcentrez&rendertype=abstract [Accessed February 12, 2014].

Campbell, B.J., Yu, L.G. & Rhodes, J.M., 2001. Altered glycosylation in inflammatory bowel disease: a possible role in cancer development. *Glycoconjugate journal*, 18(11-12), pp.851–8. Available at: http://www.ncbi.nlm.nih.gov/pubmed/12820718 [Accessed June 5, 2015].

Cao, J. et al., 2013. Studying extracellular signaling utilizing a glycoproteomic approach: lectin blot surveys, a first and important step. *Methods in molecular biology (Clifton, N.J.)*, 1013, pp.227–33. Available at: http://www.pubmedcentral.nih.gov/articlerender.fcgi?artid=3985769&tool=pmcentrez&rendertype=abstract [Accessed May 13, 2015].

Carlson, P.E. et al., 2015. Anaerobe Variation in germination of Clostridium dif fi cile clinical isolates correlates to disease severity. *Anaerobe*, (February), pp.1–7. Available at: http://dx.doi.org/10.1016/j.anaerobe.2015.02.003.

Carlson, P.E. et al., 2013. The relationship between phenotype, ribotype, and clinical disease in human Clostridium difficile isolates. *Anaerobe*, 24, pp.109–16. Available at: http://www.ncbi.nlm.nih.gov/pubmed/23608205 [Accessed February 16, 2014].

Carlson, P.E. et al., 2015. Variation in germination of Clostridium difficile clinical isolates correlates to disease severity. *Anaerobe*, 33, pp.64–70. Available at: http://linkinghub.elsevier.com/retrieve/pii/S1075996415000244.

Castagliuolo, I. et al., 1998. Oligosaccharides containing sialic acid and N-acetylglucosamine mediate Clostridium difficile toxin B (TxB) binding and biologic effects in human colonic mucosa. *Gastroenterology*, 114, p.A949. Available at: http://www.gastrojournal.org/article/S001650859883864X/fulltext [Accessed January 16, 2015].

Cerovic, V. et al., 2014. Intestinal macrophages and dendritic cells: what's the difference? *Trends in Immunology*. Available at: http://www.sciencedirect.com/science/article/pii/S147149061400060X [Accessed May 5, 2014].

Cerquetti, M., 2002. Binding of Clostridium difficile to Caco-2 epithelial cell line and to extracellular matrix proteins. *FEMS Immunology and Medical Microbiology*, 32, pp.211–218.

Cerquetti, M. et al., 2000. Characterization of surface layer proteins from different Clostridium difficile clinical isolates. *Microbial pathogenesis*, 28(6), pp.363–72. Available at: http://www.ncbi.nlm.nih.gov/pubmed/10839973 [Accessed January 19, 2014].

Cerquetti, M. et al., 1992. Purification and characterization of an immunodominant 36 kDa antigen present on the cell surface of Clostridium difficile. *Microbial pathogenesis*, 13(4), pp.271–9. Available at: http://www.ncbi.nlm.nih.gov/pubmed/1298866 [Accessed May 13, 2015].

Chai, C., Lee, K.-S. & Oh, S.-W., 2015. Synergistic inhibition of Clostridium difficile with nisin-lysozyme combination treatment. *Anaerobe*, 34, pp.24–26. Available at: http://linkinghub.elsevier.com/retrieve/pii/S1075996415300044.

Champasa, K. et al., 2013. Targeted identification of glycosylated proteins in the gastric pathogen Helicobacter pylori (Hp). *Molecular & cellular proteomics : MCP*, 12(9), pp.2568–86. Available at: http://www.pubmedcentral.nih.gov/articlerender.fcgi?artid=3769331&tool=pmcentrez&rendertype=abstract [Accessed July 27, 2015].

Chapetón Montes, D., Collignon, A. & Janoir, C., 2013. Influence of environmental conditions on the expression and the maturation process of the Clostridium difficile surface associated protease Cwp84. *Anaerobe*, 19, pp.79–82. Available at: http://www.ncbi.nlm.nih.gov/pubmed/23257307 [Accessed February 15, 2014].

Charo, I.F. & Ransohoff, R.M., 2006. The many roles of chemokines and chemokine receptors in inflammation. *The New England journal of medicine*, 354(6), pp.610–21. Available at: http://www.ncbi.nlm.nih.gov/pubmed/16467548 [Accessed May 14, 2015].

Cheknis, A.K. et al., 2009. Distribution of Clostridium difficile strains from a North American, European and Australian trial of treatment for *C. difficile* infections: 2005-2007. *Anaerobe*, 15(6), pp.230–3. Available at: http://www.ncbi.nlm.nih.gov/pubmed/19737618 [Accessed May 11, 2015].

Chen, X. et al., 2008. A mouse model of Clostridium difficile-associated disease. *Gastroenterology*, 135(6), pp.1984–92. Available at: http://www.sciencedirect.com/science/article/pii/S0016508508016648 [Accessed January 27, 2014].

Chow, W.L. & Lee, Y.K., 2008. Free fucose is a danger signal to human intestinal epithelial cells. *The British Journal of Nutrition*, 99(3), pp.449–54. Available at: http://www.ncbi.nlm.nih.gov/pubmed/17697405 [Accessed November 4, 2014].

Chu, H.W. et al., 2005. TLR2 signaling is critical for Mycoplasma pneumoniae-induced airway mucin expression. *Journal of immunology (Baltimore, Md.: 1950)*, 174(9), pp.5713–9. Available at: http://www.ncbi.nlm.nih.gov/pubmed/15843573 [Accessed July 22, 2015].

Clabots, C. et al., 1988. Clostridium difficile plasmid isolation as an epidemiologic tool. *European journal of clinical microbiology & infectious diseases : official publication of the European Society of Clinical Microbiology*, 7(2), pp.312–5. Available at: http://www.ncbi.nlm.nih.gov/pubmed/3134239 [Accessed March 5, 2014].

Collins, L.E. et al., 2014. Surface layer proteins isolated from Clostridium difficile induce clearance responses in macrophages. *Microbes and infection / Institut Pasteur*, pp.1–10. Available at: http://www.ncbi.nlm.nih.gov/pubmed/24560642 [Accessed April 4, 2014].

Cotter, P.D., Ross, R.P. & Hill, C., 2013. Bacteriocins - a viable alternative to antibiotics? *Nature reviews. Microbiology*, 11(2), pp.95–105. Available at: http://www.ncbi.nlm.nih.gov/pubmed/23268227.

Dapa, T. et al., 2013. Multiple factors modulate biofilm formation by the anaerobic pathogen Clostridium difficile. *Journal of bacteriology*, 195(3), pp.545–55. Available at: http://www.pubmedcentral.nih.gov/articlerender.fcgi?artid=3554014&tool=pmcentrez&rendertype=abstract [Accessed August 14, 2014].

Dave, M. et al., 2012. The human gut microbiome: current knowledge, challenges, and future directions. *Translational research : the journal of laboratory and clinical medicine*, 160(4), pp.246–57. Available at: http://www.ncbi.nlm.nih.gov/pubmed/22683238 [Accessed July 17, 2014].

Dawson, L.F., Valiente, E. & Wren, B.W., 2009. Clostridium difficile--a continually evolving and problematic pathogen. *Infection, genetics and evolution : journal of molecular epidemiology and evolutionary genetics in infectious diseases*, 9(6), pp.1410–7. Available at: http://www.ncbi.nlm.nih.gov/pubmed/19539054 [Accessed February 9, 2014].

Debabov, V.G., 2004. Bacterial and Archaeal S-Layers as a Subject of Nanobiotechnology. *Molecular Biology*, 38(4), pp.482–493. Available at: http://link.springer.com/10.1023/B:MBIL.0000036999.77762.6a.

Denève, C. et al., 2008. Antibiotics involved in Clostridium difficile-associated disease increase colonization factor gene expression. *Journal of medical microbiology*, 57(Pt 6), pp.732–8. Available at: http://www.ncbi.nlm.nih.gov/pubmed/18480330 [Accessed February 15, 2014].

Denève, C. et al., 2009. New trends in Clostridium difficile virulence and pathogenesis. *International journal of antimicrobial agents*, 33 Suppl 1, pp.S24–8. Available at: http://www.ncbi.nlm.nih.gov/pubmed/19303565 [Accessed February 1, 2014].

DeSchoolmeester, M.L., Manku, H. & Else, K.J., 2006. The innate immune responses of colonic epithelial cells to Trichuris muris are similar in mouse strains that develop a type 1 or type 2 adaptive immune response. *Infection and immunity*, 74(11), pp.6280–6. Available at: http://www.pubmedcentral.nih.gov/articlerender.fcgi?artid=1695505&tool=pmcentrez&rendertype=abstract [Accessed March 24, 2014].

Dingle, K.E. et al., 2013. Recombinational switching of the Clostridium difficile S-layer and a novel glycosylation gene cluster revealed by large-scale whole-genome sequencing. *The Journal of infectious diseases*, 207(4), pp.675–86. Available at: http://www.ncbi.nlm.nih.gov/pubmed/23204167 [Accessed November 10, 2013].

Dramsi, S. & Cossart, P., 2002. Listeriolysin O: a genuine cytolysin optimized for an intracellular parasite. *The Journal of cell biology*, 156(6), pp.943–6. Available at: http://www.pubmedcentral.nih.gov/articlerender.fcgi?artid=2173465&tool=pmcentrez&rendertype=abstract [Accessed June 17, 2015].

Drudy, D. et al., 2004. Human antibody response to surface layer proteins in Clostridium difficile infection. *FEMS immunology and medical microbiology*, 41(3), pp.237–42. Available at: http://www.ncbi.nlm.nih.gov/pubmed/15196573 [Accessed February 11, 2014].

Eichler, J., 2013. Extreme sweetness: protein glycosylation in archaea. *Nature reviews. Microbiology*, 11(3), pp.151–6. Available at: http://www.ncbi.nlm.nih.gov/pubmed/23353769 [Accessed January 30, 2014].

Eidhin, D.N. et al., 2006. Sequence and phylogenetic analysis of the gene for surface layer protein, SlpA, from 14 PCR ribotypes of Clostridium difficile. *Journal of medical microbiology*, 55(Pt 1), pp.69–83. Available at: http://www.ncbi.nlm.nih.gov/pubmed/16388033 [Accessed February 11, 2014].

Emerson, J.E. et al., 2008. Microarray analysis of the transcriptional responses of Clostridium difficile to environmental and antibiotic stress. *Journal of medical microbiology*, 57, pp.757–64. Available at: http://www.ncbi.nlm.nih.gov/pubmed/18480334 [Accessed February 14, 2014].

Engevik, M. a et al., 2014. Human Clostridium difficile infection: Altered mucus production and composition. *American journal of physiology. Gastrointestinal and liver physiology*, p.ajpgi.00091.2014. Available at: http://www.ncbi.nlm.nih.gov/pubmed/25552581 [Accessed January 5, 2015].

Fabich, A.J. et al., 2008. Comparison of carbon nutrition for pathogenic and commensal Escherichia coli strains in the mouse intestine. *Infection and immunity*, 76(3), pp.1143–52. Available at: http://www.pubmedcentral.nih.gov/articlerender.fcgi?artid=2258830&tool=pmcentrez&rendertype=abstract [Accessed November 11, 2014].

Fagan, R.P. et al., 2011. A proposed nomenclature for cell wall proteins of Clostridium difficile. *Journal of medical microbiology*, 60(Pt 8), pp.1225–8. Available at: http://www.ncbi.nlm.nih.gov/pubmed/21252271 [Accessed February 14, 2014].

Fagan, R.P. et al., 2009. Structural insights into the molecular organization of the S-layer from Clostridium difficile. *Molecular microbiology*, 71(5), pp.1308–22. Available at: http://www.ncbi.nlm.nih.gov/pubmed/19183279 [Accessed February 11, 2014].

Fagan, R.P. & Fairweather, N.F., 2014. Biogenesis and functions of bacterial S-layers. *Nature reviews. Microbiology*, 12(3), pp.211–22. Available at: http://www.ncbi.nlm.nih.gov/pubmed/24509785 [Accessed September 24, 2014].

Ferreyra, J.A. et al., 2014. Gut Microbiota-Produced Succinate Promotes *C. difficile* Infection after Antibiotic Treatment or Motility Disturbance. *Cell Host & Microbe*, 16(6), pp.770–777. Available at: http://linkinghub.elsevier.com/retrieve/pii/S1931312814004193 [Accessed December 11, 2014].

Foglia, G. et al., 2012. Clostridium difficile: development of a novel candidate vaccine. *Vaccine*, 30(29), pp.4307–9. Available at: http://www.ncbi.nlm.nih.gov/pubmed/22682287 [Accessed February 14, 2014].

Fournier, B.M. & Parkos, C.A., 2012. The role of neutrophils during intestinal inflammation. *Mucosal Immunology*, 5(4), pp.354–366. Available at: http://dx.doi.org/10.1038/mi.2012.24 [Accessed June 25, 2015].

Freitas, M. et al., 2002. Microbial-host interactions specifically control the glycosylation pattern in intestinal mouse mucosa. *Histochemistry and cell biology*, 118(2), pp.149–61. Available at: http://www.ncbi.nlm.nih.gov/pubmed/12189518 [Accessed January 24, 2014].

Freitas, M. & Chantal, C., 2000. Microbial Modulation of Host Intestinal Glycosylation Patterns. *Microbial Ecology in Health and Disease*, 12(2), pp.165–178. Available at: http://informahealthcare.com/doi/abs/10.1080/089106000750060422.

Frosali, S. et al., 2015. How the Intricate Interaction among Toll-Like Receptors, Microbiota, and Intestinal Immunity Can Influence Gastrointestinal Pathology. *Journal of Immunology Research*, 2015, pp.1–12. Available at: http://www.hindawi.com/journals/jir/2015/489821/.

Garrett, W.S., Gordon, J.I. & Glimcher, L.H., 2010. Homeostasis and inflammation in the intestine. *Cell*, 140(6), pp.859–70. Available at: http://www.pubmedcentral.nih.gov/articlerender.fcgi?artid=2845719&tool=pmcentrez&rendertype=abstract [Accessed January 22, 2014].

Genth, H. et al., 2008. Clostridium difficile toxins: more than mere inhibitors of Rho proteins. *The international journal of biochemistry & cell biology*, 40(4), pp.592–7. Available at: http://www.ncbi.nlm.nih.gov/pubmed/18289919 [Accessed February 15, 2014].

George, R.H. et al., 1978. Identification of Clostridium difficile as a cause of pseudomembranous colitis. *British medical journal*, 1(6114), p.695. Available at: http://www.pubmedcentral.nih.gov/articlerender.fcgi?artid=1603073&tool=pmcentrez&rendertype=abstract.

Ghantoji, S.S. et al., 2010. Economic healthcare costs of Clostridium difficile infection: a systematic review. *The Journal of hospital infection*, 74(4), pp.309–18. Available at: http://www.ncbi.nlm.nih.gov/pubmed/20153547 [Accessed January 23, 2015].

Guarner, F., 2015. The gut microbiome: What do we know? *Clinical Liver Disease*, 5(4), pp.86–90. Available at: http://doi.wiley.com/10.1002/cld.454.

Guichard, A. et al., 2013. Cholera toxin disrupts barrier function by inhibiting exocyst-mediated trafficking of host proteins to intestinal cell junctions. *Cell host & microbe*, 14(3), pp.294–305. Available at:

http://www.pubmedcentral.nih.gov/articlerender.fcgi?artid=3786442&tool=pmcentrez&rendertype=abstract [Accessed June 17, 2015].

Guo, L. et al., 1997. Regulation of lipid A modifications by Salmonella typhimurium virulence genes phoP-phoQ. *Science (New York, N.Y.)*, 276(5310), pp.250–3. Available at: http://www.ncbi.nlm.nih.gov/pubmed/9092473 [Accessed June 17, 2015].

Guo, X. et al., 2014. Induction of innate lymphoid cell-derived interleukin-22 by the transcription factor STAT3 mediates protection against intestinal infection. *Immunity*, 40(1), pp.25–39. Available at: http://dx.doi.org/10.1016/j.immuni.2013.10.021.

Gurler, V., 1993. Typing of Clostridium dificile strains by PCR-amplification of variable length 16s-23s rDNA spacer regions. *Journal of General Microbiology*, 139, pp.3089–3097.

Hall, I.C. & O'Toole, E., 1935. Intestinal flora in new-born infants with description of pathogenic anaerobe, Bacillus difficilis. *American Journal of Diseases of Children*, 49(2), p.390. Available at: http://archpedi.jamanetwork.com/article.aspx?articleid=1176814 [Accessed February 26, 2014].

Hansson, G.C., 2012. Role of mucus layers in gut infection and inflammation. *Current Opinion in Microbiology*, 15(1), pp.57–62.

Hao, J. et al., 2005. Cloning, expression, and characterization of sialic acid synthases. *Biochem Biophys Res Commun*, 338(3), pp.1507–14. Available at: http://www.ncbi.nlm.nih.gov/pubmed/16274664 [Accessed July 23, 2015].

Hasegawa, M. et al., 2014. Interleukin-22 Regulates the Complement System to Promote Resistance against Pathobionts after Pathogen-Induced Intestinal Damage. *Immunity*, 41(4), pp.620–632. Available at: http://linkinghub.elsevier.com/retrieve/pii/S1074761314003446 [Accessed October 16, 2014].

Hasegawa, M. et al., 2011. Nucleotide-binding oligomerization domain 1 mediates recognition of Clostridium difficile and induces neutrophil recruitment and protection against the pathogen. *Journal of immunology (Baltimore, Md.: 1950)*, 186(8), pp.4872–80. Available at: http://www.ncbi.nlm.nih.gov/pubmed/21411735 [Accessed February 14, 2014].

Hellickson, L.A. & Owens, K.L., 2007. Cross-Contamination of Clostridium difficile Spores on Bed Linen During Laundering. *American Journal of Infection Control*, 35(5), pp.E32–E33. Available at: http://www.ajicjournal.org/article/S0196655307002039/fulltext [Accessed June 3, 2015].

Hemmi, H. et al., 2000. A Toll-like receptor recognizes bacterial DNA. *Nature*, 408(6813), pp.740–5. Available at: http://www.ncbi.nlm.nih.gov/pubmed/11130078 [Accessed December 22, 2014].

Hennequin, C., Porcheray, F., et al., 2001. GroEL (Hsp60) of Clostridium difficile is involved in cell adherence. *Microbiology (Reading, England)*, 147(Pt 1), pp.87–96. Available at: http://www.ncbi.nlm.nih.gov/pubmed/11160803.

Hennequin, C. et al., 2003. Identification and characterization of a fibronectin-binding protein from Clostridium difficile. *Microbiology*, 149(10), pp.2779–2787. Available at: http://mic.sgmjournals.org/cgi/doi/10.1099/mic.0.26145-0 [Accessed February 15, 2014].

Hennequin, C., Collignon, A. & Karjalainen, T., 2001. Analysis of expression of GroEL (Hsp60) of Clostridium difficile in response to stress. *Microbial pathogenesis*, 31(5), pp.255–60. Available at: http://www.ncbi.nlm.nih.gov/pubmed/11710845 [Accessed June 4, 2015].

Hill, D.A. et al., 2010. Metagenomic analyses reveal antibiotic-induced temporal and spatial changes in intestinal microbiota with associated alterations in immune cell homeostasis. *Mucosal immunology*, 3(2), pp.148–158. Available at: http://www.nature.com/mi/journal/v3/n2/abs/mi2009132a.html.

Hill, S.F., 2014. Clostridium difficile infection targets. *Journal of Hospital Infection*, pp.11–15. Available at: http://linkinghub.elsevier.com/retrieve/pii/S0195670114003600 [Accessed December 12, 2014].

Hoebler, C. et al., 2006. MUC genes are differently expressed during onset and maintenance of inflammation in dextran sodium sulfate-treated mice. *Digestive diseases and sciences*, 51(2), pp.381–9. Available at: http://www.ncbi.nlm.nih.gov/pubmed/16534686 [Accessed September 30, 2014].

Hooper, L. V & Gordon, J.I., 2001. Glycans as legislators of host-microbial interactions: spanning the spectrum from symbiosis to pathogenicity. *Glycobiology*, 11(2), p.1R–10R. Available at: http://www.ncbi.nlm.nih.gov/pubmed/11287395.

Hooper, L. V & Macpherson, A.J., 2010. Immune adaptations that maintain homeostasis with the intestinal microbiota. *Nature reviews. Immunology*, 10(3), pp.159–69. Available at: http://www.ncbi.nlm.nih.gov/pubmed/20182457 [Accessed January 24, 2014].

Hooper, L. V & Xu, J., 1999. A molecular sensor that allows a gut commensal to control its nutrient foundation in a competitive ecosystem. *Proceedings of the National Academy of Sciences of the United States of America*, 96(August), pp.9833–9838. Available at: http://www.pnas.org/content/96/17/9833.short [Accessed November 4, 2014].

Hornef, M.W. et al., 2002. Bacterial strategies for overcoming host innate and adaptive immune responses. *Nature Immunology*, 3(11), pp.1033–1040.

Hu, B. et al., 2013. Microbiota-induced activation of epithelial IL-6 signaling links inflammasome-driven inflammation with transmissible cancer. *Proceedings of the National Academy of Sciences of the United States of America*, 110(24), pp.9862–7. Available at: http://www.pubmedcentral.nih.gov/articlerender.fcgi?artid=3683709&tool=pmcentrez&rendertype=abstract [Accessed July 25, 2014].

Huang, H. et al., 2009. Antimicrobial resistance in Clostridium difficile. *International journal of antimicrobial agents*, 34(6), pp.516–22. Available at: http://www.ncbi.nlm.nih.gov/pubmed/19828299 [Accessed February 14, 2014].

Huang, J. et al., 2009. Overexpression of MUC15 activates extracellular signal-regulated kinase 1/2 and promotes the oncogenic potential of human colon cancer cells. *Carcinogenesis*, 30(8), pp.1452–8. Available at: http://www.ncbi.nlm.nih.gov/pubmed/19520792 [Accessed September 26, 2014].

Hundsberger, T. et al., 1997. Transcription analysis of the genes tcdA-E of the pathogenicity locus of Clostridium difficile. *European journal of biochemistry / FEBS*, 244(3), pp.735–42. Available at: http://www.ncbi.nlm.nih.gov/pubmed/9108241 [Accessed November 18, 2014].

Imler, J.L. & Hoffmann, J.A., 2001. Toll receptors in innate immunity. *Trends in cell biology*, 11(7), pp.304–11. Available at: http://www.ncbi.nlm.nih.gov/pubmed/11413042 [Accessed July 29, 2014].

Ivanov, A.I., 2012. Structure and regulation of intestinal epithelial tight junctions: current concepts and unanswered questions. *Advances in experimental medicine and biology*, 763, pp.132–48. Available at: http://www.ncbi.nlm.nih.gov/pubmed/23397622 [Accessed June 9, 2015].

Ivanov, I.I. et al., 2009. Induction of intestinal Th17 cells by segmented filamentous bacteria. *Cell*, 139(3), pp.485–98. Available at: http://www.pubmedcentral.nih.gov/articlerender.fcgi?artid=2796826&tool=pmcentrez&rendertype=abstract [Accessed January 23, 2014].

Jafari, N. V et al., 2013. Clostridium difficile modulates host innate immunity via toxin-independent and dependent mechanism(s). *PloS one*, 8(7), p.e69846. Available at: http://www.pubmedcentral.nih.gov/articlerender.fcgi?artid=3726775&tool=pmcentrez&rendertype=abstract [Accessed May 11, 2015].

Jain, S. et al., 2011. Quantitative proteomic analysis of the heat stress response in Clostridium difficile strain 630. *Journal of proteome research*, 10(9), pp.3880–90. Available at: http://www.ncbi.nlm.nih.gov/pubmed/21786815 [Accessed June 4, 2015].

Jakobsson, H.E. et al., 2015. The composition of the gut microbiota shapes the colon mucus barrier. *EMBO reports*, 16(2), pp.164–77. Available at: http://www.pubmedcentral.nih.gov/articlerender.fcgi?artid=4328744&tool=pmcentrez&rendertype=abstract [Accessed March 8, 2015].

Janesch, B., Messner, P. & Schäffer, C., 2013. Are the surface layer homology domains essential for cell surface display and glycosylation of the S-layer protein from Paenibacillus alvei CCM 2051T? *Journal of bacteriology*, 195(3), pp.565–75. Available at: http://www.pubmedcentral.nih.gov/articlerender.fcgi?artid=3554001&tool=pmcentrez&rendertype=abstract [Accessed November 10, 2013].

Janoir, C. et al., 2013. Adaptive strategies and pathogenesis of Clostridium difficile from *in vivo* transcriptomics. *Infection and Immunity*, 81(10), pp.3757–3769.

Janoir, C. et al., 2007. Cwp84, a surface-associated protein of Clostridium difficile, is a cysteine protease with degrading activity on extracellular matrix proteins. *Journal of bacteriology*, 189(20), pp.7174–80. Available at: http://www.pubmedcentral.nih.gov/articlerender.fcgi?artid=2168428&tool=pmcentrez&rendertype=abstract [Accessed February 15, 2014].

Jarchum, I. et al., 2012. Critical role for MyD88-mediated neutrophil recruitment during Clostridium difficile colitis. *Infection and immunity*, 80(9), pp.2989–96. Available at: http://www.pubmedcentral.nih.gov/articlerender.fcgi?artid=3418725&tool=pmcentrez&rendertype=abstract [Accessed June 9, 2014].

Johansson, M.E. V et al., 2011. Composition and functional role of the mucus layers in the intestine. *Cellular and Molecular Life Sciences*, 68, pp.3635–3641.

Johansson, M.E. V et al., 2008. The inner of the two Muc2 mucin-dependent mucus layers in colon is devoid of bacteria. *Proceedings of the National Academy of Sciences of the United States of America*, 105(39), pp.15064–9. Available at: http://www.pubmedcentral.nih.gov/articlerender.fcgi?artid=2567493&tool=pmcentrez&rendertype=abstract.

Johansson, M.E.V. & Hansson, G.C., 2013. Mucus and the Goblet Cell. *Digestive Diseases*, 31(3-4), pp.305–309. Available at: http://www.pubmedcentral.nih.gov/articlerender.fcgi?artid=4282926&tool=pmcentrez&rendertype=abstract [Accessed March 16, 2015].

Jono, H. et al., 2002. Transforming growth factor-beta -Smad signaling pathway cooperates with NF-kappa B to mediate nontypeable Haemophilus influenzae-induced MUC2 mucin transcription. *The Journal of biological chemistry*, 277(47), pp.45547–57. Available at: http://www.jbc.org/content/277/47/45547.full [Accessed August 9, 2015].

Juge, N., 2012. Microbial adhesins to gastrointestinal mucus. *Trends in microbiology*, 20(1), pp.30–9. Available at: http://www.sciencedirect.com/science/article/pii/S0966842X11001879 [Accessed July 13, 2014].

Kabat, A.M., Srinivasan, N. & Maloy, K.J., 2014. Modulation of immune development and function by intestinal microbiota. *Trends in Immunology*, 35(11), pp.507–517. Available at: http://www.cell.com/article/S1471490614001318/fulltext [Accessed August 28, 2014].

Kalisz, H.M., Hendle, J. & Schmid, R.D., 1997. Structural and biochemical properties of glycosylated and deglycosylated glucose oxidase from Penicillium amagasakiense. *Applied microbiology and biotechnology*, 47(5), pp.502–7. Available at: http://www.ncbi.nlm.nih.gov/pubmed/9210339 [Accessed September 7, 2015].

Kalueff, a V et al., 2006. Hair barbering in mice: implications for neurobehavioural research. *Behavioural processes*, 71(1), pp.8–15. Available at: http://www.ncbi.nlm.nih.gov/pubmed/16236465 [Accessed May 26, 2014].

Kamada, N. et al., 2013. Control of pathogens and pathobionts by the gut microbiota. *Nature Immunology*, 14(7), pp.685–690. Available at: http://www.pubmedcentral.nih.gov/articlerender.fcgi?artid=4083503&tool=pmcentrez&rendertype=abstract [Accessed June 18, 2013].

Kanai, T., Mikami, Y. & Hayashi, A., 2015. A breakthrough in probiotics: Clostridium butyricum regulates gut homeostasis and anti-inflammatory response in inflammatory bowel disease. *Journal of Gastroenterology*. Available at: http://link.springer.com/10.1007/s00535-015-1084-x.

Kang, H.M. et al., 2008. Effects of Helicobacter pylori Infection on gastric mucin expression. *Journal of clinical gastroenterology*, 42(1), pp.29–35. Available at: http://www.ncbi.nlm.nih.gov/pubmed/18097286 [Accessed October 3, 2014].

Kang, S.S. et al., 2008. An antibiotic-responsive mouse model of fulminant ulcerative colitis. *PLoS Medicine*, 5(3), p.e41. Available at: http://www.pubmedcentral.nih.gov/articlerender.fcgi?artid=2270287&tool=pmcentrez&rendertype=abstract [Accessed November 6, 2013].

Karadsheh, Z. & Sule, S., 2013. Fecal transplantation for the treatment of recurrent Clostridium difficile infection. *North American journal of medical sciences*, 5(6), pp.339–43. Available at: http://www.pubmedcentral.nih.gov/articlerender.fcgi?artid=3731863&tool=pmcentrez&rendertype=abstract [Accessed January 22, 2014].

Karczewski, J. et al., 2014. Development of a recombinant toxin fragment vaccine for Clostridium difficile infection. *Vaccine*, pp.1–7. Available at: http://linkinghub.elsevier.com/retrieve/pii/S0264410X14001996 [Accessed March 24, 2014].

Karjalainen, T. et al., 2002. Clostridium difficile genotyping based on slpA variable region in S-layer gene sequence: an alternative to serotyping. *Journal of clinical microbiology*, 40(7), pp.2452–8. Available at: http://www.pubmedcentral.nih.gov/articlerender.fcgi?artid=120536&tool=pmcentrez&rendertype=abstract [Accessed May 13, 2015].

Karjalainen, T. et al., 2001. Molecular and Genomic Analysis of Genes Encoding Surface-Anchored Proteins from Clostridium difficile. *Infection and immunity*, 69(5), pp.3442–3446.

Kawai, T. & Akira, S., 2010. The role of pattern-recognition receptors in innate immunity: update on Toll-like receptors. *Nature immunology*, 11(5), pp.373–84. Available at: http://www.ncbi.nlm.nih.gov/pubmed/20404851 [Accessed January 20, 2014].

Kawashima, H., 2012. Roles of the Gel-Forming MUC2 Mucin and Its O-Glycosylation in the Protection against Colitis and Colorectal Cancer. *Biological and Pharmaceutical Bulletin - J-Stage*, 35(October), pp.1637–1641.

Kayama, H., Nishimura, J. & Takeda, K., 2013. Regulation of intestinal homeostasis by innate immune cells. *Immune network*, 13(6), pp.227–34. Available at: http://www.pubmedcentral.nih.gov/articlerender.fcgi?artid=3875780&tool=pmcentrez&rendertype=abstract.

Kelly, C.J. et al., 2015. Crosstalk between Microbiota-Derived Short-Chain Fatty Acids and Intestinal Epithelial HIF Augments Tissue Barrier Function. *Cell Host & Microbe*. Available at: http://www.sciencedirect.com/science/article/pii/S1931312815001225 [Accessed April 13, 2015].

Kelly, C.P. & Kyne, L., 2011. The host immune response to Clostridium difficile. *Journal of medical microbiology*, 60(Pt 8), pp.1070–9. Available at: http://www.ncbi.nlm.nih.gov/pubmed/21415200 [Accessed February 11, 2014].

Khoruts, A. & Weingarden, A.R., 2014. Emergence of fecal microbiota transplantation as an approach to repair disrupted microbial gut ecology. *Immunology letters*, pp.1–5. Available at: http://www.ncbi.nlm.nih.gov/pubmed/25106113 [Accessed August 16, 2014].

Kim, J. et al., 2014. Clinical characteristics of relapses and re-infections in Clostridium difficile infection. *Clinical microbiology and infection : the official publication of the European Society of Clinical Microbiology and Infectious Diseases*, 20(11), pp.1198–204. Available at: http://www.sciencedirect.com/science/article/pii/S1198743X14653180 [Accessed January 5, 2015].

Kim, S.H. et al., 2014. Three-dimensional intestinal villi epithelium enhances protection of human intestinal cells from bacterial infection by inducing mucin expression. *Integrative Biology*, 6, pp.1122–1131. Available at: http://www.ncbi.nlm.nih.gov/pubmed/25200891 [Accessed September 26, 2014].

Kim, Y.S. & Ho, S.B., 2010. Intestinal goblet cells and mucins in health and disease: recent insights and progress. *Current gastroenterology reports*, 12(5), pp.319–30. Available at: http://www.pubmedcentral.nih.gov/articlerender.fcgi?artid=2933006&tool=pmcentrez&rendertype=abstract [Accessed June 3, 2014].

Knoop, K. a et al., 2015. Microbial sensing by goblet cells controls immune surveillance of luminal antigens in the colon. *Mucosal immunology*, 8(1), pp.198–210. Available at: http://www.ncbi.nlm.nih.gov/pubmed/25005358 [Accessed December 16, 2014].

Koenigsknecht, M.J. & Young, V.B., 2013. Fecal microbial transplantation for the treatment of Difficile Infection: Current Promise and Future Needs. *Current opinion in gastroenterology*, 29(6), pp.628–632.

Koroleva, E.P. et al., 2015. Citrobacter rodentium-induced colitis: A robust model to study mucosal immune responses in the gut. *Journal of Immunological Methods*. Available at: http://linkinghub.elsevier.com/retrieve/pii/S002217591500037X.

Koval, S.F. & Murray, R.G., 1984. The isolation of surface array proteins from bacteria. *Canadian journal of biochemistry and cell biology = Revue canadienne de biochimie et biologie cellulaire*, 62(11), pp.1181–9. Available at: http://www.ncbi.nlm.nih.gov/pubmed/6525568 [Accessed May 6, 2015].

Kucharzik, T. et al., 2001. Neutrophil transmigration in inflammatory bowel disease is associated with differential expression of epithelial intercellular junction proteins. *The American journal of pathology*, 159(6), pp.2001–9. Available at: http://www.pubmedcentral.nih.gov/articlerender.fcgi?artid=1850599&tool=pmcentrez&rendertype=abstract [Accessed June 17, 2015].

Kuehne, S. a et al., 2010. The role of toxin A and toxin B in Clostridium difficile infection. *Nature*, 467(7316), pp.711–3. Available at: http://www.ncbi.nlm.nih.gov/pubmed/20844489 [Accessed February 3, 2014].

Kuen, B., Sleytr, U.B. & Lubitz, W., 1994. Sequence analysis of the sbsA gene encoding the 130-kDa surface-layer protein of Bacillus stearothermophilus strain PV72. *Gene*, 145(1), pp.115–20. Available at: http://www.ncbi.nlm.nih.gov/pubmed/8045409 [Accessed May 13, 2015].

Kühl, A.A. et al., 2007. Aggravation of different types of experimental colitis by depletion or adhesion blockade of neutrophils. *Gastroenterology*, 133(6), pp.1882–92. Available at: http://www.sciencedirect.com/science/article/pii/S0016508507016307 [Accessed August 11, 2015].

Kühn, R. et al., 1993. Interleukin-10-deficient mice develop chronic enterocolitis. *Cell*, 75(2), pp.263–74. Available at: http://www.ncbi.nlm.nih.gov/pubmed/8402911 [Accessed June 6, 2015].

Kuo, I.-H. et al., 2013. Activation of epidermal toll-like receptor 2 enhances tight junction function: implications for atopic dermatitis and skin barrier repair. *The Journal of investigative dermatology*, 133(4), pp.988–98. Available at: http://www.pubmedcentral.nih.gov/articlerender.fcgi?artid=3600383&tool=pmcentrez&rendertype=abstract [Accessed July 22, 2015].

Larrgy, R., 2011. *The cloning, expression and characterisation of bacterial chitin-binding proteins from Pseudomonas aeruginosa, Serratia marcescens, Photorhabdus luminescens and Photorhabdus asymbiotica*. Dublin City University.

Larson, H.E. et al., 1978. Clostridium difficile and the aetiology of pseudomembranous colitis. *Lancet*, 1(8073), pp.1063–6. Available at: http://www.ncbi.nlm.nih.gov/pubmed/77366 [Accessed June 3, 2015].

Larsson, J.M.H. et al., 2011. Altered O-glycosylation profile of MUC2 mucin occurs in active ulcerative colitis and is associated with increased inflammation. *Inflammatory bowel diseases*, 17(11), pp.2299–307. Available at: http://www.ncbi.nlm.nih.gov/pubmed/21290483 [Accessed September 24, 2014].

Lee, C.-S. et al., 2013. An improved lectin-based method for the detection of mucin-type O-glycans in biological samples. *Analyst*, (138), pp.3522–3529. Available at: http://www.academia.edu/6780110/An_improved_lectin-based_method_for_the_detection_of_mucin-type_O-glycans_in_biological_samples [Accessed May 13, 2015].

Leriche, V., Sibille, P. & Carpentier, B., 2000. Use of an enzyme-linked lectinsorbent assay to monitor the shift in polysaccharide composition in bacterial biofilms. *Applied and Environmental Microbiology*, 66(5), pp.1851–1856.

Lessa, F.C., 2013. Community-associated Clostridium difficile infection: how real is it? *Anaerobe*, 24, pp.121–3. Available at: http://www.ncbi.nlm.nih.gov/pubmed/23403280 [Accessed February 11, 2014].

Ley, R.E. et al., 2008. Evolution of mammals and their gut microbes. *Science (New York, N.Y.)*, 320(5883), pp.1647–51. Available at: http://www.pubmedcentral.nih.gov/articlerender.fcgi?artid=2649005&tool=pmcentrez&rendertype=abstract [Accessed July 22, 2014].

Liang, S.C. et al., 2006. Interleukin (IL)-22 and IL-17 are coexpressed by Th17 cells and cooperatively enhance expression of antimicrobial peptides. *The Journal of experimental medicine*, 203(10), pp.2271–9. Available at: http://www.pubmedcentral.nih.gov/articlerender.fcgi?artid=2118116&tool=pmcentrez&rendertype=abstract [Accessed October 30, 2014].

Linden, S.K. et al., 2008. Mucins in the mucosal barrier to infection. *Mucosal immunology*, 1(3), pp.183–197.

Lindén, S.K., Florin, T.H.J. & McGuckin, M.A., 2008. Mucin dynamics in intestinal bacterial infection. N. Gay, ed. *PloS one*, 3(12), p.e3952. Available at: http://www.pubmedcentral.nih.gov/articlerender.fcgi?artid=2601037&tool=pmcentrez&rendertype=abstract [Accessed September 26, 2014].

Ling, L.L. et al., 2015. A new antibiotic kills pathogens without detectable resistance. *Nature*. Available at: http://www.ncbi.nlm.nih.gov/pubmed/25561178 [Accessed January 7, 2015].

Linz, B. et al., 2007. An African origin for the intimate association between humans and Helicobacter pylori. *Nature*, 445(7130), pp.915–8. Available at: http://dx.doi.org/10.1038/nature05562 [Accessed March 15, 2015].

Liquori, G.E. et al., 2012. In situ characterization of O-linked glycans of Muc2 in mouse colon. *Acta histochemica*, 114(7), pp.723–32. Available at: http://www.ncbi.nlm.nih.gov/pubmed/22261557 [Accessed April 27, 2014].

Littman, D.R. & Pamer, E.G., 2011. Role of the commensal microbiota in normal and pathogenic host immune responses. *Cell host & microbe*, 10(4), pp.311–23. Available at: http://www.pubmedcentral.nih.gov/articlerender.fcgi?artid=3202012&tool=pmcentrez&rendertype=abstract [Accessed May 22, 2013].

Liu, S. et al., 2015. Identification of fecal microRNAs and their role in regulating gut microbiota. In *Gut Microbiota Modulation of Host Physiology: The Search for Mechanism*. p. 76.

Llorente, L. et al., 2000. Clinical and biologic effects of anti-interleukin-10 monoclonal antibody administration in systemic lupus erythematosus. *Arthritis and rheumatism*, 43(8), pp.1790–800. Available at: http://www.ncbi.nlm.nih.gov/pubmed/10943869 [Accessed August 9, 2015].

Lynch, M., 2014. *Surface Layer Proteins as virulence factors in Clostridium difficile infection*. Dublin City University.

MacFaddin, J.F., 1985. *Media for isolation, cultivation, identification, maintenance of bacteria Vol. 1.*, Baltimore: Williams & Wilkins.

Mack, D. et al., 2003. Extracellular MUC3 mucin secretion follows adherence of Lactobacillus strains to intestinal epithelial cells in vitro. *Gut*, 52, pp.827–834. Available at: http://gut.bmj.com/content/52/6/827.abstract [Accessed September 26, 2014].

Madan, R. & Petri Jr, W.A., 2012. Immune responses to Clostridium difficile infection. *Trends in molecular medicine*, 18(11), pp.658–66. Available at: http://www.ncbi.nlm.nih.gov/pubmed/23084763 [Accessed June 26, 2013].

Maloy, K.J. & Kullberg, M.C., 2008. IL-23 and Th17 cytokines in intestinal homeostasis. *Mucosal immunology*, 1(5), pp.339–349.

Maloy, K.J. & Powrie, F., 2011. Intestinal homeostasis and its breakdown in inflammatory bowel disease. *Nature*, 474(7351), pp.298–306. Available at: http://dx.doi.org/10.1038/nature10208 [Accessed August 11, 2015].

Mantle, M. & Allen, A., 1978. A colorimetric assay for glycoproteins based on the periodic acid/Schiff stain [proceedings]. *Biochemical Society transactions*, 6(3), pp.607–9. Available at: http://europepmc.org/abstract/med/208893 [Accessed May 14, 2015].

Manzo, C.E. et al., 2014. International Typing Study of Clostridium difficile. *Anaerobe*, (April), pp.1–4. Available at: http://linkinghub.elsevier.com/retrieve/pii/S1075996414000377 [Accessed April 24, 2014].

Marafini, I. et al., 2013. TGF-Beta signaling manipulation as potential therapy for IBD. *Current drug targets*, 14(12), pp.1400–4. Available at: http://www.ncbi.nlm.nih.gov/pubmed/23489130 [Accessed August 9, 2015].

Martinson, J.N. V. et al., 2015. Evaluation of portability and cost of a fluorescent PCR ribotyping protocol for Clostridium difficile epidemiology. *Journal of Clinical Microbiology*, (January), pp.JCM.03591–14. Available at: http://jcm.asm.org/lookup/doi/10.1128/JCM.03591-14.

Mathur, H. et al., 2013. Analysis of anti-Clostridium difficile activity of thuricin CD, vancomycin, metronidazole, ramoplanin, and actagardine, both singly and in paired combinations. *Antimicrobial agents and chemotherapy*, 57(6), pp.2882–6. Available at: http://www.pubmedcentral.nih.gov/articlerender.fcgi?artid=3716125&tool=pmcentrez &rendertype=abstract [Accessed June 3, 2015].

Mauri, P.L. et al., 1999. Characterization of surface layer proteins from Clostridium difficile by liquid chromatography/electrospray ionization mass spectrometry. *Rapid communications in mass spectrometry : RCM*, 13(8), pp.695–703. Available at: http://www.ncbi.nlm.nih.gov/pubmed/10343411 [Accessed March 8, 2014].

McAuley, J.L. et al., 2007. MUC1 cell surface mucin is a critical element of the mucosal barrier to infection. *The Journal of clinical investigation*, 117(8), pp.2313–24. Available at: http://www.pubmedcentral.nih.gov/articlerender.fcgi?artid=1913485&tool=pmcentrez &rendertype=abstract [Accessed September 26, 2014].

Mccoubrey, J. & Poxton, I.R., 2001. Variation in the surface layer proteins of Clostridium difficile. *FEMS Immunology and Medical Microbiology*, (31), pp.131–135.

McFarland, L. V et al., 1994. A randomized placebo-controlled trial of Saccharomyces boulardii in combination with standard antibiotics for Clostridium difficile disease. *JAMA*, 271(24), pp.1913–8. Available at: http://www.ncbi.nlm.nih.gov/pubmed/8201735 [Accessed June 16, 2015].

McGuckin, M. a et al., 2011. Mucin dynamics and enteric pathogens. *Nature reviews. Microbiology*, 9(4), pp.265–78. Available at: http://www.ncbi.nlm.nih.gov/pubmed/21407243 [Accessed July 18, 2014].

Mege, J.-L. et al., 2006. The two faces of interleukin 10 in human infectious diseases. *The Lancet. Infectious diseases*, 6(9), pp.557–69. Available at: http://www.ncbi.nlm.nih.gov/pubmed/16931407 [Accessed July 22, 2015].

Melgar, S., 2005. Acute colitis induced by dextran sulfate sodium progresses to chronicity in C57BL/6 but not in BALB/c mice: correlation between symptoms and inflammation. *AJP: Gastrointestinal and Liver Physiology*, 288(6), pp.G1328–G1338. Available at: http://ajpgi.physiology.org/content/288/6/G1328 [Accessed June 11, 2014].

Merrigan, M. et al., 2010. Human hypervirulent Clostridium difficile strains exhibit increased sporulation as well as robust toxin production. *Journal of bacteriology*, 192(19), pp.4904–11. Available at: http://www.pubmedcentral.nih.gov/articlerender.fcgi?artid=2944552&tool=pmcentrez&rendertype=abstract [Accessed November 3, 2014].

Merrigan, M.M. et al., 2013. Surface-layer protein A (SlpA) is a major contributor to host-cell adherence of Clostridium difficile. *PloS One*, 8(11), p.e78404. Available at: http://www.pubmedcentral.nih.gov/articlerender.fcgi?artid=3827033&tool=pmcentrez&rendertype=abstract [Accessed January 10, 2014].

Messner, P. et al., 2008. S-layer nanoglycobiology of bacteria. *Carbohydrate research*, 343(12), pp.1934–51. Available at: http://www.ncbi.nlm.nih.gov/pubmed/18336801 [Accessed November 10, 2013].

Min, Y.W. & Rhee, P.-L., 2015. The Role of Microbiota on the Gut Immunology. *Clinical Therapeutics*, pp.1–8. Available at: http://linkinghub.elsevier.com/retrieve/pii/S0149291815001460.

Mizrahi, A., Collignon, A. & Péchiné, S., 2014. Passive and active immunization strategies against Clostridium difficile infections: State of the art. *Anaerobe*. Available at: http://www.sciencedirect.com/science/article/pii/S1075996414000924 [Accessed July 29, 2014].

Moehle, C. et al., 2006. Aberrant intestinal expression and allelic variants of mucin genes associated with inflammatory bowel disease. *Journal of molecular medicine (Berlin, Germany)*, 84(12), pp.1055–66. Available at: http://www.ncbi.nlm.nih.gov/pubmed/17058067 [Accessed September 9, 2014].

Moncada, D.M., Kammanadiminti, S.J. & Chadee, K., 2003. Mucin and Toll-like receptors in host defense against intestinal parasites. *Trends in Parasitology*, 19(7), pp.305–311. Available at: http://linkinghub.elsevier.com/retrieve/pii/S1471492203001223 [Accessed January 12, 2015].

Moolenbeek, C. & Ruitenberg, E.J., 1981. The "Swiss roll": a simple technique for histological studies of the rodent intestine. *Laboratory animals*, 15(1), pp.57–9. Available at: http://www.ncbi.nlm.nih.gov/pubmed/7022018 [Accessed February 18, 2014].

Moran, A.P., Gupta, A. & Joshi, L., 2011. Sweet-talk: role of host glycosylation in bacterial pathogenesis of the gastrointestinal tract. *Gut*, 60(10), pp.1412–25. Available at: http://www.ncbi.nlm.nih.gov/pubmed/21228430 [Accessed May 30, 2013].

Mühl, H., 2013. Pro-inflammatory signaling by IL-10 and IL-22: Bad habit stirred up by interferons? *Frontiers in Immunology*, 4(FRB), pp.1–10.

Mullany, P. & Roberts, A., 2010. *Clostridium difficile - Methods and Protocols* 1st ed., Humana Press. Available at: http://www.springer.com/gp/book/9781603273640 [Accessed June 4, 2015].

Ng, J. et al., 2010. Clostridium difficile toxin-induced inflammation and intestinal injury are mediated by the inflammasome. *Gastroenterology*, 139(2), pp.542–52, 552.e1–3. Available at: http://www.ncbi.nlm.nih.gov/pubmed/20398664 [Accessed September 17, 2014].

Ng, K.M. et al., 2013. Microbiota-liberated host sugars facilitate post-antibiotic expansion of enteric pathogens. *Nature*, 502(7469), pp.96–9. Available at: http://www.pubmedcentral.nih.gov/articlerender.fcgi?artid=3825626&tool=pmcentrez&rendertype=abstract [Accessed July 11, 2014].

Nicholson, A. et al., 2009. The response of C57BL/6J and BALB/cJ mice to increased housing density. *Journal of the American Association for Laboratory Animal Science*, 48(6), pp.740–53. Available at: http://www.pubmedcentral.nih.gov/articlerender.fcgi?artid=2786928&tool=pmcentrez&rendertype=abstract.

Noonan, B., 1997. The synthesis, secretion and role in virulence of the paracrystalline surface protein layers of Aeromonas salmonicida and A. hydrophila. *FEMS Microbiology Letters*, 154(1), pp.1–7. Available at: http://www.sciencedirect.com/science/article/pii/S0378109797002577 [Accessed August 12, 2015].

Nothaft, H. & Szymanski, C.M., 2010. Protein glycosylation in bacteria: sweeter than ever. *Nature reviews. Microbiology*, 8(11), pp.765–78. Available at: http://www.ncbi.nlm.nih.gov/pubmed/20948550 [Accessed January 23, 2014].

Nutsch, K.M. & Hsieh, C.-S., 2012. T cell tolerance and immunity to commensal bacteria. *Current opinion in immunology*, 24(4), pp.385–91. Available at: http://www.pubmedcentral.nih.gov/articlerender.fcgi?artid=3423487&tool=pmcentrez&rendertype=abstract [Accessed February 24, 2014].

O'Brien, J.B. et al., 2005. Passive immunisation of hamsters against Clostridium difficile infection using antibodies to surface layer proteins. *FEMS microbiology letters*, 246(2), pp.199–205. Available at: http://www.ncbi.nlm.nih.gov/pubmed/15899406 [Accessed February 18, 2014].

O'Neill, L. a J., Golenbock, D. & Bowie, A.G., 2013. The history of Toll-like receptors - redefining innate immunity. *Nature reviews. Immunology*, 13(6), pp.453–460. Available at: http://www.ncbi.nlm.nih.gov/pubmed/23681101 [Accessed May 21, 2013].

Ohkusa, T. et al., 2009. Commensal bacteria can enter colonic epithelial cells and induce proinflammatory cytokine secretion: a possible pathogenic mechanism of ulcerative colitis. *Journal of medical microbiology*, 58(Pt 5), pp.535–45. Available at: http://www.pubmedcentral.nih.gov/articlerender.fcgi?artid=2887547&tool=pmcentrez&rendertype=abstract [Accessed August 24, 2014].

Ohnmacht, C. et al., 2011. Intestinal microbiota, evolution of the immune system and the bad reputation of pro-inflammatory immunity. *Cellular microbiology*, 13(5), pp.653–9. Available at: http://www.ncbi.nlm.nih.gov/pubmed/21338464 [Accessed June 5, 2015].

Ohtsuka, Y. et al., 2001. MIP-2 secreted by epithelial cells increases neutrophil and lymphocyte recruitment in the mouse intestine. *Gut*, 49(4), pp.526–33. Available at: http://www.ncbi.nlm.nih.gov/pubmed/11559650 [Accessed July 23, 2015].

Ouyang, W. et al., 2011. Regulation and functions of the IL-10 family of cytokines in inflammation and disease. *Annual review of immunology*, 29, pp.71–109.

Pamer, E.G., 2014. Fecal microbiota transplantation: effectiveness, complexities, and lingering concerns. *Mucosal immunology*, 7(2), pp.210–214. Available at: http://www.nature.com/mi/journal/v7/n2/full/mi2013117a.html?WT.ec_id=MI-201403 [Accessed February 20, 2014].

Paredes-Sabja, D., Shen, A. & Sorg, J.A., 2014. Clostridium difficile spore biology: sporulation, germination, and spore structural proteins. *Trends in microbiology*, 22(7), pp.406–416. Available at: http://www.cell.com/article/S0966842X14000742/fulltext [Accessed May 30, 2014].

Péchiné, S. et al., 2013. Immunization using GroEL decreases Clostridium difficile intestinal colonization. *PloS One*, 8(11), p.e81112. Available at: http://www.pubmedcentral.nih.gov/articlerender.fcgi?artid=3841151&tool=pmcentrez&rendertype=abstract [Accessed February 15, 2014].

Péchiné, S., Gleizes, A., et al., 2005. Immunological properties of surface proteins of Clostridium difficile. *Journal of medical microbiology*, 54(Pt 2), pp.193–6. Available at: http://www.ncbi.nlm.nih.gov/pubmed/15673516 [Accessed June 4, 2015].

Péchiné, S., Janoir, C. & Collignon, A., 2005. Variability of Clostridium difficile surface proteins and specific serum antibody response in patients with Clostridium difficile-associated disease. *Journal of clinical microbiology*, 43(10), pp.5018–25. Available at: http://www.pubmedcentral.nih.gov/articlerender.fcgi?artid=1248434&tool=pmcentrez&rendertype=abstract [Accessed June 4, 2015].

Pelaseyed, T. et al., 2014. The mucus and mucins of the goblet cells and enterocytes provide the first defense line of the gastrointestinal tract and interact with the immune system. *Immunological reviews*, 260(1), pp.8–20. Available at: http://www.ncbi.nlm.nih.gov/pubmed/24942678 [Accessed September 26, 2014].

Pender, S.L.-F. et al., 2005. Systemic administration of the chemokine macrophage inflammatory protein 1alpha exacerbates inflammatory bowel disease in a mouse model. *Gut*, 54(8), pp.1114–20. Available at: http://www.pubmedcentral.nih.gov/articlerender.fcgi?artid=1774881&tool=pmcentrez&rendertype=abstract [Accessed September 17, 2014].

Peterson, L.W. & Artis, D., 2014. Intestinal epithelial cells: regulators of barrier function and immune homeostasis. *Nature reviews. Immunology*, 14(3), pp.141–53. Available at: http://dx.doi.org/10.1038/nri3608 [Accessed May 24, 2014].

Petersson, J. et al., 2011. Importance and regulation of the colonic mucus barrier in a mouse model of colitis. *American journal of physiology. Gastrointestinal and liver*

physiology, 300(2), pp.G327–33. Available at: http://www.pubmedcentral.nih.gov/articlerender.fcgi?artid=3302190&tool=pmcentrez&rendertype=abstract [Accessed September 28, 2014].

Pettit, L.J. et al., 2014. Functional genomics reveals that Clostridium difficile Spo0A coordinates sporulation, virulence and metabolism. *BMC genomics*, 15, p.160. Available at: http://www.pubmedcentral.nih.gov/articlerender.fcgi?artid=4028888&tool=pmcentrez&rendertype=abstract [Accessed June 4, 2015].

Pham, T.A.N. et al., 2014. Epithelial IL-22RA1-mediated fucosylation promotes intestinal colonization resistance to an opportunistic pathogen. *Cell host & microbe*, 16(4), pp.504–16. Available at: http://www.pubmedcentral.nih.gov/articlerender.fcgi?artid=4190086&tool=pmcentrez&rendertype=abstract [Accessed January 12, 2015].

Pickard, J.M. et al., 2014. Rapid fucosylation of intestinal epithelium sustains host–commensal symbiosis in sickness. *Nature*. Available at: http://www.nature.com/doifinder/10.1038/nature13823 [Accessed October 1, 2014].

Pickard, J.M. & Chervonsky, a. V., 2015. Intestinal Fucose as a Mediator of Host-Microbe Symbiosis. *The Journal of Immunology*, 194(12), pp.5588–5593. Available at: http://www.jimmunol.org/cgi/doi/10.4049/jimmunol.1500395.

Posch, G. et al., 2011. Characterization and scope of S-layer protein O-glycosylation in Tannerella forsythia. *The Journal of biological chemistry*, 286(44), pp.38714–24. Available at: http://www.pubmedcentral.nih.gov/articlerender.fcgi?artid=3207478&tool=pmcentrez&rendertype=abstract [Accessed December 6, 2014].

Pott, J. & Hornef, M., 2012. Innate immune signalling at the intestinal epithelium in homeostasis and disease. *EMBO reports*, 13(8), pp.684–98. Available at: http://www.pubmedcentral.nih.gov/articlerender.fcgi?artid=3410395&tool=pmcentrez&rendertype=abstract [Accessed February 14, 2014].

Qazi, O. et al., 2009. Mass spectrometric analysis of the S-layer proteins from Clostridium difficile demonstrates the absence of glycosylation. *Journal of mass spectrometry: JMS*, 44(3), pp.368–74. Available at: http://www.ncbi.nlm.nih.gov/pubmed/18932172 [Accessed January 16, 2014].

Radaeva, S. et al., 2004. Interleukin 22 (IL-22) plays a protective role in T cell-mediated murine hepatitis: IL-22 is a survival factor for hepatocytes via STAT3 activation. *Hepatology (Baltimore, Md.)*, 39(5), pp.1332–42. Available at: http://www.ncbi.nlm.nih.gov/pubmed/15122762 [Accessed April 15, 2015].

Rakoff-Nahoum, S. et al., 2004. Recognition of commensal microflora by toll-like receptors is required for intestinal homeostasis. *Cell*, 118(2), pp.229–41. Available at: http://www.ncbi.nlm.nih.gov/pubmed/15260992.

Rao, K., Erb-Downward, J.R., et al., 2014. The systemic inflammatory response to Clostridium difficile infection. *PLoS ONE*, 9(3).

Rao, K., Young, V.B. & Aronoff, D.M., 2014. Fecal Microbiota Therapy: ready for Prime Time? *Infectious Disease Clinics of North America*, 35(1), pp.28–30.

Rea, M.C. et al., 2010. Thuricin CD, a posttranslationally modified bacteriocin with a narrow spectrum of activity against Clostridium difficile. *Proceedings of the National Academy of Sciences of the United States of America*, 107(20), pp.9352–7. Available at: http://www.pubmedcentral.nih.gov/articlerender.fcgi?artid=2889069&tool=pmcentrez&rendertype=abstract [Accessed January 21, 2014].

Redgrave, L.S. et al., 2014. Fluoroquinolone resistance: mechanisms, impact on bacteria, and role in evolutionary success. *Trends in microbiology*, 22(8), pp.438–445. Available at: http://www.ncbi.nlm.nih.gov/pubmed/24842194 [Accessed July 29, 2014].

Reid, C.W. et al., 2012. Structural characterization of surface glycans from Clostridium difficile. *Carbohydrate research*, 354, pp.65–73. Available at: http://www.ncbi.nlm.nih.gov/pubmed/22560631 [Accessed January 16, 2014].

Rhodes, J., 2007. The role of intestinal glycosylation in determining individual responses to foods in inflammatory and neoplastic bowel diseases. *Journal of Nutritional and Environmental Medicine*, 16(2), pp.106–111. Available at: http://informahealthcare.com/doi/abs/10.1080/13590840701343723 [Accessed February 14, 2014].

Ridaura, V.K. et al., 2013. Gut microbiota from twins discordant for obesity modulate metabolism in mice. *Science (New York, N.Y.)*, 341(6150), p.1241214. Available at: http://www.pubmedcentral.nih.gov/articlerender.fcgi?artid=3829625&tool=pmcentrez&rendertype=abstract [Accessed July 9, 2014].

Ristl, R. et al., 2011. The S-layer glycome-adding to the sugar coat of bacteria. *International journal of microbiology*, 2011. Available at: http://www.pubmedcentral.nih.gov/articlerender.fcgi?artid=2943079&tool=pmcentrez&rendertype=abstract [Accessed May 25, 2013].

Robbe, C. et al., 2003. Evidence of regio-specific glycosylation in human intestinal mucins: presence of an acidic gradient along the intestinal tract. *The Journal of biological chemistry*, 278(47), pp.46337–48. Available at: http://www.ncbi.nlm.nih.gov/pubmed/12952970 [Accessed November 10, 2014].

Robinson, C.J. & Young, V.B., 2010. Antibiotic administration alters the community structure of the gastrointestinal micobiota. *Gut Microbes*, 1(4), pp.279–284.

Rodriguez, C. et al., 2014. Clostridium difficile infection in elderly nursing home residents. *Anaerobe*, (August), pp.8–11. Available at: http://linkinghub.elsevier.com/retrieve/pii/S1075996414001139 [Accessed August 25, 2014].

Roe, D.E. et al., 2002. Multilaboratory comparison of growth characteristics for anaerobes, using 5 different agar media. *Clinical infectious diseases : an official publication of the Infectious Diseases Society of America*, 35(Suppl 1), pp.S36–9. Available at: http://www.ncbi.nlm.nih.gov/pubmed/12173106.

Rohlke, F. & Stollman, N., 2012. Fecal microbiota transplantation in relapsing Clostridium difficile infection. *Therapeutic Advances in Gastroenterology*, 5(6), pp.403–420.

Rolfe, R.D. & Finegold, S.M., 1979. Purification and characterization of Clostridium difficile toxin. *Infection and immunity*, 25(1), pp.191–201. Available at: http://www.pubmedcentral.nih.gov/articlerender.fcgi?artid=414437&tool=pmcentrez&rendertype=abstract.

Round, J.L. et al., 2011. The Toll-like receptor 2 pathway establishes colonization by a commensal of the human microbiota. *Science (New York, N.Y.)*, 332(6032), pp.974–7. Available at: http://www.pubmedcentral.nih.gov/articlerender.fcgi?artid=3164325&tool=pmcentrez&rendertype=abstract [Accessed December 23, 2014].

Rupnik, M., 2005. Revised nomenclature of Clostridium difficile toxins and associated genes. *Journal of Medical Microbiology*, 54(2), pp.113–117. Available at: http://jmm.sgmjournals.org/cgi/doi/10.1099/jmm.0.45810-0 [Accessed March 9, 2014].

Rupnik, M., Wilcox, M.H. & Gerding, D.N., 2009. Clostridium difficile infection: new developments in epidemiology and pathogenesis. *Nature reviews. Microbiology*, 7(7), pp.526–36. Available at: http://www.ncbi.nlm.nih.gov/pubmed/19528959 [Accessed January 28, 2014].

Ryan, A. et al., 2011. A role for TLR4 in Clostridium difficile infection and the recognition of surface layer proteins. *PLoS Pathogens*, 7(6), p.e1002076. Available at: http://www.pubmedcentral.nih.gov/articlerender.fcgi?artid=3128122&tool=pmcentrez&rendertype=abstract [Accessed July 1, 2013].

Rydström, A. & Wick, M.J., 2009. Monocyte and neutrophil recruitment during oral Salmonella infection is driven by MyD88-derived chemokines. *European journal of immunology*, 39(11), pp.3019–30. Available at: http://www.ncbi.nlm.nih.gov/pubmed/19839009 [Accessed July 23, 2015].

Sabat, R., Ouyang, W. & Wolk, K., 2014. Therapeutic opportunities of the IL-22-IL-22R1 system. *Nature reviews. Drug discovery*, 13(1), pp.21–38. Available at: http://www.ncbi.nlm.nih.gov/pubmed/24378801.

Sadighi Akha, A. a. et al., 2013. Acute infection of mice with Clostridium difficile leads to eIF2α phosphorylation and pro-survival signalling as part of the mucosal inflammatory response. *Immunology*, 140(1), pp.111–22. Available at: http://www.pubmedcentral.nih.gov/articlerender.fcgi?artid=3809711&tool=pmcentrez&rendertype=abstract [Accessed March 19, 2014].

Sadighi Akha, A.A. et al., 2015. Interleukin-22 and CD160 play additive roles in the host mucosal response to Clostridium difficile infection in mice. *Immunology*, 144(4), pp.587–97. Available at: http://www.ncbi.nlm.nih.gov/pubmed/25327211 [Accessed June 16, 2015].

Saeland, E. et al., 2012. Differential glycosylation of MUC1 and CEACAM5 between normal mucosa and tumour tissue of colon cancer patients. *International journal of cancer*, 131(1), pp.117–28. Available at: http://www.ncbi.nlm.nih.gov/pubmed/21823122 [Accessed January 10, 2015].

Sakaguchi, T. et al., 2002. Shigella flexneri regulates tight junction-associated proteins in human intestinal epithelial cells. *Cellular microbiology*, 4(6), pp.367–81. Available at: http://www.ncbi.nlm.nih.gov/pubmed/12067320 [Accessed May 11, 2015].

Sára, M. & Sleytr, U.B., 2000. S-Layer Proteins. *Journal of bacteriology*, 182(4), pp.859–868.

Sassone-Corsi, M. & Raffatellu, M., 2015. No Vacancy: How Beneficial Microbes Cooperate with Immunity To Provide Colonization Resistance to Pathogens. *The Journal of Immunology*, 194(9), pp.4081–4087. Available at: http://www.jimmunol.org/cgi/doi/10.4049/jimmunol.1403169.

Saxena, M. & Yeretssian, G., 2014. NOD-Like Receptors: Master Regulators of Inflammation and Cancer. *Frontiers in immunology*, 5, p.327. Available at: http://www.pubmedcentral.nih.gov/articlerender.fcgi?artid=4095565&tool=pmcentrez&rendertype=abstract [Accessed August 1, 2015].

Schäffer, C., Graninger, M. & Messner, P., 2001. Prokaryotic glycosylation. *Proteomics*, 1, pp.248–261.

Schäffer, C. & Messner, P., 2004. Surface-layer glycoproteins: an example for the diversity of bacterial glycosylation with promising impacts on nanobiotechnology. *Glycobiology*, 14(8), p.31R–42R. Available at: http://www.ncbi.nlm.nih.gov/pubmed/15044388 [Accessed February 14, 2014].

Schwan, C. et al., 2014. Clostridium difficile toxin CDT hijacks microtubule organization and reroutes vesicle traffic to increase pathogen adherence. *Proceedings of the National Academy of Sciences of the United States of America*, 111(6), pp.2313–8.

Schwan, C. et al., 2009. Clostridium difficile toxin CDT induces formation of microtubule-based protrusions and increases adherence of bacteria. *PLoS Pathogens*, 5(10).

Seekatz, A.M. et al., 2015. Fecal microbiota transplant eliminates Clostridium difficile in a murine model of relapsing disease. *Infection and immunity*. Available at: http://www.ncbi.nlm.nih.gov/pubmed/26169276 [Accessed July 27, 2015].

Seekatz, A.M. et al., 2014. Recovery of the Gut Microbiome following Fecal Microbiota Transplantation. *mBio*, 5(3), pp.1–9.

Seekatz, A.M. & Young, V.B., 2014. Clostridium difficile and the microbiota. *The Journal of clinical investigation*, 124(22), pp.1–8. Available at: http://europepmc.org/abstract/med/25036699.

Sekirov, I. et al., 2008. Antibiotic-induced perturbations of the intestinal microbiota alter host susceptibility to enteric infection. *Infection and immunity*, 76(10), pp.4726–36. Available at: http://www.pubmedcentral.nih.gov/articlerender.fcgi?artid=2546810&tool=pmcentrez&rendertype=abstract [Accessed November 6, 2013].

Senoh, M. et al., 2015. Inhibition of adhesion of Clostridium difficile to human intestinal cells after treatment with serum and intestinal fluid isolated from mice immunized with nontoxigenic *C. difficile* membrane fraction. *Microbial Pathogenesis*. Available at: http://linkinghub.elsevier.com/retrieve/pii/S0882401015000285.

Shaoul, R. et al., 2004. Colonic expression of MUC2, MUC5AC, and TFF1 in inflammatory bowel disease in children. *Journal of pediatric gastroenterology and nutrition*, 38(5), pp.488–93. Available at: http://www.ncbi.nlm.nih.gov/pubmed/15097436 [Accessed September 26, 2014].

Sheng, Y.H. et al., 2013. MUC1 and MUC13 differentially regulate epithelial inflammation in response to inflammatory and infectious stimuli. *Mucosal immunology*, 6(3), pp.557–68. Available at: http://www.ncbi.nlm.nih.gov/pubmed/23149663 [Accessed September 28, 2014].

Shields, K. et al., 2015. Recurrent Clostridium difficile infection: From colonization to cure. *Anaerobe*. Available at: http://linkinghub.elsevier.com/retrieve/pii/S1075996415300135.

Shull, M.M. et al., 1992. Targeted disruption of the mouse transforming growth factor-beta 1 gene results in multifocal inflammatory disease. *Nature*, 359(6397), pp.693–9. Available at: http://www.pubmedcentral.nih.gov/articlerender.fcgi?artid=3889166&tool=pmcentrez&rendertype=abstract [Accessed July 8, 2015].

Sleytr, U.B. & Beveridge, T.J., 1999. Bacterial S-layers. *Trends in microbiology*, 7(6), pp.253–60. Available at: http://www.ncbi.nlm.nih.gov/pubmed/10366863.

Solomon, K., 2013. The host immune response to Clostridium difficile infection. *Therapeutic Advances in Infectious Disease*, 1(1), pp.19–35. Available at: http://tai.sagepub.com/lookup/doi/10.1177/2049936112472173 [Accessed August 10, 2013].

Sommer, F. et al., 2014. Altered mucus glycosylation in core 1 O-glycan-deficient mice affects microbiota composition and intestinal architecture. *PLoS ONE*, 9(1).

Sommer, F. & Bäckhed, F., 2013. The gut microbiota--masters of host development and physiology. *Nature reviews. Microbiology*, 11(4), pp.227–38. Available at: http://www.ncbi.nlm.nih.gov/pubmed/23435359.

Sonnenberg, G.F. et al., 2010. Pathological versus protective functions of IL-22 in airway inflammation are regulated by IL-17A. *The Journal of experimental medicine*, 207(6), pp.1293–1305.

Sonnenberg, G.F., Fouser, L. a & Artis, D., 2011. Border patrol: regulation of immunity, inflammation and tissue homeostasis at barrier surfaces by IL-22. *Nature immunology*, 12(5), pp.383–390. Available at: http://dx.doi.org/10.1038/ni.2025.

Sorg, J.A., 2014. Microbial Bile Acid Metabolic Clusters: The Bouncers at the Bar. *Cell Host & Microbe*, 16(5), pp.551–552. Available at: http://linkinghub.elsevier.com/retrieve/pii/S193131281400393X [Accessed November 13, 2014].

Spigaglia, P. et al., 2013. Surface-layer (S-layer) of human and animal Clostridium difficile strains and their behaviour in adherence to epithelial cells and intestinal colonization. *Journal of medical microbiology*, 62(Pt 9), pp.1386–93. Available at: http://www.ncbi.nlm.nih.gov/pubmed/23518658 [Accessed February 3, 2014].

Stabler, R.A. et al., 2009. Comparative genome and phenotypic analysis of Clostridium difficile 027 strains provides insight into the evolution of a hypervirulent bacterium. *Genome biology*, 10(9), p.R102. Available at: http://www.pubmedcentral.nih.gov/articlerender.fcgi?artid=2768977&tool=pmcentrez&rendertype=abstract [Accessed February 9, 2014].

Stanley, J.D. et al., 2013. Clostridium difficile infection. *Current Problems in Surgery*, 50(7), pp.302–37. Available at: http://www.sciencedirect.com/science/article/pii/S0011384013000646 [Accessed March 4, 2014].

Stevenson, E., Minton, N.P. & Kuehne, S.A., 2015. The role of flagella in Clostridium difficile pathogenicity. *Trends in Microbiology*, pp.1–8. Available at: http://dx.doi.org/10.1016/j.tim.2015.01.004.

Sugimoto, K. & Ogawa, A., 2008. IL-22 ameliorates intestinal inflammation in a mouse model of ulcerative colitis. *The Journal of Clinical Investigation*, 118(2). Available at: http://www.ncbi.nlm.nih.gov/pmc/articles/PMC2157567/.

Sun, X. et al., 2011. Mouse relapse model of Clostridium difficile infection. *Infection and immunity*, 79(7), pp.2856–64. Available at: http://www.pubmedcentral.nih.gov/articlerender.fcgi?artid=3191975&tool=pmcentrez&rendertype=abstract [Accessed July 1, 2013].

Sun, X. & Hirota, S. a, 2015. The roles of host and pathogen factors and the innate immune response in the pathogenesis of Clostridium difficile infection. *Molecular immunology*, 63(2), pp.193–202. Available at: http://www.ncbi.nlm.nih.gov/pubmed/25242213 [Accessed November 18, 2014].

Suzuki, T., 2012. Regulation of intestinal epithelial permeability by tight junctions. *Cellular and Molecular Life Sciences*, pp.631–659.

Szymanski, C.M. & Wren, B.W., 2005. Protein glycosylation in bacterial mucosal pathogens. *Nature reviews. Microbiology*, 3(3), pp.225–237.

Takeuchi, O. et al., 1999. Differential roles of TLR2 and TLR4 in recognition of gram-negative and gram-positive bacterial cell wall components. *Immunity*, 11(4), pp.443–51. Available at: http://www.ncbi.nlm.nih.gov/pubmed/10549626 [Accessed June 11, 2015].

Tam Dang, T.H. et al., 2012. Novel inhibitors of surface layer processing in Clostridium difficile. *Bioorganic & medicinal chemistry*, 20(2), pp.614–21. Available at: http://www.ncbi.nlm.nih.gov/pubmed/21752656 [Accessed February 14, 2014].

Tanner, M.E., 2005. The enzymes of sialic acid biosynthesis. *Bioorganic chemistry*, 33(3), pp.216–28. Available at: http://www.ncbi.nlm.nih.gov/pubmed/15888312 [Accessed March 6, 2015].

Tasteyre, A. et al., 2001. Role of FliC and FliD Flagellar Proteins of Clostridium difficile in Adherence and Gut Colonization. *Infection and immunity*, 69(12), pp.7937–7940. Available at: http://www.pubmedcentral.nih.gov/articlerender.fcgi?artid=98895&tool=pmcentrez&rendertype=abstract [Accessed March 5, 2014].

Taur, Y. & Pamer, E.G., 2014. Harnessing Microbiota to Kill a Pathogen: Fixing the microbiota to treat Clostridium difficile infections. *Nature Medicine*, 20(3), pp.246–247. Available at: http://www.nature.com/doifinder/10.1038/nm.3492 [Accessed March 7, 2014].

Teena Chopra et al., 2015. Burden of Clostridium difficile infection on hospital readmissions and its potential impact under the Hospital Readmission Reduction Program. *American Journal of Infection Control*, 43(4), pp.314–317. Available at: http://www.sciencedirect.com/science/article/pii/S0196655314013029 [Accessed March 30, 2015].

Tenover, F.C., Tickler, I.A. & Persing, D.H., 2012. Antimicrobial-resistant strains of Clostridium difficile from North America. *Antimicrobial agents and chemotherapy*, 56(6), pp.2929–32. Available at: http://aac.asm.org/content/56/6/2929.full [Accessed May 5, 2015].

Thaiss, C. a et al., 2014. The interplay between the innate immune system and the microbiota. *Current opinion in immunology*, 26C, pp.41–48. Available at: http://www.ncbi.nlm.nih.gov/pubmed/24556399 [Accessed March 22, 2014].

Theriot, C.M. et al., 2014. Antibiotic-induced shifts in the mouse gut microbiome and metabolome increase susceptibility to Clostridium difficile infection. *Nature communications*, 5, p.3114. Available at: http://www.nature.com/ncomms/2014/140120/ncomms4114/pdf/ncomms4114.pdf [Accessed March 19, 2014].

Theriot, C.M. et al., 2015. Effects of Tigecycline and Vancomycin Administration on Established Clostridium difficile Infection. *Antimicrobial Agents and Chemotherapy*, 59(3), pp.1596–1604. Available at: http://aac.asm.org/lookup/doi/10.1128/AAC.04296-14.

Theriot, C.M. & Young, V.B., 2014. Microbial and metabolic interactions between the gastrointestinal tract and Clostridium difficile infection. *Gut Microbes*, 5(1), pp.86–95. Available at: http://www.ncbi.nlm.nih.gov/pubmed/24335555 [Accessed March 19, 2014].

Thompson, R. et al., 2011. Optimization of the enzyme-linked lectin assay for enhanced glycoprotein and glycoconjugate analysis. *Analytical biochemistry*, 413(2), pp.114–22. Available at: 85% [Accessed February 4, 2014].

Thompson, S.A., 2002. Campylobacter surface-layers (S-layers) and immune evasion. *Annals of periodontology / the American Academy of Periodontology*, 7(1), pp.43–53. Available at: http://www.pubmedcentral.nih.gov/articlerender.fcgi?artid=2763180&tool=pmcentrez&rendertype=abstract [Accessed August 12, 2015].

Tobisawa, Y. et al., 2010. Sulfation of colonic mucins by N-acetylglucosamine 6-O-sulfotransferase-2 and its protective function in experimental colitis in mice. *The Journal of biological chemistry*, 285(9), pp.6750–60. Available at: http://www.pubmedcentral.nih.gov/articlerender.fcgi?artid=2825469&tool=pmcentrez&rendertype=abstract [Accessed April 28, 2014].

Tortora, G.J., Funke, B.R. & Case, C.L., 2010. *Microbiology. An Introduction.* 10th ed., San Francisco: Person Education Inc.

Tremaroli, V. & Bäckhed, F., 2012. Functional interactions between the gut microbiota and host metabolism. *Nature*, 489(7415), pp.242–249.

Turnbaugh, P.J. et al., 2007. The human microbiome project. *Nature*, 449(7164), pp.804–10. Available at: http://dx.doi.org/10.1038/nature06244 [Accessed July 10, 2014].

Twine, S.M. et al., 2009. Motility and flagellar glycosylation in Clostridium difficile. *Journal of bacteriology*, 191(22), pp.7050–62. Available at: http://www.pubmedcentral.nih.gov/articlerender.fcgi?artid=2772495&tool=pmcentrez&rendertype=abstract [Accessed November 10, 2013].

Ubeda, C. & Pamer, E.G., 2013. Antibiotics, microbiota, and immune defense. *Trends in immunology*, 33(9), pp.459–466.

Ueno, K. et al., 2008. MUC1 mucin is a negative regulator of toll-like receptor signaling. *American journal of respiratory cell and molecular biology*, 38(3), pp.263–8. Available at: http://www.pubmedcentral.nih.gov/articlerender.fcgi?artid=2258447&tool=pmcentrez&rendertype=abstract [Accessed December 5, 2014].

Ulluwishewa, D. et al., 2011. Regulation of tight junction permeability by intestinal bacteria and dietary components. *The Journal of nutrition*, 141(5), pp.769–76. Available at: http://jn.nutrition.org/content/141/5/769.full [Accessed May 11, 2015].

University of Colorado Denver/Anschutz Medical Campus, Guidelines for Establishing Humane Endpoints in Animal Study Proposals. Available at: http://www.ucdenver.edu/academics/research/AboutUs/animal/Documents/Guidelines for Animal_Study_Endpoints.pdf.

Vardakas, K.Z. et al., 2012. Treatment failure and recurrence of Clostridium difficile infection following treatment with vancomycin or metronidazole: a systematic review of the evidence. *International journal of antimicrobial agents*, 40(1), pp.1–8. Available at: http://www.ncbi.nlm.nih.gov/pubmed/22398198 [Accessed February 14, 2014].

Varki, A., 2009. Multiple changes in sialic acid biology during human evolution. *Glycoconjugate journal*, 26(3), pp.231–45. Available at: http://www.ncbi.nlm.nih.gov/pubmed/18777136 [Accessed October 23, 2014].

Varki, A., 2008. Sialic acids in human health and disease. *Trends in molecular medicine*, 14(8), pp.351–60. Available at: http://www.sciencedirect.com/science/article/pii/S1471491408001330 [Accessed July 9, 2014].

Versalovic, J. et al., 2008. Commensal-derived probiotics as anti-inflammatory agents. *Microbial Ecology in Health and Disease*, 20(2). Available at: http://www.microbecolhealthdis.net/index.php/mehd/article/view/7627 [Accessed July 22, 2015].

Vijay-Kumar, M., Aitken, J.D. & Gewirtz, A.T., 2008. Toll like receptor-5: Protecting the gut from enteric microbes. *Seminars in Immunopathology*, 30(1), pp.11–21.

Vohra, P. & Poxton, I.R., 2012. Induction of cytokines in a macrophage cell line by proteins of Clostridium difficile. *FEMS immunology and medical microbiology*, 65(1), pp.96–

104. Available at: http://www.ncbi.nlm.nih.gov/pubmed/22409477 [Accessed February 14, 2014].

Voth, D.D.E. & Ballard, J.J.D., 2005. Clostridium difficile toxins: mechanism of action and role in disease. *Clinical microbiology reviews*, 18(2), pp.247–263. Available at: http://cmr.asm.org/content/18/2/247.short [Accessed November 18, 2014].

Waligora, A.J. et al., 2001. Characterization of a cell surface protein of Clostridium difficile with adhesive properties. *Infection and immunity*, 69(4), pp.2144–53. Available at: http://www.pubmedcentral.nih.gov/articlerender.fcgi?artid=98141&tool=pmcentrez&rendertype=abstract [Accessed February 14, 2014].

Waligora, A.J. et al., 1999. Clostridium difficile cell attachment is modified by environmental factors. *Applied and environmental microbiology*, 65(9), pp.4234–8. Available at: http://www.pubmedcentral.nih.gov/articlerender.fcgi?artid=99767&tool=pmcentrez&rendertype=abstract [Accessed January 21, 2014].

Walsh, C., 2003. *Antibiotics: actions, origins, resistance*. 1st ed., Washington D.C.: ASM Press. Available at: http://capitadiscovery.co.uk/dcu/items/377301?query=antibiotics&resultsUri=items%3Fquery%3Dantibiotics [Accessed February 4, 2015].

Walsh, M.D. et al., 2013. Expression of MUC2, MUC5AC, MUC5B, and MUC6 mucins in colorectal cancers and their association with the CpG island methylator phenotype. *Modern pathology : an official journal of the United States and Canadian Academy of Pathology, Inc*, 26(12), pp.1642–56. Available at: http://www.ncbi.nlm.nih.gov/pubmed/23807779 [Accessed May 28, 2015].

Wang, Z.-X. et al., 2012. Global identification of prokaryotic glycoproteins based on an Escherichia coli proteome microarray. D. Chatterji, ed. *PloS one*, 7(11), p.e49080. Available at: http://dx.plos.org/10.1371/journal.pone.0049080 [Accessed December 12, 2014].

Weil, A.A. & Hohmann, E.L., 2015. Fecal Microbiota Transplant: Benefits and Risks. *Open Forum Infectious Diseases*, 2(2), pp.1–2. Available at: http://ofid.oxfordjournals.org/content/early/2014/06/01/ofid.ofu038.short.

Weingarden, A.R. et al., 2014. Microbiota transplantation restores normal fecal bile acid composition in recurrent Clostridium difficile infection. *American journal of physiology. Gastrointestinal and liver physiology*, 306(4), pp.G310–9. Available at: http://www.ncbi.nlm.nih.gov/pubmed/24284963.

Weis, W.I. & Drickamer, K., 1996. Structural basis of lectin-carbohydrate recognition. *Annual review of biochemistry*, (65), pp.441–473.

Weisburg, W.G. et al., 1991. 16S ribosomal DNA amplification for phylogenetic study. *Journal of bacteriology*, 173(2), pp.697–703. Available at: http://www.pubmedcentral.nih.gov/articlerender.fcgi?artid=207061&tool=pmcentrez&rendertype=abstract.

Wlodarska, M. et al., 2011. Antibiotic treatment alters the colonic mucus layer and predisposes the host to exacerbated Citrobacter rodentium-induced colitis. *Infection*

and immunity, 79(4), pp.1536–45. Available at: http://www.pubmedcentral.nih.gov/articlerender.fcgi?artid=3067531&tool=pmcentrez&rendertype=abstract [Accessed November 6, 2013].

Wlodarska, M., Kostic, A.D. & Xavier, R.J., 2015. An Integrative View of Microbiome-Host Interactions in Inflammatory Bowel Diseases. *Cell Host & Microbe*, 17(5), pp.577–591. Available at: http://www.cell.com/article/S1931312815001663/fulltext.

Wojciechowski, A.L. et al., 2014. Corticosteroid use is associated with a reduced incidence of Clostridium difficile-associated diarrhea: A retrospective cohort study. *Anaerobe*. Available at: http://www.sciencedirect.com/science/article/pii/S1075996414001024 [Accessed August 19, 2014].

Wolfensohn, S. & Lloyd, M., 2012. *Handbook of Laboratory Animal managment and Welfare* 3rd Editio., Blackwell Publishing.

Wright, A. et al., 2005. Proteomic analysis of cell surface proteins from Clostridium difficile. *Proteomics*, 5(9), pp.2443–52. Available at: http://www.ncbi.nlm.nih.gov/pubmed/15887182 [Accessed February 14, 2014].

Wüst, J. et al., 1982. Investigation of an outbreak of antibiotic-associated colitis by various typing methods. *Journal of clinical microbiology*, 16(6), pp.1096–101. Available at: http://www.pubmedcentral.nih.gov/articlerender.fcgi?artid=272546&tool=pmcentrez&rendertype=abstract [Accessed March 5, 2014].

Xu, X. et al., 2013. Gut microbiota, host health, and polysaccharides. *Biotechnology advances*, 31(2), pp.318–37. Available at: http://www.ncbi.nlm.nih.gov/pubmed/23280014 [Accessed June 3, 2013].

Young, V.B. & Hanna, P.C., 2014. Overlapping roles for toxins in Clostridium difficile infection. *Journal of Infectious Diseases*, 209(1), pp.9–11.

Yuki, T. et al., 2011. Activation of TLR2 enhances tight junction barrier in epidermal keratinocytes. *Journal of immunology (Baltimore, Md. : 1950)*, 187(6), pp.3230–7. Available at: http://www.ncbi.nlm.nih.gov/pubmed/21841130 [Accessed July 22, 2015].

Zaneveld, J. et al., 2008. Host-bacterial coevolution and the search for new drug targets. *Current opinion in chemical biology*, 12(1), pp.109–14. Available at: http://www.pubmedcentral.nih.gov/articlerender.fcgi?artid=2348432&tool=pmcentrez&rendertype=abstract [Accessed June 5, 2015].

Zarepour, M. et al., 2013. The mucin Muc2 limits pathogen burdens and epithelial barrier dysfunction during Salmonella enterica serovar Typhimurium colitis. *Infection and immunity*, 81(10), pp.3672–83. Available at: http://www.pubmedcentral.nih.gov/articlerender.fcgi?artid=3811786&tool=pmcentrez&rendertype=abstract [Accessed September 24, 2014].

Zeissig, S. & Blumberg, R.S., 2014. Life at the beginning: perturbation of the microbiota by antibiotics in early life and its role in health and disease. *Nature Immunology*, 15(4), pp.307–310. Available at: http://www.nature.com/doifinder/10.1038/ni.2847 [Accessed March 19, 2014].

Zenewicz, L.A. et al., 2007. Interleukin-22 but not interleukin-17 provides protection to hepatocytes during acute liver inflammation. *Immunity*, 27(4), pp.647–59. Available at: http://www.pubmedcentral.nih.gov/articlerender.fcgi?artid=2149911&tool=pmcentrez&rendertype=abstract [Accessed August 11, 2015].

Zhang, C. et al., 2014. Helicobacter pylori dwelling on the apical surface of gastrointestinal epithelium damages the mucosal barrier through direct contact. *Helicobacter*, 19(5), pp.330–42. Available at: http://www.ncbi.nlm.nih.gov/pubmed/24826891 [Accessed December 6, 2014].

Zhang, D. et al., 2004. A toll-like receptor that prevents infection by uropathogenic bacteria. *Science (New York, N.Y.)*, 303(5663), pp.1522–6. Available at: http://www.ncbi.nlm.nih.gov/pubmed/15001781 [Accessed July 12, 2015].

Zhang, Y. et al., 2015. Impacts of Gut Bacteria on Human Health and Diseases. *International Journal of Molecular Sciences*, 16, pp.7493–7519.

Zheng, Y. et al., 2008. Interleukin-22 mediates early host defense against attaching and effacing bacterial pathogens. *Nature medicine*, 14(3), pp.282–289.

Zindl, C.L. et al., 2013. IL-22-producing neutrophils contribute to antimicrobial defense and restitution of colonic epithelial integrity during colitis. *Proceedings of the National Academy of Sciences of the United States of America*, 110(31), pp.12768–73. Available at: http://www.pubmedcentral.nih.gov/articlerender.fcgi?artid=3732935&tool=pmcentrez&rendertype=abstract [Accessed February 12, 2015].

APPENDIX A – BUFFERS AND SOLUTIONS

***Clostridium difficile* washing solution.** Made up in dH_2O to 1 L. HCl was used to adjust pH to pH 7.4. Solution was used ice cold to wash harvested *C. difficile* cells.	
Tris:HCl	50 mM

S-layer isolation solution. Solution was made fresh on the day. Made up in dH_2O to 100 ml. HCl was used to adjust pH to pH 8.3. Protease inhibitor was added and left to dissolve. Incubation was carried out at 37°C for 90 min.	
Tris:HCl	50 mM
Urea	8 M
Protease inhibitor	5 tablets per 100 ml

S-layer dialysis buffer. Made up in dH_2O to 5 L x 4. HCl was used to adjust pH to pH 8.5. Solution was used at 4°C, changed every 2 h.	
Tris:HCl	20 mM

FPLC Elution Buffer (Buffer A). Made up in dH_2O to 2 L and pH was adjusted with HCl to pH 8.5.	
Tris:HCl	20 mM

FPLC Elution Buffer (Buffer B). Made up in dH_2O to 2 L and pH was adjusted with HCl to pH 8.5.	
Trizma Base	20 mM
NaCl	0.3 M

5X Loading Buffer. 1 M DTT was added to 5X loading buffer just before use and 3 µl of 5X loading buffer was added to 12 µl of each sample. This sample preparation was used for SDS PAGE during SLP characterisation, Periodic acid–Schiff Glycoprotein Staining and lectin blotting.	
Trizma Base	125 mM
Glycerol	10%
SDS	2%
Bromophenol Blue	0.05% (w/v)
DTT	0.25 M

Separating gel (12.5% (w/v)). Solution was dissolved in dH_2O to required volume. Ammonium persulphate and TEMED were added last before pouring over the gels. Gel was covered with isopropanol to exclude air and aid the polymerisation. This sample preparation was used for SDS PAGE during SLP characterisation, Periodic acid–Schiff Glycoprotein Staining and lectin blotting.

Acrylamide/Bisacrylamide (30% stock)	12.5%
Tris-HCl pH 8.8	1.5 M
SDS	1%
Ammonium persulphate	0.5% (w/v)
TEMED	0.1% (v/v)

Stacking gel (5% (w/v)). Formulation was dissolved in dH_2O to required volume. Ammonium persulphate and TEMED were added last before pouring over the gels. This sample preparation was used for SDS PAGE during SLP characterisation, Periodic acid–Schiff Glycoprotein Staining and lectin blotting.

Acrylamide/Bisacrylamide (30% stock)	5%
Tris-HCl pH 8.8	0.5 M
SDS	1%
Ammonium persulphate	0.5% (w/v)
TEMED	0.1% (v/v)

Electrode running buffer. Buffer was dissolved in dH_2O to required volume.

Trizma Base	25 mM
Glycine	200 mM
SDS	17 mM

Coomassie Stain. Solution was made up in dH_2O to required volume.

Brilliant Blue	0.2%
Methanol	45%
Acetic Acid	10%

Destain Solution. Solution was made up in dH_2O to required volume.

Methanol	25%
Acetic Acid	10%

Wash buffer for fluorescent lectin staining. Solution was made up in dH_2O to required volume.	
TBS	1X
$MgCl_2$	1 mM
$CaCl_2$	1 mM

Fluorescent lectin buffer. Solution was made up in dH_2O to required volume.	
TBS	1X
$MgCl_2$	1 mM
$CaCl_2$	1 mM
BSA	1%

Tris-buffered Saline (TBS) 10X. Buffer was made up in dH_2O and pH was adjusted to pH 7.6. Buffer was used for lectin blotting and fluorescent lectin staining analysis.	
NaCl	150 mM
Trizma Base	50 mM

MEDIA

Fastidious Anaerobe Broth (FAB) for *C. difficile* culture. Broth powder was soaked in water for 10 min and then brought to boil. Solution was autoclaved for 15 min and 121°C.	
Broth powder	29.7 g per 1 L

Brain Heart Infusion Broth (BHI) for *C. difficile* culture. Broth powder was soaked in water for 10 min and warmed gently to dissolve. Solution was autoclaved for 15 min and 121°C.	
Broth powder	37 g per 1 L

***Ex vivo* colon culture.** Media was prepared freshly on the day.	
RPMI	50 ml
Penicillin (10 000 U/ml) and Streptomycin (10 000 µg/ml)	0.5 ml

APPENDIX B – SLP CHARACTERISATION

A

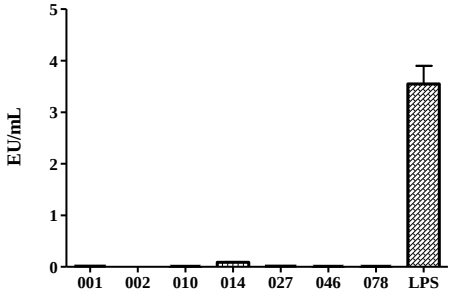

B

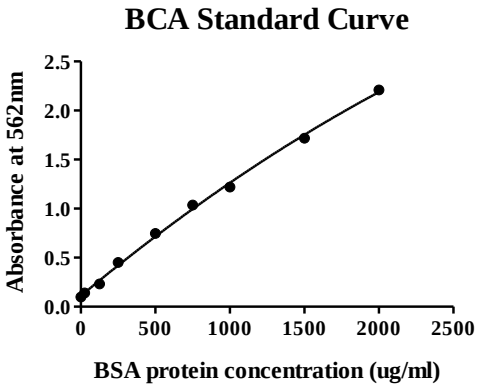

C

Table A1 The concentration of the SLP stocks.

C. difficile Ribotype	SLP Concentration (µg/ml)
001	3335
002	1195
010	1037
014	2456
027	2100
046	800
078	7234

Figure A1 SLPs from various ribotypes were examined for presence of endotoxin contamination and protein concentration was measured using BCA assay. LAL endotoxin assay was carried out to ensure that any immune response was indeed due to the SLPs and not due to potential contamination from other bacterial sources (**A**). A Bicinchoninic acid (BCA) assay was performed on all samples to determine the protein concentration for each batch of SLPs. This was of great importance as a standard volume of each SLP was required for cell stimulation. The standard curve was calculated with a four-parameter (quadratic) curve (**B**) and equation of the line was used to calculate total concentration (**C**). This table presents representative results for each ribotype used in this project.

APPENDIX C – RT QPCR QUALITY ASSURANCE

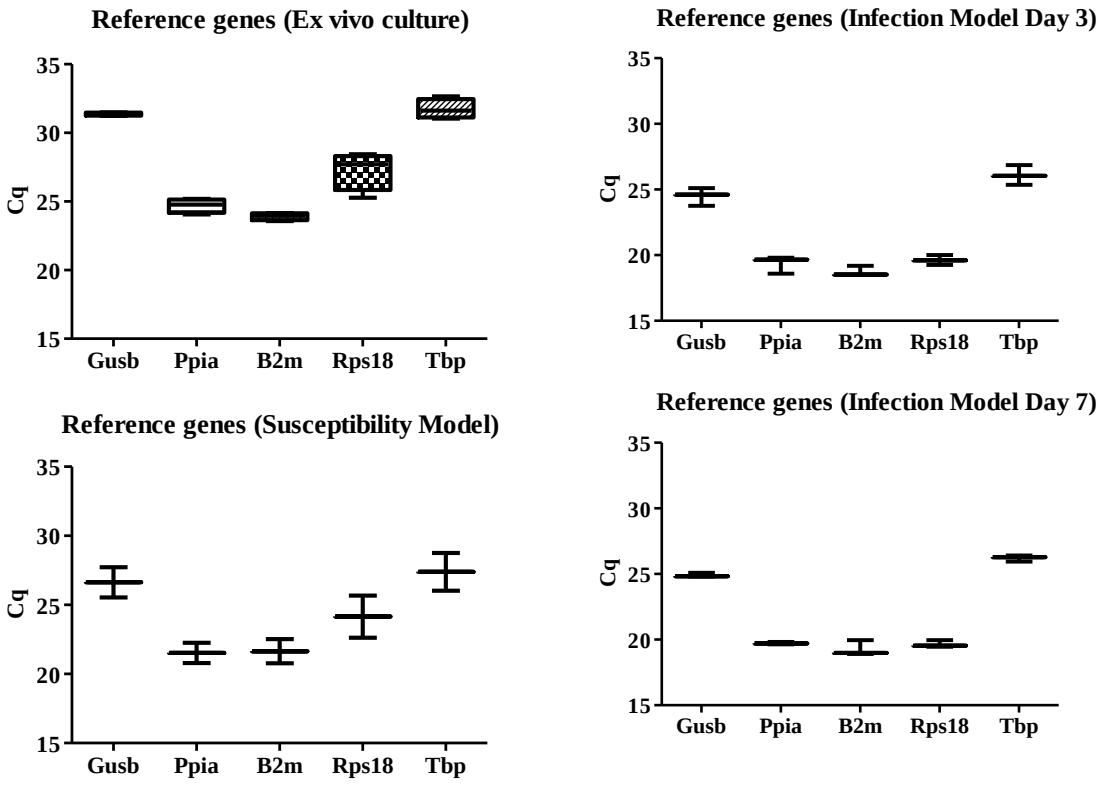

Figure A2 *Ppia* and *B2m* were identified as endogenous controls for colonic gene expression. Normalised amounts of mRNA from *ex vivo* culture, susceptibility model and infection model were converted into cDNA using a High Capacity cDNA Mastermix. The cDNA was mixed with primers for GUSB, *PPIA*, B2M, RPS18 and TBP and FAST SYBR Mastermix. Samples were assayed in triplicates and analysed on LightCycler®96. Results are mean geometric of Cq values.

Table A2 Sequences of Prime Time® qPCR Primers used in this study. All primers were sourced from IDT.

Gene	Protein	Ref Seq ID	Forward Primer (5' → 3')	Reverse Primer (3' → 5')	Exon Location
Muc1	MUC1	NM_013605	GACTGCTACTGCCATTACCTG	CCTACCATCCTATGAGTGAATACC	6 – 7
Muc2	MUC2	NM_023566	TCAAAGTGCTCTCCAAACTCTC	CAGCTCCTCTCAGAATTCCAC	40 – 43
Muc3	MUC3	XM_355711	CTTGTCACCTGTCCAGAACC	AACCACTACAGAAGTTGCCA	13 – 14
Muc4	MUC4	NM_080457	GACAAGTTAGTCCTGACATCCC	CAGCCTCTCCAAGAAATGTAGT	18 – 19
Muc5ac	MUC5AC	NM_010844	CTGGTTGAGTGGTTGTGTGT	CCCATGTGTATTCCTCTCCCA	31 – 32
Muc6	MUC6	NM_181729	GCAGTTGGAGACACAAAGGTA	CATGACATCCACTCTCACACC	31 – 33
Muc13	MUC13	NM_010739	CTCCTTGTCCTTAAGACCGTAG	CCTAATCCCTACGCAAACCAG	12 – 13
Muc15	MUC15	NM_172979	GTTCTGGTGCATTGTCTAATCG	GTGCTTCACTGCTTAGCCTT	3 – 4
Muc20	MUC20	NM_146071	GCCTGTCCCTTTGAGTGAAG	CCCTCCTTGTCTTCTGCTG	1 – 2
Ccl2	MCP1	NM_011333	AACTACAGCTTCTTTGGGACA	CATCCACGTGTTGGCTCA	1 – 3
Ccl3	MIP1α	NM_011337	CGATGAATTGGCGTGGAATC	CCTTGCTGTTCTTCTCTGTACC	1 – 2
Ccl5	RANTES	NM_013653	GCTCCAATCTTGCAGTCGT	CCTCTATCCTAGCTCATCTCCA	2 – 3
Cxcl2	MIP1β	NM_009140	CAGAAGTCATAGCCACTCTCAAG	CTTTCCAGGTCAGTTAGCCTT	2 - 4
Il1b	IL-1β	NM_008361	GACCTGTTCTTTGAAGTTGAC	CTCTTGTTGATGTGCTGCTG	3 – 4
Il2	IL-2	NM_008366	GCAGGATGGAGAATTACAGGAA	GCAGAGGTCCAAGTTCATCTTC	1 – 3
Il6	IL-6	NM_031168	AGCCAGAGTCCTTCAGAGA	TCCTTAGCCACTCCTTCTGT	4 – 5
Il10	IL-10	NM_010548	GGCATCACTTCTACCAGGTAA	TCAGCCAGGTGAAGACTTTC	1 – 3
Il12a	IL-12p35	NM_001159424	CACTGGAACTACACAAGAACGA	AAGTCCTCATAGATGCTACCAAG	3 – 5
Il23a	IL-23	NM_031252	GATCCTTTGCAAGCAGAACTG	ACCAGCGGGACATATGAATC	1 – 3
Il17a	IL-17A	NM_010552	AGACTACCTCAACCGTTCCA	GAGCTTCCCAGATCACAGAG	2 – 3
Tnfa	TNFα	NM_013693	AGACCCTCACACTCAGATCA	TCTTTGAGATCCATGCCGTTG	2 – 4
Tgfb	TGFα	NM_019919	CCGAATGTCTGACGTATTGAAGA	GCGGACTACTATGCTAAAGAGG	20 – 21
Tlr2	TLR2	NM_011905	CAACTTACCGAAACCTCAGACA	CCAGAAGCATCACATGACAGA	2 – 3
Tlr4	TLR4	NM_021297	AGCTCAGATCTATGTTCTTGGTTG	GAAGCTTGAATCCCTGCATAG	1 – 2

Table A2 Sequences of Prime Time® qPCR Primers used in this study. All primers were sourced from IDT.

Gene	Protein	Ref Seq ID	Forward Primer (5' → 3')	Reverse Primer (3' → 5')	Exon Location
Tlr5	TLR5	NM_016928	GGAACATATGCCAGACACATCT	TGAAGATCACACTCATGAGCAAG	3 – 4
Tlr9	TLR9	NM_031178	GAATCCTCCATCTCCCAACA	TCACAGGGTAGGAAGGCA	1 – 2
Stat3	STAT3	NM_213660	AGTCTCGAAGGTGATCAGGT	GTTCAAGCACCTGACCCTTAG	13 - 15
Il22b (Ilfifb)	IL-22	NM_054079	AATGAATCTTTGTGGTTATCAAGTCT	AAGTGAGAAGCTAACGTCCAC	5 - 5
Reg3g	REGIIIγ	NM_011260	GATTCGTCTCCCAGTTGATGT	CTCCATGACCCGACACTG	4 - 5
Fut2	FUT2	NM_018876	CCAGAGGAAAGGAGAAAGGT	GTCCTGAACGAAGAGCCAAG	1a – 3b
Nans	NANS	NM_053179	GTTAGTGTCCCCAGATCCAAC	GAATTCAGCCACGACCAGTA	2 - 3
Cdh1	CDH1	NM_009864	AGTCTCGTTTCTGTCTTCTGAG	GAGCTGTCTACCAAAGTGACG	3 – 4
Ocln	OCLN	NM_008756	GTTGATCTGAAGTGATAGGTGGA	CACTATGAAACAGACTACACGACA	6 – 7
Gusb	GUSB	NM_010368	GAGAACTGGTATAAGACGCATCA	GAACAGCCTTCTGGTACTCC	1 – 2
Ppia	PPIA	NM_008907	CAAACACAAACGGTTCCCAG	TTCACCTTCCCAAAGACCAC	4 – 5
B2m	B2M	NM_009735	GGGTGGAACTGTGTTACGTAG	TGGTCTTTCTGGTGCTTGTC	1 – 2
Rps18	RPS18	NM_011296	ACACCACATGAGCATATCTCC	CCTGAGAAGTTCCAGCACAT	2 – 3
Tbp	TBP	NM_013684	CCAGAACTGAAAATCAACGCAG	TGTATCTACCGTGAATCTTGGC	4 – 5

APPENDIX D – FLUORESCENT LECTIN STAINING CONTROLS

A BUFFER

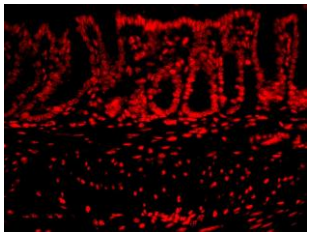

D DBA

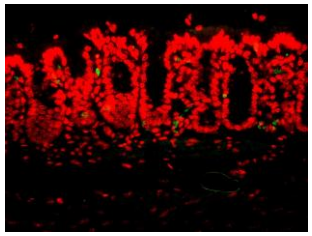

G PNA

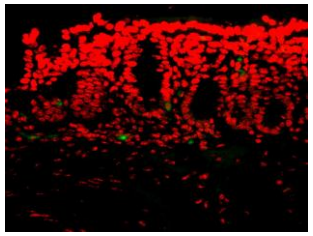

J UEA I

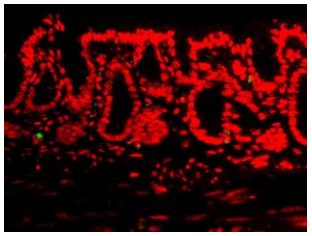

B AAL

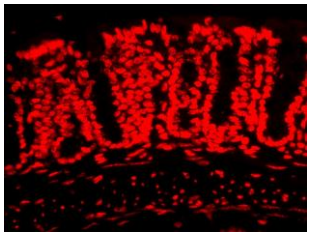

E GSL II

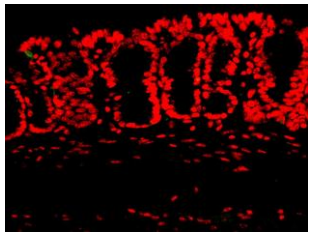

H SNA

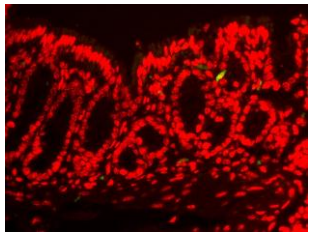

K WGA

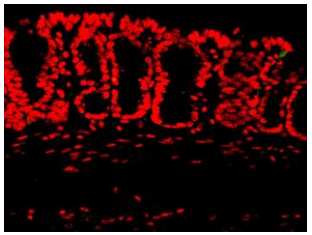

C ConA

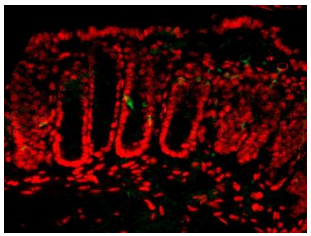

F MAL I

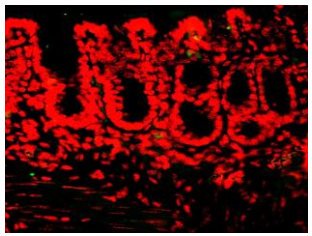

I sWGA

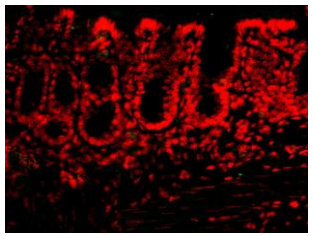

Figure A3 Buffer-only probing and pre-incubation with corresponding monosaccharide confirmed lectin specificity. Slides were probed with buffer and fluorescence was not detected (**A**). FITC-labelled lectins were pre-incubated for 30 min with 0.5 M of corresponding monosaccharide sugar. Lectins-monosaccharide solutions were then used to probe the surface of colonic epithelium. The fluorescent signal was reduced in case of all lectins used in this study, as observed on tissue histochemistry images (**B-K**),

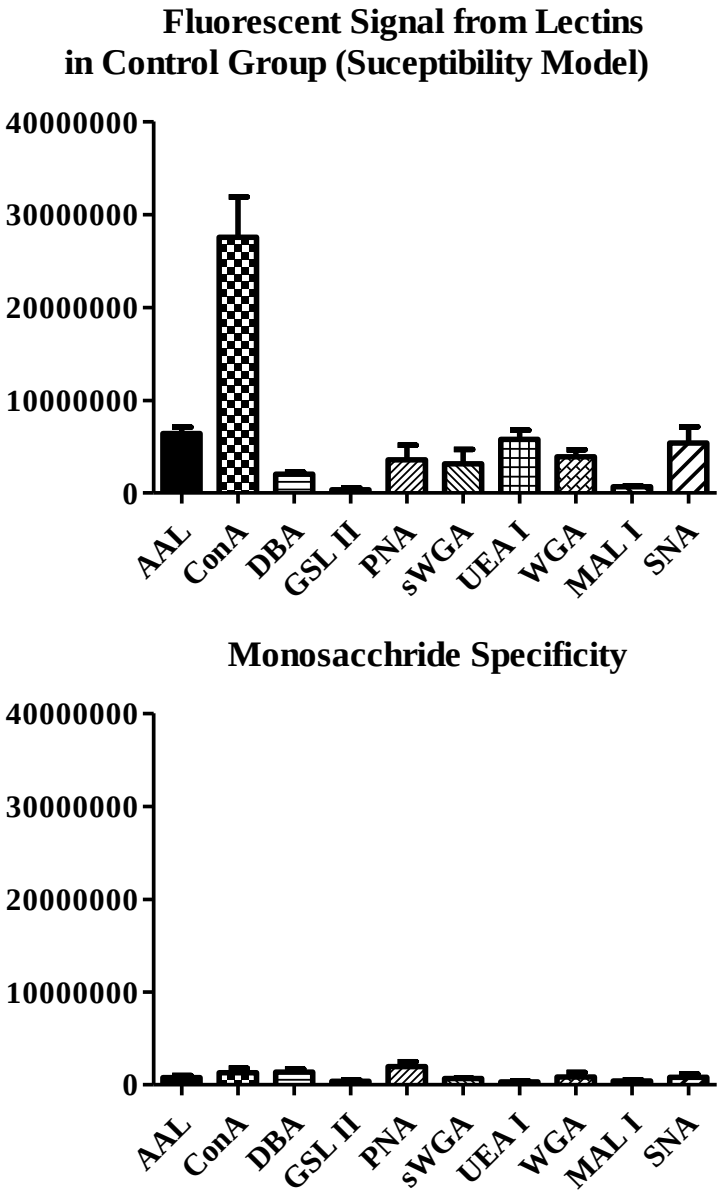

Figure A4. Monosaccharide Specificity total fluorescence signal (**B**) was compared to signal in susceptibility study (**A**).